Dissertation
submitted to the
Combined Faculties for the Natural Sciences and for Mathematics
of the Ruperto-Carola University of Heidelberg, Germany
for the degree of
Doctor of Natural Sciences

presented by
Diplom-Biochemiker Johannes Hermle
born in: Offenbach a.M., Germany
Oral-examination: July 26, 2017

siRNA SCREEN FOR IDENTIFICATION OF HUMAN KINASES INVOLVED IN ASSEMBLY AND RELEASE OF HIV-1

Referees: Prof. Dr. Hans-Georg Kräusslich
Prof. Dr. Dirk Grimm

Meiner Familie

Summary

The replication of the human immunodeficiency virus type 1 (HIV-1) is as yet not fully understood. In particular the knowledge of interactions between viral and host cell proteins and the understanding of complete virus-host protein networks are still imprecise. An integral picture of the hijacked cellular machinery is essential for a better comprehension of the virus. And as a prerequisite, new tools are needed for this purpose.

To create such a novel tool, a screening platform for host cell factors was established in this work. The screening assay serves as a powerful method to gain insights into virus-host-interactions. It was specifically tailored to addressing the stage of assembly and release of viral particles during the replication cycle of HIV-1. It was designed to be suitable for both RNAi and chemical compound screening. The first phase of this work comprised the setup and optimization of the assay. It was shown, that it was robust and reliable and delivered reproducible results. As a subsequent step, a siRNA library targeting 724 human kinases and accessory proteins was examined. After the evaluation of the complete siRNA library in a primary screen, all primary hits were validated in a second reconfirmation screen using different siRNAs. The purpose of this two-step approach was to identify and exclude false positives.

In the end, 43 genes were reconfirmed to influence the assembly and release of HIV-1. Out of those, 39 were host dependency and 4 host restriction factors. Several of them had already been described in the literature to interact with HIV-1. However, various so far unknown host cell proteins were identified within this work. A subsequent combinatory pathway analysis including hits from other published screens identified several important signaling pathways to be important for HIV-1 assembly and release. The described single key proteins and their underlying protein networks provide a basis for the next steps toward understanding the virus and improving treatment in the future.

Zusammenfassung

Noch immer gibt es große Lücken im Verständnis der Replikationsmechanik des Humanen Immundefizienz-Virus Typ 1 (HIV-1). Im Besonderen das Wissen um Interaktionen von HIV-1 mit Wirtszellproteinen ist weiterhin unvollständig, sowie das Wissen über den Aufbau der Virus-Wirt Proteinnetzwerke. Ein umfassendes Bild der, durch das Virus zweckentfremdeten, Zellmaschinerie ist essentiell, um das Virus im Ganzen zu verstehen.

Die vorliegende Arbeit beschreibt die Etablierung einer Hochdurchsatz-Screening Plattform als äußerst leistungsfähige Methode, um Einblicke in die Virus-Wirt Wechselbeziehungen zu generieren. Die Plattform ist spezifisch auf die Untersuchung der Partikelbildung und –freisetzung von HIV-1 zugeschnitten. Sie wurde entwickelt, um sowohl mit RNA-Interferenzbibliotheken, als auch mit Bibliotheken chemischer Moleküle verwendbar zu sein. Die erste Phase dieser Arbeit umfasste die Entwicklung und den Aufbau der Plattform unter Durchführung der notwendigen Qualitätstests. Die Ergebnisse zeigten, dass die entwickelte Plattform robust war und verlässliche und reproduzierbare Ergebnisse lieferte. Als erste Anwendung wurde eine Bibliothek von „short interfering RNAs“ (siRNAs) getestet, die 724 humane Kinasen und verwandte Proteine abdeckte. Zunächst wurde in einem primären Test die komplette Bibliothek untersucht. Um die gefundenen, potenziellen Wirtszellfaktoren zu bestätigen und um mögliche fälschlich-Positive auszusondern, wurden diese Treffer in einem zweiten Bestätigungssuchtest überprüft.

Insgesamt wurden hierbei 43 Proteine bestätigt – davon 39 Abhängigkeits- und 4 Restriktionsfaktoren. Einige davon waren schon vorher in der Literatur in Bezug zu HIV-1 beschrieben, jedoch war auch ein Teil in diesem Kontext bisher unbekannt und stellt daher vielversprechende, neue Ziele für das Verständnis von der HIV-1-Replikation dar. Eine anschließend durchgeführte Kombinations-Netzwerk-Analyse unter Einbeziehung anderer Publikationen identifizierte wichtige Signalkaskaden. Die in dieser Arbeit gewonnen

Erkenntnisse bilden die Basis für zukünftige Untersuchungen, um die spezifischen Rollen dieser Proteine und Netzwerke für die Formation und Freisetzung von HIV-1 aufzudecken.

Table of contents

1 Introduction

Great advances have been made in the therapy of the human immunodeficiency virus type 1 (HIV-1), which is the causative agent of the acquired immunodeficiency syndrome (AIDS). However, it still poses an enormous burden for patients and health care systems worldwide. This is in part due to the fact that there are uncharted areas in its replication cycle - especially regarding its interactions with the host cells.

1.1 Human immunodeficiency virus type 1

1.1.1 Clinical relevance

In 1983 HIV-1 was first described to be the cause of a newly emerging epidemic of an immunodeficiency syndrome called AIDS (1-3). According to the United Nations Joint Program on HIV/AIDS (UNAIDS) approximately 36.7 million people were estimated to be living with a HIV-1 infection at the end of 2015. Furthermore, the UNAIDS fact sheet 2016 records 1.1 million AIDS related deaths and approximately 2.1 million newly infected people within 2015 alone (4, 5).

HIV-1 is transmitted sexually or via contaminated blood transfusions and needles. After an acute infection the number of $CD4^+$ T-cells is diminished until the $CD8^+$ T-cell response sets in and controls the initial viremia. An infection with HIV-1 is commonly not recognized early on as only unspecific symptoms occur during this phase. In addition, HIV-1 is not detectable through routine ELISA testing during the first three to six months after infection, although proviral DNA can be detected by PCR. The acute phase is followed by a latency phase of variable duration. HIV-1 infects cells of the host immune system, mostly $CD4^+$ T-cells but also macrophages and dendritic cells. In the final stage the viral load in the system rises while the $CD4^+$ T-cell count drops rapidly. Thus, the capacity of the immune system is disrupted and other bacterial, fungal or viral infections, which are normally suppressed by the immune defense, can

now manifest and cause serious diseases. Characteristic examples are meningitis, pneumonia, candidiasis or Kaposi's sarcoma (6).

Although a cure for an HIV-1 infection has not yet been found, antiretroviral drugs are available targeting various steps of the replication cycle. To prevent the rise of resistance mutations, a combination anti-retroviral therapy (cART or HAART for Highly Active Antiretroviral Therapy) is used, in which several distinct drugs are administered (7-10). Available drugs are targeting either the entry step by impairing binding to or fusion with the cellular membrane, or early steps of replication through viral proteins (e.g. RT or IN). Another prospect of suppressing viral spread could be the inhibition of the virus assembly and/or maturation (11) as done for other viruses like herpes simplex (12). At the point of time of the experiments described in this thesis, several assembly inhibitors with promising preclinical results were in the development pipeline, but to date none of them is commercially available (13-16). For example, the clinical development of Bevirimat, a betulinic acid derivative that interferes with the production of the HIV capsid, was stopped because of low efficacy in treated patients due to polymorphisms (17, 18). And just recently, GlaxoSmithKline announced discontinuation of the phase IIb study of the second generation maturation inhibitor BMS-955176 (19). Of note, the maturation inhibitors that failed during development targeted mutation prone viral proteins instead of host proteins, which might have facilitated the virus's fast development of resistance to the respective drug.

The occurrence of HIV-1 variants resistant to standard of care drugs poses an important issue for the future of antiviral therapy (20). This is based on the high probability of mutations and recombinations of the RNA genome of the virus during the error-prone step of reverse transcription (21). The pressure to select for evasive mutations gives rise to resistant variants. Additional therapy approaches, for example offering a potent block of viral assembly and/or maturation could broaden the arsenal and overcome mutations. As cellular proof-reading functions are much more reliable, host proteins are not as prone to mutations as viral proteins. The identification of crucial host cell factors

controlling or enhancing viral replication will therefore open up a new angle for effective antiviral treatment.

The next sections outline current knowledge on the biochemical mechanisms of HIV-1 replication and the genes known to date to be responsible for virus-host-interactions.

1.1.2 Genomic and structural composition of HIV-1

HIV-1 belongs to the genus of lentiviruses in the family of retroviruses. Its single stranded and positive orientated RNA genome has the size of approximately 9.7 kb. Similar to all members of the retrovirus families, HIV-1 contains three major reading frames named *group specific antigen* (*gag*), *polymerase* (*pol*) and *envelope* (*env*). In addition, it encodes for six accessory genes with regulatory and/or auxiliary functions (22).

The precursor protein Gag consists of the domains MA (matrix), CA (capsid), SP1 (spacer peptide 1), NC (nucleocapsid), SP2 (spacer peptide 2) and p6 (protein domain 6). They are proteolytically cleaved during maturation by the viral protease (23). The *pol* gene encodes the viral protease (PR), the reverse transcriptase (RT) - harboring DNA polymerase and RNase H activities - and integrase (IN), which is essential for the integration into the host genome. The *env* gene encodes for the glycoprotein precursor gp160, which is cleaved by cellular proteases into the transmembrane anchor protein gp41 and the surface protein gp120 (24, 25). Essential for replication and reverse transcription of the genome are the flanking long-terminal repeats (LTR) which carry enhancer and promoter elements (Figure 1-1).

The accessory proteins Vif, Vpu, Vpr, and Nef influence replication and pathogenicity and possess the ability to alter the response of the host cell. Tat and Rev are necessary for viral protein expression (26, 27).

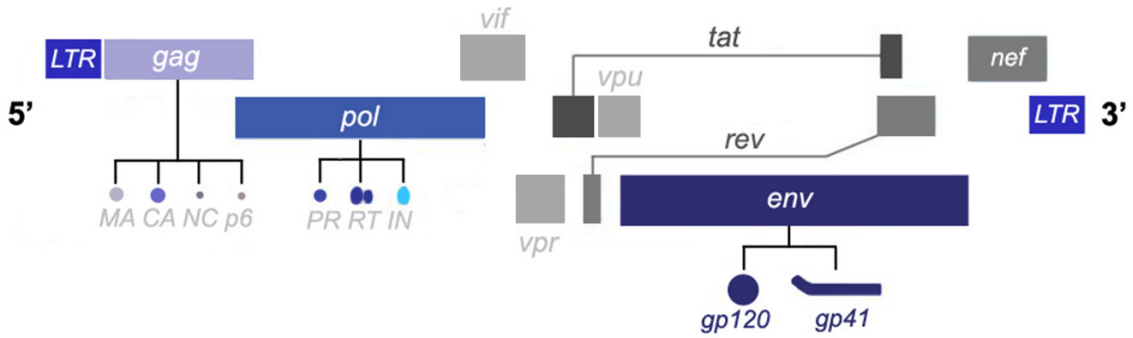

Figure 1-1 HIV-1 genome.

Schematic drawing of HIV-1's genomic organization. The major open reading frames *gag*, *pol* and *env* are depicted in light blue, blue and dark blue squares, respectively. The proteins arising after proteolytic cleavage from these genes are depicted as circles and lines in the respective colors below. The accessory genes are shown in grey squares and the long terminal repeats (LTRs) in blue. Not shown are the spacer peptides 1 and 2 and the intermediate product gp160. Figure adapted from (28, 29).

HIV-1 virions are enveloped by a membrane derived from the host cell plasma membrane with a diameter of approximately 145 nm (30) and contain two copies of the viral genome (Figure 1-2). Approximately ten trimers of the heterodimer gp120/gp41 spikes are incorporated into the membrane by the interaction of the cytoplasmic tail of gp41 and MA (31-34). During and directly after budding (see chapter 1.1.3) from the producer cell, the virion is in its immature form with an incomplete shell of Gag molecules beneath the membrane, forming a hexameric lattice (30, 35-37). The Gag molecules only cover approximately two third of the membrane that envelops the viral particle (37, 38).

The released immature viral particles are not infectious. After budding, the immature virion rapidly undergoes maturation. This process is mediated by the cleavage of Gag into its elements MA, CA, NC, SP1, SP2, and p6 by the viral protease. Maturation results in the fully infectious mature virion. The places of these cleavage events are marked by arrowheads in the lower part of Figure 1-2. Whereas the Gag polyprotein initially forms a layer beneath the membrane (Figure 1-2 upper left), after maturation only MA remains at the membrane, while CA is rearranged into hexamer and pentamer sub-structures to form its characteristically cone shaped structure (Figure 1-2 upper right) (30, 39-41).

This shell contains the viral RNA, to which multiple copies of NC are bound, forming a ribonucleoprotein complex. Several additional copies of RT and IN are in close proximity to the NC-RNA-complex and the accessory proteins Vpr, Vif and Nef are incorporated in the complex as well.

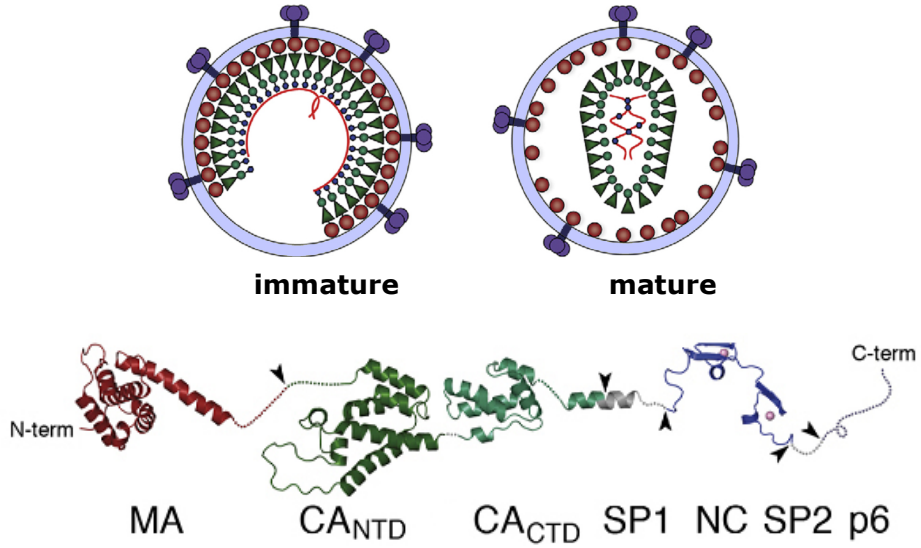

Figure 1-2 Immature and mature HIV-1 virions and model of Gag polypeptide.
Upper panel: Schematic drawing of immature (left) and mature (right) HIV-1 virions. The light blue ring indicates the membrane with the Env trimers in purple. Located beneath the membrane is the incomplete Gag shell with its subunits MA (red dots), CA (green triangle and green dot) and NC (small blue dot). The viral RNA is depicted as a red line. During maturation Gag is cleaved and MA remains at the membrane, CA forms the conic capsid comprising the viral RNA which is bound by NC proteins. **Lower panel**: Structural model of Gag, derived from high-resolution structures and models of isolated domains. Matrix (MA, dark red), Capsid N-terminal domain (CA_{NTD}, dark green), Capsid C-terminal domain (CA_{CTD}, light green), spacer peptide 1 (SP1), Nucleocapsid (NC, blue), spacer peptide 2 (SP2), Env (dark blue), viral membrane (light blue). Protease cleavage sites are indicated by arrowheads. Figure adapted from (42).

1.1.3 HIV-1 replication

The replication cycle of HIV-1 is depicted in Figure 1-3 and is discussed in the subsequent sub-chapters. In short, replication involves transcription and translation of the viral proteins followed by assembly and budding of the newly assembled virion. Shortly after budding maturation takes place which renders

the HIV-1 virion fully infective. The infectious virus binds to a target cell where interaction with the receptor and co-receptor complex allows the virion to enter the cell. Following an uncoating step the reverse transcription takes place. The viral genome is then imported into the nucleus and integrated into the host genome.

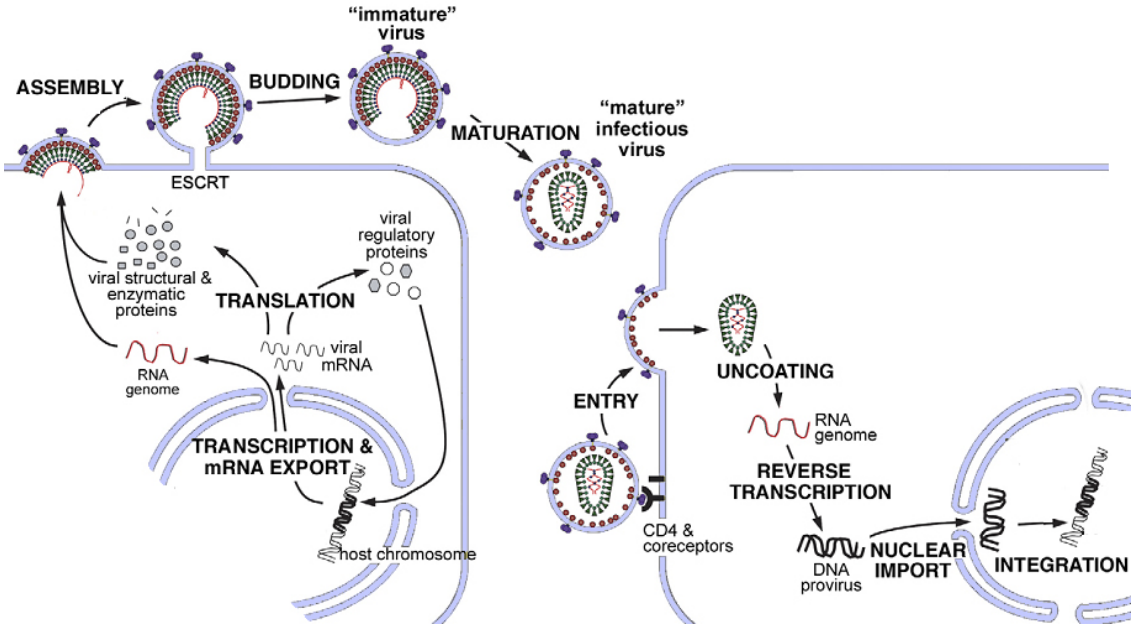

Figure 1-3 Replication of HIV-1.

Schematic drawing of the HIV-1 replication cycle showing the complete replication cycle from transcription/mRNA export from the host nucleus via assembly, budding, and maturation until the newly formed viral particles bind to and infect a new target cell. Figure adapted from (42).

Viral assembly and release

In an infected cell the provirus (the genome of HIV-1) is integrated into the host genome and can be latent for several years with a half-life time of the latent reservoir of ~44 months in resting memory $CD4^+$ T cells (43, 44). Upon cell activation it gets transcribed by the cellular RNA polymerase II. At first the fully spliced gene products Tat, Rev and Nef undergo transcription. Tat then in turn facilitates efficient gene expression by binding to the LTR. Rev is responsible for the export of incompletely spliced mRNAs from the nucleus. The Env glycoprotein originates from singly spliced RNA and is synthesized in the ER. It

is subsequently transported to the plasma membrane via the secretory pathway (31).

The unspliced RNA is used to express the polyproteins Gag and Gag-Pol. All viral structural proteins are transported to the plasma membrane where the assembly takes place (45-47). A fraction of the unspliced viral genomes is carried along to the plasma membrane due to the interaction between certain zinc-fingers in NC and the packaging sequence (psi) in the 5' UTR of the RNA (48, 49). In the cytosol, Gag in its precursor form is present as monomers and low-order oligomers (48, 50, 51). The major amount of Gag is localized at the plasma membrane (52) where it multimerizes (Figure 1-4).

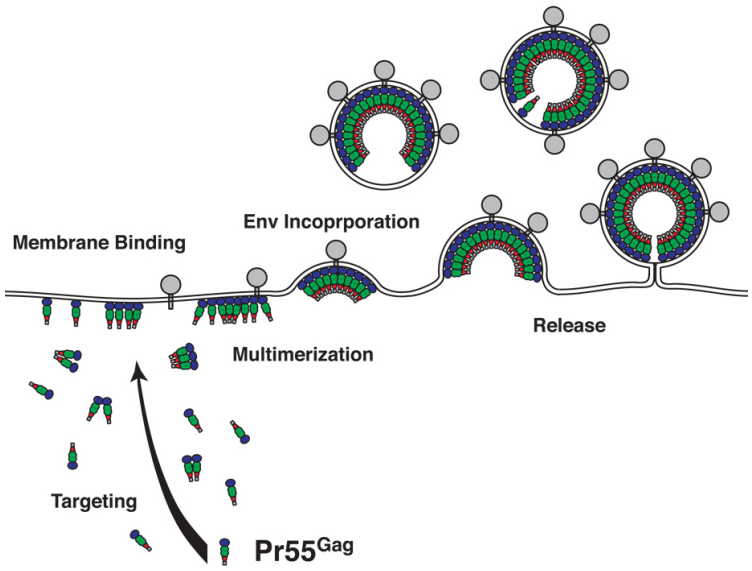

Figure 1-4 Gag assembly.
Gag is present in the cytoplasm as monomers or low-order oligomers. Upon binding to the membrane Gag multimerizes and recruits ENV. The Gag lattice induces curvature of the membrane. Figure modified from (45).

The occurrence of an active targeting mechanism to the plasma membrane is still debated. Some evidence can be found in the literature that endosomal pathways play a role in the transport of viral proteins as the adaptor complex AP-3 is interacting with Gag and seems to be important for release of HIV-1 (53). Alternatively it is discussed that viral particles might assemble on and bud into vesicles and might be transported to the plasma membrane in some cell

types (54). Membrane binding is achieved by MA with its covalently linked N-terminal myristoyl group (55, 56) and some basic amino acids which both interact with phosphatidylinositol-(4,5)-bisphosphate (PI(4,5)P2) (57-59). This interaction is crucial for membrane binding and localization (60). Oligomerization of Gag and PI(4,5)P2 binding to Gag releases the myristoyl group resulting in increased membrane affinity (myristyl switch model (61, 62)) and targets Gag to lipid-raft like domains (63-68).

Gag multimerizes at the membrane and thus induces a local curvature leading to the viral bud (35, 69, 70). This process is promoted by interactions of CA domains and RNA binding by NC (36, 42, 71, 72). The latter might be dispensable, however (73). Electron density and x-ray reconstructions revealed that the N-terminal domain of CA is involved in forming a hexameric structure while the C-terminal domain is involved in linking adjacent hexamers (35, 37, 38, 74). The cellular endosomal sorting complex required for transport (ESCRT) machinery is recruited to the bud and ultimately facilitates the scission of the stalk and releases the virion (75-77). This important complex and its function are described in more detail in chapter 1.3.

Although Gag alone is sufficient for assembly and release of immature and non-infectious viral like particles (78) viral proteins like Env, RT, IN, PR, Vpr, Vif, and Nef are incorporated into the assembling viral particle. RNA binding to NC seems to be important for particle stability *in vitro* (79). Furthermore, several cellular proteins can be detected in viral particles (80, 81), e.g. Cyclophilin A (82, 83), APOBEC3G (84, 85). Although their role during replication of HIV-1 was identified for some proteins, it is still unclear for their majority.

Recent studies addressed the assembly kinetics by using fluorescently tagged Gag (86, 87). Gag monomers were shown to form initial oligomers in the cytosol prior to cell membrane binding (51). It was shown that Gag assembly at the cell membrane is a rapid process comprised of three distinct phases (87, 88). After the detection of an assembly site an exponential increase in fluorescence was detected in phase I, taking about 8 - 9 minutes until 90 % completion. Phase II was defined as a relative static assembly site both in

fluorescence intensity and movement. In the last phase, rapid movement and a decline in fluorescence intensity was observed. In total the complete assembly process from nucleation to release takes around 25 minutes (87).

During budding or directly after its completion a structural rearrangement of the Gag shell takes place. It is called maturation and is triggered by the sequential cleavage of the precursor Gag polyproteins at five positions (arrowheads in Figure 1-2 lower panel) into their functional counterparts by the viral enzyme protease (35, 89-91). It results in mature, fully infectious, viral particles. Maturation can be blocked by protease (PR) inhibitors, which target the crucial CA-SP1 region of Gag (92).

Infection of a new cell: from entry to integration

As a first step, the infectious HIV-1 particle binds unspecifically to the heparin sulfate proteoglycans (HSPG) of a target cell (93, 94). In order to infect this cell, the viral particle then has to pass the barrier of the plasma membrane. Originally it was thought that the membrane fusion occurs exclusively at the plasma membrane (95). Recent studies showed an alternative pathway in which clathrin mediated endocytosis of the bound particles and their fusion with endosomal membranes may play a role (96, 97). However, the significance of this mechanism for establishing a productive infection is currently disputed and seems to be cell type dependent (98-101). Regardless of the type of the membrane, fusion is imagined to start with binding of the viral envelope protein gp120 to the cellular CD4 receptor (Cluster of differentiation 4) (27). CD4 is a 55 kDa transmembrane protein and a member of the immunoglobulin (Ig) superfamily. Under normal circumstances CD4 is involved in T-cell receptor and MHC class II function on T-cells (102, 103). Subsequently a co-receptor is recruited by a specific binding motif in gp120 (104) – either CXCR4 (CXC chemokine receptor 4) or CCR5 (CC chemokine receptor 5) according to the tropism of the virus. The binding of the co-receptor to gp120 leads to major structural reorganization in Env, resulting in insertion of the fusion peptide of gp41 into the cellular membrane (105). In the next step a six-helix-bundle is formed, which facilitates the fusion of the viral and the cellular membrane (106).

After the lipid envelope is lost, the capsid shell is set free. This process has until recently been thought to fully take place in the cytosol (107). However, viral capsid (CA) protein was lately found in the nucleus, suggesting that uncoating might as well be finalized there (108-111). Different models of viral uncoating like immediate uncoating, biphasic uncoating or uncoating at the nuclear pore complex are currently under discussion (112). Regardless of the model it is clear that during the uncoating of the capsid shell the reverse transcription complex (RTC), composed of the genomic RNA and a number of HIV-1 encoded proteins, is formed and reverse transcription of the viral genome takes place.

The early phase of RTC building events includes still coated HIV-1 cores, which can also be called pre-RTCs. The interaction of phosphorylated MA and Nef with microfilaments of the actin cortex results in local rearrangements of the actin cytoskeleton. Afterwards, pre-RTCs pass through the actin cortex at the plasma membrane and get into the cytosol where they interact with dynein to be transported along microtubules (MT) to their minus (–) ends (113). In this phase the cyclophilin A (CypA), which is bound to approximately 10% of CA molecules, protects RTCs from attack by the host restriction factor TRIM5α which would facilitate too rapid capsid disassembly. Furthermore, the HIV-1 nucleocapsid protein NCp7, a highly conserved 55-amino acid protein, is thought to promote reverse transcription (114-116).

This very early phase is followed by a subsequent phase involving uncoated HIV-1 RTC starting with completion of reverse transcription which results in double-strand cDNA. This process is likely associated with uncoating of pre-RTCs to RTCs (113). After completion of viral cDNA synthesis the preintegration complex (PIC) is formed consisting of cDNA, IN, MA, Vpr and several cellular proteins (117-119). The PIC facilitates transfer of the cDNA into the nucleus through the nuclear pore and HIV-1 is therefore independent of cell division. The viral genome is finally integrated into the host genome by IN. Although the PIC makes HIV-1 independent of cell division as stated above, the virus is still an obligate cell parasite and relies on the exploitation of cellular enzymes,

transportation and signaling networks ("host cell factors") for its own replication.

1.2 Virus host interactions

Several host cell factors are known to play an important role during replication of HIV-1 (120-122). The function of those cellular proteins can be either disadvantageous for the virus (host restriction factor, HRF) or advantageous (host dependency factor, HDF). A complete comprehension of the interplay of HIV-1, HRFs, and HDFs is required to better understand viral replication.

Subsequently, some examples for HRFs and HDFs are introduced to show the bandwidth of possible interactions. Several HRFs have been described to counteract certain steps during replication of HIV-1. Table 1 summarizes the most relevant HRF proteins. Of note, HRFs are not limited to proteins in the table - even microRNAs play a role in inhibition of viral translation as shown for miR-28, miR-29a, miR-125b, miR-133b, miR-138, miR-149, miR-150, miR-223, and miR-382 (123).

Table 1 List of host restriction factors

Host restriction factor	Proposed function	Counter-acted by	IFN-dep.	Ref
90K/ LGALS3BP	Unknown, upregulated in cancer and HIV-1 infection; reduces infectivity of new viral particles	-	Yes	(124, 125)
APOBEC3	Cytidine deaminase; causes hypermutations during reverse transcription	Vif	Yes	(84, 85, 126-128)
GBP5	TRAFAC class dynamin-like GTPase; interferes with Env processing and incorporation into new viral particles	(Vpu mutations)	Yes	(129-131)

Host restriction factor	Proposed function	Counter-acted by	IFN-dep.	Ref
IFITM	IFN induced transmembrane proteins; modify membrane composition and properties and thereby reducing infectivity of viral particles	-	Yes	(132)
MARCH8	Membrane-bound RING E3 ubiquitin ligase; reduces HIV-1 infectivity by impairment of Env incorporation	-	Yes	(133)
Mx2	Member of both the dynamin family and the family of large GTPases; involved in type I interferon inhibition of HIV-1 probably by blocking nuclear import	-	Yes	(134-136)
SAMHD1	Phosphohydrolase; may play a role in regulation of the innate immune response; impairs reverse transcription of HIV-1	Vpx	Yes	(137-141)
SERINC3, SERINC5	Sphingolipids and phosphatidylserine synthesis; incorporated into viral particles and reduce their fusion capacity	Nef	No	(142-146)
SLFN11	RNA binding protein; Reduces mRNA translation	-	Yes	(147)
Syntenin-1/ SDCBP	Multifunctional adapter protein involved in diverse array of functions including trafficking of transmembrane proteins; Actin remodeling by Synthenin-1 interferes with viral cell entry	-	No	(148)
Tetherin	Membrane glycoprotein; blocks release of new viruses	Vpu	Yes	(149-151)
TRIM5α	Tripartite motif (TRIM) family member; species specific impairment of uncoating/reverse transcription	-	Yes	(152-154)

Host restriction factor	Proposed function	Counter-acted by	IFN-dep.	Ref
TRIM22	Tripartite motif (TRIM) family member; E3 ubiquitin-ligase; reduces HIV-1 transcription	-	Yes	(155, 156)

In the course of the host-virus coevolution, several viral proteins have emerged to counteract or circumvent these host restrictions (157, 158). For example, the host proteins APOBEC3G and TRIM5α (152, 153) take part in innate antiviral immunity and interfere with retroviral replication. APOBEC3G (and other proteins of the APOBEC3 family) are cytidine deaminases, which are packaged into the newly formed viral particles and lead to hypermutations during reverse transcription in the target cells (84, 85, 126-128, 159). To circumvent this, the HIV-1 protein Vif recruits an ubiquitin ligase complex leading to APOBEC3G degradation (126). TRIM5α is a multi domain protein which impairs the uncoating and reverse transcription by binding to CA (152, 153). In contrast to Vif counteracting APOBEC3 restriction, HIV-1 has no viral counterpart to TRIM5α. However, it was shown that Cyclophilin A protects the virus from TRIM5α activity in humans (154). As another example, the HIV-1 component Vpu antagonizes a different mechanism of innate antiviral immunity, the retention of virus particles at the plasma membrane by CD317/Tetherin (149-151). Lastly, the cellular enzyme SAMHD1 was identified to be responsible for blocking HIV-1 infection in macrophages, monocytes, dendritic cells (137-141), and resting T-cells (160). This block can be overcome by co-expression of Vpx from HIV-2 while HIV-1 does not contain an antagonist of its own (137, 161), making HIV-1 infection of the respective cells inefficient. Activated T-cells are susceptible to HIV-1 infection despite similar expression levels of SAMHD1 (160), suggesting additional, yet unknown factors involved in HIV-1 replication in this cell type, possibly kinases like CDK1 and CDK2 (162-165). Many of the aforementioned host restriction factors are part of the innate immune response and are responsive to interferons (IFNs) (166, 167). These IFN induced host restriction factors, their site of action during the HIV-1 replication and their specific counterparts are depicted in Figure 1-5.

IFNs are a family of pro-inflammatory and immunomodulatory cytokines and consist of three IFN types, of which type I IFNs are the ones mainly involved in antiviral responses (166). For example, the type I interferon IFN epsilon is reported to reduce HIV-1 infectivity through several stages during its replication cycle (168). In addition, expression and/or activity of many anti-viral host cell factors are increased after HIV-1 infection of a cell in an IFN dependent manner. The beneficial roles of IFNs in the acute state of HIV-1 infection like control of infection and reduction of virus load are contrasted by several recent studies pointing towards viruses dysregulating IFN signaling pathways e.g. in chronic persistent HIV-related disease (166).

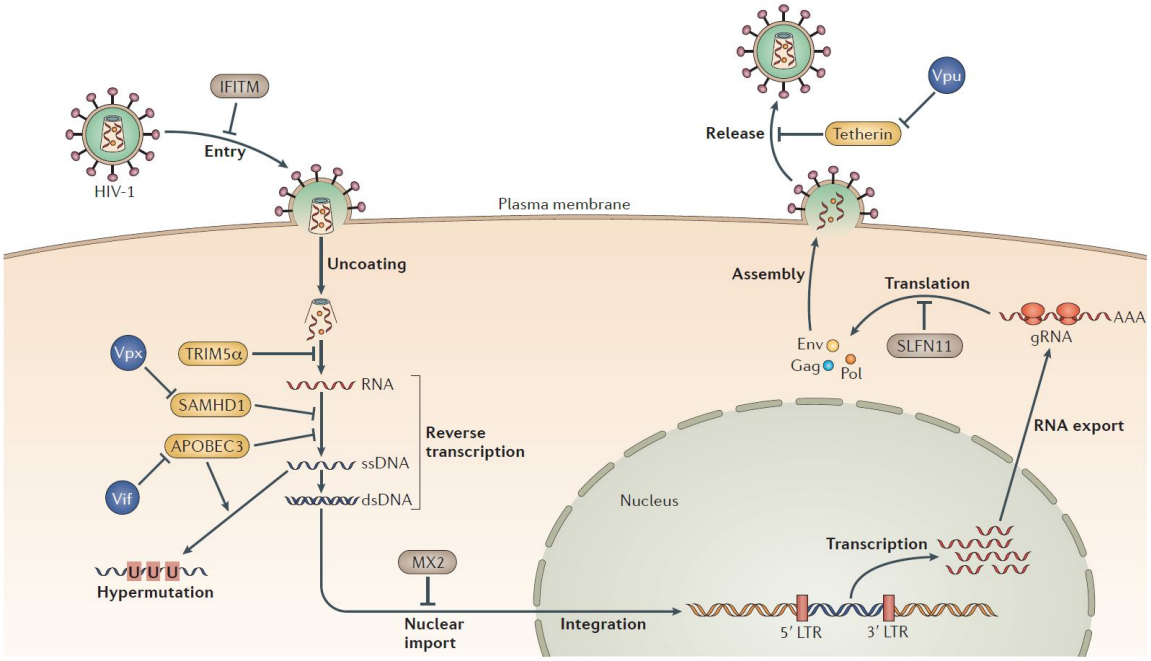

Figure 1-5 Overview of IFN induced host restriction factors
Several cellular proteins are restricting the replication cycle of HIV-1. Yellow and brown boxes show IFN induced host restriction factors (for more information see Table 1). Blue circles indicate viral accessory proteins preventing the restriction of their respective counterparts. Figure from (166).

Interestingly, IFN dependence has recently been shown not to be a mutual feature of all HRFs. The most recently discovered Serine incorporator 5 (SERINC5), for example, is constitutively expressed and not IFN-induced (142-146). SERINC5 is incorporated into budding HIV-1 virions and impairs

subsequent virion penetration of susceptible target cells. This action is prevented by the HIV-1 factor Nef which excludes SERINC5 from viral particles by diverting it to another endosomal compartment (144).

In addition to the cell-advantageous host restriction factors, some well characterized HDFs, whose presence is advantageous for the virus, are known to date and the numbers of newly described HDFs are continuously rising (169). Although the actual importance of some proteins for the replication of HIV-1 is controversially discussed, several examples are summarized in Table 2.

Table 2 List of the host dependency factors.

Host dependency factor	Proposed function	Ref
ALCAM	Cell to cell transmission of HIV-1	(170)
ALIX	Interacts with p6 GAG, involved in viral budding	(171)
aPKC	Phosphorylates p6 and leads to Vpr incorporation	(172)
CBF-beta	Essential for Vif induced ubiquitination and degradation of APOBEC3G	(173)
CDK family	Increase of viral replication by Tat interaction with CDK9	(174)
CPSF6	Binds to HIV-1 CA and facilitates transport by TNPO3	(175-177)
Cullin-5	Essential for Vif induced ubiquitination and degradation of APOBEC3G	(178)
DDX3	Important for nuclear export of HIV-1 RNA splice variants	(179, 180)
DOCK2-ELMO1	Enables Nef to influence Rac regulated pathways	(181)
ERK2 / MAPK	Phosphorylation of GAG	(182, 183)
ESCRT complex	Multi protein complex essential for release of new viral particles from the plasma membrane	(184-187)
Ezrin & EHD4	Interact with Nef to affect its infectivity	(188)
hNAP-1	Correlates with Tat-mediated viral expression	(189)
hnRNP E1	Affects Rev expression	(190)
hnRNP K	Participates in viral RNA splicing process	(191)
HSP70	Promotes import of HIV-1 PIC into nucleus	(192)

Host dependency factor	Proposed function	Ref
JNK	Phosphorylation of IN, promotion of integration	(193)
LEDGF/p75	Essential for viral integration	(194)
LRPPRC	Affects viral replication	(195)
LYRIC	Interacts with MA and NC, regulates infectivity	(196)
Matrin 3	Required for nuclear export of viral RNAs	(197)
Mortalin	Affects Nef secretion	(198)
Nucleoporins (Nup98, Nup153, Nup358),	Facilitate nuclear import and involvement in integration	(108, 109, 199-201)
pTEF-b	Stimulates HIV-1 transcription together with Tat and Tar	(202, 203)
RHA	Promotes viral reverse transcription	(204, 205)
Splicing regulator p32	Associates with viral splicing inhibition induced by Tat acetylation	(206)
Staufen 1	Interacts with viral genomic DNA	(207, 208)
TNPO3 (Karyopherins)	Transport of HIV-1 proteins	(209-213)
TPST2, SLC35B2	Sulfonation of CCR5 increases CCR5 and Env interaction	(170)
YB-1	Potentiates viral transactivation	(214, 215)

Obvious examples for HDFs are the receptor CD4 and the co-receptors CXCR4 and CCR5 which are important for a productive infection of T-cells. Examples of factors, which have been discussed for many years, are the cellular protein Cyclophilin A (82, 83) or LEDGF (194). Cyclophilin A was shown to bind CA and an impaired binding led to a reduction of nuclear import and infectivity in some cell lines (216). In addition, Cyclophilin A was shown to be packaged into HIV-1 particles, although the role of this interaction is not yet identified (217). LEDGF was described to bind IN and to be essential for integration (194, 218). In addition to an integrase binding domain, LEDGF contains a second

domain binding chromatin – revealing LEDGF's role as an adaptor to guide IN to the host DNA. It was shown that by exchanging its chromatin binding domain (CBD) to other CBDs with specific binding sites in the host DNA, the integration site can be redirected artificially (219). Kinases like ERK2/MAPK (182, 183, 220) or aPKC (172) were as well described as HDFs (see chapter 1.4). Not only single proteins interact and modulate the infectivity of HIV-1, but as well huge multi-protein complexes. One example is the endosomal sorting complex required for transport (ESCRT) complex, which is described in more detail in the following chapter.

1.3 The ESCRT complex

The ESCRT complex orchestrates a crucial step during the assembly and release of HIV-1. ESCRT's role in the cell is the sorting of ubiquitinated membrane proteins into the multi-vesicular body to transport them to the lysosome for degradation (221, 222). In addition, the ESCRT complex plays a role during abscission, the scission of the mid-body at the end of cytokinesis (223). Many viruses including HIV-1 use this complex for their own purposes, namely budding and release of newly formed virions. For an extensive review of viruses using the ESCRT complex please refer to (184) and (187).

The ESCRT complex comprises four sub-complexes ESCRT-0 to ESCRT-III, consisting of several proteins each (Figure 1-6). The multi-step process of abscission starts with binding of ESCRT-I by ESCRT-0, which is then followed by the recruitment of ESCRT-II so that ESCRT-I interacts with ESCRT-0 and ESCRT-II, linking them to a chain-like structure (186). ESCRT-1 contains amongst other proteins the important tumor susceptibility gene 101 protein (TSG101). ESCRT-II then binds to and activates the ESCRT-III sub-complex, which initially exists in an auto inhibited state in the cytoplasm (186). In addition to the main complex, two more loosely connected auxiliary proteins play a role in the abscission process. On the one hand ALG-2 interacting protein X (AIP1 or ALIX) acts as an adaptor or scaffolding agent (171), while the ATPase VPS4 has a crucial role to facilitate the disassembly and recycling of the ESCRT machinery (224).

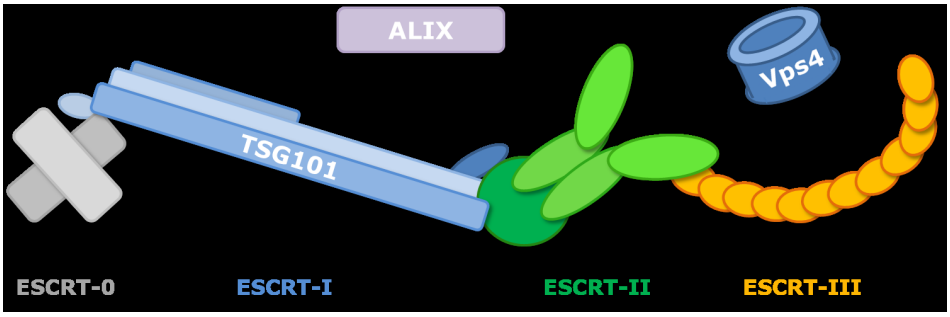

Figure 1-6 The ESCRT machinery.
The ESCRT complex comprises of four complexes ESCRT-0 to ESCRT-III. ESCRT-0 is depicted in grey, ESCRT-I in blue including TSG101, ESCRT-II in green, and ESCRT-III in orange. The auxiliary proteins ALIX and Vps4 are in indicated in lilac and dark blue, respectively. Figure adapted from (225).

HIV-1 requires the recruitment of the ESCRT complex to the site of its assembly for a successful release of the newly formed virions from the plasma membrane. ESCRT is indispensable for this step, as the Gag induced membrane curvature on its own does not suffice to facilitate release (35, 70, 226). For this step, the regular function of the ESCRT complex is exploited in a way that it abscises the neck of the newly formed buds (77, 187, 227, 228). Impairing the functionality of the ESCRT complex, for example by knockdown of TSG101 or utilizing a dominant negative VPS4 mutant, interferes with HIV-1 release (185). Furthermore, Gag proteins having a mutation in or lacking the entire C-terminal p6 domain (the so called “late domain”) lead to a diminished release of viral particles. Electron microscopy demonstrated the formation and accumulation of viral buds at the plasma membrane which show an immature or irregular morphology (76, 229, 230). This demonstrated that blocking the interaction of the virus with the ESCRT complex does not affect assembly and multimerization of Gag but rather the last step – the scission of the readymade bud.

Within the above mentioned p6 domain of Gag a specific amino acid motif is important for the interaction with the ESCRT complex. A common feature of late domains is the presence of highly conserved motifs mediating protein-protein interactions with host cell proteins (231), for example the facilitation of the scission event. Regarding HIV-1, mutation studies led to the discovery of a PTAP amino acid motif in the N-terminus of the Gag-derived p6 protein (232). Mutation of these four amino acids led to impaired release of HIV-1 while alterations in the residual parts of p6 had no significant effect (232). The PTAP

motif was shown to interact with the N-terminus of Tsg101 (185, 233, 234), the major part of the cellular ESCRT-1 complex (223, 235, 236) (Figure 1-7).

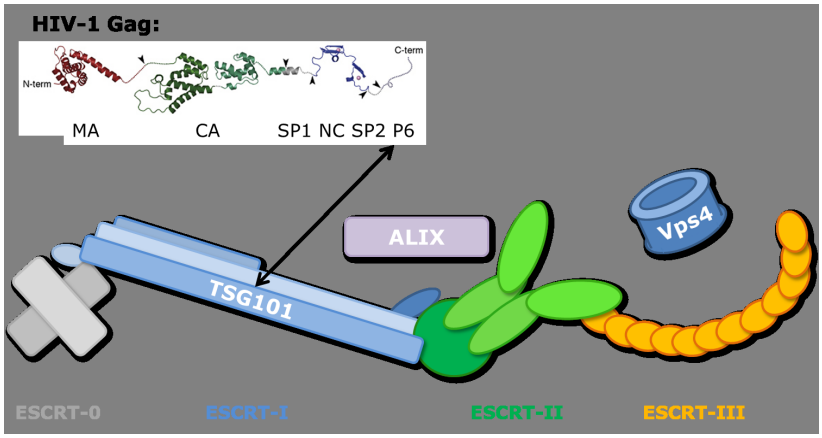

Figure 1-7 The ESCRT machinery and its interaction with Gag.
The PTAP motif within the p6 domain of Gag interacts with TSG101, which is a component of the ESCRT-I complex. By this interaction the ESCRT machinery is recruited to the site of budding. Figure modified from (42, 225).

Various late domains were identified in retroviruses and the switching of distinct late domain motifs from one virus type to another revealed their exchangeability and modular character (237). The interaction partners of several other viruses' late domain motifs were identified as well and some examples are given in Table 3.

Table 3Viral late domain motifs.

Virus	Late domain motif	Cellular interaction partner
HIV-1	PTAP	Tsg101
EIAV	YPXL	AIPa/ALIX
HTLV-1, RSV	PPXY	NEDD4

In this work, a release-impaired variant of HIV-1 is used as a control, which harbors a p6 domain with its PTAP motif mutated to LIRL (indicated as "Late(-)" throughout the work) (232, 238). The p6 protein was shown to be

multi-phosphorylated. At the time of this work this phosphorylation of p6 was thought to be important for HIV-1 release which sparked the focus on kinases.

1.4 Kinases and HIV-1

Some kinases were reported to be involved in p6 phosphorylation and the budding process: The cellular ERK-2 kinase, a member of the important MAP kinase family (220, 239), or the TANK-1 binding kinase (TBK) (240). However, to date it is known that phosphorylation of p6 is dispensable for HIV-1 replication (241, 242), leaving the exact role of the p6 multi-phosphorylation unknown.

Even though the phosphorylation of the p6 domain is dispensable, kinases and the phosphorylation of viral proteins and/or host factors still play a very important role in the regulation of several steps of HIV-1 replication. Until today several cellular kinases were identified to play a role in the replication of HIV-1.

The nuclear import of the pre-integration complexes (PICs), for example, involves phosphorylation of the three viral proteins MA, Vpr and IN. MA has been shown to be phosphorylated by cellular serine-threonine kinases and kinases of the MAPK pathway (182, 183, 243, 244), some of which are even incorporated into virions (182). However, as viruses bearing large deletions in the phosphorylated N-terminal region of MA were still mostly able to replicate it was considered that MA was dispensable for nuclear import of HIV-1 (245, 246). An alternative function of MA phosphorylation might be that it facilitates proper detachment of MA from the viral envelope, which was shown to be required for the formation of PICs (247).

The accessory protein Vpr is phosphorylated at different sites, with serine 79 being of major functional importance. Phosphorylation at this site is responsible for induction of G2 cell cycle arrest (248, 249) and for efficient nuclear import (250). Protein kinase A was suggested as the responsible kinase for serine 79 (249).

As another example, the phosphorylation of the viral integrase (IN) by cellular c-Jun N-terminal kinase (JNK) at serine 57 is crucial for efficient HIV-1 integration and infection (193). Phosphorylated IN binds the isomerase Pin1 and thus increases viral protein stability. As JNK is only expressed in activated, but not resting, CD4+ T-lymphocytes, this phosphorylation might explain the cellular selectivity of HIV-1 infections (193), underlining the importance of kinases in the biology of HIV-1.

Cellular kinases are also involved in viral transcription. For example, human positive transcription elongation factor b (p-TEFb) is required for transcription of HIV-1 (202). P-TEFb is a heterodimer composed of the cyclin-dependent kinase 9 (CDK9) and its regulatory partner cyclin T1 (251). Phosphorylation by p-TEFb/CDK9 is required to release polymerase II from pausing, leading to the production of full-length HIV-1 transcripts (251). Other members of the CDK family, namely CDK 1, -2, and -6, are responsible for phosphorylation of SAMHD1 (252, 253), enabling control of HIV-1 replication.

In sum, inhibition of cellular kinases interacting with HIV-1 has been shown to affect the viral replication cycle, suggesting potential new therapeutic approaches (254). However, a detailed picture of the involved kinases and their regulation and especially those kinases with an enhancing role in assembly and release of HIV-1 is still missing and has yet to be elucidated. The data of Radestock and coworkers and the history of the p6 phosphorylation debate suggest inverting the direction of investigations into kinases important for HIV-1 replication: Instead of assuming relevance of certain phosphorylations and searching for the respective kinases from there, it might make more sense to search for kinases which cause a functional impact on viral replication in the first place. Therefore, a far-reaching screening approach is needed to shed light on the essential network of host cell kinases regulating viral release.

1.5 Identification of host cell factors

In order to investigate cellular proteins on a broad and genome-wide scale, there are a few techniques suitable for a high throughput screening (HTS) approach. One potent tool is a loss-of-function screen using RNA interference (RNAi). RNAi is a post-translational gene silencing mechanism and was first described in *C. elegans* (255). Through it, single-stranded RNAs (ssRNA) with approximately 22 nucleotides are bound by the ribonucleoprotein complex RNA induced silencing complex (RISC). This complex binds and cleaves the complimentary mRNA (256). The short ssRNA molecules are either naturally derived from miRNAs expressed from the cellular genome for gene expression fine-tuning, or are added artificially to the system for example as siRNAs. The latter are ready-made 22-nucleotide RNA duplexes which can be directly transfected or electroporated into the target cells and directly start with recruiting the RISC. The process is depicted in Figure 1-8 and please see (257) for an in-depth review of the RNAi pathway.

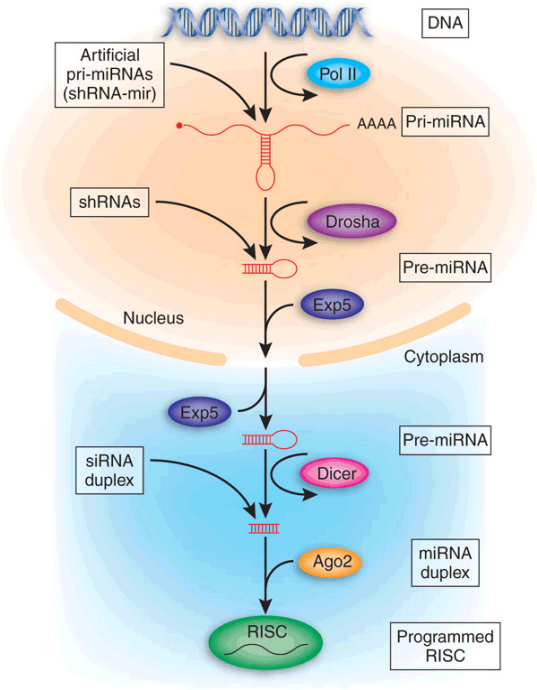

Figure 1-8 RNAi pathway.
Artificial siRNAs can enter this pathway as synthetic siRNA duplexes, as short-hairpin RNAs (shRNA) transcribed by Pol III or as artificial pri-miRNAs (shRNA-mir). For simplicity, not all factors involved in miRNA biogenesis are shown. Ago2, Argonaute-2; Exp5, Exportin-5. Figure from (257).

There are two distinct ways to use RNAi for identifying host cell factors involved in the mechanism of interest. If applicable, specific genes can be chosen through educated guessing and tested with tailor-made experiments. On the other hand, to get a broader understanding, whole libraries of RNAi molecules can be tested in a medium- to high-throughput screening. Those genome-wide siRNA, shRNA or even miRNA screens are often used to identify so far unknown cellular proteins. There are two main settings of RNAi libraries used in today's screening platforms. Either the RNAi reagents are distributed separately or several distinct RNAi against the same target gene are pooled together. Both approaches have different (dis-) advantages in regard to off-target effects and technical/budget requirements.

In the last years, several high-throughput siRNA screens with HIV-1 were published, which identified many putative host cell factors involved in HIV-1 replication (212, 258, 259). However, they did not show a big overlap of identified cellular proteins. In addition, as only two of the screens encompassed the assembly phase in their methodology and the other focused more on the early steps of an infection, only a limited number of essential cofactors for viral egress are known. (120, 122, 260). Thus, there is still a need for a better understanding of the assembly and release of HIV-1.

Although providing the most comprehensive image of a virus-host interaction landscape, the specific setting of a genome wide screen predefines its usability to answer specific questions. Huge genome-wide approaches are challenging to yield clear and un-convoluted results and smaller approaches may be superior in a limited setting (261, 262). A screening assay specifically tailored to investigate the late phase in viral replication has not yet been established.

2 Aim of the study

HIV-1 depends on cellular proteins for its replication. While much is known about their involvement in the steps from binding to a target cell up to integration and replication, there is still a substantial knowledge gap for the assembly and release of newly built viral particles. To shed light on these crucial phases during HIV-1 replication a detailed picture of the involved cellular factors is required. The hypothesis of this work is that a broad screening approach may lead to the identification of these factors. Based on this idea, the aim of this thesis is the establishment of an efficient high-throughput screening (HTS) assay specifically tailored to address assembly and release of HIV-1.

This HTS assay should be versatile to test not only libraries of siRNAs to determine key host cell factors involved in this phase of the viral replication, but as well chemical compound libraries with molecules potentially interfering with assembly or release of HIV-1 particles. The establishment includes both the experimental setup as well as the organization of various collaboration partners for a joint approach e.g. on statistics or bioinformatics.

Subsequent to the completion of the screening platform establishment, a siRNA library, targeting the complete set of human kinases, shall be investigated. As kinases and the phosphorylation of their target proteins may play a fundamental role in assembly and release of HIV-1, the screening of such a library may lead to the discovery of candidate kinases, so far not described in the context of HIV-1, or protein networks regulating this crucial phase of the viral replication cycle.

3 Materials & Methods

3.1 Materials

3.1.1 Chemicals, reagents, enzymes, and materials

Table 4 Chemicals, reagents, enzymes, and materials

Materials	Supplier
6-well- and 12-well plates, 384-well plates (#353962), cell culture flasks with 75 or 150 cm^2	BD Falcon, Germany
96-well plates Costar plates #3603 or #3916 (black)	Corning Life Sciences, Netherlands
Acrylamide	Rotiphorese Gel, Roth, Karlsruhe, Germany
Ampicillin	Roth, Karlsruhe, Germany.
Blotting paper	3 MM Chr, Whatman, Dassel, Germany
Confocal laser scanning microscope Leica SP2	Leica Microsystems GmbH, Wetzlar, Germany
DMEM	Gibco/Invitrogen, Karlsruhe, Germany
DNA gel extraction kit	Nucleospin® Extraction II, Macherey-Nagel, Düren, Germany
ECL Western blotting substrate	Pierce, Rockford, IL,USA
ELISA plates	Maxisorb, Nunc, Wiesbaden, Germany
Epifluorescence screening Microscope Olympus Scan^R	Olympus Soft Imaging Solutions GmbH, Münster, Germany
FCS	Biochrom AG / seromed, Berlin, Germany
Fibronectin	Sigma-Aldrich, Steinheim, Germany
FuGENE® 6	Roche, Basel, Switzerland
FuGENE® HD	Roche, Basel, Switzerland
Hoechst 33258	Molecular Probes, Germany
Igepal CA630	Sigma-Aldrich, Steinheim, Germany
Infrared scanner Odyssey	LI-COR Inc., Lincoln, NE, USA
Kanamycin	Roth, Karlsruhe, Germany

Materials	Supplier
LiCor blocking buffer	LI-COR Inc., Lincoln, NE, USA
Lipofectamine® 2000	Thermo Fisher, Germany
Matrix Hydra® DT	Thermo Fisher, Germany
Multi Drop® Combi	Thermo Fisher, Germany
Nitrocellulose membrane	Protran, Schleicher & Schüll/Whatman, Dassel, Germany
Penicillin-streptomycin solution (10,000U/mL + 10 mg/mL)	Invitrogen/GIBCO, Germany
Plasmid purification kit	NucleoBond MaxiPrep Kit, Macherey-Nagel, Düren, Germany
PocketBloc Thermomixer	Biozyme, Germany
Restriction enzymes and buffers	NEB (New England Biolabs GmbH, Frankfurt, Germany) Fermentas (Fermentas GmbH, St. Leon-Rot, Germany)
SDS-PAGE electrophoresis chamber	Mighty small, Hoefer, Almstetten, Germany
Semi-Dry Blotter Fastblot B32	Whatman Biometra, Göttingen
Size standard DNA (1kB Plus DNA Ladder)	Thermo Fisher, Germany
Size standard Protein (PageRuler™ Plus)	Thermo Fisher, Germany
Spectrophotometer DU 640	Beckman Coulter, Fullerton, CA, USA
Tecan SAFIRE™	Thermo Fisher, Germany
Trypsin	Biochrom AG, Berlin, Germany
Ultracentrifuge Optima XL-70	Beckman Coulter, Fullerton, CA, USA

3.1.2 Buffer, solutions, and reagents

Table 5 Buffer, solutions, and reagents.

Buffer	Concentrations
Acrylamide 30%	0.15 % bisacrylamide 30 % acrylamide
Acrylamide for stacking gels (30:0.8%)	0.8 % bisacrylamide 30 % acrylamide
DNA loading buffer (10x)	50 % sucrose 10 mM EDTA 2 % bromphenol blue 2 % orange G
LB agar	13 % agar in LB Medium
LB medium	1 % peptone 0.5 % yeast extract 171 mM NaCl
PBS (10x)	1.37 M NaCl 27 mM KCl 80 mM Na_2HPO_4 18 mM KH_2PO_4
RIPA lysis buffer	0.1 M Tris-HCl (pH 8.0) 0.33 M NaCl 2 % SDS 0.4 % deoxycholate 1 % Triton X-100
TAE buffer (50x)	2 M Tris-acetate 500 mM EDTA
TBS	20 mM Tris 150 mM NaCl
TBST (10x)	200 mM 1M Tris 150 mM NaCl 0.5 % Triton-X100
SDS-PAGE electrophoresis buffer	25 mM Tris 19.2 M glycine 0.1 % SDS

Buffer	Concentrations
Separating gel	17.5 % acrylamide 375 mM Tris-HCl pH 8.8 0.1 % SDS 0.1 % APS 0.0017 % TEMED
Stacking gel	2 % acrylamide 125 mM Tris-HCl pH 6.8 0.1 % SDS 0.0025 % APS 0.0025 % TEMED
Western blot blocking buffer	5 % milkpowder in PBS or TBST
Semi dry Western blot buffer	20 mM Tris 150 mM Glycine 20 % Methanol
Western blot transfer buffer	48 mM Tris 39 mM Glycine 0.375 % SDS 20 % Methanol

3.1.3 Antibodies

Table 6 Antibodies.

Antibody	Application	Dilution	Supplier
Mouse anti Actin	WB	1:2500	Santa Cruz
Mouse anti PAPSS1	WB	1:250	Abcam
Rabbit anti ERK2	WB	1:1000	Santa Cruz
Rabbit anti HIV CA	WB	1:5000	Kräusslich lab
Rabbit anti HIV MA	WB	1:5000	Kräusslich lab
Rabbit anti MAP2K3	WB/IF	1:500 / 1:150	Abcam
Rabbit anti MAP3K14	WB/IF	1:250	Abcam
Sheep anti-HIV CA	WB/IF	1:5000	Kräusslich lab

3.1.4 Plasmids

Table 7 Plasmids.

Plasmid	Description	Reference
pNL4-3	Proviral infectious plasmid	(263)
pCHIV	Non-infectious subviral plasmid	(264)
pCHIV.late(-)	Non-infectious subviral plasmid; PTAP→LIRL	(232, 238)
pCHIV^{eYFP}	Non-infectious subviral plasmid harboring the e*yfp* gene within the *gag* ORF	(238, 264)
pCHIV^{eYFP}.late(-)	Non-infectious subviral plasmid; PTAP→LIRL; e*yfp* gene within the *gag* ORF	(232, 238)

3.1.5 Cell lines

Table 8 Cell lines.

Name	Description	Reference
293T	Human embryonic kidney fibroblast, Transduced with SV40 large T antigen	(265)
HeLa	human cervix carcinoma	(266)
HeLaP4	HeLa stably expressing CD4	(267)
SupT1/CCR5	Human Non Hodgkin's T cell lymphoma, stably expressing CCR5	R. Doms
MT-4	Human T cells isolated from a patient with adult T cell leukemia, HTLV-I transformed	(268)

3.1.6 siRNAs

In the primary screen, the Silencer® Human Kinase siRNA Library V3 (AM80010V3) from Ambion was used. It contains three distinct siRNAs per target gene. For sequences and more information about the human kinase siRNA library see 12.1 Appendix 1: Primary screen kinase library. Three independent Silencer® Select siRNAs from Ambion were used for each of the identified primary hits in the reconfirmation screen (12.2 Appendix 2:

Reconfirmation screen library). In addition, the following siRNAs were used for controls experiments:

Table 9 siRNAs.

Name	Gene Name	Sequence	Reference
siTSG101	Tumor susceptibility gene 101	CCUCCAGUCUUCUCUCGUCTT	(185)

Name	Gene Name	siRNA ID	Supplier
siVPS4A	Vacuolar protein sorting 4A (yeast)	SI00760767	QIAGEN GmbH - Germany
siVPS4B	Vacuolar protein sorting 4B (yeast)	SI00760809	QIAGEN GmbH - Germany
siEAP20	Vacuolar protein sorting 25 homolog (S. cerevisiae)	SI00631295	QIAGEN GmbH - Germany
siALIX	Programmed cell death 6 interacting protein (AIP1/ALIX)	SI02655345	QIAGEN GmbH - Germany

3.2 Methods

3.2.1 (Quantitative) Western Blot

Cell lysates for western blot experiments were generated by incubating the cell with RIPA lysis buffer. The homogenate was transferred to a tube and denaturized at 95 °C for 5 min. Samples were then loaded onto SDS-Polyacrylamide Gel Electrophoresis (SDS-PAGE) gels and were run at ~200 V for approximately one hour. Afterwards, proteins were transferred from the gels to nitrocellulose membranes in a semi-dry blotting machine (Fastblot B32, Whatman Biometra, Gottingen, Germany) at 400 V, 240 mA, and 10 W. The resulting membranes were blocked with 5% milk powder in TBST to reduce unspecific binding of the antibodies and washed with TBST. Incubation of the primary antibody was conducted over night at 4 °C. Subsequently, the membranes were washed with TBST for three times. The membranes were then incubated with the secondary antibodies were diluted in LiCor blocking buffer (LI-COR Inc., Lincoln, NE, USA) at room temperature for one hour. After washing the membranes for two times with TBST and one time with PBS, the

membranes were scanned with the Infrared scanner Odyssey (LI-COR Inc., Lincoln, NE, USA) and images were analyzed using the standard Odyssey Aerius v 2.1 analysis software.

3.2.2 Transformation of bacteria and DNA amplification

For plasmid DNA amplification, 100 ng plasmid DNA were added to chemically competent bacteria (DH5α or Stable II *E.coli*). Following an incubation period on ice for 10 minutes, the bacteria underwent a heat shock at 42 °C for 45 seconds. 450 µL LB medium were added and incubated for 1 hour at 37 °C before they were transferred to LB Agar plates containing the respective antibiotic. The plates were incubated at 37 °C over night. At the following day, single colonies were added to 1.5 mL or 200 mL LB medium for mini or maxi preparations, respectively. The bacteria were then incubated under the appropriate antibiotic selection pressure at 37 °C over night. Plasmid DNA was purified using the NucleoBondR miniprep or maxiprep kits (Macherey-Nagel, Duren, Germany) according to the description of the supplier. Concentration and purity of the resulting DNA was checked with an UV spectrophotometer (Spectrophotometer DU 640, Beckman Coulter, Fullerton, CA, USA).

3.2.3 DNA digestion and ligation

DNA was digested using restriction enzymes and their respective buffers from NEB (New England Biolabs GmbH, Frankfurt, Germany) or Fermentas (Fermentas GmbH, St. Leon-Rot, Germany). The restriction enzyme was incubated together with its appropriate buffer and 1 µg of the purified plasmid DNA at the temperature recommended by the manufacturer for approximately one hour. Gel electrophoresis was performed subsequently, to check the sizes of the restriction products. The individual DNA bands were compared to a molecular mass standard ladder (1 kb Plus DNA ladder, Invitrogen Ltd., Paisley, UK).

3.2.4 DNA amplification by polymerase chain reaction (PCR)

For amplification of DNA, a standard PCR was used. 40 ng of purified plasmid DNA served as a template and were mixed with forward and reverse primers (40 pmol each), 250 µM desoxy nucleotide triphospates (dNTPs), and the proofreading polymerase Pfu or the standard Taq polymerase with the respective buffer. The standard PCR settings were: Denaturation (94°C for 5 min); Short denaturation cycles (20-30x, 94°C); Annealing (48°C for 45 seconds); Synthesis (72°C for 1 min/kb template length).

3.2.5 Cell culture

Cells were routinely cultivated and grown in flasks (75 or 150 cm^2, BD Falcon, Germany) or multi well plates of different formats (6-well or 12-well plates, BD Falcon, Germany; 96-well plates Costar plates #3603 or #3916, Corning Life Sciences, Netherlands). Cells were kept in DMEM medium containing 10 % fetal calf serum (FCS, Biochrom AG / Seromed, Berlin, Germany) and Penicillin-streptomycin solution (10,000U/mL + 10 mg/mL, Invitrogen/GIBCO, Germany) in a 5 % CO_2 atmosphere at 37 °C. For passaging, cells were washed with PBS and harvested by trypsin incubation for 5 minutes. After counting, the required number of cells was distributed to other flasks or multi-well plates.

3.2.6 Transfection of cells

Cells were seeded approximately one day prior to transfection with one of the different methods.

3.2.6.1 Calcium phosphate precipitation method

DNA was diluted in H2O and mixed with 1/10 2.5 M CaCl2. This mixture was then slowly pipetted to the same volume of 2x HeBS buffer while vortexing, incubated for 30 min at RT and then slowly added to the cells. Medium change was performed app. 6 h post transfection.

3.2.6.2 FuGENE® 6, FuGENE® HD, Lipofectamine® 2000

These commercially available transfection reagents were used according to the respective manufacturer's instructions. FuGENE® 6 and FuGENE® HD were acquired from Roche, Basel, Switzerland. Lipofectamine® 2000 was supplied by Thermo Fisher, Germany.

3.2.7 Screening assay

The screening procedure was partly published previously in Hermle et al., BMC Biotechnology, 2010 (238). All 96- or 384-well plates were prepared for reverse transfection in advance of the conduct of the actual screening. This step was based on and done with the support of our collaboration partners (269, 270). The transfection mixture contained OptiMEM (with 0.4 M sucrose), the respective siRNA, Lipofectamine® 2000, gelatin and fibronectin.

On the day of the experimental start, cells were harvested and a stock cell suspension was prepared in a sufficient volume to be distributed to all plates of the screen at the same time to avoid unequal cell numbers. Then, 15,000 293T cells/96 well or 2,500 cells/384-well were seeded in 100 µl / 25 µl cell culture medium using the automated Multi Drop® Combi Reagent Dispenser (Thermo Fisher). After 30 hours, the transfection mixture of pCHIVeYFP:pCHIV (1:1 ratio) was prepared using FuGENE® 6 as a transfection reagent. Per 96-well plate, 960 µl of DMEM without FCS was mixed with 38.4 µl FuGENE® 6 (Roche). Following 5 min incubation at room temperature, 19.2 µg of total plasmid DNA were added and the mixture was incubated for further 15 min at room temperature. Subsequently, 9.6 ml of the cell suspension were added and mixed. The supernatant were removed and 100 µl of the transfection mixture were added per well onto 96-well plates (Corning COSTAR #3603) or 25 µl per well onto 384-well plates (BD FALCON 353962, BD Biosciences) using an automated reagent dispenser (MultiDrop® Combi). This resulted in a total amount of 100 ng proviral plasmid DNA per 96-well or 25 ng per 384-well.

Supernatants (~87.5 µl/96-well or ~20 µl/384-well) were collected 42 hours post transfection using the Matrix Hydra® DT automated liquid handling

platform (Thermo Fisher) and transferred to separate 96-well plates (Corning COSTAR #3916) or 384-well plate. The residual supernatant over the cells was aspirated and 100 µl/96-well or 25 µl/384-well of the lysis buffer (PBS/0.5% Igepal) were added to each well to generate cell lysate suspensions. All plates were frozen at -20 °C and thawn at room temperature prior to measurement. Fluorescence intensities of the cell lysate plates and the supernatant plates were subsequently measured with the Tecan SAFIRE™ (Thermo Fisher).

The raw fluorescence signal intensities were exported to Microsoft EXCEL. For initial experiments, the ratio of supernatant intensity versus the total intensity from supernatant plus cell lysates is calculated (SN/(SN+CL), indicated as SN/Total). For the siRNA primary and reconfirmation screen, statistical analysis was performed by the collaboration partners Johanna Mazur and Lars Kaderali (Viroquant Research Group Modeling, BioQuant, University of Heidelberg, Germany). The analysis for the release screen was done in R (Version 2.8.0, R Development Core Team, http://www.R-project.org) and was based on their previously published analysis process for evaluation of microscopy based siRNA screens (Bioconductor packages RNAither (271) and cellHTS (272). Briefly, raw signal intensities of the cell lysates and the supernatant were normalized by locally weighted scatterplot smoothing (LOWESS). Then all wells with the lowest 5 % of signal intensity in the cell lysate were discarded to exclude potential cytotoxic siRNAs followed by z-score normalization in relation to the median of all wells for the primary screen and the non-silencing control siRNAs on each plate for the reconfirmation screen. The resulting z-score was a measure to rank the results in dependence of the individual standard deviations. In addition p-values were calculated to test for statistical significance.

4 Results

The results section of this thesis is subdivided into four parts. It starts with a description of the assay's setup, including the optimization in regard to reliability and robustness. The second part covers the primary screen of the siRNA library. The identified primary hits were then re-tested in the so called reconfirmation screen, which is shown in the third part. The fourth part contains results of the bioinformatic analysis of the identified host cell factors.

The crucial step during the screening is the detection of released particles outside the cells. This assay has to be robust, reproducible, and has to be applicable for high-throughput approaches. The method covering all of these requirements is a fluorescence based assay. It offers a mixture of high sensitivity, reliability, reproducibility, and relatively low work-demand (e.g. compared to conducting ELISAs on a HTS scale) and is therefore ideal as a HTS detection method. Our group previously described a non-infectious clone of HIV-1 (pCHIV) harboring an eGFP (264, 273) or eYFP within *gag* (238). The construct lacks the LTRs and protein expression is driven by a CMV promoter leading to a normal expression of all viral proteins apart from Nef (Figure 4-1).

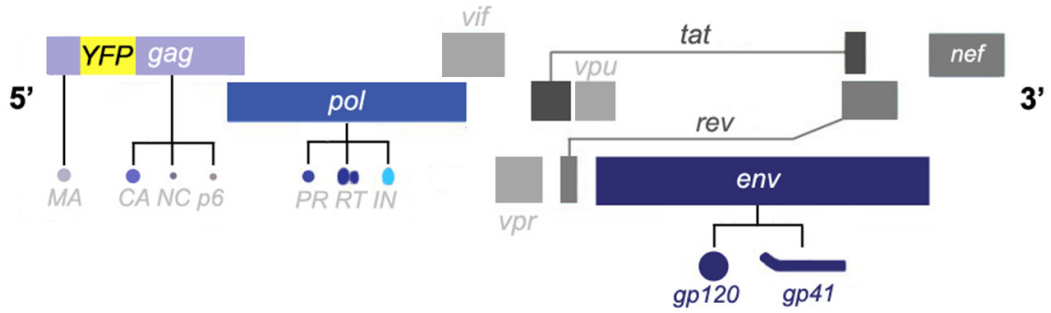

Figure 4-1 Genome of pCHIV^{eYFP}.
Schematic drawing of the genomic organization of pCHIV^{eYFP}. The major open reading frames *gag*, *pol* and *env* are depicted in light blue, blue and dark blue, respectively. Below them are the products shown after proteolytic cleavage. The eYFP is inserted between MA and CA within *gag* and depicted in yellow. The accessory proteins are shown in grey. Figure adapted from (28, 29).

Wild type budding kinetics, maturation and appearance were proven using transfections of an equimolar ratio of pCHIV^{eYFP} with the parent pCHIV plasmid lacking the reporter insert. The need to apply equimolar mixtures of labelled and unlabeled plasmids stems from previously published studies from our department in which it was shown that only labelled plasmid led to Gag assembly at the plasma membrane and only the equimolar mixtures yielded wild-type like budding (273). The viral particles, which result from the transfection of this mixture, are able to bind and enter new target cells but do not lead to a productive infection due to the lack of the LTRs. Approximately 50 % of all Gag molecules of the newly formed viral particles carry a fluorescent protein, which allow detection and quantification directly in the supernatant (273). Current monochromator-based microplate detection systems allow a rapid, reliable, and economic quantification of the fluorescence intensity and are therefore suitable for high throughput screening. A previously described variant of pCHIV is used as a positive control, which harbors a p6 domain with its PTAP motif mutated to LIRL (indicated as pCHIV.late(-) or pCHIV^{eYFP}.late(-), respectively) (232, 238). This late domain defective variant leads to a strongly impaired release of viral particles. It was shown previously by the group of Barbara Müller that the fluorescence measurement yields comparable results as a standard ELISA detection of HIV-1 CA Figure 4-2 (238).

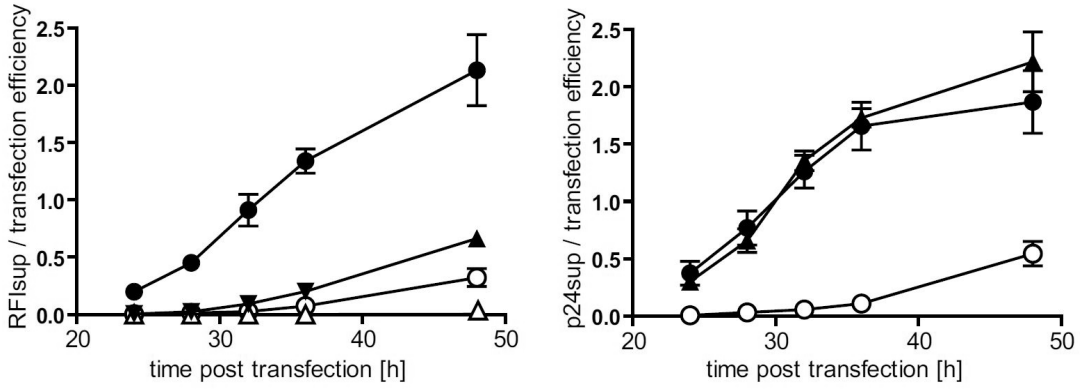

Figure 4-2 Release of pCHIV^{eYFP} measured by fluorescence and ELISA.
Comparison of the fluorescence detection of the YFP signal (left) and quantification of HIV CA by an ELISA (right). Filled circles (●) indicate the equimolar mixture of pCHIV^{eYFP}:pCHIV; open circles (o) the mixture of pCHIV^{eYFP}.late(-):pCHIV.late(-) constructs; filled triangles (▲) show peYFP:pCHIV mixtures and open triangles (△) peYFP/empty vector. Experiments performed by Barbara Müller, Maria Anders and Anke-Mareil Heuser. Figure taken from (238).

These published findings show that the pCHIV^{eYFP} approach offers a simple and direct quantification of released particles. Therefore, the fluorescence detection method was chosen as the read-out for the hereby described siRNA screening platform analyzing HIV-1 assembly and release.

Briefly, the assay is based on the quantification of eYFP fluorescence intensity in cell lysates and supernatant of pCHIV^{eYFP} transfected cells. A microplate reader yields raw fluorescence intensity from the supernatant and the cell lysates from multi-well plates. Raw fluorescence intensities are not easy to be directly compared, as depend on cell numbers, cell viability, or other variable factors. Any unspecific effect on general cell viability would cause reduced fluorescence in the supernatant and would yield a false-positive hit. To avoid this, the supernatant fluorescence is always normalized to the total combined fluorescence of supernatants plus cell lysates. This is indicated as "SN/Total" throughout all experiments.

For the siRNA libraries the already established method of "reverse transfection" from our collaboration group of Dr. Holger Erfle (BioQuant, University of Heidelberg, Germany) was applied. In brief, siRNAs, the transfection reagent, and fibronectin are mixed and added to a well of a 96-well plate. The plates are dried and can be prepared in advance. The cells are then added on top of the coated well and are directly transfected (269, 270).

4.1 Setup of the screening assay

Several steps have to be optimized in order to establish a screening assay suitable to screen siRNA libraries in a medium/high throughput approach. First of all the cell seeding procedure has to be optimized using automated procedures. This is followed by fine tuning of the transfection efficiency to ensure optimal transfection rates. Sample collection and detection of the eYFP signal are the next two steps in data creation followed by two steps dealing with quality control – namely the assay stability and robustness and the efficacy of control siRNAs. The last point deals with the establishment of the statistical analysis of the raw data (conducted by external collaborators) and the

bioinformatic evaluation. Please note, the order of the steps is chosen for comprehensibility and many steps were conducted in parallel. Figure 4-3 shows a schematic overview of the seven individual stages of this process. The complete assay was established for the usage of both 96- and 384-well plates. This allows the conduct of low-to-medium high-throughput (96-well) up to high-throughput screening approaches. The screen of the kinase library was conducted in the 96-well plate format. Therefore, the establishment of the 384-well format is not described in the similar high grade of detail.

Figure 4-3 Schematic process of the screening platform
The flowchart shows the individual steps of the screening platform from optimization of cell seeding until the bioinformatic analysis. Each step had to be established specifically for the HIV-1 screening platform. The sole exception was the statistical analysis, which was conducted by external collaborators (indicated by an asterisk).

Seeding optimization

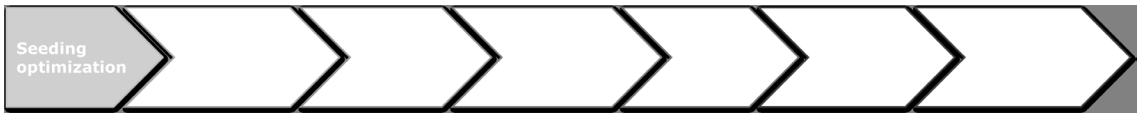

At first, the seeding of cells had to be adapted for medium/high throughput screening. For large sets of multi-well plates a homogenous and reproducible preparation of cell suspensions and the even distribution on single wells is an important step. Manual distribution of the cell suspension is error prone and therefore automated dispensers have to be utilized to ensure equal and rapid dispersion to all multi-well plates. Thereby it is crucial to seed as many cells as possible to facilitate efficient reverse transfection later on. However, the density has to be that low to have a confluent cell layer at the end of the whole assay to ensure that the cell viability is not impaired, e.g. due to space limitations and overgrowing. In addition, the variation between the wells has to be low.

The establishment started with experiments on different protocols to prepare the cell suspension for different automated cell dispensers (cell numbers, volumes, seeding speed, and centrifugation post seeding). Cell growth and density was monitored by widefield microscopy. Based on these results, a Multi Drop® Combi Reagent Dispenser (Thermo Fisher) and 293T cells were chosen for the screening assay. Other cell lines (e.g. HeLa or HeLa-P4 cells) were compared as well but did overall not yield acceptable results (data not shown).

Determination of the optimal procedure included as well testing different cell densities of 293T cells (30,000, 15,000, 7,500, and 2,500 cells/well). All wells were transfected with an equimolar ratio of pCHIV^{eYFP}:pCHIV (indicated as “WT”, wild type), a 1:1 ratio of the late domain deficient pCHIV^{eYFP}.late(-): pCHIV.late(-) (indicated as “Late (-)”), or peYFP at 30 hours post seeding. For each cell density 8 wells were used on a 96-well plate. Figure 4-4 shows example photomontages of 3x3 individual images for the different cell densities. They were acquired using an automated Olympus ScanR microscope and montaged using the program ImageJ. Centrifugation after seeding had no influence on cell densities and was therefore not used for the screening assay (data not shown). The wells with 30,000 cells/well were over fluent and cell debris was visible at the time point of harvest. The wells with 15,000 cell per well showed an even and 80-90 % confluent cell layer with no cell debris. Fewer cell numbers yielded too low confluency (Figure 4-4).

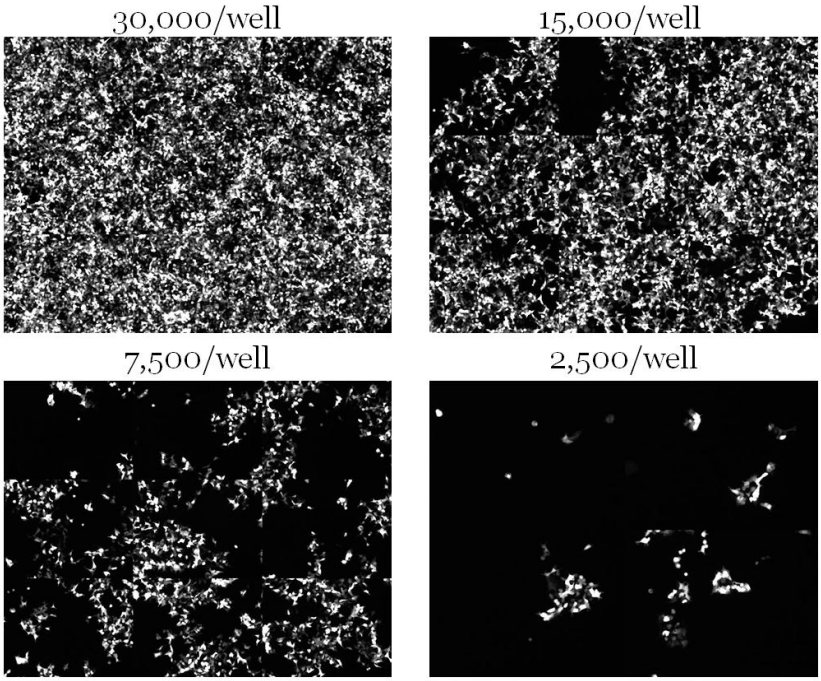

Figure 4-4 Examples of cell densities
Different cell numbers of 293T cells were seeded into the wells of 96-well plates (30,000, 15,000, 7,500 and 2,500 cells/well). Shown are montages of 3x3 individual pictures of the same well (YFP channel = ~529 nm).

At 44 hours post transfection (74 hours after seeding), the supernatants and cell lysates were harvested and the fluorescence intensity quantified. Figure 4-5 shows one example of three independent experiments. Normalized fluorescence intensity of supernatant versus total fluorescence for 15,000 cells/well gave the best ratio between wildtype and late(-) of ~8 fold, the best statistical significance of $p < 0.001$ (unpaired t-test, GraphPad Prism 6.05), and the lowest variability. Wells with 30,000 cells/well resulted in the highest net fluorescence intensity. However, microscopic inspection of the wells revealed overgrown wells which resulted in cell death. Damaged cells led to shedding of cytoplasm content which was reflected by relatively high results for the Late(-). Wells with lower cell numbers yielded smaller fold differences and cell density in wells with 2,500 cells/well was too low which resulted in greater variance.

Based on those results, the density of 15,000 293T cells per 96-well was used for the screen. For the 384-well format, 2,500 cells/well in 25 µl medium were determined to be optimal.

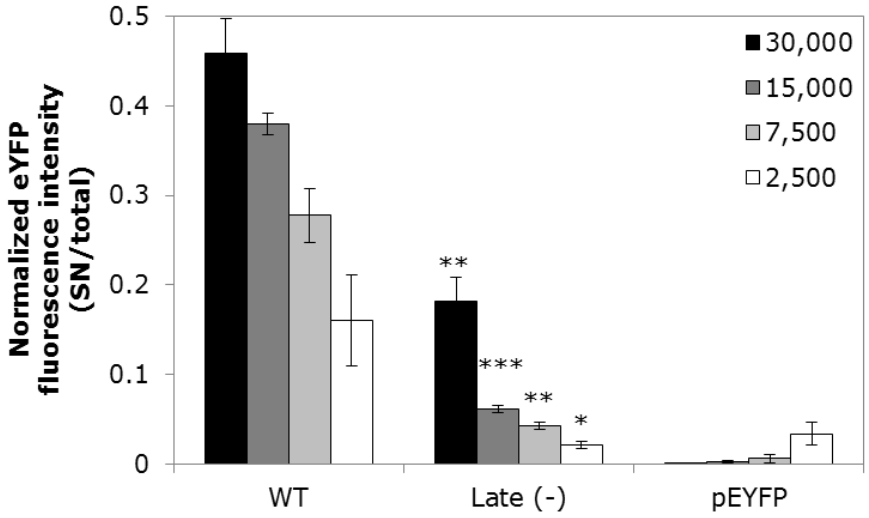

Figure 4-5 Optimal cell seeding conditions were established with 15,000 cells/well
Different cell numbers of 293T cells were seeded into the wells of 96-well plates (30,000, 15,000, 7,500, and 2,500 cells/well). For each cell density one column (8 wells) of the 96-well plate was used. 30 hours post seeding, the wells were transfected either with a 1:1 mixture of pCHIV^{eYFP}:pCHIV (indicated as "WT", wild type), a 1:1 ratio of the late domain deficient pCHIV^{eYFP}.late(-): pCHIV.late(-) (indicated as "Late (-)"), or peYFP. Depicted are the normalized fluorescence intensities, calculated by division of supernatant intensity by total intensity in lysate and supernatant (mean ± standard deviation). The experiment was performed in triplicates and one representative graph is shown. Statistical analysis (unpaired t-test, GraphPad Prism 6.05) of Late(-) value compared to the respective WT result: ***= $p<0.001$; **= $p<0.01$; *= $p<0.05$.

Transfection efficiency

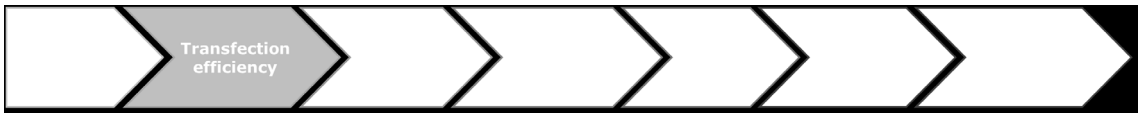

Transfection efficiency has to be optimized. This prevents skewed results by using the optimal amounts of plasmid DNA and the transfection reagent. This is important to avoid not transfected cells or over-transfected wells leading to cytotoxicity. 15,000 293T cells were seeded per well. 30 hours later, the 1:1 mixtures of pCHIV^{eYFP}:pCHIV (indicated as "WT") or the late domain deficient pCHIV^{eYFP}.late(-):pCHIV.late(-) (indicated as "Late(-)") were transfected with different total plasmid amounts (200, 100, 50, 25, 12.5, 6.25 ng plasmid

DNA/well). Eight wells per condition were tested and the complete experiment was conducted in triplicates (only one representative experiment is shown in Figure 4-6).

All wells were visually inspected using a fluorescence microscope for cell viability, cell numbers, and transfection efficiency (proportion of YFP positive cells). Wells transfected with 200 ng plasmid DNA showed high cytotoxicity. The 100 ng/well showed no visible cytotoxicity, an almost 100 % transfection efficiency based on presence of fluorescent cells, and a low variability of fluorescence intensities between single wells. The transfection efficiency decreased in correlation with lower amounts of plasmid DNA. In addition, lower plasmid DNA amounts led to increased variability. The relative release of WT was comparable for all settings, however with lower amounts of proviral plasmid DNA the WT:late(-) ratio decreased strongly from ~8 fold at 100 ng/well to only ~2.5 fold at 6.25 ng/well (Figure 4-6).

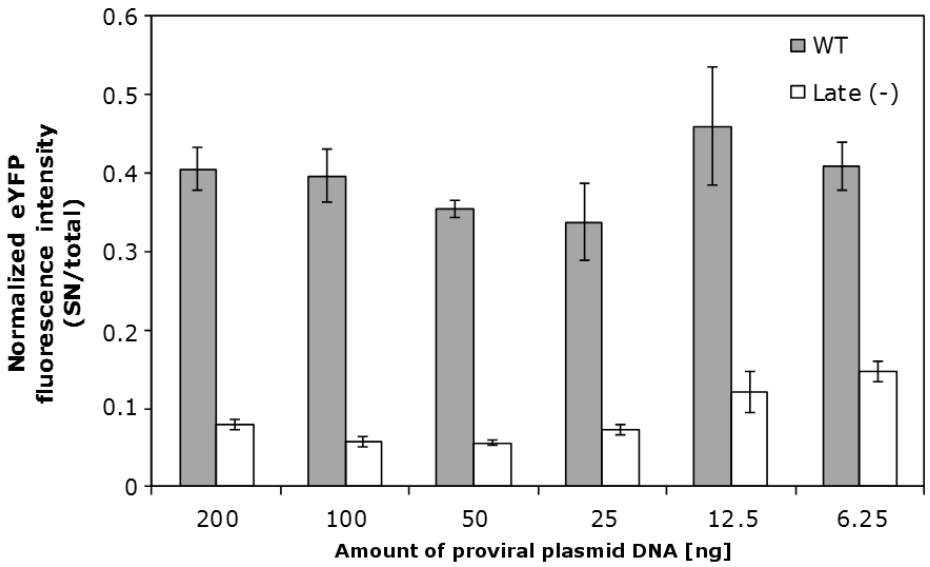

Figure 4-6 Best signal ratio of WT vs.-Late(-) control achieved with 100 ng proviral plasmid/well

293T cells in a 96-well plate were transfected with different amounts of proviral plasmid DNA. Either a 1:1 mixture of pCHIVeYFP:pCHIV (indicated as "WT) or a 1:1 mixture of the late domain deficient pCHIVeYFP.late(-): pCHIV.late(-)(indicated as "Late(-). Depicted are the normalized fluorescence intensities (SN/total, mean ± standard deviation). Relative release efficiency was comparable for WT between the different conditions. However, variability increased with lower plasmid amounts and the ratio of WT:late(-) diminished from ~8 fold for 100 ng/well to ~2.5 fold for 6.25 ng/well.

As it resulted in the optimal efficiency with no cytotoxicity and a good signal to control ratio of ~8 flog, 100 ng/well total proviral plasmid DNA were used for the screening assay. For the 384-well format, 25 ng/well in 25 µl medium were determined to be optimal.

Time point of sample collection

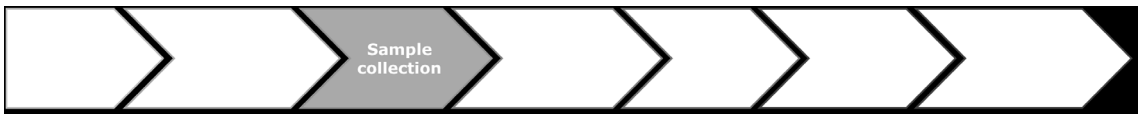

The next step was the determination of the appropriate sample collection time point after transfection. From previous experiments from our and Barbara Müller's group, it was known that first viral particles from the pcHIV plasmid are released ~24 hours post transfection. It was published that 33-36 hours post transfection would yield good results and a broad signal:control ratio (238). Shorter duration did not lead to sufficient production and release of viral particles, while more than 48 hours led to a decreased ratio of WT:late(-) presumably due to unspecific shedding of cellular content e.g. due to cell damage and death (238). In addition, very long time points are generally not suitable, as the starting cell density would have to be too low to yield good initial transfection rates with the siRNAs.

In order to optimize the signal intensity and the time point of sample collection for this specific assay, several time points around the published window of 33-36 hours post transfection were tested: namely 32, 38, and 44 hours. For this experiment, 15,000 293T cells were seeded per well. 30 hours after seeding the cells were transfected with "WT" or "Late(-)". Eight wells per conditions were tested. Cell lysates and supernatants were harvested after 32, 38, or 44 hours post transfection. Figure 4-7 shows the normalized fluorescence intensity (SN/total) as mean ± standard deviation.

In contrast to the published harvest time point of 33-36 hours post transfection, 44 hours yielded best results in this format. Both the relative

release (~0.35) as well as the WT:Late(-) ratio or 8 fold was best for this time point. As discussed above, later time points > 44 hours did result in decreasing WT : Late(-) ratios as expected (results not shown). From these experiments, 44 hours were determined as optimal duration from transfection to sample collection for the screening assay.

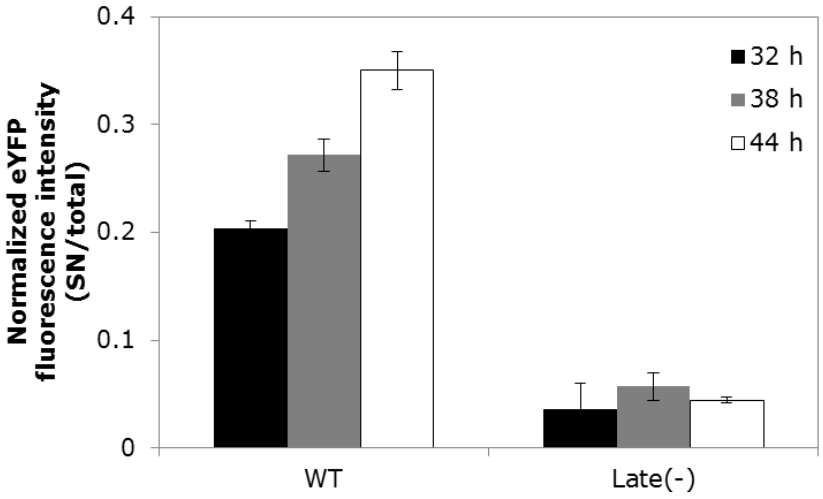

Figure 4-7 Harvest time of 44 hours yielded the best WT:Late (-) ratio
293T cells in a 96-well plate were transfected with different amounts of proviral plasmid DNA. Either a 1:1 mixture of pCHIVeYFP:pCHIV (indicated as "WT) or a 1:1 mixture of the late domain deficient pCHIVeYFP.late(-): pCHIV.late(-)(indicated as "Late(-). Supernatant and cell lysates were harvested at 32, 38 or 44 hours post transfection. Depicted is the normalized fluorescence intensity, calculated by division of supernatant intensity (SN) by total intensity in lysate and supernatant (total). Values are given as mean ± standard deviation. Relative release efficiency and the WT:Late(-) ratio was best for the 44 hour time point.

Signal detection

To ensure the best measurement of the peYFP signal in the collected cell lysates and supernatants, four different plate reader systems were tested: Tecan SAFIRE™, Tecan INFINITE™, Thermo VARIOSCAN™, and Mithras LB940.

For this experiment, 293T cells were seeded and transfected with "WT", "Late(-)", or peYFP with three wells per condition. The same samples were

measured with the four indicated plate readers and are depicted as mean ± standard deviation of the normalized fluorescence intensity in Figure 4-8.

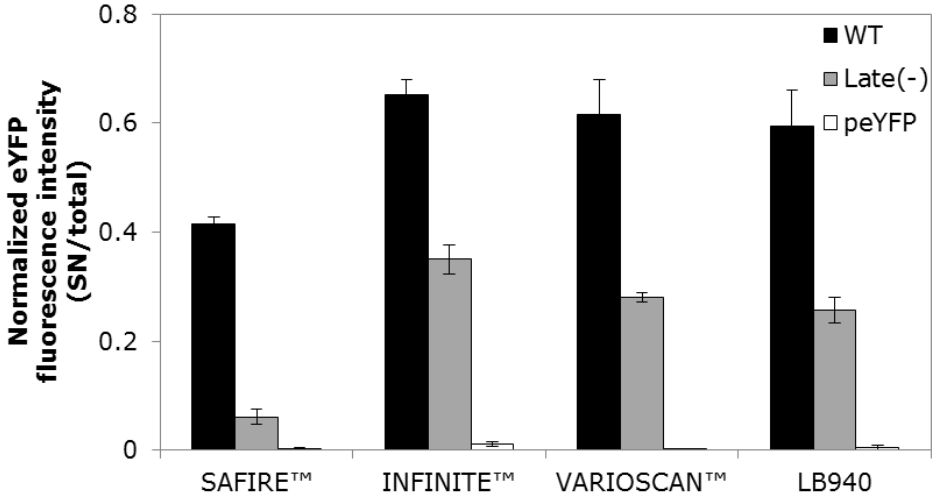

Figure 4-8 Comparison of different plate readers.
293T cells in a 96-well plate were transfected either a 1:1 mixture of pCHIVeYFP:pCHIV (indicated as "WT), a 1:1 mixture of the late domain deficient pCHIVeYFP.late(-): pCHIV.late(-) (indicated as "Late(-)") or peYFP. Supernatant and cell lysates were harvested at 44 hours post transfection. The same samples were measured with a TECAN SAFIRE™, TECAN INFINITE™, Thermo VARIOSCAN™, MITHRAS LB940. Depicted is the normalized fluorescence intensity, calculated by division of supernatant intensity by total intensity in lysate and supernatant (mean ± standard deviation).

The Tecan SAFIRE™ yielded the lowest relative release of the WT group (~0.4 vs. ~0.6). However, the Late(-) results were much higher for the other three devices, which diminishes the WT:Late(-) Signal:Control ratio. Albeit using the identical samples, all four plate reader gave out different values and especially the difference for the Late(-) group is remarkable. One option could be different sensitivities and the resulting different signal to noise ratios of the four devices. In order to test this hypothesis, the mean of the three WT values were divided by the mean of the 18 non transfected background wells for each of the devices. The signal to noise ratio differed greatly between all of the four devices as shown in Table 10. The Tecan SAFIRE™ excelled in this regard with a ratio of >40 fold while the MITHRAS LB940 yielded only a poor ratio of two fold.

Table 10 Signal to noise ratio of the different devices

Device	Signal:Background ratio
Tecan SAFIRE™	41
Tecan INFINITE™	15
Thermo Varioscan™	16
MITHRAS LB940	2

Not only the signal-to-background ratio is crucial for a successful assay. In addition, the width of the signal window between WT and the positive control Late(-) is of importance.

Table 11 lists the WT:Late(-) ratios for all four devices. The Tecan SAFIRE™ excelled here as well with a ratio of ~7 fold while all the other devices only had ratios of 2-3 fold. This is presumably caused by the much higher sensitivity of the Tecan SAFIRE™.

Table 11 Ratio of WT to Late(-) values

Device	WT:Late(-) ratio
Tecan SAFIRE™	7
Tecan INFINITE™	< 2
Thermo Varioscan™	3
MITHRAS LB940	2

Another important factor for the conduct of the complete screen was the duration of the measurement of one single plate. The time spans for one measurement are listed in Table 12. In this category the MITHRAS LB940 was best with less than 1 minute per plate while the Tecan SAFIRE™ took more than 30 minutes per plate. In this time the SAFIRE™ measured each well 4 times to yield more robust values while the MITHRAS LB940 measured only a single time. These results correlate inversely with the sensitivity of the devices.

Table 12 Time to measure one 96-well plate

Device	Time [minutes]
Tecan SAFIRE™	> 30
Tecan INFINITE™	12
Thermo Varioscan™	8
MITHRAS LB940	< 1

Although being the slowest of the test devices, the Tecan SAFIRE™ resulted in the most robust data with the best signal:noise and WT:Late(-) ratios, and the lowest variability. Because of these results, the SAFIRE™ was used for the screening assay.

Assay stability

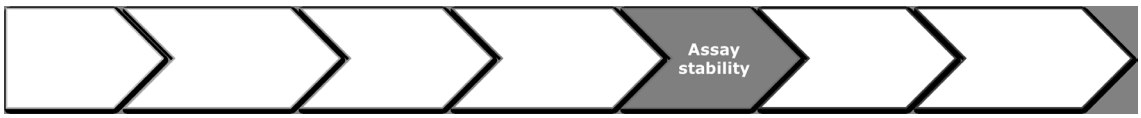

Another important part of the assay establishment is the testing for stability and robustness. Only with reproducible procedures, reliable results can be generated from a medium/high throughput screen. This means that results must be reproducible and constant between different replicates and that the results have to be constant regardless of the placing within the same plate. Especially the latter, the intra-plate variability, is crucial to ensure equal results throughout the plates in order to not falsely identify “hits” just based on their location on the plate. As the screening assay was established for 96- and for 384-well plates, both these points were addressed for both plate formats to demonstrate their usability.

For the 96-well format, 293T cells in 90 wells per plate were transfected with “WT”. Two wells per plate remained untransfected, two wells received the “Late(-)”, and two wells were transfected with peYFP. Fluorescence intensities were measures and normalized by dividing the supernatant intensity by the

total. Figure 4-9 shows the mean and standard deviation of the three replicates to illustrate the variation within a plate. The results show no statistical differences between single wells and low variability between the same wells on different plates. This indicates an equal measurement throughout the same plate and low inter- and intra-plate variability.

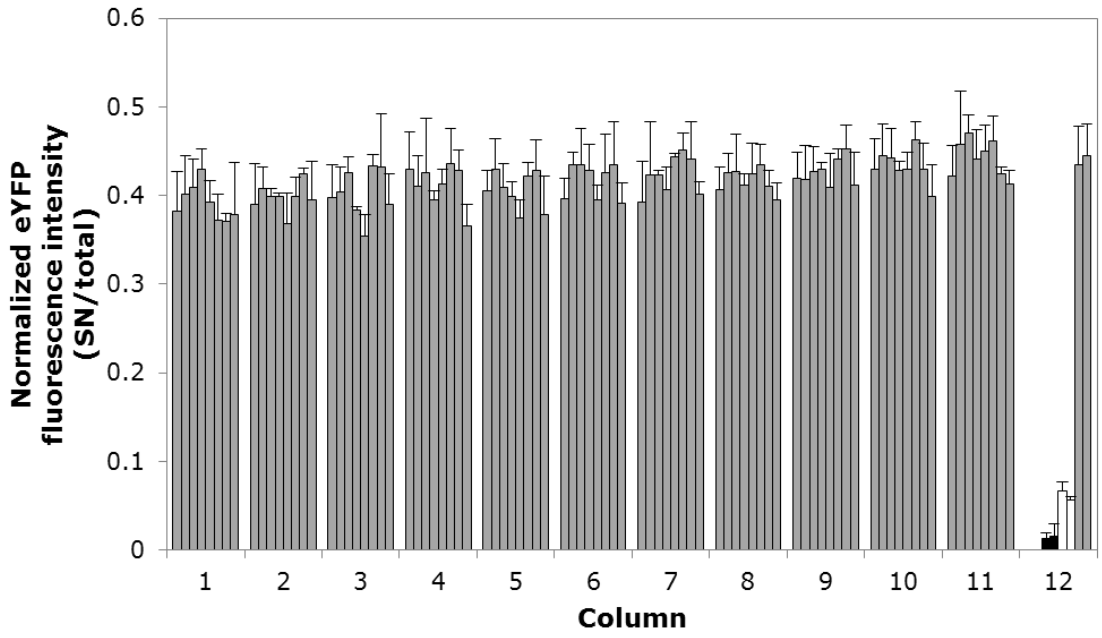

Figure 4-9 No significant differences detectable throughout a 96-well plate.
Three 96-well plates were transfected with a 1:1 mixture of pCHIV^{eYFP}:pCHIV (indicated as "WT", grey columns), the 1:1 mixture of the late domain deficient pCHIVeYFP.late(-): pCHIV.late(-) (indicated as "Late(-), white columns), or peYFP (black columns). The fluorescence intensity of both the cell lysates and the supernatants were measured. Depicted are the mean normalized fluorescence intensities of all 96 wells, calculated by division of supernatant intensity by total intensity in lysate and supernatant. (mean ± standard deviation). No statistical differences between any wells were detected.

For the 384-well format, 2,500 293T cells were seeded per well on three plates. 30 hours post seeding, 138 wells per plate were transfected with 25 ng of total plasmid DNA of a 1:1 mixture of pCHIVeYFP:pCHIV (indicated as "WT). 92 wells per plate received the 1:1 mixture of the late domain deficient pCHIVeYFP.late(-): pCHIV.late(-) (indicated as "Late(-)), and 138 wells were transfected with peYFP. 16 wells remained untransfected. Cell lysates and supernatants were collected at 44 hours post transfection and analyzed with the Tecan SAFIRE™ plate reader, as established previously. Fluorescence

intensities were normalized by dividing the supernatant intensity by the total. Figure 4-10 shows the mean and standard deviation of the three replicates to illustrate the variation within a plate. The results show no statistical differences between single wells and low variability between the same wells on different plates. This indicates an equal measurement throughout the same plate and low inter- and intra-plate variability. However, the 384-well plates yield a higher variance compared to the 96-well plates.

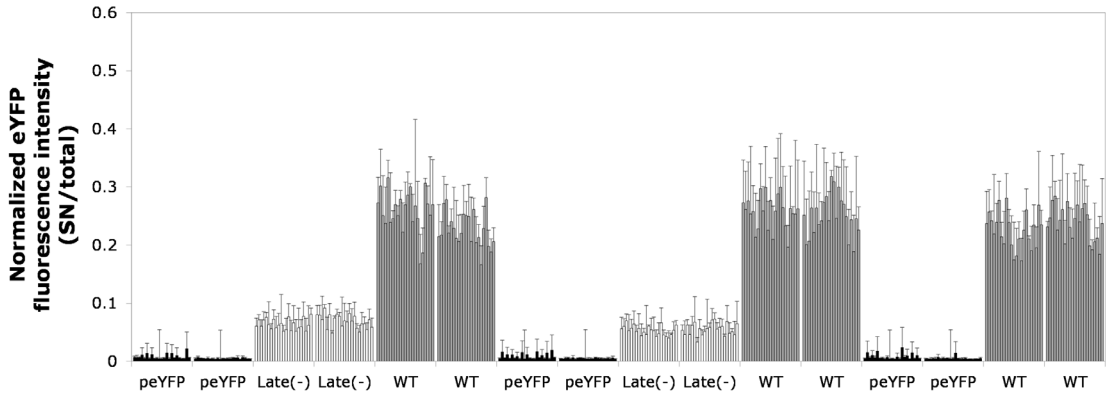

Figure 4-10 No significant differences detectable throughout a 384-well plate.
Three 384-well plates were transfected with a 1:1 mixture of pCHIVeYFP:pCHIV (indicated as "WT", grey columns), the 1:1 mixture of the late domain deficient pCHIVeYFP.late(-): pCHIV.late(-) (indicated as "Late(-), white columns), or peYFP (black columns). The fluorescence intensity of both the cell lysates and the supernatants were measured. Depicted is the normalized fluorescence intensity, calculated by division of supernatant intensity by total intensity in lysate and supernatant (mean ± standard deviation). No statistical differences between any wells were detected.

For a better comparison of the two plate formats, Figure 4-11 depicts the overall means for the 96- and the 384-well plates. Both formats were applicable for screening approaches. 96-well plates yielded in average a superior WT : Late(-) ratio of ~8 compared to a ratio of ~4 for the 384-well plates. In addition, the variances in the 96-well plates were smaller. On the other side, 384-well plates have the advantage to be used in high-throughput screens for e.g. genome wide screens. In order to compensate for the smaller signal window and the higher variance, more replicates have to be used for the 384-well plates.

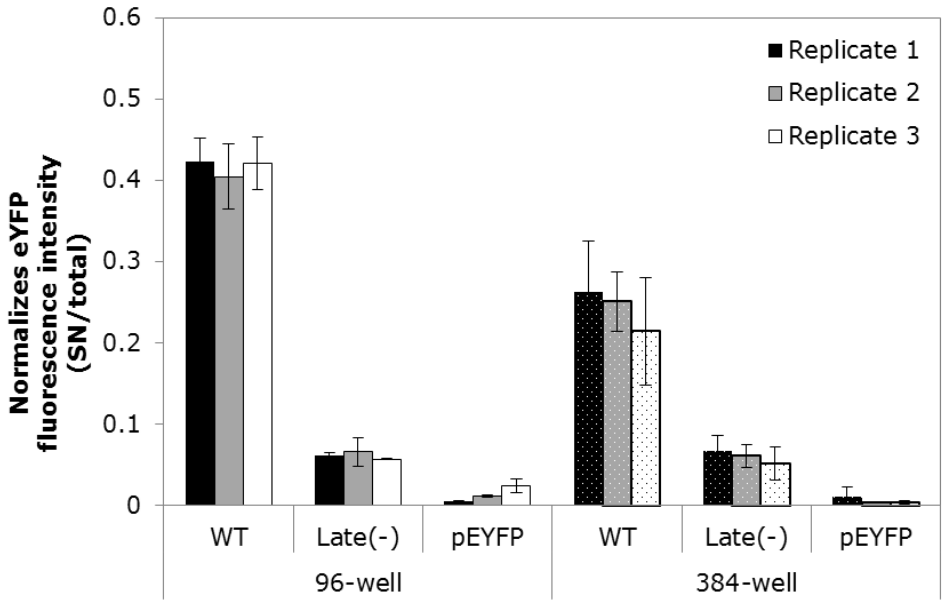

Figure 4-11 Low inter- and intra-plate variance
Depicted are the mean normalized fluorescence intensities of three 96-well and three 384-well plates (mean ± standard deviation). No statistical differences between any wells were detected.

A second experiment was conducted to address the question of the variability between replicates on a broader scale. It was conducted in collaboration with the group of Barbara Müller while applying the hereby described screening assay for testing a library of small chemical molecules to identify novel lead candidates for inhibition of HIV-1 assembly and release (results not shown). Control wells from 88 96-well plates from this compound screen were used for this comparison. Two wells per plate were transfected with a 1:1 mixture of pCHIV^{eYFP}:pCHIV (indicated as "WT") and two wells per plate with the 1:1 mixture of the late domain deficient pCHIV^{eYFP}.late(-): pCHIV.late(-) (indicated as "Late(-)"). Figure 4-12 shows the mean and standard deviation of the normalized eYFP fluorescence from all wells over the 176 wells. The low error bars indicate a very low inter-plate variability. In summary, the assay shows neither intra- nor inter-plate variability and is therefore suitable for mid- to high-throughput screening.

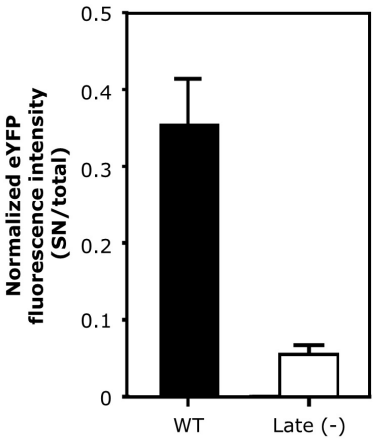

Figure 4-12 Very low inter-plate variability between 88 different 96-well plates. For each of 88 different 96-well plates two wells were transfected with a 1:1 mixture of pCHIV^{eYFP}:pCHIV (indicated as "WT") and two with a 1:1 ratio of pCHIV^{eYFP}.late(-): pCHIV.late(-) (indicated as "Late (-)") established in the previous experiments (total n = 176). The fluorescence intensity of both the cell lysates and the supernatants were measured. Depicted is the normalized fluorescence intensity, calculated by division of supernatant intensity by total intensity in lysate and supernatant (mean ± standard deviation). Figure from (238) and experiment conducted together with Barbara Müller, Maria Anders and Anke-Mareil Heuser.

Efficacy of controls

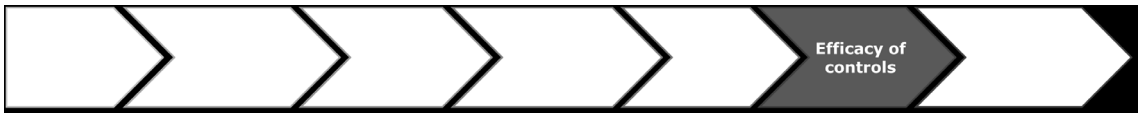

In parallel to addressing the technical questions, it is of similar importance to test appropriate controls to demonstrate the applicability of the assay. Preparation of the siRNA test plates and the complete library was performed in collaboration with the ViroQuant-CellNetworks RNAi Screening Facility headed by Dr. Holger Erfle and was based on their previously published method (269, 270).

At first, a siRNA targeting TSG101 (185) was tested. TSG101 is an important part of the cellular ESCRT complex required for the budding of HIV-1 particles. The wells of 96-well plates were pre-coated with the reverse transfection mixture including either a non-silencing control siRNA or a siRNA targeting TSG101 (indicated as "non-silencing control" and "siTSG101"). 15,000 293T cells/well were seeded into 96-well plates. 6, 18, and 36 hours post siRNA transfection, 96-wells were transfected with 100 ng of total plasmid DNA of a 1:1

mixture of pCHIV^{eYFP}:pCHIV (indicated as "WT") or with the 1:1 mixture of the late domain deficient pCHIV^{eYFP}.late(-): pCHIV.late(-) (indicated as "Late(-)") with eight wells each. Cell lysates and supernatants were collected at 44 hours post transfection and were analyzed with the Tecan SAFIRE™ platereader. In addition, cell lysates from an identical set of plates were collected to perform Western-Blot analysis of TSG101 protein expression after 24 and 48 hours post siRNA transfection. The results show that the reverse transfection with a siRNA targeting TSG101 significantly impairs the release of the newly formed viral particles (Figure 4-13). However, the relative release of the siTSG101 treated wells was higher than the results with the Late(-) construct. In addition it shows that TSG101 required a short incubation time to achieve an optimal knockdown (18 hours plus 44 hours = 62 hours). Western Blot analysis using an anti-TSG101 antibody shows the knockdown on protein level. Longer incubation led to marked cell toxicity (widefield microscopy, not shown) and increased fluorescence signals in the supernatant (Figure 4-13).

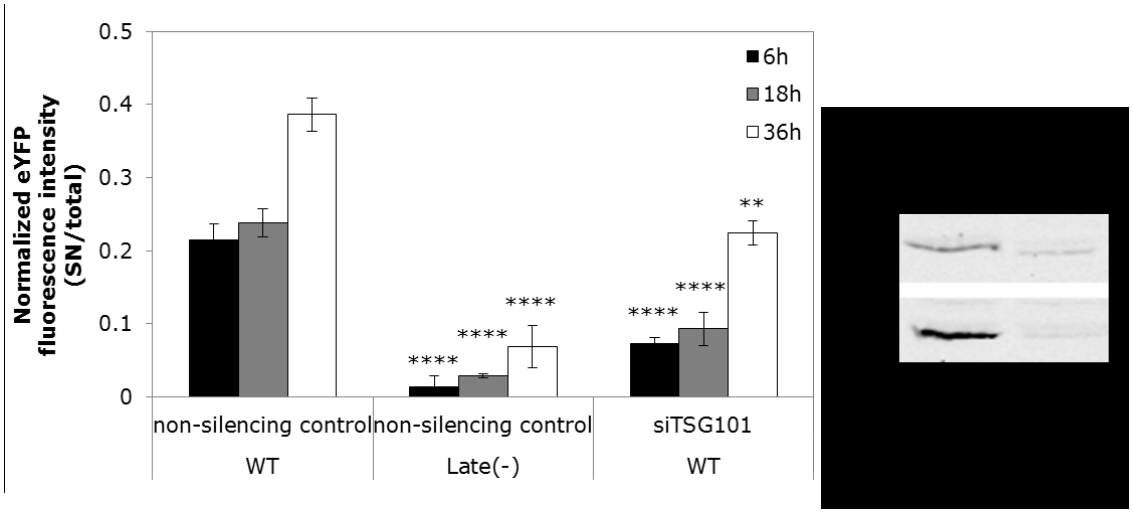

Figure 4-13 A siRNA against TSG101 is a suitable control to impair the release of viral particles by specific protein knockdown.
The wells of a 96-well plate were coated with the reverse transfection mix including a non-silencing control siRNA or a siRNA targeting TSG101 (siTSG101). 293T cells were transfected with 100 ng/well of proviral plasmid DNA. Either a 1:1 mixture of pCHIVeYFP:pCHIV (indicated as "WT) or a 1:1 mixture of the late domain deficient pCHIVeYFP.late(-): pCHIV.late(-) (indicated as "Late(-)). Supernatant and cell lysates were harvested at 44 hours post transfection. At 44 hours post transfection the cell lysates and supernatants were harvested and the fluorescence intensity was measured. Left: Normalized fluorescence intensity, calculated by division of supernatant intensity by total intensity in lysate and supernatant (mean ± standard deviation, n = 3). Right: Anti-TSG101 western blot of the cell lysates. Statistical analysis (one-sided ANOVA with Dunnett's multiple comparisons post-test, GraphPad Prism 6.05) compared to the respective WT result: ****= p<0.0001, ***= p<0.001, **= p<0.01, *= p<0.05, ns= not significant.

As a second positive control, siRNAs targeting the subunits A and B of the ATPase VPS4 were tested. As TSG101, VPS4 is involved in the ESCRT complex. The wells of 96-well plates were pre-coated with the reverse transfection mixture including either a non-silencing control siRNA or a siRNA mixture targeting VPS4A and VPS4B (indicated as "non-silencing control" and "siVPS4A/B"). Two different amounts of the siVPS4 A and B were tested (0.5 ng + 0.5 ng or 1 ng + 1 ng per 96-well, Qiagen Flexitube SI00760767 + SI00760802). 15,000 293T cells/well were seeded in the 96-well plates. 6, 18, and 36 hours post transfection, the wells were transfected with 100 ng of total plasmid of a 1:1 mixture of pCHIV^{eYFP}:pCHIV (indicated as "WT) or with the 1:1 mixture of the late domain deficient pCHIV^{eYFP}.late(-): pCHIV.late(-) (indicated as "Late(-)") with eight wells each. Cell lysates and supernatants were collected at 44 hours post transfection and were analyzed with the Tecan SAFIRE™ platereader. No effect on HIV-1 release was detectable at the earliest knockdown duration (6 hours) and only a slight reduction at 18 hours. The knockdown of VPS4A/B led to a ~50% decreased release of viral particles at the latest time points (Figure 4-14).

The results of this part show that knockdown of known host dependency factors indeed lead to a strong reduction of released viral particles using the eYFP readout. Protein turnover rates depend the time and duration of a knockdown. This can be seen as TSG101 showed highest efficacy at the shortest knockdown time point while the VPS4A/B knockdown only caused some reduction of release efficiency at the latest time point. Although the effect of siTSG101 was almost as pronounced as the effect of the Late(-) variant, it could not be used as a positive control in the kinase screen as it was not included in the pre-designed library.

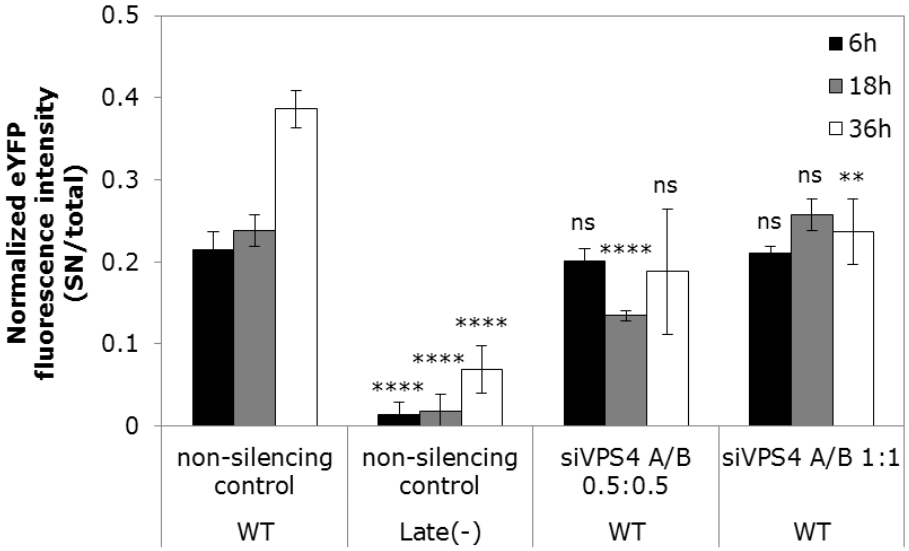

Figure 4-14 Knockdown of VPS4 leads to an impairment of HIV-1 viral particle release at 36 hours.
The wells of a 96-well plate were coated with the reverse transfection mix including a non-silencing control siRNA or a siRNA targeting VPS4 subunits A and B (siVPS4 A/B). 293T cells were seeded with 15,000 cells per well. The wells were transfected with 100 ng DNA/well at 6, 18, or 36 hours after seeding either with a 1:1 mixture of pCHIV^{eYFP}:pCHIV (indicated as "WT") or a 1:1 ratio of pCHIV^{eYFP}.late(-): pCHIV.late(-) (indicated as "Late (-)") with n = 3. At 44 hours post transfection the cell lysates and supernatants were harvested and the fluorescence intensity was measured. The graph shows the normalized fluorescence intensity, calculated by division of supernatant intensity by total intensity in lysate and supernatant (mean ± standard deviation). Statistical analysis (one-sided ANOVA with Dunnett's multiple comparisons post-test, GraphPad Prism 6.05) compared to the respective WT result: ****= p<0.0001, ***= p<0.001, **= p<0.01, *= p<0.05, ns= not significant.

Statistical & bioinformatical analysis

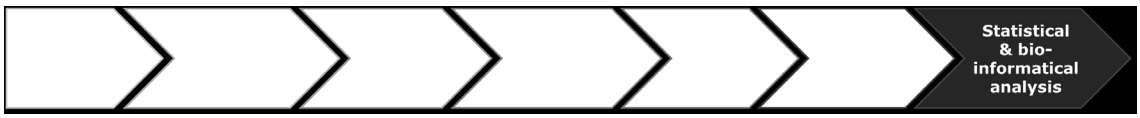

Raw data were exported from the plate reader into Microsoft EXCEL format. For single experiments, the raw values were analyzed manually. As discussed above, the raw eYFP fluorescence intensities were normalized to remove bias by e.g. cell numbers. For this, the intensities of the supernatant were divided by the sum of the supernatant and cell lysate fluorescence intensities using Microsoft Excel. Results for which this type of analysis was used are indicated by SN/total. For statistical analyses, GraphPad Prism (version 6.05) was used to calculate statistical significance values by using either

a t-test for comparison of two groups or a one-sided ANOVA with Dunnett's multiple comparisons post-test for multi-group experiments.

Manual analyses were not possible for the primary and reconfirmation screens. The Excel files were therefore transferred to the Viroquant Research Group Modeling lead by Dr. Lars Kaderali for statistical analysis and hit list generation (271, 274). The calculations were conducted by Johanna Mazur using R version 2.8.0 with a custom-tailored analysis workflow based on cellHTS and the Bioconductor package RNAither (271). As a first step the wells with the lowest 5 % of signal intensity in the cell lysate were discarded in order to exclude potential cytotoxic siRNAs. Then, instead of the manual normalization of the supernatant intensity divided by the total intensity, the locally weighted scatterplot smoothing (LOWESS) method (275) was applied for normalization of the raw eYFP fluorescence intensities. LOWESS is a very flexible non-parametric regression method which applies a low degree polynomial fit per data point. It is the most suitable method for normalization of complex non-linear data sets. This was followed by z-score normalization and p-value calculation. The resulting z-score is a measure to rank the results for each siRNA in the library in dependence of the individual standard deviation and allows comparing the results of different plates. The formula to calculate the z-score in the primary and reconfirmation screens are given below. With the assumption that the majority of siRNA have no effect of HIV-1 release, the z-scores were calculated in relation to the median of all wells in the primary screen. As this assumption is not true anymore in the reconfirmation screen, the z-scores were here calculated in relation to the non-silencing control siRNAs on each plate:

z-score calculation:

$$\text{Primary screen}: \frac{\text{Normalized intensity (well)} - \text{Median intensity (plate)}}{\text{Median of the standard deviation (plate)}}$$

$$\text{Reconfirmation screen}: \frac{\text{Normalized intensity (well)} - \text{Median intensity (non - silencing siRNAs)}}{\text{Median of the standard deviation (non - silencing siRNAs)}}$$

After receiving the hit lists, threshold criteria were defined together with the biostatisticians. For stringent hit definition two thresholds were defined for the results of the primary and the reconfirmation screen. Based on the experience with other siRNA screens and according to the range of z-scores resulting from this kinase screen, a cut-off threshold of z-score ± 2 was chosen. A second threshold of p-value ≤ 0.05 was applied additionally in order to take the reproducibility and variance of the different replicates into account.

After the definition of the final set of hits after the analysis of the reconfirmation screen, biostatistical pathway analyses were performed with publicly available tools.
Enriched biological properties, for example Gene Ontology (GO) terms, were identified to determine enriched functional-related gene groups and networks. Two open source dataset tools for large-scale datasets were used according to the description on the respective websites:

- Database for Annotation, Visualization and Integrated Discovery (DAVID v6.8, http://david.abcc.ncifcrf.gov/, (276-279))
- Kyoto Encyclopedia of Genes and Genomes (KEGG, http://www.genome.jp/kegg/mapper.html, (280-282))

4.2 Primary siRNA screen

After successful establishment of the screening assay, a siRNA library was tested to identify host cell factors involved in the replication and release of HIV-1. The library comprised siRNAs against 724 human proteins including mainly all known kinases and some auxiliary proteins interacting with those kinases. The library was a custom-made library manufactured by Ambion and designed by the group of Dr. Holger Erfle (BioQuant, University of Heidelberg, Germany). All gene symbols, RefSeq identification numbers and siRNA IDs are listed in chapter 12.1 Appendix 1. Three different siRNAs directed against each of the targets were included in the siRNA library. The siRNAs were randomly distributed onto 28 different 96-well plates plus one control plate. The complete

set of plates was screened in triplicates – which led to a total sum of 87 different 96-well plates. All 96-well plates were prepared in advance by coating of the siRNA libraries. In brief, siRNAs, the transfection reagent, and fibronectin were mixed and added to a well of a 96-well plate prior to drying in a miVac Modular Concentrator (Wolf Laboratories) (269, 270). All stock solutions (e.g. cell suspensions or transfection mixtures) were prepared in ample quantity for the complete set of 87 plates to ensure even and homogenous distribution.

All steps from cell seeding, transfection, sample collection and analysis were performed in parallel at the same time for the complete screening library as described above. On the day of the experimental start, cells were harvested and a stock cell suspension was prepared in a sufficient volume to be distributed to all plates of the screen at the same time. Then, 15,000 293T cells/96-well were seeded in 100 µl cell culture medium using the automated Multi Drop® Combi Reagent Dispenser (Thermo Fisher). After 30 hours, the supernatant was removed from the plates and 100 µl/96-well of the pCHIV^{eYFP}:pCHIV transfection mixture was added to each well using again the Multi Drop® Combi.

In addition, three additional 96-well plates were used as controls. The reason was to monitor whether the time point of plate treatment would have an influence on the results. For this, the first control plate was treated as the very first plate at cell seeding and distribution of the transfection mixture. The second was treated (seeding and transfection) after the first 42 of the 84 plates of the complete library and the third control plate as the very last plate of the screen. For the three control plates, both the bulk preparations of the cell suspension and the pCHIV^{eYFP}:pCHIV (indicated as “WT”) transfection mixture was used as for the other 84 plates of the library. A second quality check to be addressed by the three control plates was to test the WT:Late(-) ratio under medium-throughput screening conditions. Therefore each of the three control plates contained wells transfected with pCHIV^{eYFP}.late(-): pCHIV.late(-) (indicated as “Late(-)”) as control. Three wells for each the WT and the Late(-) were used per control plate.

Approximately 42 hours post transfection, the supernatants were harvested using the Matrix Hydra® DT automated liquid handling platform (Thermo Fisher) and transferred to separate 96-well plates. The residual supernatant over the cells was discarded and 100 µl/96-well lysis buffer were added to generate cell lysate suspensions. All plates were then frozen at -20 °C until measurement. Figure 4-15 shows all 174 96-well plates (87 plates supernatant + 87 plates cell lysates).

Figure 4-15 Image of the 174 96-well plates
The complete screen comprised of 87 96-well plates containing the harvested supernatant and another 87 96-well plates with the cell lysates. All plates were frozen at -20 °C and batch-wise thawn for measurement in the Tecan SAFIRE™ platereader.

Fluorescence intensities of the cell lysate supernatant plates were subsequently measured with the Tecan SAFIRE™ (Thermo Fisher). Resulting raw fluorescence signal intensities were automatically exported to Microsoft Excel. The analysis for the control plates were conducted manually in Microsoft Excel and the normalized fluorescence intensities (SN/total) for each of the three are shown in Figure 4-16. The comparison of the WT intensity to the Late(-) results yielded a signal-to-control ratio of ~8 fold with very small standard deviations. This was consistent with the results from the establishment phase. As the plates were transfected at the beginning, mid and end of the library, the comparable results from these three plates indicate that the distribution of the bulk cell suspension and transfection mixture was homogenous and did not cause any time-dependent gradient of the results.

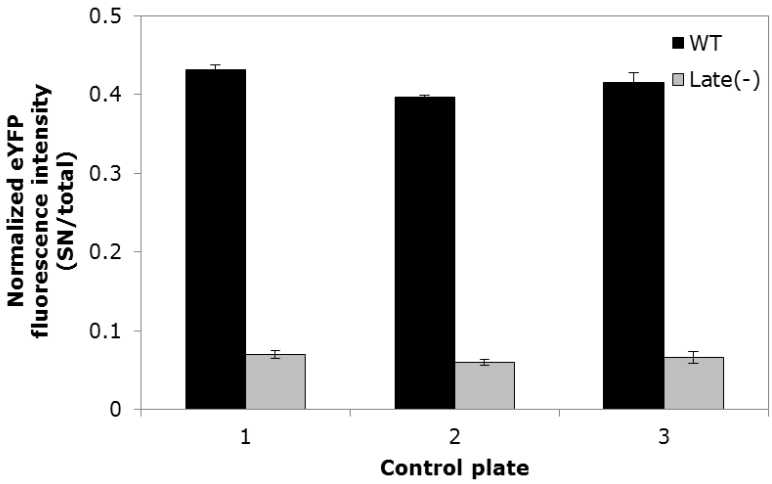

Figure 4-16 Quality controls confirmed validity and low variation of the primary screen.
293T cells were seeded into three 96-well control plates with 15,000 cells per well. The wells were transfected with 100 ng DNA/well at 30 hours after seeding either with a 1:1 mixture of pCHIV^{eYFP}:pCHIV (indicated as "WT", wild type) or a 1:1 ratio of pCHIV^{eYFP}.late(-): pCHIV.late(-) (indicated as "Late (-)") with n = 3. At 44 hours post transfection the cell lysates and supernatants were harvested and the fluorescence intensity was measured. All results were comparable and showed very small standard deviation. Depicted is the normalized fluorescence intensity, calculated by division of supernatant intensity by total intensity in lysate and supernatant (mean ± standard deviation).

The raw data were then transferred to the group of Dr. Lars Kaderali for statistical analysis as described above. Figure 4-17 shows the raw eYFP intensities of the cell lysates (left) and the supernatants (right) for each of the three replicates. For each replicate, the 28 different plates are depicted as box plots. The black line indicates the median intensity of all wells of the 28 96-well plates per replicate. The median intensities and distributions/variations of the intensities of three replicates (size of box and whiskers with only a few outliers) were equal, indicating a very homogenous distribution over all plates of the screen.

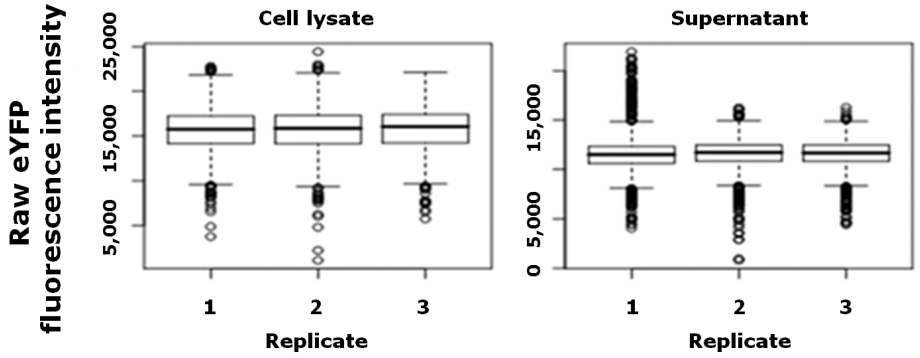

Figure 4-17 Comparable distribution of raw eYFP intensities between the different replicates of the screen.
Depicted in this graph are box plots of the raw eYFP intensities of cell lysates (left) and supernatants (right). The box plots include the raw intensity values for all wells of the 28 96-well plates per replicate. The black bar indicates the median, the box the first and third quartiles, the whiskers indicate the 1.5 inter quartile range and the open dots show single outliers. Both the median intensity and the variability (box and whiskers) are equal in the different replicates, indicating a high homogeneity. Figure created by Johanna Mazur and Lars Kaderali using R during the process of statistical analysis of my experimental results.

After sample measurement the raw data underwent statistical data analysis and normalization as discussed above. In short, the 5% wells with lowest cell lysate intensity were removed to exclude potential cytotoxic effects, followed by normalization of the raw eYFP fluorescence intensities over all plates and the calculation of z-score and p-values for ranking and hit definition. From the results, all siRNAs were defined as a hit when they a) had a z-score of > +2 or< -2 and b) had a p-value < 0.05 to take the reproducibility between the replicates into account. Figure 4-18 depicts the distribution of the z-scores over all siRNAs in the screen. The red and the green vertical lines indicate the threshold of z-score ≤ -2 (red) or z-score ≥ +2 (green), respectively. Z-scores of ≤ -2 indicate a reduced release of viral particles and were defined as potential host dependency factors (HDF). At the other end of the distribution curve, all siRNAs with a z-score of ≥ +2 were defined as potential host restriction factors (HRF). The statistical analyses of the raw values were performed by Johanna Mazur and Lars Kaderali to generate the z-scores, which are shown in Figure 4-18 and Table 13 List of the 50 potential host dependency factors.Table 13 to Table 16.

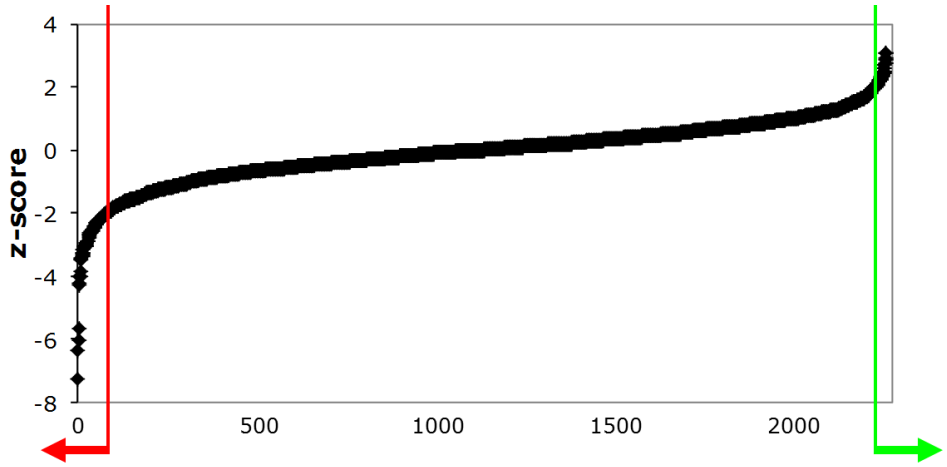

Figure 4-18 Distribution of all z-scores
Shown is the distribution of all z-scores for all individual sample of the kinase screen. Values below or equal to a z-score ≤-2 were defined as potential host dependency factors (left side, red arrow). Potential host restriction factors were above the threshold of a z-score ≥ 2 (right side, green arrow). In addition to the z-score criterion all hits have to comply with the additional threshold of p-value ≤ 0.05.

Table 13 lists all 50 potential HDFs with at least one of the three siRNAs fulfilling the aforementioned thresholds. The table lists the gene symbol, the RefSeq ID, the full gene name, the maximum z-score and the number of siRNAs reaching the threshold criteria. Only those siRNA were counted as a hit when they had a p-value below 0.05. The majority of those potential HDFs scored with one of the three individual siRNAs. Out of the 50, only three genes scored as hits with 2 of the three individual siRNAs and none with all three. Those three hits were Nemo-like kinase (NLK), Cyclin-dependent kinase 7 (CDK7) and PAS domain containing serine/threonine kinase (PASK).

Table 13 List of the 50 potential host dependency factors.
Hit definition threshold: Minimum one siRNA yielding a z-score ≤ -2 (sorted by z-score). All hits comply with the second threshold of p < 0.05. Indicated in grey are the hits with more than one siRNA fulfilling the threshold.

Gene Symbol	RefSeq ID	Full gene name	Max. z-score	No. of siRNAs out of 3 > threshold
KSR2	NM_173598	Kinase suppressor of ras 2	-8.456	1/3
PRKG2	NM_006259	Protein kinase, cGMP-dependent, type II	-4.387	1/3
ITPKA	NM_002220	Inositol 1,4,5-trisphosphate 3-kinase A	-4.064	1/3

Gene Symbol	RefSeq ID	Full gene name	Max. z-score	No. of siRNAs out of 3 > threshold
PLXNA3	NM_017514	Plexin A3	-3.993	1/3
NLK	NM_016231	Nemo-like kinase	-3.703	2/3
PAPSS1	NM_005443	3'-phosphoadenosine 5'-phosphosulfate synthase 1	-3.469	1/3
PRPS1	NM_002764	Phosphoribosyl pyrophosphate synthetase 1	-3.350	1/3
PLXNC1	NM_005761	Plexin C1	-3.325	1/3
EPHA10	NM_001004338	EPH receptor A10	-3.325	1/3
PAPSS2	NM_001015880	3'-phosphoadenosine 5'-phosphosulfate synthase 2	-3.111	1/3
AKAP8L	NM_014371	A kinase (PRKA) anchor protein 8-like	-2.952	1/3
CDK6	NM_001259	Cyclin-dependent kinase 6	-2.870	1/3
CDK7	NM_001799	Cyclin-dependent kinase 7	-2.846	2/3
GLYCTK	NM_145262	Glycerate kinase	-2.770	1/3
MAP4K2	NM_004579	Mitogen-activated protein kinase kinase kinase kinase 2	-2.728	1/3
FES	NM_002005	Feline sarcoma oncogene	-2.707	1/3
MAP2K3	NM_002756	Mitogen-activated protein kinase kinase 3	-2.696	1/3
RPS6KA2	NM_001006932	Ribosomal protein S6 kinase, 90kDa, polypeptide 2	-2.660	1/3
MAP3K14	NM_003954	Mitogen-activated protein kinase kinase kinase 14	-2.613	1/3
PXK	NM_017771	PX domain containing serine/threonine kinase	-2.583	1/3
NME1	NM_000269	NME/NM23 nucleoside diphosphate kinase 1	-2.580	1/3
NRGN	NM_006176	Neurogranin (protein kinase C substrate, RC3)	-2.504	1/3
STK32B	NM_018401	Serine/threonine kinase 32B	-2.503	1/3
AKAP7	NM_004842	A kinase (PRKA) anchor protein 7	-2.421	1/3
MAST4	NM_198828	Microtubule associated serine/threonine kinase family member 4	-2.404	1/3
CDK10	NM_052987	Cyclin-dependent kinase 10	-2.390	1/3

Gene Symbol	RefSeq ID	Full gene name	Max. z-score	No. of siRNAs out of 3 > threshold
SPHK1	NM_021972	Sphingosine kinase 1	-2.375	1/3
SPHK2	NM_020126	Sphingosine kinase 2	-2.350	1/3
IRAK4	NM_016123	Interleukin-1 receptor-associated kinase 4	-2.325	1/3
SLK	NM_014720	STE20-like kinase (yeast)	-2.320	1/3
RPS6KB1	NM_003161	Ribosomal protein S6 kinase, 70kDa, polypeptide 1	-2.312	1/3
PTK6	NM_005975	PTK6 protein tyrosine kinase 6	-2.288	1/3
PASK	NM_015148	PAS domain containing serine/threonine kinase	-2.254	2/3
HKDC1	NM_025130	Hexokinase domain containing 1	-2.207	1/3
UCK2	NM_012474	Uridine-cytidine kinase 2	-2.207	1/3
RIPK3	NM_006871	Receptor-interacting serine-threonine kinase 3	-2.202	1/3
CDKL1	NM_004196	Cyclin-dependent kinase-like 1 (CDC2-related kinase)	-2.133	1/3
PIK3CG	NM_002649	Phosphoinositide-3-kinase, catalytic, gamma polypeptide	-2.126	1/3
PLXNA2	NM_025179	Plexin A2	-2.125	1/3
BRAF	NM_004333	V-raf murine sarcoma viral oncogene homolog B1	-2.116	1/3
EPHB4	NM_004444	EPH receptor B4	-2.104	1/3
FRK	NM_002031	Fyn-related kinase	-2.100	1/3
DCAKD	NM_024819	Dephospho-CoA kinase domain containing	-2.099	1/3
IGF1R	NM_000875	Insulin-like growth factor 1 receptor	-2.080	1/3
ALPK3	NM_020778	Alpha-kinase 3	-2.078	1/3
FGFR2	NM_000141	Fibroblast growth factor receptor 2 (bacteria-expressed kinase, keratinocyte growth factor receptor, craniofacial dysostosis 1, Crouzon syndrome, Pfeiffer syndrome, Jackson-Weiss syndrome)	-2.064	1/3
PIM1	NM_002648	Pim-1 oncogene	-2.055	1/3

Gene Symbol	RefSeq ID	Full gene name	Max. z-score	No. of siRNAs out of 3 > threshold
SGK269	XM_370878	NKF3 kinase family member	-2.046	1/3
ROR1	NM_001083592	Receptor tyrosine kinase-like orphan receptor 1	-2.008	1/3
NAGK	NM_017567	N-acetylglucosamine kinase	-2.003	1/3

26 potential HRFs fulfilled with at least one of the three siRNAs the threshold of z-score > +2 and p-value < 0.05. Similar to the table above, Table 14 lists the gene symbol, the RefSeq ID, the full gene name, the maximum z-score and the number of siRNAs reaching the threshold criteria for each of those 26 genes. Similar to the HDFs, the majority of the potential HRFs scored with only one of the three individual siRNAs. Out of the 26, only one gene scored as hit with 2 of the three individual siRNAs and none with all three. This hit was C-src tyrosine kinase (CSK).

Table 14 List of the 26 potential host restriction factors.
Hit definition threshold: Minimum one siRNA yielding a z-score > +2 (sorted by z-score). All hits comply with the second threshold of p < 0.05. Indicated in grey are the hits with more than one siRNA fulfilling the threshold.

Gene Symbol	RefSeq ID	Full gene name	Max. z-score	No. of siRNAs out of 3 > threshold
MAPK3	NM_001040056	Mitogen-activated protein kinase 3	3.210	1/3
SYK	NM_003177	Spleen tyrosine kinase	3.110	1/3
NRK	NM_198465	Nik related kinase	3.088	1/3
GSK3B	NM_002093	Glycogen synthase kinase 3 beta	3.078	1/3
TAF1L	NM_153809	TAF1 RNA polymerase II, TATA box binding protein (TBP)-associated factor, 210kDa-like	3.042	1/3
MAP4K4	NM_004834	Mitogen-activated protein kinase kinase kinase kinase 4	2.984	1/3
GAK	NM_005255	Cyclin G associated kinase	2.958	1/3
PSKH1	NM_006742	Protein serine kinase H1	2.810	1/3

Gene Symbol	RefSeq ID	Full gene name	Max. z-score	No. of siRNAs out of 3 > threshold
CSK	NM_004383	C-src tyrosine kinase	2.727	2/3
SNF1LK2	NM_015191	SNF1-like kinase 2	2.631	1/3
LIMK1	NM_002314	LIM domain kinase 1	2.604	1/3
BLK	NM_001715	B lymphoid tyrosine kinase	2.530	1/3
DGKH	NM_152910	Diacylglycerol kinase, eta	2.374	1/3
FGFR4	NM_002011	Fibroblast growth factor receptor 4	2.330	1/3
GRK4	NM_001004056	G protein-coupled receptor kinase 4	2.328	1/3
AURKAIP 1	NM_017900	Aurora kinase A interacting protein 1	2.304	1/3
MAP4K1	NM_001042600	Mitogen-activated protein kinase kinase kinase kinase 1	2.274	1/3
STK16	NM_001008910	Serine/threonine kinase 16	2.215	1/3
ACVR2A	NM_001616	Activin A receptor, type IIA	2.172	1/3
IPMK	NM_152230	Inositol polyphosphate multikinase	2.150	1/3
CD2	NM_001767	CD2 molecule	2.149	1/3
CDK4	NM_000075	Cyclin-dependent kinase 4	2.128	1/3
ILK	NM_001014794	Integrin-linked kinase	2.109	1/3
RBKS	NM_022128	Ribokinase	2.099	1/3
PLK2	NM_006622	Polo-like kinase 2 (Drosophila)	2.093	1/3
BRSK2	NM_003957	BR serine/threonine kinase 2	2.015	1/3

4.3 Reconfirmation screen

Having the risk of false-positive hits arising from any screening approach in mind, a subsequent reconfirmation screen was performed. For this all 76 primary hits (50 potential host dependency factors and 26 potential host restriction factors) listed above were tested again for re-validation. For each of

the hits, three new siRNAs were ordered from Ambion which were distinct from the siRNAs used in the primary screen. This was to exclude potential off-target effects caused if a siRNAs used in the primary screen would have been bound to an unspecific off-target gene. While the siRNAs in the primary screen library were normal Ambion Silencer® siRNAs, chemically modified Silencer® Select siRNAs (Ambion) were used in the reconfirmation screen.

The three siRNAs per hit gene were distributed onto 5 different 96-well plates as described above. As only a small fraction of siRNAs were tested in this screen, several improvements in regard to statistical power and quality could be included which were not possible for the big screen. To improve the quality, no siRNAs were used on the edge wells in order to avoid potential edge effects on cell growth. To increase the robustness of the reconfirmation screen, each of the 96-well plates was tested with five replicates (compared to the three replicates in the primary screen). The complete experimental procedure was similar to the primary screen. The only difference was in the statistical analysis: For the primary screen LOWESS normalization the median fluorescence intensity was used. This was possible under the assumption that the majority of siRNAs in the library would have no effect on HIV-1 release. This assumption is, however, by definition not true for the reconfirmation screen. Therefore each plate contained 9x the non-silencing siRNA randomly distributed and the results were normalized to the median result of these control siRNAs. After measurement of the raw fluorescence intensities and statistical analyses, the similar thresholds were used as criteria for hit definition for the reconfirmation screen as for the primary screen (z-score $\leq$ -2 or z-score $\geq$ +2, p-value $<$ 0.05). From the complete set of 76 primary hits, 43 were reconfirmed which equals a reconfirmation rate of ~57%. Interestingly, the reconfirmation rate was not equal for host dependency or restriction factors.

Out of the 50 primary HDFs, 39 were validated. This equaled a reconfirmation rate of approximately ~78%. Of note, all three HDFs from the primary screen with more than one siRNA fulfilling the hit criterion were reconfirmed in this second screen. The reconfirmed HDF with the highest z-score was Sphingosine kinase 1 (SPHK1) with a z-score of -8.024. Out of the 43

reconfirmed hits, 15 were reconfirmed with two of the three individual siRNAs and one gene even with all three siRNAs (3'-phosphoadenosine 5'-phosphosulfate synthase 1, PAPSS1). These 16 hits and the three hits from the primary screen were categorized as "Strong HDFs". The "Strong HDF" with the highest z-score of -7.910 was Neurogranin (NRGN). Table 15 lists the 39 confirmed host dependency factors sorted by their maximum z-score. In addition, the table indicates the gene symbol, the RefSeq ID, the full gene name, and the number of individual siRNAs from the three siRNAs used in the primary and the three from the reconfirmation screen which reached the threshold.

Table 15 List of the 39 reconfirmed host dependency factors.
Hit definition threshold: Minimum one siRNA yielding a z-score > +2 (sorted by z-score). All hits comply with the second threshold of $p < 0.05$. "Strong HDFs" are indicated in grey.

Gene Symbol	RefSeq ID	Full gene name	Max. z-score (primary)	Max. z-score (reconfirm.)	no. siRNA primary + reconfirm. above threshold
SPHK1	NM_021972	Sphingosine kinase 1	-2.375	-8.024	1/3 + 1/3
NRGN	NM_006176	Neurogranin (protein kinase C substrate, RC3)	-2.504	-7.910	1/3 + 2/3
PLXNA2	NM_025179	Plexin A2	-2.125	-7.067	1/3 + 1/3
MAP3K14	NM_003954	Mitogen-activated protein kinase kinase kinase 14	-2.613	-6.539	1/3 + 2/3
PAPSS1	NM_005443	3'-phosphoadenosine 5'-phosphosulfate synthase 1	-3.469	-5.492	1/3 + 3/3
GLYCTK	NM_145262	Glycerate kinase	-2.770	-4.611	1/3 + 2/3
PLXNC1	NM_005761	Plexin C1	-3.325	-4.544	1/3 + 1/3
UCK2	NM_012474	Uridine-cytidine kinase 2	-2.207	-4.141	1/3 + 2/3
NME1	NM_000269	NME/NM23 nucleoside diphosphate kinase 1	-2.580	-3.988	1/3 + 1/3
PIK3CG	NM_002649	Phosphoinositide-3-kinase, catalytic, gamma polypeptide	-2.126	-3.892	1/3 + 1/3
CDK10	NM_052987	Cyclin-dependent kinase 10	-2.390	-3.863	1/3 + 2/3
AKAP7	NM_004842	A kinase (PRKA) anchor protein 7	-2.421	-3.815	1/3 + 1/3
PXK	NM_017771	PX domain containing serine/threonine kinase	-2.583	-3.801	1/3 + 1/3

Gene Symbol	RefSeq ID	Full gene name	Max. z-score (primary)	Max. z-score (reconfirm.)	no. siRNA primary + reconfirm. above threshold
ITPKA	NM_002220	Inositol 1,4,5-trisphosphate 3-kinase A	-4.064	-3.761	1/3 + 1/3
RPS6KA2	NM_001006932	Ribosomal protein S6 kinase, 90kDa, polypeptide 2	-2.660	-3.673	1/3 + 1/3
FRK	NM_002031	Fyn-related kinase	-2.100	-3.612	1/3 + 2/3
CDK7	NM_001799	Cyclin-dependent kinase 7	-2.846	-3.563	2/3 + 1/3
KSR2	NM_173598	Kinase suppressor of ras 2	-8.456	-3.559	1/3 + 1/3
MAP2K3	NM_002756	Mitogen-activated protein kinase kinase 3	-2.696	-3.441	1/3 + 1/3
PASK	NM_015148	PAS domain containing serine/threonine kinase	-2.254	-3.405	2/3 + 1/3
STK32B	NM_018401	Serine/threonine kinase 32B	-2.503	-3.391	1/3 + 2/3
FGFR2	NM_000141	Fibroblast growth factor receptor 2 (bacteria-expressed kinase, keratinocyte growth factor receptor, craniofacial dysostosis 1, Crouzon syndrome, Pfeiffer syndrome, Jackson-Weiss syndrome)	-2.064	-3.381	1/3 + 2/3
IRAK4	NM_016123	Interleukin-1 receptor-associated kinase 4	-2.325	-3.010	1/3 + 2/3
NLK	NM_016231	Nemo-like kinase	-3.703	-2.998	2/3 + 1/3
BRAF	NM_004333	V-raf murine sarcoma viral oncogene homolog B1	-2.116	-2.892	1/3 + 1/3
PRKG2	NM_006259	Protein kinase, cGMP-dependent, type II	-4.387	-2.837	1/3 + 2/3
IGF1R	NM_000875	Insulin-like growth factor 1 receptor	-2.080	-2.791	1/3 + 2/3
FES	NM_002005	Feline sarcoma oncogene	-2.707	-2.676	1/3 + 1/3
MAP4K2	NM_004579	Mitogen-activated protein kinase kinase kinase kinase 2	-2.728	-2.617	1/3 + 2/3
RPS6KB1	NM_003161	Ribosomal protein S6 kinase, 70kDa, polypeptide 1	-2.312	-2.606	1/3 + 2/3
SPHK2	NM_020126	Sphingosine kinase 2	-2.350	-2.554	1/3 + 1/3
DCAKD	NM_024819	Dephospho-CoA kinase domain containing	-2.099	-2.524	1/3 + 1/3
CDKL1	NM_004196	Cyclin-dependent kinase-like 1 (CDC2-related kinase)	-2.133	-2.407	1/3 + 2/3
PIM1	NM_002648	Pim-1 oncogene	-2.055	-2.317	1/3 + 1/3

Gene Symbol	RefSeq ID	Full gene name	Max. z-score (primary)	Max. z-score (reconfirm.)	no. siRNA primary + reconfirm. above threshold
NAGK	NM_017567	N-acetylglucosamine kinase	-2.003	-2.277	1/3 + 1/3
ALPK3	NM_020778	Alpha-kinase 3	-2.078	-2.252	1/3 + 1/3
HKDC1	NM_025130	Hexokinase domain containing 1	-2.207	-2.131	1/3 + 2/3
MAST4	NM_198828	Microtubule associated serine/threonine kinase family member 4	-2.404	-2.049	1/3 + 1/3
SGK269	XM_370878	NKF3 kinase family member	-2.046	-2.015	1/3 + 1/3

From the 26 potential HRFs, only 4 could be validated. This equals a reconfirmation rate of approximately 15%. Of note, the HRF from the primary screen with more than one siRNA fulfilling the hit criterion (CSK) was reconfirmed in this second screen. In addition, it was the hit with the top z-score of +4.936 in the reconfirmation screen. Out of the 26 reconfirmed HRFs, none scored with more than one of the siRNAs. Therefore only CSK was defined as "Strong HRF" based on the two scoring siRNAs from the primary screen. Table 16 lists the four confirmed host dependency factors sorted by their maximum z-score. In addition, the table indicates the gene symbol, the RefSeq ID, the full gene name, and the number of individual siRNAs from the three siRNAs used in the primary and the three from the reconfirmation screen which reached the threshold.

Table 16 List of the 4 reconfirmed host restriction factors.
Hit definition threshold: Minimum one siRNA yielding a z-score > +2 (sorted by z-score). All hits comply with the second threshold of $p < 0.05$. "Strong HDFs" are indicated in grey.

Gene Symbol	Ref Seq ID	Full gene name	Max. z-score (primary)	Max. z-score (reconfirm.)	no. siRNA primary + reconfirm. above threshold
CSK	NM_004383	C-src tyrosine kinase	2.727	4.936	2/3 + 1/3
TAF1L	NM_153809	TAF1 RNA polymerase II, TATA box binding protein (TBP)-associated factor, 210kDa-like	3.042	3.185	1/3 + 1/3

Gene Symbol	Ref Seq ID	Full gene name	Max. z-score (primary)	Max. z-score (reconfirm.)	no. siRNA primary + reconfirm. above threshold
SNF1LK2	NM_015191	SNF1-like kinase 2	2.631	2.362	1/3 + 1/3
CD2	NM_001767	CD2 molecule	2.149	2.111	1/3 + 1/3

4.4 Exemplary single hit characterization

The next step was to follow up on individual genes in order to validate the results from the screening assay. A detailed characterization of the role, relevance and function of each of the hits for HIV-1 assembly and release will be elucidated by future studies. However, as a proof for their relevance, a single hit was chosen for initial follow-up experiments.

The bioinformatic analysis indicated the MAPK pathway as the top enriched pathway in the set of reconfirmed hits. Included in this pathway is Mitogen-activated protein kinase kinase kinase 14 (MAP3K14), one of the strongest hits of our screen. Furthermore, MAP3K14 was identified in the siRNA screen by Zhou et al. as a hit in their part addressing the late stages of HIV-1 replication (283). See chapter 5.3 for further information regarding overlap with other RNAi screens. MAP3K14 is the crucial activator of the alternative NFkB activation pathway and is therefore also called NFkB inducing kinase (NIK) (284). Additional literature studies revealed that HIV-1 Tat enhances MAP3K14 activity (285) and that MAP3K14 expression is increased after RSV infection (286). Paul Bieniasz's group showed, that MAP3K14 influences the replication of several human viruses in response to type I interferon (287, 288). *In silico* sequence analyses for protein interaction motifs using the open source tool "Eukaryotic Linear Motif resource for functional sites in proteins" (ELM) (289, 290) predicted binding sites in HIV-1 p6 for TRAF proteins, which are important activators of MAP3K14. Because of these reasons, MAP3K14 was chosen as an ideal example for follow-up studies at the time of the experiments.

The screen was based on bulk readout of fluorescence intensities in 96-well plates. As a first step towards the follow-up characterization of single hit proteins, the effect was re-assessed in a different format. For this purpose, 293T cells were seeded into 12-well plates. The plates were incubated for ~7 hours in order to let the cells settle down and attach to the wells prior to transfection with the siRNAs: either a non-silencing control (nsc) siRNA or the top siRNA against MAP3K14 from the reconfirmation screen (siM3K14). Similar to the screening conditions, 30 hours post siRNA transfection, the wells were transfected with the 1:1 mixtures of WT or Late(-) proviral plasmid DNAs. After 44 hours, supernatants and cell lysates were harvested and fluorescence intensities of the samples were measured. The experiment confirmed that siM3K14 reduced the relative release of Gag significantly in a different format and setting compared to the screening assay (Figure 4-19).

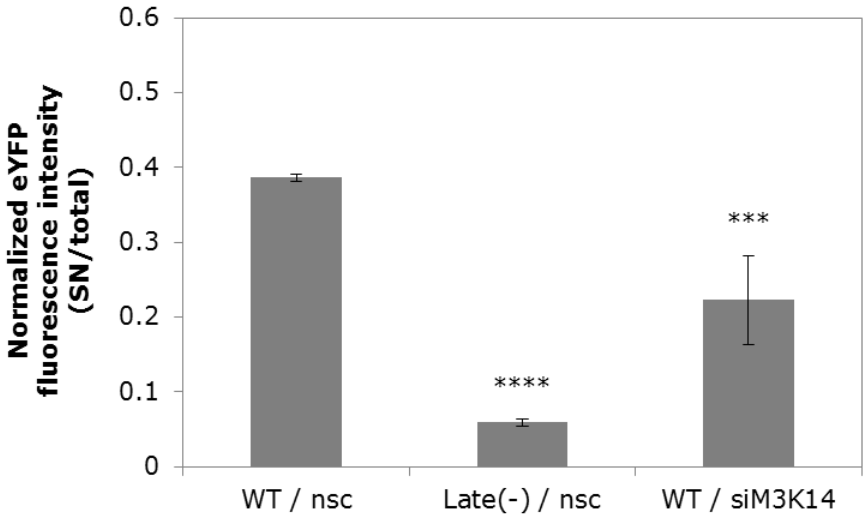

Figure 4-19 siRNA against MAP3K14 reduced release in 12-well format (fluorescence)
The graph shows the normalized fluorescence intensity, calculated by division of supernatant intensity by total intensity in lysate and supernatant (mean ± standard deviation) with n=3. Statistical analysis (one-sided ANOVA with Dunnett's multiple comparisons post-test, GraphPad Prism 6.05) compared to the WT/nsc result: ****= p<0.0001, ***= p<0.001.

As a next step a different readout was chosen to address the effect independently of fluorescence. For this purpose, the release efficiency was measured using direct quantitation of HIV-1 CA. For this experiment, the same conditions were applied as above just using only the unlabeled WT and Late(-)

proviral plasmid DNAs. Figure 4-20 shows the results of the quantitative western blot with signals of supernatant normalized to total signal. Release efficiency was reduced by the siRNA targeting MAP3K14 by ~50%. This was comparable to the effect using eYFP fluorescence readout.

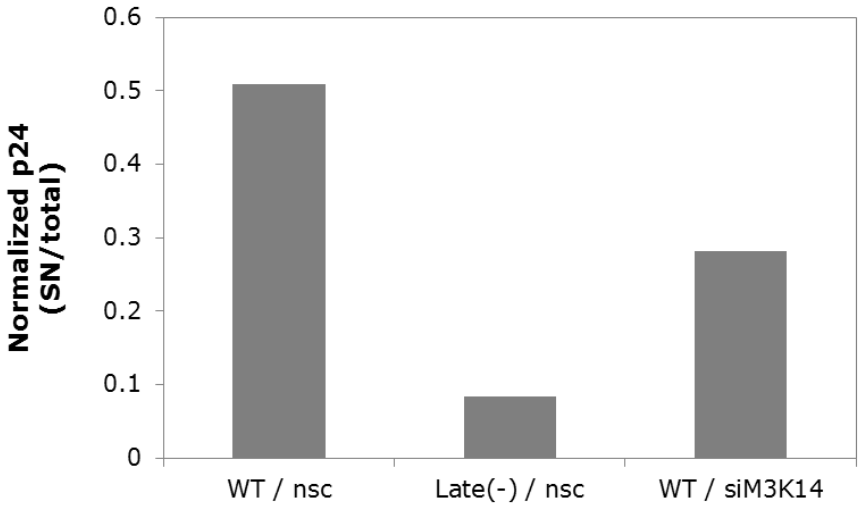

Figure 4-20 siRNA against MAP3K14 reduced release in 12-well format (Western Blot)
The graph shows the normalized p24 values obtained by quantitative Western Blot measurement of the intensities of the single bands using the LICOR Odyssey. Normalized values were calculated by division of supernatant intensity by total intensity in lysate and supernatant.

Choudhary et al. showed that MAP3K14 expression was increased after RSV infection (286). In order to address the question if HIV-1 infection leads to a similar MAP3K14 increase, the expression was addressed by immunofluorescence of cells transfected with pcHIV. For this purpose, 293T cells were seeded in 6-well plates containing glass coverslips. 24 hours later, the cells were transfected with pcHIV proviral plasmid DNA. 36 hours later, cells were fixed and stained with antibodies against HIV-1 capsid (sheep anti p24, Kräusslich lab) and MAP3K14 (rabbit anti MAP3K14, Abcam). Nuclei were stained 4´,6-Diamidin-2-phenylindol (Dapi) in addition. Figure 4-21 shows increased MAP3K14 signal intensities in p24-positive cells.

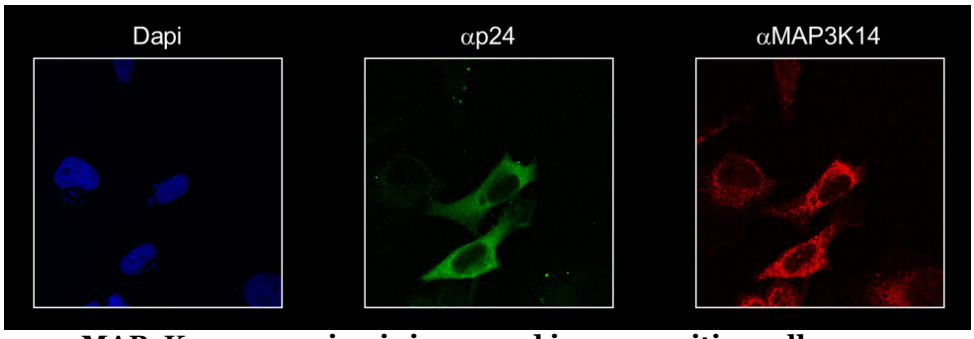

Figure 4-21 MAP3K14 expression is increased in p24 positive cells
293T cells were fixed and stained with Dapi 1:2000, sheep αp24 1:500, rabbit αMAP3K14 1:150. Capsid positive cells show an increased signal of MAP3K14.

The exemplary follow-up of MAP3K14 shows clearly, that the results of the screen can be transferred to and confirmed by other experimental settings. Furthermore, Khan et al. showed that knockdown of TRAF proteins indeed caused a reduction of HIV-1 Gag release into the supernatant of macrophages in the meantime (291). The established screening assay yielded a list of novel host cell factors. Each of these hits has to be addressed by specific experiments in the future in order to fully understand their respective roles in HIV-1 assembly and release. For this purpose, the impact of the hereby identified proteins has to be confirmed for example in more relevant primary cells or by using specific inhibitors.

4.5 Bioinformatical analysis

To focus on single proteins is one aspect of the interpretation of the results. On the other side, cellular kinases are interlinked in big multi-step processes which orchestrate the different networks and signaling pathways in the cell. This screening assay identified 43 host cell factors (39 HDFs and 4 HRFs) to be important for HIV-1 assembly and release. In order to understand the underlying processes, bioinformatical analyses were conducted. Parts of our previously described analysis roadmap were used for this bioinformatical analysis (292).

All hits were tested using the "Database for Annotation, Visualization and Integrated Discovery (DAVID, v6.7, 2015, http://david.abcc.ncifcrf.gov/) (276-279). This set of algorithms was designed to generate functional annotations to gene sets in order to detect enriched groups or clusters of genes. As a background dataset, the complete list of genes included in the primary siRNA library was used in order to detect specifically enriched pathways and functional annotations from the set of kinases.

As a first step, potential gene clustering was analyzed. The given data set of the 43 reconfirmed hits is hereby analyzed for certain keywords regarding the gene function. Mostly several generic kinase-specific enriched terms (e.g. phosphotransferase, ATP binding,…) were detected. In addition, the term "TNF/Stress related signaling" was found to be enriched. The results are listed in Table 17 stating the category, the term, the number of genes in the respective group, the p-value, and the fold enrichment.

Table 17 DAVID gene clustering analysis of reconfirmed hits versus the complete kinase library as background

Category	Term	Genes in group	p-value	Fold enrichment
SP_PIR_KEYWORDS	ATP	11	0.052	1.6
SP_PIR-KEYWORDS	Phosphotransferase	12	0.072	1.5
GOTERM_MF_FAT	Adenyl nucleotide binding	27	0.076	1.1
GOTERM_MF_FAT	Purine nucleoside binding	27	0.076	1.1
GOTERM_MF_FAT	Nucleoside binding	27	0.076	1.1
GOTERM_MF_FAT	ATP binding	27	0.076	1.1
GOTERM_MF_FAT	Adenyl ribonucleoside binding	27	0.076	1.1
BIOCARTA	TNF/Stress related signaling	3	0.078	3.6
GOTERM_MF_FAT	Purine nucleotide binding	27	0.08	1.1
UP_SEQ_FEATURE	Nucleotide phosphate-binding region:ATP	23	0.093	1.1

As gene cluster categories are rather generic and too unspecific for pinning down crucial pathways, a functional annotation analysis was conducted subsequently. This analysis was based on gene ontology (GO) terms, which groups and identifies genes according to their networks and their functions in specific biological processes. This analysis gave hints to functions which were shared by several of the identified hits. Categories involved in regulation of apoptosis, cell death as well as cell metabolism were especially enriched – each with 7 hits per category. Table 18 lists the results from the functional annotation analysis including the category, the term, the number of genes in the respective group, and the p-value.

Table 18 DAVID functional annotation analysis of reconfirmed hits versus the complete kinase library as background

Category	Term	Genes in group	p-value
GOTERM_MF_FAT	Negative regulation of apoptosis	7	0.025
GOTERM_MF_FAT	Negative regulation of cell death	7	0.028
GOTERM_MF_FAT	Negative regulation of programmed cell death	7	0.028
GOTERM_MF_FAT	Regulation of transcription, DNA-dependent	5	0.035
GOTERM_MF_FAT	Regulation of RNA metabolic process	5	0.047
SP_PIR-KEYWORDS	Transcription	4	0.06
SP_PIR-KEYWORDS	Transcription regulation	4	0.06
GOTERM_MF_FAT	Regulation of cell proliferation	8	0.063
GOTERM_MF_FAT	Transcription	4	0.073

In addition to the DAVID database tool, the Kyoto Encyclopedia of Genes and Genomes (KEGG) Mapper v2.5 (http://www.genome.jp/kegg/mapper.html, Copyright 1995-2015 Kanehisa Laboratories) was applied to the 43 validated hits as well. KEGG Mapper clusters proteins in well-defined signaling pathways. In comparison to the GO terms, the KEGG networks are

much more detailed and specific. It is especially suited to address interactions of proteins on the level of specific signaling pathways. Similar to the DAVID database tool, KEGG mapper revealed clusters or pathways related to both cell proliferation and cellular maintenance. In total, 10 pathways were identified with at least 4 of the reconfirmed hits. The highest numbers of genes were found in the MAP kinase signaling pathway (7 hits), followed by the RAP1 (5 hits) and mTOR pathways (4 hits). Table 19 lists all identified signaling pathways listing all identified genes.

Table 19 KEGG Mapper signaling pathway analysis of the reconfirmed hits.
Listed are pathways with 4 or more identified genes.

KEGG term	Number of Genes
MAPK signaling pathway ▪ FGFR2; fibroblast growth factor receptor 2 ▪ NLK; nemo-like kinase ▪ MAP2K3; mitogen-activated protein kinase kinase 3 ▪ MAP4K2; mitogen-activated protein kinase kinase kinase kinase 2 ▪ RPS6KA2; ribosomal protein S6 kinase, 90kDa, polypeptide 2 ▪ BRAF; B-Raf proto-oncogene, serine/threonine kinase ▪ MAP3K14; mitogen-activated protein kinase kinase kinase 14	7
RAP1 signaling pathway ▪ FGFR2; fibroblast growth factor receptor 2 ▪ IGF1R; insulin-like growth factor 1 receptor ▪ PIK3CG; phosphatidylinositol-4,5-bisphosphate 3-kinase, catalytic subunit γ ▪ MAP2K3; mitogen-activated protein kinase kinase 3 ▪ BRAF; B-Raf proto-oncogene, serine/threonine kinase	5
mTOR signaling pathway ▪ PIK3CG; phosphatidylinositol-4,5-bisphosphate 3-kinase, catalytic subunit γ ▪ RPS6KA2; ribosomal protein S6 kinase, 90kDa, polypeptide 2 ▪ RPS6KB1; ribosomal protein S6 kinase, 70kDa, polypeptide 1 ▪ BRAF; B-Raf proto-oncogene, serine/threonine kinase	4
Insulin signaling pathway ▪ PIK3CG; phosphatidylinositol-4,5-bisphosphate 3-kinase, catalytic subunit γ ▪ RPS6KB1; ribosomal protein S6 kinase, 70kDa, polypeptide 1 ▪ BRAF; B-Raf proto-oncogene, serine/threonine kinase ▪ HKDC1; hexokinase domain containing 1	4
PI3K-Akt signaling pathway ▪ FGFR2; fibroblast growth factor receptor 2 ▪ IGF1R; insulin-like growth factor 1 receptor ▪ PIK3CG; phosphatidylinositol-4,5-bisphosphate 3-kinase, catalytic subunit γ ▪ RPS6KB1; ribosomal protein S6 kinase, 70kDa, polypeptide 1	4
HIF-1 signaling pathway ▪ IGF1R; insulin-like growth factor 1 receptor ▪ PIK3CG; phosphatidylinositol-4,5-bisphosphate 3-kinase, catalytic subunit γ ▪ RPS6KB1; ribosomal protein S6 kinase, 70kDa, polypeptide 1 ▪ hsa:80201 HKDC1; hexokinase domain containing 1	4

KEGG term	Number of Genes
RAS signaling pathway ▪ FGFR2; fibroblast growth factor receptor 2 ▪ KSR2; kinase suppressor of ras 2 ▪ IGF1R; insulin-like growth factor 1 receptor ▪ PIK3CG; phosphatidylinositol-4,5-bisphosphate 3-kinase, catalytic subunit γ	4
Fc gamma R-mediated phagocytosis ▪ IGF1R; insulin-like growth factor 1 receptor ▪ NLK; nemo-like kinase ▪ PIK3CG; phosphatidylinositol-4,5-bisphosphate 3-kinase, catalytic subunit gamma ▪ BRAF; B-Raf proto-oncogene, serine/threonine kinase	4
FoxO signaling pathway ▪ IGF1R; insulin-like growth factor 1 receptor ▪ NLK; nemo-like kinase ▪ PIK3CG; phosphatidylinositol-4,5-bisphosphate 3-kinase, catalytic subunit γ ▪ BRAF; B-Raf proto-oncogene, serine/threonine kinase	4
Neurotrophin signaling pathway ▪ IRAK4; interleukin-1 receptor-associated kinase 4 ▪ PIK3CG; phosphatidylinositol-4,5-bisphosphate 3-kinase, catalytic subunit ▪ RPS6KA2; ribosomal protein S6 kinase, 90kDa, polypeptide 2 ▪ BRAF; B-Raf proto-oncogene, serine/threonine kinase	4

The KEGG pathway database contains in addition maps for all the described pathways. For all 10 enriched pathways, the respective map was adapted to indicate the genes which were validated in the reconfirmation screen. As an example, Figure 4-22 shows the map of the MAPK signaling pathway, showing the seven hits highlighted in pink color. Interestingly, the 7 hits identified are not in direct interaction with each other but from different parts of the MAPK signaling pathway. The maps of the other pathways are included in the appendix 3. All maps were generated using KEGG Mapper and all hit genes are indicated in red.

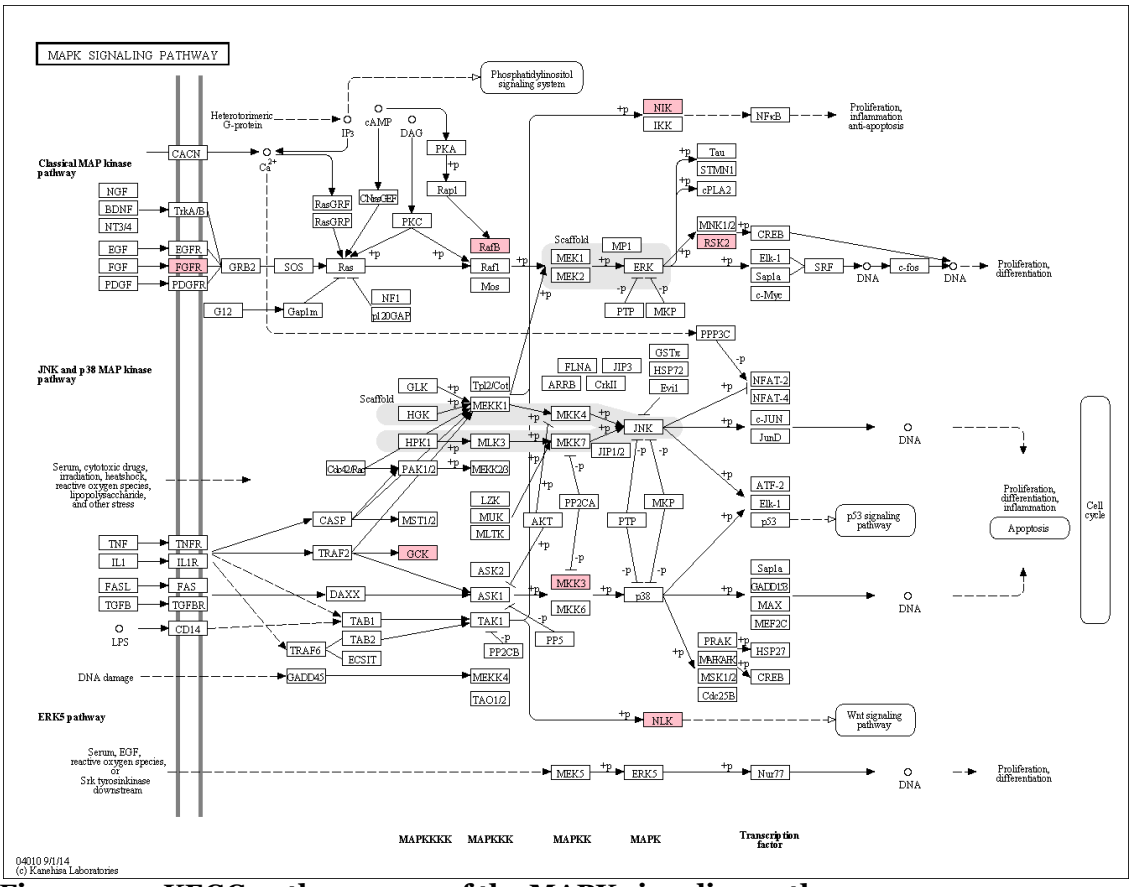

Figure 4-22 KEGG pathway map of the MAPK signaling pathway.
The map shows the MAPK signaling pathway based on the KEGG database. The seven hits, falling into this network, are indicated in red. Figure created using KEGG Mapper v2.5.

The results from the bioinformatical analysis offer a promising starting point to understand the specific role and importance of the identified host cell factors. Several screens were performed at the point of time of this work. Each was conducted in distinct technical settings with only a limited overlap of single proteins (discussed in chapter 5.3). However, comparing the identified signaling networks leads to the realization that the underlying pathways of the respective hits overlap to a much greater extent than the mere protein level. This indicates the importance of combinatory pathway analyses for screening approaches which are elucidated in more depth in chapter 5.4 in the following discussion.

5 Discussion

Having novel tools available to illuminate the virus host interactions is essential for a better understanding of HIV-1 replication. In recent years, screening platforms using RNAi emerged as a powerful tool to address that interaction (260).

5.1 Establishment of the screening assay

In this work, a novel screening assay was successfully established to address the interplay between cellular proteins and the assembly and release of new viral particles. The platform is versatile and requires only a limited set of manual steps supported by automated liquid handling machines, which allow its application for high throughput screening. It is tailored for a use of 96-well plates but 384-well plates can be used as well. It was shown, that the platform is robust, easy to use, and yields stable and reproducible results and signal-to-background ratios. The assay was tailored to screening medium to large sets of reverse transfected siRNAs. However, it is as well suitable for other screening approaches, such as testing of chemical compounds. Figure 5-1 gives an overview of the assay from the beginning with pre-spotted multi-well plates to the statistical and bioinformatical analysis.

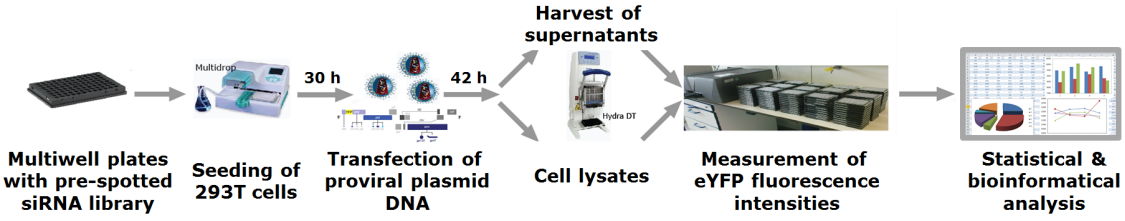

Figure 5-1 Overview of the established screening assay
The complete siRNA screening assay covers all steps from preparation of the siRNAs, conduct of the actual assay to the statistical and bioinformatical analysis of the results.

There are several options to detect and quantify HIV-1 release, as discussed below. Current automatic microscopy techniques offer a lot of possibilities for high content screening. Another, microscope based, siRNA screening assay was established in our group simultaneously (274). However, microscopy excels at observations of cells but the newly formed viral particles are released into the supernatant, which makes a microscopic readout unsuitable. An in-house ELISA to detect the HIV-1 capsid protein (p24), for example, would have given the sufficient sensitivity and specificity to measure viral particle release. However, it lacks the technical feasibility to run many samples in a very concise time frame, which is indispensable for a HTS format. Previous siRNA screens used reporter enzymes such as luciferase (258, 293) or β-galactosidase (283), which were responsive to HIV-1 transcription. These readouts give a strong signal and a good signal-to-background ratio. But these reporter enzymes are not incorporated into the viral particles and can therefore hardly be applied to directly measuring released viruses. Methods exist to directly quantify released viral particles as well. One of them would be to harvest the supernatant containing the newly released viruses and to measure the reverse transcriptase activity (294). However, this type of assay is costly which makes it more suitable for smaller sets of target proteins. A second option would be to apply the supernatant to new cells and thereby allowing a second round of infection during which a reporter gene is expressed in the new target cell (212, 283). However, this poses a disadvantage, as it only yields an indirect indication of release efficiency, as signals could be shrouded by release independent effects between entry and translation in the reporter cell. In contrast to these limitations of the various aforementioned methods, the previously published viral construct pcHIV^{eYFP} harboring an fluorescently labeled Gag (238) is uniquely suitable for this specific purpose. The readout is a unique feature of this platform, enabling the direct quantification of released virus like particles. The assay consequently requires only a few handling steps, no costly reagents and offers a high signal-to-noise ratio.

The technique of reverse transfection offers a great flexibility for genome wide siRNA screening, as the plates, which contain the siRNAs and the transfection reagent, can be prepared and stored (269, 270). This reduces the

workload on the actual day of conducting the screen, which is especially advantageous for the screening of large libraries. The standardized production process ensures high quality and reproducible transfection results. Protocols for both 96-well and 384-well plates are available from our collaborator Holger Erfle (BioQuant, University of Heidelberg, Germany). Both parts of the screening of human kinases (primary and reconfirmation screen) used three different siRNAs per target gene each (in total six), which is crucial for excluding off-target effects. In addition, it is important not to place siRNAs against the same target into adjacent wells of the same multi-well plate. This could cause artifacts such as edge-well effects or other technical inhomogeneity.

For this assay, 293T cells were chosen, as they resulted in the optimal signal strength and lowest variance. However, cell lines like 293T cells or even T-cell lines do not fully represent all aspects of cell types relevant for HIV-1 infections *in vivo*, e.g. primary T-cells. However, 293T cells are routinely used by many labs for HIV particle production. But of course, all hits from this initial screening assay will have to be separately evaluated in other assays, including primary T-cells.

The results of the establishment phase showed, that the screen yielded a very low variability within a plate and between different plates (Figure 4-9). In general, the variance in the 96-well plate format is much lower compared to the 384-well plates. In addition, the signal ratio between “WT” and “Late(-)” is bigger (~8 fold vs. ~4 fold, Figure 4-11). However, the 384-well format is nevertheless applicable for high-throughput screens in the future.

The relevance of the established assay’s results was proven by testing siRNAs against known dependency factors. Especially a knockdown of TSG101 resulted in a strong decrease of the fluorescence intensity in the supernatant (Figure 4-13). Although not as strong as TSG101, siRNAs targeting VPS4 showed a statistical significant effect as well (Figure 4-14). Interestingly, the knockdown times for both targets to generate an optimal result differed greatly. While for TSG101 shorter knockdown durations gave better results, VPS4 needed a longer time period. Knockdown durations can be optimized for single targets.

However, a general limitation of high throughput RNAi screens *per* se is, that a routine and comprehensive parallel examination of the knockdown efficacy (e.g. by RT-qPCR or quantitative Western Blotting) is not feasible with time and budget restraints. Therefore it is not guaranteed that the siRNA transfection indeed led to reduction of the protein expression in the cell. Furthermore, as proteins differ in their respective turn-over times it is not possible to silence every gene equally efficiently. Regardless of the limitations, RNAi screening assays are a very powerful tool to identify host cell factors.

In comparison to other published HIV-1 screens (212, 258, 283), the hereby described platform is the first of its kind especially tailored to investigate the steps between transcription and viral egress. Altogether, this screening platform offers a novel, stable and valuable addition to the existing approaches.

5.2 Focus on the cellular conductors: Results from the kinase screen

After successful establishment of the screening assay, a siRNA library targeting 724 human kinases and accessory proteins were tested. Hits from the primary screen were re-tested in the reconfirmation screen. For this, siRNAs which were distinct from the ones used in the primary screen were used. The screening of a kinase library revealed 43 validated hits. These include 39 HDFs (Table 15) and four HRFs (Table 16). Out of those, 19 HDFs and 1 HRF were defined as “Strong HDF” or “Strong HRF”, respectively. Table 20 gives a summary of the results from the primary and the reconfirmation screen.

Table 20 Summary of the results of the primary and reconfirmation screen

Screen	No. of genes tested	HDF	HRF
Primary	724	50	26
Reconfirmation	76	39	4

Interestingly, the screening assay yielded more HDFs than HRFs. This may hint to the fact that late stages of HIV-1 replication do not face similar tight restrictions as early stages, e.g. uncoating and reverse transcription being counteracted by TRIM5a or APOBEC3G. Alternatively, the possibility exists that this bias may be due to technical specificities of the detection method.

Kinases of different pathways regulating growth, proliferation, differentiation, and survival of cells were suggested to play a role during the late phase of HIV-1 replication as shown in the results section 4.5 and discussed in section 5.4. In general, it makes sense for a virus to stimulate growth and survival of the infected cell to ensure consistent infection and survival of the virus itself. And it makes even more sense for the virus not to rely on a single pathway, but to make sure via the use of redundant signal modulation that the cell will rather survive and proliferate than undergo apoptosis or necrosis.

In the following section, the results are discussed in the context of the current literature, in order to distinguish truly novel kinases arising from this work in contrast to previously described kinases from the literature. Of note, by the normalization of the supernatant signal to the total signal, any influence on cell numbers and translation or transcription should be removed from the set. The fact that some of the host cell factors below are described to be involved in gene transcription is intriguing on the first glance. One possible explanation would be that this host cell factor for example influences the transcription of a specific release relevant cellular protein. Alternatively this host cell factor may also have a separate function independent on its known role during e.g. transcription. The exact relevance and mode of action has to be determined in future studies.

5.2.1 Host dependency factors

The following proteins were identified in the primary screen and then validated during the reconfirmation screen. Host dependency factors elicit a positive effect on HIV-1 and a knockdown of these proteins leads to a diminished assembly and release of viral particles.

- **Sphingosine kinase 1 and sphingosine kinase 2 (SPHK1, SPHK2)**

Sphingosine kinases phosphorylate sphingosine to the lipid mediator sphingosine-1-phosphat (295). Sphingosine kinase 1 (SPHK1) is located at the plasma membrane, while SPHK2 is located in the endoplasmic reticulum, the nucleus and mitochondria (296). SPHK1 and S1P play a role in cell signaling, cell survival, and (pro-inflammatory) immunomodulation (296). Infections may lead to either increased (human cytomegalovirus, respiratory syncytial virus) or reduced (bovine viral diarrhea virus, dengue virus) SPHK1 activity (297). A recent microarray of human B cells reported upregulation of SPHK1 by the HIV-1 gp120 protein when interacting with the integrin α4β7 (298). In our study, silencing of SPHK1 led to the strongest impairment of virus release of the complete siRNA set, further corroborating the relevance of the enzyme for HIV-1 life cycle. In addition, targeting SPHK2 led to an impaired release of HIV-1 as well, albeit in a lesser extent compared to SPHK1. To date, the effect of modulation of the SPHK1/S1P axis before or after HIV-1 infection was only tested in preclinical studies with the S1P analog Fingolimod (FTY720) in macaques without benefits regarding virus permission or lymphocyte trafficking (299, 300). However, the modulation of SPHK1 is an emerging field and future studies might be required to discover the point of vantage for SPHK1/S1P axis modulation in HIV-1 infection. Of note, recent studies showed that inhibition of SPHK2, the intracellular sphingosine kinase, can lead to tumor regression (301, 302). The effect of SPHK1 on HIV-1 associated tumors like Kaposi's sarcoma remains to be determined.

- **Neurogranin (NRGN)**

The protein neurogranin is not a kinase itself, it participates in the protein kinase C signaling pathway and regulates the availability of the second messenger calmodulin (303). Calmodulin is involved in the modulation of inflammatory signals. In peripheral blood mononuclear cells (PBMCs) of HIV-1 patients, neurogranin mRNA was shown to be downregulated in response to virus replication (304). This seems at first glance to be at odds with our results, however, it might indicate that, although neurogranin plays a role in HIV-1 replication and release, the virus leads to a downregulation of neurogranin and thus a modulation of inflammation at a later stage.

- **Plexin A2, Plexin C1**

The kinase siRNA library used in this study was predesigned by our collaboration partners and contained additional non-kinase proteins. Two of these proteins, plexin A2 and plexin C1, belong to the family of plexins, namely transmembrane receptors for semaphorins. Viral semaphorins were shown to modulate the immune response by binding to plexins such as Plexin A2 or Plexin C1 (305). A role of plexins in HIV-1 infections has not yet been described.

- **Mitogen-activated protein kinase kinase kinase 14 (MAP3K14)**

MAP3K14 stimulates NFkB activity and is therefore also called NFkB inducing kinase (NIK) (284). The effect of silencing of this MAP kinase for HIV replication was already shown in another siRNA screen by Zhou et *al.* (283) and HIV Tat was revealed as the HIV component that enhances the activity of this kinase (285). In addition, Paul Bieniasz's group showed, that MAP3K14 influences the replication of several human viruses in response to type I interferon (287). Interestingly, the HIV p6 domain contains a motif, which has been predicted to be able to bind TRAF proteins which activate MAP3K14 (*in silico* sequence analysis with Eukaryotic Linear Motif, ELM, http://elm.eu.org/, (289, 290)). In the meantime, Khan et al. showed that knockdown of TRAF proteins indeed caused a reduction of HIV-1 Gag release into the supernatant of macrophages (291).

- **3'-phosphoadenosine 5'-phosphosulfate synthase 1 (PAPSS1)**

PAPSS1 is a bifunctional enzyme involved in the production of 3'-phosphoadenylylsulfate (PAPS), the co-factor of sulfotransferases. The kinase part transfers a phosphate group from ATP to adenosine 5'-phosphosulfate (APS) yielding PAPS. Sulfotransferases catalyze the sulfonation of endogenous substrates like lipids, peptides or hormones as well as xenobiotics (306). HIV-1 transcription in different cell types was reported to be dependent on this sulfonation (306) and sulfonation inhibitors can block HIV-1 transcription initiation (307). As discussed at the beginning of this section, effects on transcription were excluded due to normalization of the HIV-1 related fluorescence in the supernatant to the total HIV-1 related fluorescence. This may be due to PAPSS1 controlling the transcription of an important release

factor or to an additional function other than direct modulation of HIV-1 transcription. PAPSS1 was the only target for which three different siRNAs showed effects above the threshold in the reconfirmation screen. This makes it a very promising candidate for future investigations.

- **Glycerate kinase (GLYCTK)**

The kinase catalyzes the phosphorylation of (R)-glycerate and may be involved in serine degradation and fructose metabolism (308). An interaction with HIV-1 or any other virus has not yet been described.

- **Uridine-cytidine kinase 2 (UCK2)**

This enzyme catalyzes the phosphorylation of uridine and cytidine (309, 310). An interaction with HIV has not yet been described.

- **NME/NM23 nucleoside diphosphate kinase 1 (NME1)**

Reduced mRNA transcript levels of NME1 were first identified in highly metastatic cells (311). It is therefore assumed to be a metastasis suppressor. An interaction with HIV-1 has not yet been described.

- **Phosphatidylinositol-4,5-bisphosphate 3-kinase, catalytic subunit gamma (PIK3CG)**

The PIK3CG is a catalytic subunit of PI3K, which phosphorylates phosphatidylinositol-4,5-bisphosphate to Phosphatidylinositol-(3,4,5)-trisphosphate (PI3P). Amongst other, PI3K is involved in AKT and mTOR signaling (312). PI3K activity is modulated by different components of HIV and plays a role in the HIV-1 modulation of the inflammatory response (313, 314), for example via expression of the cytokine CCL5 (315, 316) and downregulation of MHC-I (317, 318). PI3K also plays a role in replication of HIV-1, as inhibitors of PI3K showed a strong reduction of HIV-1 production in human PBMCs (319). The gp120 and the Tat proteins are responsible for PI3K induced virus replication and survival of the host cell (320, 321). The Nef protein “hides” the infected cell from the immune system by blocking the transport of MHC class I molecules to the cell surface in a PI 3-kinase-dependent way (322).

- **Cyclin-dependent kinase 10 (CDK10)**

Cyclin-dependent kinases are essential for cell cycle progression (323). All CDKs depend on specific cyclins to be active, which is cyclin M in case of CDK10 (324). An interaction of CDK10 and HIV-1 has not yet been described.

- **A kinase (PRKA) anchor protein 7 (AKAP7)**

The A-kinase anchoring proteins are a group of functionally related proteins that bind to a regulatory subunit of cAMP-dependent protein kinase A (PKA) and target the enzyme to specific subcellular compartments depending on their targeting motifs (325). No direct interactions of AKAP7 and HIV-1 have been described. Interestingly, association of PKA to the virus is required as a cofactor for optimal reverse transcription of HIV-1 (326). Jiang et al. (293) described PRKACB, a subunit of PKA, to be involved in the replication of HIV-1. Our results are the first to indicate that AKAP7 might play a role in the release of HIV-1, while the specific role of the cAMP-dependent protein kinase A (PKA) enzyme remains to be determined.

- **PX domain containing serine/threonine kinase (PXK)**

PXK contains a phox (PX) domain and is involved in the trafficking of cellular receptors like the epidermal growth factor receptor and the B-cell receptor (327, 328). It may be associated with susceptibility to systemic lupus erythematosus (328), but an interaction with HIV-1 has not yet been described.

- **Inositol 1,4,5-trisphosphate 3-kinase A (ITPKA)**

ITPKA is responsible for regulating the levels of a large number of inositol polyphosphates that are important in cellular signaling (329-331). Direct interaction of ITPKA with neither HIV nor other viruses has yet been described.

- **Ribosomal protein S6 kinase, 90 kDa, polypeptide 2 (RPS6KA2)**

The ribosomal protein S6 kinase, 90 kDa, polypeptide 2 (RPS6KA2) is a member of the RSK family of kinases. In human peripheral blood monocytes, the RSK2 was overexpressed on the mRNA level after HIV-1 infection (332). It is recruited and activated by Tat (333) and is reciprocally important for Tat function.

- **Fyn-related kinase (FRK)**

The Fyn-related kinase (FRK) is a nuclear tyrosine kinase that regulates cell survival, differentiation and proliferation (334). Direct interactions with HIV-1 have not yet been described.

- **Cyclin-dependent kinase 7 (CDK7)**

This enzyme interacts with cyclin H and MAT1, which results in a complex responsible for the activating of other CDKs (CDK activating kinase (CAK)) and regulation of the cell cycle (335). To achieve hyperphosphorylation of C-terminal domain (CTD) repeats of RNA polymerase II (Pol II), a prerequisite for transcriptional elongation of HIV-1, Tat binds directly to CDK7 (336, 337). Of note, in this study virus release and not direct effects on transcription were tested as described for PAPSS1, this could indicate an additional role of CDK7 in a later step of HIV-1 infection.

- **Kinase suppressor of ras 2 (KSR2**)

KSR2 is involved in cell proliferation and differentiation (338, 339) and has been suggested as a marker for immortalized cells (338). Interactions with HIV-1 have not yet been described.

- **Mitogen-activated protein kinase kinase 3 (MAP2K3)**

The mitogen-activated protein kinase kinase 3 phosphorylates and thus activates MAPK14/p38-MAPK which is linked to inflammation, cell cycle, cell death, development, cell differentiation, senescence and tumorigenesis in specific cell types (340). HIV-1 Tat associates with the respective kinase promoter and thus leads to increased gene expression of MAP2K3 (341).

- **PAS domain containing serine/threonine kinase (PASK)**

PASK is a nutrient responsive kinase regulating energy balance of the cell (342-344) as well as cell proliferation and survival (345). Interactions with HIV-1 have not yet been described, however, energy metabolism is essential for cell viability and virus replication, and thus it makes sense that HIV-1 could intervene here as well.

- **Serine/threonine kinase 32B (STK32B)**

The function of STK32B is not known and therefore no deduction is possible regarding its relevance for HIV-1.

- **Fibroblast growth factor receptor 2 (FGFR2)**

The transmembrane fibroblast growth factor receptor 2 (FGFR2) consists of a cytosolic tyrosine kinase domain, which transduces the signals of different fibroblast growth factors (FGFs) to the MAPK cascade. HIV-1 Tat synergizes with the FGFR-2 ligand FGF-2 to prevent apoptosis (346), but although the basic domain of HIV-1 Tat was already identified as an essential component for this interaction (347), the exact mechanism remains to be elucidated. Both HIV-1 Tat and FGF-2 compete for the secreted Fibroblast Growth Factor Binding Protein-1 (FGFBP1) a protein that potentiates the effect of FGFs in target cells (348). Pre-treatment of endothelial cells with FGF2 protects cells from HIV-1 toxicity (349), maybe by competing for the same receptor. It may be hypothesized that HIV-1 Tat might use the FGFR-2 in a FGFBP1-dependent manner, leading to activation of the MAPK pathway and increased cell proliferation.

- **Interleukin-1 receptor-associated kinase 4 (IRAK4)**

IRAK4 is involved in signaling innate immune responses from Toll-like or T-cell receptors (350). HIV-1 infection is associated with an increased risk of bacterial infections, and indeed HIV-1 was reported to downregulate IRAK4 expression, leading to impaired TLR signaling (351), hindering the appropriate immune response. In our study, HIV-1 release was reduced after silencing of IRAK4, indicating that the virus first might use the kinase IRAK4 for release and afterwards or even thereby disturbs its function to suppress the innate immune response.

- **Nemo-like kinase (NLK)**

The nemo-like kinase (NLK) is an atypical member of the MAPK pathway (352). Similar to other MAP kinases, its predominant role is in cell proliferation and differentiation via the WnT signaling pathway (353). Interactions of neither HIV-1 nor other viruses with NLK have yet been described.

- **B-Raf proto-oncogene, serine/threonine kinase**

B-Raf is a member of the Raf kinase family, which consists of A-Raf, B-Raf and C-Raf (Raf-1). These kinases transduce growth signals via the MAPK/ERK signaling pathway leading to cell division and differentiation. Interactions of HIV-1 with C-Raf have been reported (354-358), while the role of B-Raf in HIV-1 life cycle remains to be determined.

- **Protein kinase, cGMP-dependent, type II (PRKG2)**

PRKG2 alias CGKII inhibits renin secretion, chloride/water secretion in the small intestine, the resetting of the clock during early night, and endochondral bone growth (359). An interaction with HIV-1 has not yet been described.

- **Insulin-like growth factor 1 receptor (IGF1R)**

Activation of the transmembrane receptor IGF-1R results in proliferation or muscle cell growth. The endogenous IGF-1R ligand IGF-1 is reduced in HIV-1 patients due to growth hormone resistance (360) and the IGF-1 receptor was shown *in vitro* to be upregulated after exposure to gp120 in neurons (361). This upregulation might suggest compensation for low IGF-1 levels, however, recently it was reported that low IGF-1 plasma and CSF levels might rather be due to treatment with antiviral drugs and not the virus itself (362, 363). The increased IGF-1R levels in HIV-exposed neurons might as well simply aim at cell proliferation facilitating virus replication as consistent with the impaired HIV-1 release after silencing of IGF-1R in this study.

- **Feline sarcoma oncogene (FES)**

FES has tyrosine-specific protein kinase activity required for maintenance of cellular transformation (364, 365). In AIDS patients, cases of lymphomas had HIV-1 integration upstream from the *c-fes* proto-oncogene (366), indicating a direct contribution of the virus to HIV-1 associated lymphomas. In our study, HIV-1 expression was impaired after silencing of FES, adding a potential new HIV-1 interaction to this oncogene.

- **Mitogen-activated protein kinase kinase kinase kinase 2 (MAP4K2)**

MAP4K2 may be a regulator of NFκB signaling and thus contributing to cancer development (367). It might as well be required to transduce signals from TGFβ receptor to p38 (368). No interactions with HIV-1 have yet been described for this underexplored MAP Kinase. However, in a recent shRNA screen with HIV-1, MAP4K2 was identified as a host cell factor influencing the replication of the virus (294).

- **Ribosomal protein S6 kinase, 70kDa, polypeptide 1 (RPS6KB1)**

This enzyme is a member of the ribosomal S6 kinase family of serine/threonine kinases promoting protein synthesis, cell growth, and cell proliferation (369). It was recently suggested as a potential biomarker or even potential target for treatment of diffuse large B-cell lymphoma (DLBCL) in patients positive for HIV-1 (370), because RPS6KB1 was more frequently detected in common variants of DLBCL associated with HIV infection. The results of our study indicate that RPS6KB1 might be required for HIV-1 release, corroborating the hypothesis that this kinase might be a potential target for future therapies.

- **Sphingosine kinase 2 (SPHK2)**

For a description of SPHK2, please see the paragraph on SPHK1.

- **Dephospho-CoA kinase containing domain (DCAKD)**

The function of DCAKD is not known and therefore not deduction is possible regarding its relevance for HIV-1.

- **Cyclin-dependent kinase-like 1 (CDC2-related kinase) (CDKL1)**

CDKL1 is overexpressed in malignant tumors (371) and plays a role in cell cycle regulation (372): Knockdown of CDKL1 in melanoma cells led to arrest of the cells in G1 phase (372). An interaction with HIV or any other virus has not yet been described.

- **Pim-1 oncogene (PIM1)**

Pim kinases are implicated in the regulation of apoptosis, metabolism, and the cell cycle (373). PIM-1 was reported to act as a key switch involved in HIV-1 latency control (374). The authors conclude that PIM-1 activity is required for HIV-1 reactivation in both T cell lines and primary CD4 T cells. This is in line with the results of our study and might indicate that HIV-1 replication is dependent on PIM-1 in the special situation of virus reactivation.

- **N-acetylglucosamine kinase (NAGK)**

NAGK is involved in posttranslational modification of amino sugars. Its metabolic pathway yields UDP-acetylglucosamine (UDP-GlcNAc), a substrate for *O*-GlcNAc transferase (OGT), which modifies cytosolic and nuclear proteins associated with regulatory functions ranging from transcription, translation, cell signaling, and stress response to carbohydrate metabolism (375, 376). Overexpression of OGT, however, seems to rather inhibit the activity of the HIV-1 LTR promoter (377). This discrepancy to our study might either point towards a direct interaction of HIV-1 with NAGK and/or the resulting UDP-GlcNAc or it might be based on experimental differences, because in our experiment a CMV promoter was used instead of a LTR promoter. However, both results link viral replication and release to the glucose metabolism of the host cell and the establishment of metabolic treatment might provide a beneficial addition to conventional HIV-1 therapies in the future.

- **Alpha-kinase 3 (ALPK3)**

Alpha-kinases were first described in the mid-nineties (378). ALPK3 plays a critical role in cardiomyocyte differentiation (379) and knock-out of ALPK3 leads to nonprogressive cardiomyopathy (380). Interactions with HIV-1 or any other virus has not yet been described.

- **Hexokinase domain containing 1 (HKDC1)**

Reduced expression of this putative hexokinase is associated with altered glucose homeostasis (381). HIV-1 Tat downregulates the HKDC1 expression in U-937 macrophages (382). This indicates a subsequent change in the glucose metabolism of these cells. In our study, HKDC1 was required for HIV-1 release.

These results again link viral replication to the glucose metabolism of the host cell as already described for NAGK.

- **Microtubule associated serine/threonine kinase family member 4 (MAST4)**

  MAST kinases are expressed throughout the body (383, 384). Their expression in brain might imply an involvement in neurological function (384), and a role in breast cancer was suggested was well (385), however, their actual substrates or biological function have not yet been identified. An interaction with HIV-1 or other viruses has not yet been reported.

- **NKF3 kinase family member (SGK269)**

  Phosphorylation of SGK269 or Pseudopodium-enriched atypical kinase 1 (PEAK1) plays a role in cell migration and proliferation (386, 387). An interaction of this recently described kinase with HIV-1 has not yet been described.

5.2.2 Host restriction factors

The following proteins were identified in the primary screen and then validated during the reconfirmation screen. The knockdown of these proteins leads to an increased release of viral particles.

- **C-src tyrosine kinase (CSK)**

  CSK is involved in cell growth, differentiation, migration, and immune response. CSK phosphorylates and thus negatively regulates the family of src kinases (388), which themselves have been shown to play a role in HIV-1 infections (389). A recent study revealed that high c-src activity is the cellular response of infected cells trying to slow the viral transcription (389). Here, our results showed an increase of HIV-1 release after CSK silencing, indicating an additional interaction of CSK and HIV-1 other than c-src mediated transcription control of the virus.

- **TAF1 RNA polymerase II, TATA box binding protein (TBP)-associated factor, 210kDa-like (TAF1L)**

TAF1L protein can bind directly to the TATA-binding protein which is required for transcription of protein-encoding genes (390). An interaction with HIV has not yet been described.

- **SNF1-like kinase 2 (SNF1LK2, SIK2)**

SIK2 is part of a cellular complex essential for glucose homeostasis (391) and thus takes part in energy metabolism of the cell. An interaction with HIV-1 has not yet been described.

- **CD2 molecule (CD2)**

CD2 is a cell surface molecule expressed on T-cells and natural killer cells and plays a role in the activation of these cells. CD2 activates and induces latent HIV-1 replication in resting $CD4^+$ T cells (392) and increases HIV-1 production *in vivo* (393). High CD2 expression also occurs in latently infected resting memory $CD4^+$ T cells (394). Our current findings propose an additional role of CD2 in HIV-1 release.

5.3 Individual hits in the context of current literature

One way to pick hits for further more detailed investigations of their specific roles could be to focus on the most impressive effects detected in this work. Obvious candidates for this approach would be SPHK1, which caused the strongest reduction of HIV-1 particle release after knockdown. Multiple hits, the so called “strong” HDFs and HRFs like MAP3K14 or PAPSS1, scored with several of the used siRNAs, making the result more robust and trustworthy. PAPPS1 was the only hit to be identified with all three distinct siRNAs reaching the threshold of the reconfirmation screen. This unambiguous result makes PAPSS1 a very promising target. The results of this work hint to a potential dual role as inhibition of PAPSS1 related sulfotransferases has already been shown to directly inhibit HIV-1 transcription (306) and this screen revealed another, not transcription related, mechanism. Maybe PAPSS1 regulates an important release factor? The clinical relevance of this finding and the potential use of

PAPSS1 antagonists will have to be determined in future studies. On the other hand, reconfirmed "strong" host cell factors not yet described in the HIV-1 context may offer exciting new fields of research. Examples for these candidates may be Glycerate kinase (GLYCKT) or Fyn-related kinase (FRK).

Follow-up testing of the identified hits are crucial to determine the real relevance and roles of the confirmed hits. MAP3K14 was chosen as an example for depicting the necessary next steps (section 4.4). At first, the transfer of the assay to bigger well format was successful and release efficacy reduction was comparable between the eYFP fluorescence measurement and a quantitative Western Blot measureing HIV-1 CA (Figure 4-19 and Figure 4-20). Also it should be addressed if the presence of HIV-1 in the cell has an influence on hit protein expression. Expression of MAP3K14 was indeed increased in HIV-1 capsid positive cells by fluorescence microscopy (Figure 4-21). These initial experients show clearly that findings from the screening setting can successfully be transferred. Further experiments should encompass additional assays. For example, the siRNA's knockdown efficacy has to be checked by quantitative Western Blot and quantitative realtime PCR. As stated above, only one knockdown time was tested during the screen. Although scoring under the assay conditions, a different knockdown duration might yield optimal results for some of the hits. This has to be evaluated in future experiments. The screening assay is based on 293T cells due to ease of handling and high transfection efficiencies. However, for subsequent experiments, the role of the host cell factors have to be addressed in more relevant T-cell lines or primary T-cells e.g. using shRNAs. Further experiments might include the investigation of direct protein-protein interactions between the hits and HIV-1 proteins. Further options would be combinatory knockdowns of hits within the same pathway to identify synergies.

In addition, it is important to examine the results of the screen in the context of other published results. This is important to assess the quality of the findings and to determine possible candidates for follow-up studies. Several identified proteins were already described before to have an interaction with HIV-1. For example, 16 of the identified host cell factors were already included in the NCBI HIV-1 interaction database. Table 25 in the appendix lists all

currently described interactions from this database with the hits from our screen and the respective publications (by their Pubmed identification number). The current version of the NCBI HIV-1 interaction database can be found at http://www.ncbi.nlm.nih.gov/genome/viruses/retroviruses/hiv-1/interactions/browse/. All of these interactions were mentioned in the individual discussion of each of the proteins above.

This indicates a certain robustness and sensitivity of our current screening method, however, there were also candidates described in the literature for HIV-1 interaction that tested negative in our screen. ERK2, for example, was described to regulate viral assembly and release via phosphorylation of the p6 domain of Gag (220). At the time of this work it was intriguing that ERK2 did not score as a hit in this screen. However, in the meantime it was shown that that p6 phosphorylation is dispensable for HIV-1 (241, 242). Therefore it is not so surprising anymore that ERK2 was not identified. Other kinases which were described in the context of HIV-1 release were LIM domain kinase 1 (LIMK1) and its activator Rho kinase 1 (ROCK1) (395), lymphocyte-specific protein tyrosine kinase (LCK) (396), or Interleukin 2 inducible T-cell kinase (ITK) (397). It was shown that inhibition of these kinases reduced HIV-1 assembly and/or release. All of these kinases were included in the siRNA library of the primary screen but none fulfilled the threshold criteria except for LIMK1 which then was not reconfirmed in the second screen. This may be due to the fact that the chosen knockdown time in this assay was not suitable for the protein turnover times of these kinases. They might score as hits at different time points. As stated above, a screening assay is only able to yield a snap-shot and cannot give a full picture.

In addition it is crucial to compare the results with other published RNAi screens. True hits should also be positive with more than one screening method. In the last years, several screenings were conducted using RNAi to identify cellular proteins important for HIV-1 replication. Three of them used siRNAs in either 293T or HeLa cells (212, 258, 283) and four other screens relied on the usage of shRNA library transduced cells (293, 294, 398, 399). Overall the overlap rate between the published screens is surprisingly low (120, 260), albeit

each identified a huge number of proteins. This may be due to different settings of the individual screening approaches. All screens differ in cell lines, RNAi libraries, duration of knockdown, reporter assays, HIV-1 types, and other important factors such as statistical analysis and hit definition. For a more detailed reviews of the difference of four of the mentioned HIV-1 screens please see the publications from Bushman (120) and Hirsch (400).

The results of this work as well show only a small overlap with the previously published screens. Only one overlap with each of Brass et al. (212), Zhou et al. (283), Jiang et al. (293), and Wen et al. (294); two overlaps with Yeung et al. (398); and no overlap with König et al. (258) or Rato et al. (399). Table 21 lists the overlap with the aforementioned screens.

Table 21 Overlaps between the results of this work and published RNAi screens.

Overlap with	Gene symbol	Ref Seq ID	Full gene name
Brass et al. (212)	ITPKA	NM_002220	Inositol 1,4,5-trisphosphate 3-kinase A
Zhou et al. (283)	MAP3K14	NM_003954	Mitogen-activated protein kinase kinase kinase 14
Jiang et al. (293)	HKDC1	NM_025130	Hexokinase domain containing 1
Wen et al. (294)	MAP4K2	NM_004579	Mitogen-activated protein kinase kinase kinase kinase 2
Yeung et al. (398)	PIK3CG	NM_002649	Phosphoinositide-3-kinase, catalytic, gamma polypeptide
Yeung et al. (398)	IRAK4	NM_016123	Interleukin-1 receptor-associated kinase 4

Interestingly some primary hits, which could not be validated during the reconfirmation screen showed up in the results of the other published screens as well. For example, BLK were identified by Jiang et al. (293) and LIMK1 was even the strongest hit in Wen et al. (294).

On the first thought is seems to be astonishing to have such a low rate of similar hits resulting from all of these screening approaches. But as mentioned before, all of the screens differ in many details from each other and some

publications only conducted primary screens without any reconfirmation tests. As each of the screens reveals a shrouded view on a specific situation, it appears to be of much higher relevance to leave the level of individual proteins and move to their connecting pathways and networks.

5.4 The broader picture: Signaling pathways

Looking more closely on the relation of the identified proteins appears to be a better option to enhance the significance of the picture. Although the results of this work and the other publications differed greatly on the level of single proteins, it is interesting to note that similar pathways were identified in each case. Table 19 lists the enriched pathways from this work. The highest ranking pathways were the MAP kinase pathway, the RAP1 pathway, and the mTOR pathway.

One striking example for the benefit of combinatory network analyses is the mechanistic Target of Rapamycin (mTOR) pathway. It is very complex and regulates several important functions in the cell – for example proliferation, survival, metabolism, growth, stress response, and cytoskeletal organization (312). Taking into account the closely related PI3K/AKT pathway, six different proteins were identified in this work, which are involved in this pathway. These include proteins from the beginning of the signaling cascade like growth factor receptors (FGFR2 and IGF1R), over intermediate regulators as PI3K and BRAF up to effectors downstream of the mTOR complex such as RPS6KA2 and RPS6KB1. In addition, the other screens reported many other parts of the mTOR pathway including the central regulator AKT (212, 283). A complete list is given in Table 22.

Table 22 Identified members of the mTOR/PI3K/AKT pathway.

Gene symbol	Gene name	Hit in
AKT	AKT serine/threonine kinase 1	(212, 283)
AMPK	5' AMP-activated protein kinase	(283)

Gene symbol	Gene name	Hit in
ARF6	ADP ribosylation factor 6	(294)
BRAF	V-raf murine sarcoma viral oncogene homolog B1	Hermle
FGFR2	Fibroblast growth factor receptor 2 (bacteria-expressed kinase, keratinocyte growth factor receptor, craniofacial dysostosis 1, Crouzon syndrome, Pfeiffer syndrome, Jackson-Weiss syndrome)	Hermle
FOXO3	Forkhead box O3	(398)
IGF1R	Insulin-like growth factor 1 receptor	Hermle
IKBKB	Inhibitor of kappa light polypeptide gene enhancer in B-cells, kinase beta	(258)
NFKB1	Nuclear factor kappa B subunit 1	(398)
NRAS	Neuroblastoma RAS viral oncogene homolog	(398)
PI3K	Phosphoinositide-3-kinase	Hermle, (258, 398)
PPP2R1A	Protein phosphatase 2 scaffold subunit Alpha	(258)
PPP2R5E	Protein phosphatase 2 regulatory subunit B'epsilon	(258)
PTEN	Phosphatase and tensin homolog	(398)
RPS6KA2	Ribosomal protein S6 kinase, 90kDa, polypeptide 2	Hermle
RPS6KB1	Ribosomal protein S6 kinase, 70kDa, polypeptide 1	Hermle
RRAS2	Related RAS viral (r-ras) oncogene homolog 2	(398)
SGK1	Serum/glucocorticoid regulated kinase 1	(399)
SHC1	SHC adaptor protein 1	(258)
YWHAB	Tyrosine 3-monooxygenase/tryptophan 5-monooxygenase activation protein beta	(258)

The identification of so many members of the PI3K/AKT/mTOR pathway makes it a very interesting candidate for follow-up studies. And indeed, recent publications added indications of an important role of this pathway for the replication of various viruses including HIV-1 (401). As an example for the interplay of factors found to be involved in the PI3K/AKT/mTOR pathway, one noticeable signaling cluster is discussed in more detail. A group of the

components listed above represents the majority of a signaling cascade, which leads to the inhibition of FOXO transcription suppressors. FOXO inhibition leads to increased expression of several genes involved in cell survival, enhanced proliferation, and improved stress responses (402). PI3K activates AKT and SGK1 (and potentially activates mTOR complex 2 (mTORC2)). Active SGK1 translocates into the nucleus and phosphorylates the transcription factor FoxO3, which in turn is excluded from the nucleus and is inactivated by additional phosphorylation by AKT. With FoxO3 inactive and removed from the nucleus, transcription of several genes is no longer blocked (403, 404). From this network, PI3K and SGK1 were identified in this work. Other screens identified PI3K, AKT, SGK1, and FoxO3. In addition, other upstream regulators of PI3K and mTORC2 were identified both in this work and other screens. An overview of the FoxO3 signaling network and its identified members are depicted in Figure 5-2. This hypothesis describes a signaling cascade, which potentially could influence HIV-1 expression in infected cells. Its role has to be elucidated in the future.

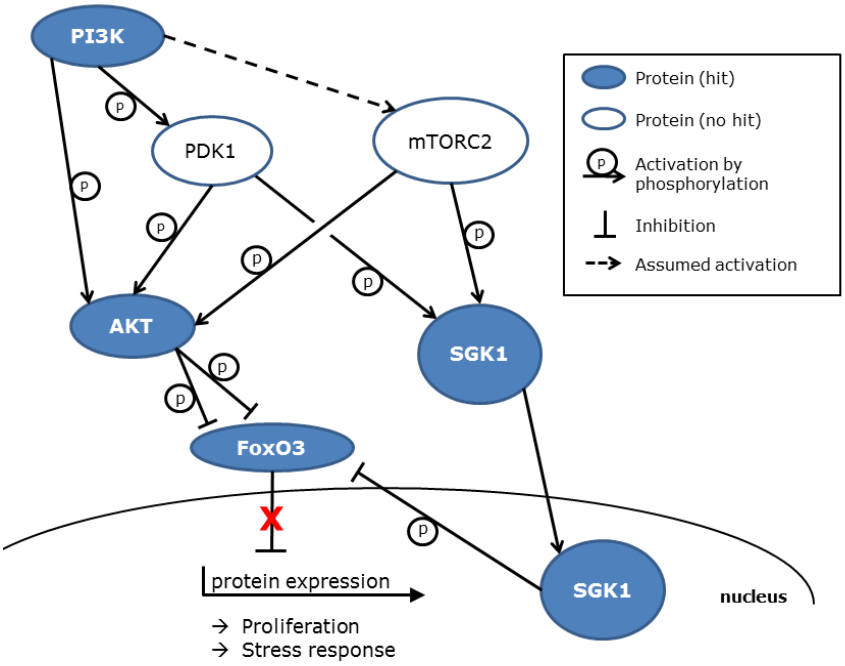

Figure 5-2: Potential Foxo3 signaling cascade regulating proliferation.
The map shows the described signaling cascade regulating FoxO3 and its role in protein expression, proliferation, and stress response. Blue circles indicate proteins, which were identified in RNAi screens (this work and other publications) to be involved in HIV-1 replication. Open circles indicate HIV-1 independent proteins. Lines with an arrowhead indicate activation by phosphorylation, while lines with a blunt end mark inhibitory phosphorylations. The dashed line shows the assumed activation of mTORC2 by PI3K, which is currently debated. Based on (403).

Several hypotheses can be based on the identified signaling networks. An alternative role of the PI3K/AKT/mTOR especially during assembly and release of HIV-1 may be its involvement in the organization of the cytoskeleton and actin remodeling (405). It was shown, that PI3K, AKT and mTOR are involved in actin polymerization and cell migration (406). This is consistent to the fact that LIMK1, a very important activator of actin polymerization, was identified by Wen et al. (294, 395). As described above, LIMK1 was a primary hit in this work as well, but missed the threshold in the reconfirmation screen. Cytoskeleton organization was linked to HIV-1 assembly in the past, as actin filaments were detected in close proximity of and directing towards budding sites by cryo-EM (407). However, recent investigations by the group of Barbara Müller showed no effect of drugs, which either stabilize or destabilize actin filaments, on assembly efficiency (408). A different process regulated by the mTOR pathway is autophagy, which was shown to be important for HIV-1, although not for assembly and release (409, 410). In addition, novel mTOR kinase inhibitors (TOR-KIs) were reported to inhibit replication of HIV-1 in humanized mice (411). All these facts combined, the PI3K/AKT/mTOR pathway appears to be a very prominent pathway involved in (but apparently not limited to) assembly and release of HIV-1 and more work has to be conducted in the future to unravel its details.

5.5 Conclusion

Multiple host cell factors were identified by this work. An involvement with HIV-1 assembly and release was already discussed for some of them in the literature but novel factors were described as well. The latter represent new targets for future investigations. Especially interesting hits represent SPHK1, which caused the strongest reduction of HIV 1 particle release after knockdown, or other “strong” host cell factors like MAP3K14 and PAPSS1. Although the overlap among several published screens is limited on a protein level, similar pathways were mutually identified, such as the MAPK or the PI3K/AKT pathways. This shows that the detection of individual hits is directly coupled to technical details such as cells type, knockdown conditions, or the readout and can barely be compared. Therefore, the focus should lie to a greater degree on

these main pathways, without neglecting the key proteins. My confirmed host cell factors in view of the published literature and the here applied combinatory pathway identification approach including hits from other screens will be a basis for follow-up studies. In this way, the next step can be taken to unravel the mechanisms of how HIV-1 utilizes these pathways to facilitate its assembly and release.

6 List of figures

7 List of tables

8 List of abbreviations

A, mA	Ampere, mili Ampere
aa	Amino acid
AA	Acrylamide
Ago2	Argonaute-2
AIDS	Acquired immunodeficiency virus
AIP1	Actin-interacting protein 1
ALG-2	Apoptosis-linked gene 2
ALIX	ALG-2 interacting protein X
APOBEC3G	Apoplipoprotein B mRNA-editing, enzyme-catalytic, polypeptide-like 3G
app.	Approximately
APS	Ammonium peroxodisulfate
ATP	Adenosine-tri-phosphate
BIS	N,N'-methylene bisacrylamide
C. elegans	Caenorhabditis elegans
CA	Capsid
CAI	Capsid assembly inhibitor, 12-mer peptide
CAP-1	Capsid assembly inhibitor; N-(3-chloro-4-methylphenyl)-N'-[2-[([5-[(dimethylamino)-methyl]-2-furyl]-methyl)-sulfanyl]ethyl]urea)
cART	Combination anti-retroviral therapy
CBD	Chromatin binding domain
CCR5	CC chemokine receptor 5
CD4	Cluster of differentiation 4 receptor
CD8	Cluster of differentiation 8 receptor
CDK1	Cyclin-dependent kinase 1
CDK2	Cyclin-dependent kinase 1
CL	Cell lysate
CTD	C-terminal domain
CXCR4	CXC chemokine receptor 4
CypA	Cyclophilin A
DLBCL	Diffuse large B-cell lymphoma

DMEM	Dulbecco's Modified Eagle Medium
DNA	Desoxyribonucleic acid
dNTPs	Deoxy-nucleoside-triphosphates
e.g.	Example given
EAP	ELL-associated protein
ECL	Enhanced chemiluminescence
EDTA	Ethylene-diamine-tetra-acetic acid
EIAV	Equine Infectious Anemia Virus
ELISA	Enzyme-linked immunosorbent assay
EM	Electron microscopy
EMBL	European Molecular Biology Laboratory
Env	Envelope
ERK-2	MAPK-1, mitogen-activated protein kinase 1
ESCRT	Endosomal trafficking complex required for transport
Exp5	Exportin-5
eYFP	Enhanced yellow fluorescent protein
FCS	Fetal calf serum
Fig.	Figure
Gag	Group specific antigen
gp	Glycoprotein
GO	Gene Onthology
h	Hour
HAART	Highly Active Antiretroviral Therapy
HDF	Host dependency factor
HIV-1	Human immunodeficiency virus-1
HRF	Host restriction factor
HSP	Heat shock protein
HSPG	Heparin sulphate proteoglycans
HTLV	Human T cell leukemia virus
HTS	High throughput screen
ID	Identifier
Ig	Immunoglobulin
IN	HIV-1 integrase

JNK	c-Jun N-terminal kinase
kb	Kilo base pairs
kDa	Kilo Dalton
KEGG	Kyoto Encyclopedia of Genes and Genomes
Late (-)	Late domain deficient; in experiments Late (-) indicates an equimolar mixture of pCHIV^{eYFP}.late(-):pCHIV.late(-)
LB	Lysogeny broth
LEDGF	Lens epithelium–derived growth factor p75 splice variant
LOWESS	Lnocally weighted scatterplot smoothing
LTR	Long terminal repeat
M	Molar, mol per litre
MA	Matrix
MAP	Mitogen-activated protein
MHC	Major histocompatibility complex
miRNA	Micro RNA
mRNA	Messenger RNA
mTOR	Mechanistic Target of Rapamycin
MVB	Multivesicular body
n	Number of repetitions
NC	Nucleocapsid
Nedd4	Neural precursor cell expressed, developmentally down-regulated 4
NIK	NFkB inducing kinase = MAP3K14
Nup	Nucleoporin
nsc	Non-silencing control siRNA
nt	Nucleotide
NTD	N-terminal domain
p24	Alternative designation of the HIV-1 CA protein
p6	Protein domain 6
PAGE	Polyacrylamide gel electrophoresis
PBMC	Peripheral blood mononuclear cell
PBS	Phosphate buffered saline

PCR	Polymerase chain reaction
PI(4,5)P2	Phosphatidylinositol-(4,5)-bisphosphate
PI3P	Phosphatidylinositol (3,4,5)-trisphosphate
PIC	Preintegration complex
pol	Polymerase
Pol II	DNA-dependend-RNA-polymerase II
PPXY	Amino acid motif, late domain
PR	Protease
PTAP	Amino acid motif, late domain
Ref Seq	Reference Sequence collection
RISC	RNA induced silencing complex
RNA	Ribonucleic acid
RNAi	RNA interference
rpm	Rotations per minute
RSV	Rous sarcoma virus
RT	Room temperature or Reverse Transcriptase
RTC	Reverse transcription complex
SAMHD1	SAM domain and HD domain-containing protein 1
SDS	Sodium dodecyl sulfate
shRNA	Short hairpin RNA
siRNA	Small interfering RNA
SN	Supernatant
SP1	Spacer peptide 1
SP2	Spacer peptide 2
ssRNA	Single strand RNA
TBK	TANK binding kinase 1
TBS	Tris buffered saline
TMB	3,3',5,5' tetramethylbenzidine
Total supernatant	Total fluorescence intensity in cell lysate and
TRIM5a	Tripartite motif-containing protein 5
Tris	Tris(hydroxymethyl)aminomethane
TSG101	Tumor suppressor gene 101
U	Unit

UNAIDS	Joint United Nations Programme on HIV/AIDS
UTR	Untranslated terminal region
V	Volt
Vps	Vacuolar protein sorting
vs.	Versus
W	Watt
WT	Wild type; in experiments WT indicates the equimolar Mixtures of pCHIV^{eYFP}:pCHIV
WW	Prolin rich protein interaction domain
YFP	Yellow fluorescent protein
YPXL	Amino acid motif, late domain

9 List of publications

Publications in peer reviewed journals *(# = contributed equally)*

Hermle J, Anders M, Heuser AM, Müller B: A simple fluorescence based assay for quantification of human immunodeficiency virus particle release. BMC Biotechnol 2010, 20; 10:32.(238)

Börner K#, **Hermle J#**, Sommer C, Brown NP, Knapp B, Glass B, Kunkel J, Torralba G, Reymann J, Beil N, Beneke J, Pepperkok R, Schneider R, Ludwig T, Hausmann M, Hamprecht F, Erfle H, Kaderali L, Kräusslich HG, Lehmann MJ: From experimental setup to bioinformatics: an RNAi screening platform to identify host factors involved in HIV-1 replication. Biotechnol J 2010, 5(1): 39-49. (274)

Perkovic M, Schmidt S, Marino D, Russell RA, Stauch B, Hofmann H, Kopietz F, Kloke BP, Zielonka J, Ströver H, **Hermle J**, Lindemann D, Pathak VK, Schneider G, Löchelt M, Cichutek K, Münk C: Species-specific inhibition of APOBEC3C by the prototype foamy virus protein bet. J Biol Chem. 2009, 27; 284(9): 5819-26. (412)

Oral presentations *(* = presenting author)*

Hermle J*, Börner K, Mazur J, Brown NP, Anders M, Müller B, Schneider R, Erfle H, Pepperkok R, Kaderali L, Lehmann MJ, Kräusslich HG. RNAi screen to identify human host cell factors required for HIV-1 release. Eurovirology Meeting, April 2010, Cernobbio, Italy

Lehmann MJ, **Hermle J***, Börner K, Kaderali L, Erfle H, Pepperkok R, Kräusslich HG. High-Througput siRNA screening to identify human host factors involved in pathogenesis of HIV-1. Jahrestagung der Gesellschaft für Virologie, März 2008, Heidelberg, Germany

Münk C*, Perković M, **Hermle J**, Kloke BP, Chareza S, Löchelt M, Cichutek K: The primate foamy virus Bet protein protects HIV and SIV against APOBEC3-induced
deamination by a novel pathway not involving the proteasome. Retrovirus Meeting, Mai 2006, Cold Spring Harbour, USA

Poster presentations

Hermle J, Lehmann MJ, Börner K, Mazur J, Brown NP, Heuser AM, Anders M,
Schneider R, Erfle H, Pepperkok R, Kaderali L, Müller B, Kräusslich HG: A random screening assay for indentification of inhibitors of, and host-cell factors involved in HIV-1 morphogenesis. Retrovirus Meeting, Mai 2010, Cold Spring Harbor, New York, USA

Börner K, Wiedtke E, Brown N, Schürmann N, **Hermle J**, Kaderali L, Kräusslich HG, Grimm D: Improvement of RNAi screens via stable Ago-2 over-expression. Keystone Meeting on RNA silencing, Januar 2010, Keystone, USA.

Hermle J, Lehmann MJ, Börner K, Mazur J, Anders M, Müller B, Erfle H, Pepperkok R, Kaderali L, Kräusslich HG: RNAi screen to identify human host cell factor networks required for HIV-1 release. German Symposium on Systems Biology, Mai 2009, Heidelberg, Germany

Börner K, **Hermle J**, Sommer C, Glass B, Brown NP, Kunkel J, Reymann J, Beil N, Beneke J, Pepperkok R, Schneider R, Ludwig T, Hamprecht F, Erfle H, Kaderali L, Lehmann MJ, Kräusslich HG: Identification of new cellular interaction partners of HIV-1 using high-throughput siRNA screening. German Symposium on Systems Biology, Mai 2009, Heidelberg, Germany

Hermle J, Lehmann MJ, Börner K, Mazur J, Anders M, Müller B, Erfle H, Pepperkok R, Kaderali L, Kräusslich HG: Identification of host cell factors involved in release of HIV-1 by siRNA screening. Jahrestagung der Gesellschaft für Virologie, März 2009, Leipzig, Germany

Lehmann MJ, **Hermle J**, Börner K, Kaderali L, Erfle H, Pepperkok R, Kräusslich HG: High-throughput siRNA screening to identify virus-host interactions involved in pathogenesis of HIV-1. FORSYS Konferenz, Juni 2008, Berlin, Germany

Lehmann MJ, Börner K, **Hermle J**, Kaderali L, Erfle H, Pepperkok R, Kräusslich HG: High-throughput siRNA screening to identify host-virus interactions involved in pathogenesis of HIV-1. System Biologie Konferenz, Mai 2008, Dresden, Germany

Börner K, **Hermle J**, Erfle H, Pepperkok R, Kräusslich HG, Lehmann MJ: Using adequate standards to enhance the robustness of high-throughput siRNA screens.
Jahrestagung der Gesellschaft für Virologie, März 2008, Heidelberg, Germany

10 Acknowledgments

At first I would like to thank my parents for everything. I am truly and always grateful for your support throughout my whole life. As well I would like to thank Nina for being at my side for the whole time, for enduring my ups and downs, and for catching me when I needed it the most. You cannot imagine how glad I am for having you in my life!

I would like to thank Hans-Georg Kräusslich for the opportunity to perform this work in his lab. I am grateful for the advice, the support, the helo and the understanding he offered to me in order to bring this work to a successful end after all. I thank the complete Kräusslich lab, all members of the Müller lab as well as Oliver Fackler, Oliver Keppler and Dirk Grimm and their entire groups for the constant support, the disussions and good working atmosphere throughout my time in the lab. In addition, I appreciate very much that Dirk Grimm agreed to be my second referee. And in advance I would like to thank Walter Nickel and Hans-Michael Müller for being reviewers in my defence. Special thanks to Maik Lehmann for supervising me; to Kathleen Börner for all the shared moments and days and evenings and for the great time; to Bärbel Glass, Walter Muranyi, Peter Koch, Maria Anders, Anke-Mareil Heuser and Heike Oberwinkler, for the invaluable support thoughout my time in the lab. In addition, I would like to thank Lars Kaderali and Johanna Mazur for the statistical support of my work and for answering my many questions. As well I want to thank Holger Erfle, Nina Beil and Jürgen Beneke from the ViroQuant CellNetworks RNAi Screening Facility. And of course many thanks to all the other participants in our “journey” to set up the different screening assays in the BioQuant.

Many thanks to Martin Westphal, Johannes Harleman, Silke Baasner and Melanie Bothe at Fresenius Kabi – I am extremely grateful that they believed in me and that they poked me often and hard enough to continue.

Last but not least I would like to thank everyone who supported the writing of this thesis by comments, discussions and critical reviews.

11 References

1. **Barré-Sinoussi F, Chermann JC, Rey F, Nugeyre MT, Chamaret S, Gruest J, Dauguet C, Axler-Blin C, Vézinet-Brun F, Rouzioux C, Rozenbaum W, Montagnier L.** 2004. Isolation of a T-lymphotropic retrovirus from a patient at risk for acquired immune deficiency syndrome (AIDS). 1983. Revista De Investigación Clínica; Organo Del Hospital De Enfermedades De La Nutrición **56:**126-129.
2. **Gallo RC, Salahuddin SZ, Popovic M, Shearer GM, Kaplan M, Haynes BF, Palker TJ, Redfield R, Oleske J, Safai B.** 1984. Frequent detection and isolation of cytopathic retroviruses (HTLV-III) from patients with AIDS and at risk for AIDS. Science (New York, NY) **224:**500-503.
3. **Gottlieb MS, Groopman JE, Weinstein WM, Fahey JL, Detels R.** 1983. The acquired immunodeficiency syndrome. Annals of Internal Medicine **99:**208-220.
4. **(UNAIDS) UJPoHA.** 2016. Global AIDS Update 2016.
5. **(UNAIDS) UJPoHA.** 2016. Fact sheet November 2016.
6. **AIDS.gov.** 11/16/2010 2010. Opportunistic Infections and Their Relationship to HIV/AIDS. https://www.aids.gov/hiv-aids-basics/staying-healthy-with-hiv-aids/potential-related-health-problems/opportunistic-infections/. Accessed
7. **Dybul M, Fauci AS, Bartlett JG, Kaplan JE, Pau AK.** 2002. Guidelines for using antiretroviral agents among HIV-infected adults and adolescents. Annals of Internal Medicine **137:**381-433.
8. **Hofmann WP, Soriano V, Zeuzem S.** 2009. Antiviral combination therapy for treatment of chronic hepatitis B, hepatitis C, and human immunodeficiency virus infection. Handbook of Experimental Pharmacology doi:10.1007/978-3-540-79086-0_12**:**321-346.
9. **Li X, Margolick JB, Jamieson BD, Rinaldo CR, Phair JP, Jacobson LP.** 2011. CD4+ T-cell counts and plasma HIV-1 RNA levels beyond 5 years of highly active antiretroviral therapy. J Acquir Immune Defic Syndr **57:**421-428.
10. **Adolescents. PoAGfAa.** Guidelines for the use of antiretroviral agents in HIV-1-infected

adults and adolescents. Department of Health and Human Services Available at http://wwwaidsinfonihgov/ContentFiles/AdultandAdolescentGL

pdf Accessed [March 26, 2017].

11. **De Clercq E.** 2002. New developments in anti-HIV chemotherapy. Biochim Biophys Acta **1587:**258-275.
12. **Akanitapichat P, Bastow KF.** 2002. The antiviral agent 5-chloro-1,3-dihydroxyacridone interferes with assembly and maturation of herpes simplex virus. Antiviral Res **53:**113-126.
13. **Sticht J, Humbert M, Findlow S, Bodem J, Müller B, Dietrich U, Werner J, Kräusslich H-G.** 2005. A peptide inhibitor of HIV-1 assembly in vitro. Nature Structural & Molecular Biology **12:**671-677.
14. **Kilgore NR.** 2007. Poster: Characterization of PA1050040, a second generation HIV-1 maturation inhibitor. (Abstract no. MOPDX05), abstr

Fourth International AIDS Society Conference on HIV Pathogenesis, Treatment and Prevention, Sydney, Australia, 22-25 July 2007.

15. **Blair WS, Cao J, Jackson L, Jimenez J, Peng Q, Wu H, Isaacson J, Butler SL, Chu A, Graham J, Malfait AM, Tortorella M, Patick AK.** 2007. Identification and characterization of UK-201844, a novel inhibitor that interferes with human immunodeficiency virus type 1 gp160 processing. Antimicrob Agents Chemother **51:**3554-3561.
16. **Spearman P.** 2016. HIV-1 Gag as an Antiviral Target: Development of Assembly and Maturation Inhibitors. Curr Top Med Chem **16:**1154-1166.
17. **Van Baelen K, Salzwedel K, Rondelez E, Van Eygen V, De Vos S, Verheyen A, Steegen K, Verlinden Y, Allaway GP, Stuyver LJ.** 2009. Susceptibility of human immunodeficiency virus type 1 to the maturation inhibitor bevirimat is modulated by baseline polymorphisms in Gag spacer peptide 1. Antimicrob Agents Chemother **53:**2185-2188.
18. **Seclen E, Gonzalez Mdel M, Corral A, de Mendoza C, Soriano V, Poveda E.** 2010. High prevalence of natural polymorphisms in Gag (CA-SP1) associated with reduced response to Bevirimat, an HIV-1 maturation inhibitor. AIDS **24:**467-469.
19. **Lawrence S.** 2016. GSK drops a pair of late stage candidates in COPD and HIV-1. FierceBiotech,
20. **Chen R, Quinones-Mateu ME, Mansky LM.** 2005. HIV-1 mutagenesis during antiretroviral therapy: implications for successful drug treatment. Front Biosci **10:**743-750.
21. **Roberts JD, Bebenek K, Kunkel TA.** 1988. The accuracy of reverse transcriptase from HIV-1. Science **242:**1171-1173.
22. **Votteler JS, Ulrich.** 2008. Human Immunodeficiency Viruses: Molecular Biology. Encyclopedia of Virology**:**517-525.
23. **de Marco A, Müller B, Glass B, Riches JD, Kräusslich H-G, Briggs JAG.** 2010. Structural Analysis of HIV-1 Maturation Using Cryo-Electron Tomography. PLoS Pathogens **6**.
24. **Hallenberger S, Moulard M, Sordel M, Klenk HD, Garten W.** 1997. The role of eukaryotic subtilisin-like endoproteases for the activation of human immunodeficiency virus glycoproteins in natural host cells. Journal of Virology **71:**1036-1045.
25. **Moulard M, Decroly E.** 2000. Maturation of HIV envelope glycoprotein precursors by cellular endoproteases. Biochim Biophys Acta **1469:**121-132.
26. **Coffin JM, Hughes SH, Varmus HE.** 1997. Retroviruses. Cold Spring Harbor Laboratory Press, Cold Spring Harbor, NY.
27. **Flint SJ, Enquist LW, Racaniello VR, Skalka AM.** 2009. Principles of Virology, 3rd Edition ed. John Wiley & Sons.
28. **Fackler OT, Geyer M.** 2002. Der Aktivität des Nef-Proteins auf der Spur: Neue Strategien für die Bekämpfung von HIV. Biologie in unserer Zeit **32:**90-100.
29. **Kuiken C, Leitner T, Foley B, Hahn B, Marx P, McCutchan F, Wolinsky S, Korber B.** HIV Sequence Compendium 2010.
30. **Briggs JAG, Wilk T, Welker R, Kräusslich H-G, Fuller SD.** 2003. Structural organization of authentic, mature HIV-1 virions and cores. The EMBO Journal **22:**1707-1715.

31. **Checkley MA, Luttge BG, Freed EO.** 2011. HIV-1 envelope glycoprotein biosynthesis, trafficking, and incorporation. Journal of Molecular Biology **410:**582-608.
32. **Chertova E, Bess JW, Jr., Crise BJ, Sowder Ii RC, Schaden TM, Hilburn JM, Hoxie JA, Benveniste RE, Lifson JD, Henderson LE, Arthur LO.** 2002. Envelope glycoprotein incorporation, not shedding of surface envelope glycoprotein (gp120/SU), Is the primary determinant of SU content of purified human immunodeficiency virus type 1 and simian immunodeficiency virus. Journal of Virology **76:**5315-5325.
33. **Zhu P, Chertova E, Bess J, Jr., Lifson JD, Arthur LO, Liu J, Taylor KA, Roux KH.** 2003. Electron tomography analysis of envelope glycoprotein trimers on HIV and simian immunodeficiency virus virions. Proceedings of the National Academy of Sciences of the United States of America **100:**15812-15817.
34. **Zhu P, Liu J, Bess J, Jr., Chertova E, Lifson JD, Grisé H, Ofek GA, Taylor KA, Roux KH.** 2006. Distribution and three-dimensional structure of AIDS virus envelope spikes. Nature **441:**847-852.
35. **Briggs JAG, Kräusslich H-G.** 2011. The molecular architecture of HIV. Journal of Molecular Biology **410:**491-500.
36. **Briggs JAG, Simon MN, Gross I, Kräusslich H-G, Fuller SD, Vogt VM, Johnson MC.** 2004. The stoichiometry of Gag protein in HIV-1. Nature Structural & Molecular Biology **11:**672-675.
37. **Carlson L-A, Briggs JAG, Glass B, Riches JD, Simon MN, Johnson MC, Müller B, Grünewald K, Kräusslich H-G.** 2008. Three-dimensional analysis of budding sites and released virus suggests a revised model for HIV-1 morphogenesis. Cell Host & Microbe **4:**592-599.
38. **Wright ER, Schooler JB, Ding HJ, Kieffer C, Fillmore C, Sundquist WI, Jensen GJ.** 2007. Electron cryotomography of immature HIV-1 virions reveals the structure of the CA and SP1 Gag shells. The EMBO Journal **26:**2218-2226.
39. **Ganser BK, Li S, Klishko VY, Finch JT, Sundquist WI.** 1999. Assembly and analysis of conical models for the HIV-1 core. Science (New York, NY) **283:**80-83.
40. **Li S, Hill CP, Sundquist WI, Finch JT.** 2000. Image reconstructions of helical assemblies of the HIV-1 CA protein. Nature **407:**409-413.
41. **Mattei S, Glass B, Hagen WJ, Krausslich HG, Briggs JA.** 2016. The structure and flexibility of conical HIV-1 capsids determined within intact virions. Science **354:**1434-1437.
42. **Ganser-Pornillos BK, Yeager M, Sundquist WI.** 2008. The structural biology of HIV assembly. Current Opinion in Structural Biology **18:**203-217.
43. **Bruner KM, Hosmane NN, Siliciano RF.** 2015. Towards an HIV-1 cure: measuring the latent reservoir. Trends Microbiol **23:**192-203.
44. **Siliciano JD, Kajdas J, Finzi D, Quinn TC, Chadwick K, Margolick JB, Kovacs C, Gange SJ, Siliciano RF.** 2003. Long-term follow-up studies confirm the stability of the latent reservoir for HIV-1 in resting CD4+ T cells. Nat Med **9:**727-728.
45. **Ono A.** 2009. HIV-1 Assembly at the Plasma Membrane: Gag Trafficking and Localization. Future Virology **4:**241-257.

46. **Ono A, Freed EO.** 2004. Cell-type-dependent targeting of human immunodeficiency virus type 1 assembly to the plasma membrane and the multivesicular body. Journal of virology **78:**1552-1563.
47. **Welsch S, Keppler OT, Habermann A, Allespach I, Krijnse-Locker J, Kräusslich H-G.** 2007. HIV-1 buds predominantly at the plasma membrane of primary human macrophages. PLoS pathogens **3**.
48. **Kutluay SB, Bieniasz PD.** 2010. Analysis of the initiating events in HIV-1 particle assembly and genome packaging. PLoS Pathogens **6**.
49. **Kuzembayeva M, Dilley K, Sardo L, Hu WS.** 2014. Life of psi: how full-length HIV-1 RNAs become packaged genomes in the viral particles. Virology **454-455:**362-370.
50. **Klein KC, Reed JC, Lingappa JR.** 2007. Intracellular destinies: degradation, targeting, assembly, and endocytosis of HIV Gag. AIDS Reviews **9:**150-161.
51. **Hendrix J, Baumgartel V, Schrimpf W, Ivanchenko S, Digman MA, Gratton E, Krausslich HG, Muller B, Lamb DC.** 2015. Live-cell observation of cytosolic HIV-1 assembly onset reveals RNA-interacting Gag oligomers. J Cell Biol **210:**629-646.
52. **Hermida-Matsumoto L, Resh MD.** 2000. Localization of human immunodeficiency virus type 1 Gag and Env at the plasma membrane by confocal imaging. Journal of Virology **74:**8670-8679.
53. **Dong X, Li H, Derdowski A, Ding L, Burnett A, Chen X, Peters TR, Dermody TS, Woodruff E, Wang J-J, Spearman P.** 2005. AP-3 directs the intracellular trafficking of HIV-1 Gag and plays a key role in particle assembly. Cell **120:**663-674.
54. **Balasubramaniam M, Freed EO.** 2011. New insights into HIV assembly and trafficking. Physiology (Bethesda) **26:**236-251.
55. **Bryant M, Ratner L.** 1990. Myristoylation-dependent replication and assembly of human immunodeficiency virus 1. Proceedings of the National Academy of Sciences of the United States of America **87:**523-527.
56. **Göttlinger HG, Sodroski JG, Haseltine WA.** 1989. Role of capsid precursor processing and myristoylation in morphogenesis and infectivity of human immunodeficiency virus type 1. Proceedings of the National Academy of Sciences of the United States of America **86:**5781-5785.
57. **Olety B, Veatch SL, Ono A.** 2015. Phosphatidylinositol-(4,5)-Bisphosphate Acyl Chains Differentiate Membrane Binding of HIV-1 Gag from That of the Phospholipase Cdelta1 Pleckstrin Homology Domain. J Virol **89:**7861-7873.
58. **Olety B, Ono A.** 2014. Roles played by acidic lipids in HIV-1 Gag membrane binding. Virus Res **193:**108-115.
59. **Vlach J, Saad JS.** 2015. Structural and molecular determinants of HIV-1 Gag binding to the plasma membrane. Front Microbiol **6:**232.
60. **Ono A, Ablan SD, Lockett SJ, Nagashima K, Freed EO.** 2004. Phosphatidylinositol (4,5) bisphosphate regulates HIV-1 Gag targeting to the plasma membrane. Proceedings of the National Academy of Sciences of the United States of America **101:**14889-14894.
61. **Resh MD.** 2004. A myristoyl switch regulates membrane binding of HIV-1 Gag. Proceedings of the National Academy of Sciences of the United States of America **101:**417-418.

62. **Tang C, Loeliger E, Luncsford P, Kinde I, Beckett D, Summers MF.** 2004. Entropic switch regulates myristate exposure in the HIV-1 matrix protein. Proceedings of the National Academy of Sciences of the United States of America **101:**517-522.
63. **Nguyen DH, Hildreth JE.** 2000. Evidence for budding of human immunodeficiency virus type 1 selectively from glycolipid-enriched membrane lipid rafts. Journal of Virology **74:**3264-3272.
64. **Ono A.** 2010. Relationships between plasma membrane microdomains and HIV-1 assembly. Biology of the Cell / Under the Auspices of the European Cell Biology Organization **102:**335-350.
65. **Ono A, Freed EO.** 2005. Role of lipid rafts in virus replication. Advances in Virus Research **64:**311-358.
66. **Saad JS, Miller J, Tai J, Kim A, Ghanam RH, Summers MF.** 2006. Structural basis for targeting HIV-1 Gag proteins to the plasma membrane for virus assembly. Proceedings of the National Academy of Sciences of the United States of America **103:**11364-11369.
67. **Lorizate M, Sachsenheimer T, Glass B, Habermann A, Gerl MJ, Krausslich HG, Brugger B.** 2013. Comparative lipidomics analysis of HIV-1 particles and their producer cell membrane in different cell lines. Cell Microbiol **15:**292-304.
68. **Brügger B, Glass B, Haberkant P, Leibrecht I, Wieland FT, Kräusslich H-G.** 2006. The HIV lipidome: a raft with an unusual composition. Proceedings of the National Academy of Sciences of the United States of America **103:**2641-2646.
69. **Resh MD.** 2005. Intracellular trafficking of HIV-1 Gag: how Gag interacts with cell membranes and makes viral particles. AIDS Reviews **7:**84-91.
70. **Ganser-Pornillos BK, Yeager M, Pornillos O.** 2012. Assembly and architecture of HIV. Adv Exp Med Biol **726:**441-465.
71. **Burniston MT, Cimarelli A, Colgan J, Curtis SP, Luban J.** 1999. Human immunodeficiency virus type 1 Gag polyprotein multimerization requires the nucleocapsid domain and RNA and is promoted by the capsid-dimer interface and the basic region of matrix protein. Journal of Virology **73:**8527-8540.
72. **Göttlinger HG.** 2001. The HIV-1 assembly machine. AIDS (London, England) **15 Suppl 5:**S13-20.
73. **O'Carroll IP, Soheilian F, Kamata A, Nagashima K, Rein A.** 2013. Elements in HIV-1 Gag contributing to virus particle assembly. Virus Res **171:**341-345.
74. **Briggs JAG, Riches JD, Glass B, Bartonova V, Zanetti G, Kräusslich HG.** 2009. Structure and assembly of immature HIV. Proceedings of the National Academy of Sciences of the United States of America **106:**11090-11095.
75. **Demirov DG, Freed EO.** 2004. Retrovirus budding. Virus Research **106:**87-102.
76. **Morita E, Sundquist WI.** 2004. Retrovirus budding. Annual Review of Cell and Developmental Biology **20:**395-425.
77. **Prescher J, Baumgartel V, Ivanchenko S, Torrano AA, Brauchle C, Muller B, Lamb DC.** 2015. Super-resolution imaging of ESCRT-proteins at HIV-1 assembly sites. PLoS Pathog **11:**e1004677.

78. **Gheysen D, Jacobs E, de Foresta F, Thiriart C, Francotte M, Thines D, De Wilde M.** 1989. Assembly and release of HIV-1 precursor Pr55gag virus-like particles from recombinant baculovirus-infected insect cells. Cell **59:**103-112.
79. **Campbell S, Rein A.** 1999. In vitro assembly properties of human immunodeficiency virus type 1 Gag protein lacking the p6 domain. Journal of Virology **73:**2270-2279.
80. **Ott DE.** 2008. Cellular proteins detected in HIV-1. Reviews in Medical Virology **18:**159-175.
81. **Swanson CM, Malim MH.** 2008. SnapShot: HIV-1 proteins. Cell **133:**742,-742.e741.
82. **Franke EK, Yuan HE, Luban J.** 1994. Specific incorporation of cyclophilin A into HIV-1 virions. Nature **372:**359-362.
83. **Thali M, Bukovsky A, Kondo E, Rosenwirth B, Walsh CT, Sodroski J, Göttlinger HG.** 1994. Functional association of cyclophilin A with HIV-1 virions. Nature **372:**363-365.
84. **Kao S, Khan MA, Miyagi E, Plishka R, Buckler-White A, Strebel K.** 2003. The human immunodeficiency virus type 1 Vif protein reduces intracellular expression and inhibits packaging of APOBEC3G (CEM15), a cellular inhibitor of virus infectivity. J Virol **77:**11398-11407.
85. **Sheehy AM, Gaddis NC, Choi JD, Malim MH.** 2002. Isolation of a human gene that inhibits HIV-1 infection and is suppressed by the viral Vif protein. Nature **418:**646-650.
86. **Gunzenhauser J, Olivier N, Pengo T, Manley S.** 2012. Quantitative super-resolution imaging reveals protein stoichiometry and nanoscale morphology of assembling HIV-Gag virions. Nano Lett **12:**4705-4710.
87. **Ivanchenko S, Godinez WJ, Lampe M, Kräusslich H-G, Eils R, Rohr K, Bräuchle C, Müller B, Lamb DC.** 2009. Dynamics of HIV-1 assembly and release. PLoS Pathogens **5**.
88. **Baumgärtel V, Ivanchenko S, Dupont A, Sergeev M, Wiseman PW, Kräusslich H-G, Bräuchle C, Müller B, Lamb DC.** 2011. Live-cell visualization of dynamics of HIV budding site interactions with an ESCRT component. Nature Cell Biology **13:**469-474.
89. **Pettit SC, Moody MD, Wehbie RS, Kaplan AH, Nantermet PV, Klein CA, Swanstrom R.** 1994. The p2 domain of human immunodeficiency virus type 1 Gag regulates sequential proteolytic processing and is required to produce fully infectious virions. Journal of Virology **68:**8017-8027.
90. **Wiegers K, Rutter G, Kottler H, Tessmer U, Hohenberg H, Kräusslich HG.** 1998. Sequential steps in human immunodeficiency virus particle maturation revealed by alterations of individual Gag polyprotein cleavage sites. Journal of Virology **72:**2846-2854.
91. **Lee SK, Potempa M, Swanstrom R.** 2012. The choreography of HIV-1 proteolytic processing and virion assembly. J Biol Chem **287:**40867-40874.
92. **Schur FK, Obr M, Hagen WJ, Wan W, Jakobi AJ, Kirkpatrick JM, Sachse C, Krausslich HG, Briggs JA.** 2016. An atomic model of HIV-1 capsid-SP1 reveals structures regulating assembly and maturation. Science **353:**506-508.
93. **Mondor I, Ugolini S, Sattentau QJ.** 1998. Human immunodeficiency virus type 1 attachment to HeLa CD4 cells is CD4 independent and gp120

dependent and requires cell surface heparans. Journal of Virology **72:**3623-3634.
94. **Ugolini S, Mondor I, Sattentau QJ.** 1999. HIV-1 attachment: another look. Trends in Microbiology **7:**144-149.
95. **Gallo SA, Finnegan CM, Viard M, Raviv Y, Dimitrov A, Rawat SS, Puri A, Durell S, Blumenthal R.** 2003. The HIV Env-mediated fusion reaction. Biochimica Et Biophysica Acta **1614:**36-50.
96. **Daecke J, Fackler OT, Dittmar MT, Kräusslich H-G.** 2005. Involvement of clathrin-mediated endocytosis in human immunodeficiency virus type 1 entry. Journal of Virology **79:**1581-1594.
97. **Miyauchi K, Kim Y, Latinovic O, Morozov V, Melikyan GB.** 2009. HIV enters cells via endocytosis and dynamin-dependent fusion with endosomes. Cell **137:**433-444.
98. **Herold N, Anders-Osswein M, Glass B, Eckhardt M, Muller B, Krausslich HG.** 2014. HIV-1 entry in SupT1-R5, CEM-ss, and primary CD4+ T cells occurs at the plasma membrane and does not require endocytosis. J Virol **88:**13956-13970.
99. **Marin M, Melikyan GB.** 2015. Can HIV-1 entry sites be deduced by comparing bulk endocytosis to functional readouts for viral fusion? J Virol **89:**2985.
100. **Herold N, Muller B, Krausslich HG.** 2015. Reply to "Can HIV-1 entry sites be deduced by comparing bulk endocytosis to functional readouts for viral fusion?". J Virol **89:**2986-2987.
101. **Kondo N, Marin M, Kim JH, Desai TM, Melikyan GB.** 2015. Distinct requirements for HIV-cell fusion and HIV-mediated cell-cell fusion. J Biol Chem **290:**6558-6573.
102. **Bour S, Geleziunas R, Wainberg MA.** 1995. The human immunodeficiency virus type 1 (HIV-1) CD4 receptor and its central role in promotion of HIV-1 infection. Microbiological Reviews **59:**63-93.
103. **Maddon PJ, Dalgleish AG, McDougal JS, Clapham PR, Weiss RA, Axel R.** 1986. The T4 gene encodes the AIDS virus receptor and is expressed in the immune system and the brain. Cell **47:**333-348.
104. **Wu L, Gerard NP, Wyatt R, Choe H, Parolin C, Ruffing N, Borsetti A, Cardoso AA, Desjardin E, Newman W, Gerard C, Sodroski J.** 1996. CD4-induced interaction of primary HIV-1 gp120 glycoproteins with the chemokine receptor CCR-5. Nature **384:**179-183.
105. **Furuta RA, Wild CT, Weng Y, Weiss CD.** 1998. Capture of an early fusion-active conformation of HIV-1 gp41. Nature Structural Biology **5:**276-279.
106. **Bullough PA, Hughson FM, Skehel JJ, Wiley DC.** 1994. Structure of influenza haemagglutinin at the pH of membrane fusion. Nature **371:**37-43.
107. **Koch P, Lampe M, Godinez WJ, Müller B, Rohr K, Kräusslich H-G, Lehmann MJ.** 2009. Visualizing fusion of pseudotyped HIV-1 particles in real time by live cell microscopy. Retrovirology **6**.
108. **Matreyek KA, Engelman A.** 2011. The requirement for nucleoporin NUP153 during human immunodeficiency virus type 1 infection is determined by the viral capsid. J Virol **85:**7818-7827.
109. **Matreyek KA, Yucel SS, Li X, Engelman A.** 2013. Nucleoporin NUP153 phenylalanine-glycine motifs engage a common binding pocket

within the HIV-1 capsid protein to mediate lentiviral infectivity. PLoS Pathog **9:**e1003693.

110. **Peng K, Muranyi W, Glass B, Laketa V, Yant SR, Tsai L, Cihlar T, Muller B, Krausslich HG.** 2014. Quantitative microscopy of functional HIV post-entry complexes reveals association of replication with the viral capsid. Elife **3:**e04114.
111. **Hulme AE, Kelley Z, Foley D, Hope TJ.** 2015. Complementary Assays Reveal a Low Level of CA Associated with Viral Complexes in the Nuclei of HIV-1-Infected Cells. J Virol **89:**5350-5361.
112. **Campbell EM, Hope TJ.** 2015. HIV-1 capsid: the multifaceted key player in HIV-1 infection. Nat Rev Microbiol **13:**471-483.
113. **Iordanskiy S, Bukrinsky M.** 2007. Reverse transcription complex: the key player of the early phase of HIV replication. Future Virol **2:**49-64.
114. **Bampi C, Bibillo A, Wendeler M, Divita G, Gorelick RJ, Le Grice SF, Darlix JL.** 2006. Nucleotide excision repair and template-independent addition by HIV-1 reverse transcriptase in the presence of nucleocapsid protein. J Biol Chem **281:**11736-11743.
115. **Darlix JL, Godet J, Ivanyi-Nagy R, Fosse P, Mauffret O, Mely Y.** 2011. Flexible nature and specific functions of the HIV-1 nucleocapsid protein. J Mol Biol **410:**565-581.
116. **Kim J, Roberts A, Yuan H, Xiong Y, Anderson KS.** 2012. Nucleocapsid protein annealing of a primer-template enhances (+)-strand DNA synthesis and fidelity by HIV-1 reverse transcriptase. J Mol Biol **415:**866-880.
117. **Bukrinsky M.** 2004. A hard way to the nucleus. Molecular Medicine (Cambridge, Mass) **10:**1-5.
118. **Craigie R, Bushman FD.** 2014. Host Factors in Retroviral Integration and the Selection of Integration Target Sites. Microbiol Spectr **2**.
119. **Bin Hamid F, Kim J, Shin CG.** 2016. Cellular and viral determinants of retroviral nuclear entry. Can J Microbiol **62:**1-15.
120. **Bushman FD, Malani N, Fernandes J, D'Orso I, Cagney G, Diamond TL, Zhou H, Hazuda DJ, Espeseth AS, König R, Bandyopadhyay S, Ideker T, Goff SP, Krogan NJ, Frankel AD, Young JAT, Chanda SK.** 2009. Host cell factors in HIV replication: meta-analysis of genome-wide studies. PLoS Pathogens **5**.
121. **Dordor A, Poudevigne E, Göttlinger H, Weissenhorn W.** 2011. Essential and supporting host cell factors for HIV-1 budding. Future Microbiology **6:**1159-1170.
122. **Goff SP.** 2007. Host factors exploited by retroviruses. Nature Reviews Microbiology **5:**253-263.
123. **Swaminathan G, Navas-Martin S, Martin-Garcia J.** 2014. MicroRNAs and HIV-1 infection: antiviral activities and beyond. J Mol Biol **426:**1178-1197.
124. **Lodermeyer V, Suhr K, Schrott N, Kolbe C, Sturzel CM, Krnavek D, Munch J, Dietz C, Waldmann T, Kirchhoff F, Goffinet C.** 2013. 90K, an interferon-stimulated gene product, reduces the infectivity of HIV-1. Retrovirology **10:**111.
125. **Goffinet C.** 2016. Cellular Antiviral Factors that Target Particle Infectivity of HIV-1. Curr HIV Res **14:**211-216.

126. **Mariani R, Chen D, Schröfelbauer B, Navarro F, König R, Bollman B, Münk C, Nymark-McMahon H, Landau NR.** 2003. Species-specific exclusion of APOBEC3G from HIV-1 virions by Vif. Cell **114:**21-31.
127. **Bishop KN, Holmes RK, Sheehy AM, Davidson NO, Cho SJ, Malim MH.** 2004. Cytidine deamination of retroviral DNA by diverse APOBEC proteins. Curr Biol **14:**1392-1396.
128. **Harris RS, Liddament MT.** 2004. Retroviral restriction by APOBEC proteins. Nature Reviews Immunology **4:**868-877.
129. **Hotter D, Sauter D, Kirchhoff F.** 2016. Guanylate binding protein 5: Impairing virion infectivity by targeting retroviral envelope glycoproteins. Small GTPases doi:10.1080/21541248.2016.1189990**:**1-7.
130. **McLaren PJ, Gawanbacht A, Pyndiah N, Krapp C, Hotter D, Kluge SF, Gotz N, Heilmann J, Mack K, Sauter D, Thompson D, Perreaud J, Rausell A, Munoz M, Ciuffi A, Kirchhoff F, Telenti A.** 2015. Identification of potential HIV restriction factors by combining evolutionary genomic signatures with functional analyses. Retrovirology **12:**41.
131. **Krapp C, Hotter D, Gawanbacht A, McLaren PJ, Kluge SF, Sturzel CM, Mack K, Reith E, Engelhart S, Ciuffi A, Hornung V, Sauter D, Telenti A, Kirchhoff F.** 2016. Guanylate Binding Protein (GBP) 5 Is an Interferon-Inducible Inhibitor of HIV-1 Infectivity. Cell Host Microbe **19:**504-514.
132. **Compton AA, Bruel T, Porrot F, Mallet A, Sachse M, Euvrard M, Liang C, Casartelli N, Schwartz O.** 2014. IFITM proteins incorporated into HIV-1 virions impair viral fusion and spread. Cell Host Microbe **16:**736-747.
133. **Tada T, Zhang Y, Koyama T, Tobiume M, Tsunetsugu-Yokota Y, Yamaoka S, Fujita H, Tokunaga K.** 2015. MARCH8 inhibits HIV-1 infection by reducing virion incorporation of envelope glycoproteins. Nat Med **21:**1502-1507.
134. **Kane M, Yadav SS, Bitzegeio J, Kutluay SB, Zang T, Wilson SJ, Schoggins JW, Rice CM, Yamashita M, Hatziioannou T, Bieniasz PD.** 2013. MX2 is an interferon-induced inhibitor of HIV-1 infection. Nature **502:**563-566.
135. **Liu Z, Pan Q, Ding S, Qian J, Xu F, Zhou J, Cen S, Guo F, Liang C.** 2013. The interferon-inducible MxB protein inhibits HIV-1 infection. Cell Host Microbe **14:**398-410.
136. **Goujon C, Moncorge O, Bauby H, Doyle T, Ward CC, Schaller T, Hue S, Barclay WS, Schulz R, Malim MH.** 2013. Human MX2 is an interferon-induced post-entry inhibitor of HIV-1 infection. Nature **502:**559-562.
137. **Hrecka K, Hao C, Gierszewska M, Swanson SK, Kesik-Brodacka M, Srivastava S, Florens L, Washburn MP, Skowronski J.** 2011. Vpx relieves inhibition of HIV-1 infection of macrophages mediated by the SAMHD1 protein. Nature **474:**658-661.
138. **Berger A, Sommer AF, Zwarg J, Hamdorf M, Welzel K, Esly N, Panitz S, Reuter A, Ramos I, Jatiani A, Mulder LC, Fernandez-Sesma A, Rutsch F, Simon V, Konig R, Flory E.** 2011. SAMHD1-deficient CD14+ cells from individuals with Aicardi-Goutieres syndrome are highly susceptible to HIV-1 infection. PLoS Pathog **7:**e1002425.

139. **Schneider C, Oellerich T, Baldauf HM, Schwarz SM, Thomas D, Flick R, Bohnenberger H, Kaderali L, Stegmann L, Cremer A, Martin M, Lohmeyer J, Michaelis M, Hornung V, Schliemann C, Berdel WE, Hartmann W, Wardelmann E, Comoglio F, Hansmann ML, Yakunin AF, Geisslinger G, Strobel P, Ferreiros N, Serve H, Keppler OT, Cinatl J, Jr.** 2016. SAMHD1 is a biomarker for cytarabine response and a therapeutic target in acute myeloid leukemia. Nat Med doi:10.1038/nm.4255.
140. **Fu W, Qiu C, Zhou M, Zhu L, Yang Y, Qiu C, Zhang L, Xu X, Wang Y, Xu J, Zhang X.** 2016. Immune Activation Influences SAMHD1 Expression and Vpx-mediated SAMHD1 Degradation during Chronic HIV-1 Infection. Sci Rep **6:**38162.
141. **Laguette N, Sobhian B, Casartelli N, Ringeard M, Chable-Bessia C, Ségéral E, Yatim A, Emiliani S, Schwartz O, Benkirane M.** 2011. SAMHD1 is the dendritic- and myeloid-cell-specific HIV-1 restriction factor counteracted by Vpx. Nature **474:**654-657.
142. **Usami Y, Wu Y, Gottlinger HG.** 2015. SERINC3 and SERINC5 restrict HIV-1 infectivity and are counteracted by Nef. Nature **526:**218-223.
143. **Trautz B, Pierini V, Wombacher R, Stolp B, Chase AJ, Pizzato M, Fackler OT.** 2016. The Antagonism of HIV-1 Nef to SERINC5 Particle Infectivity Restriction Involves the Counteraction of Virion-Associated Pools of the Restriction Factor. J Virol **90:**10915-10927.
144. **Rosa A, Chande A, Ziglio S, De Sanctis V, Bertorelli R, Goh SL, McCauley SM, Nowosielska A, Antonarakis SE, Luban J, Santoni FA, Pizzato M.** 2015. HIV-1 Nef promotes infection by excluding SERINC5 from virion incorporation. Nature **526:**212-217.
145. **Beitari S, Ding S, Pan Q, Finzi A, Liang C.** 2016. The effect of HIV-1 Env on SERINC5 antagonism. J Virol doi:10.1128/JVI.02214-16.
146. **Fackler OT.** 2015. Spotlight on HIV-1 Nef: SERINC3 and SERINC5 Identified as Restriction Factors Antagonized by the Pathogenesis Factor. Viruses **7:**6730-6738.
147. **Li M, Kao E, Gao X, Sandig H, Limmer K, Pavon-Eternod M, Jones TE, Landry S, Pan T, Weitzman MD, David M.** 2012. Codon-usage-based inhibition of HIV protein synthesis by human schlafen 11. Nature **491:**125-128.
148. **Gordon-Alonso M, Rocha-Perugini V, Alvarez S, Moreno-Gonzalo O, Ursa A, Lopez-Martin S, Izquierdo-Useros N, Martinez-Picado J, Munoz-Fernandez MA, Yanez-Mo M, Sanchez-Madrid F.** 2012. The PDZ-adaptor protein syntenin-1 regulates HIV-1 entry. Mol Biol Cell **23:**2253-2263.
149. **Neil SJD, Zang T, Bieniasz PD.** 2008. Tetherin inhibits retrovirus release and is antagonized by HIV-1 Vpu. Nature **451:**425-430.
150. **Madjo U, Leymarie O, Fremont S, Kuster A, Nehlich M, Gallois-Montbrun S, Janvier K, Berlioz-Torrent C.** 2016. LC3C Contributes to Vpu-Mediated Antagonism of BST2/Tetherin Restriction on HIV-1 Release through a Non-canonical Autophagy Pathway. Cell Rep **17:**2221-2233.
151. **Pujol FM, Laketa V, Schmidt F, Mukenhirn M, Muller B, Boulant S, Grimm D, Keppler OT, Fackler OT.** 2016. HIV-1 Vpu

Antagonizes CD317/Tetherin by Adaptor Protein-1-Mediated Exclusion from Virus Assembly Sites. J Virol **90:**6709-6723.

152. **Stremlau M, Owens CM, Perron MJ, Kiessling M, Autissier P, Sodroski J.** 2004. The cytoplasmic body component TRIM5alpha restricts HIV-1 infection in Old World monkeys. Nature **427:**848-853.
153. **Campbell EM, Weingart J, Sette P, Opp S, Sastri J, O'Connor SK, Talley S, Diaz-Griffero F, Hirsch V, Bouamr F.** 2015. TRIM5alpha-Mediated Ubiquitin Chain Conjugation Is Required for Inhibition of HIV-1 Reverse Transcription and Capsid Destabilization. J Virol **90:**1849-1857.
154. **Sayah DM, Sokolskaja E, Berthoux L, Luban J.** 2004. Cyclophilin A retrotransposition into TRIM5 explains owl monkey resistance to HIV-1. Nature **430:**569-573.
155. **Tissot C, Mechti N.** 1995. Molecular cloning of a new interferon-induced factor that represses human immunodeficiency virus type 1 long terminal repeat expression. J Biol Chem **270:**14891-14898.
156. **Turrini F, Marelli S, Kajaste-Rudnitski A, Lusic M, Van Lint C, Das AT, Harwig A, Berkhout B, Vicenzi E.** 2015. HIV-1 transcriptional silencing caused by TRIM22 inhibition of Sp1 binding to the viral promoter. Retrovirology **12:**104.
157. **Kirchhoff F.** 2010. Immune evasion and counteraction of restriction factors by HIV-1 and other primate lentiviruses. Cell Host Microbe **8:**55-67.
158. **Harris RS, Hultquist JF, Evans DT.** 2012. The restriction factors of human immunodeficiency virus. J Biol Chem **287:**40875-40883.
159. **Yu Q, Chen D, Konig R, Mariani R, Unutmaz D, Landau NR.** 2004. APOBEC3B and APOBEC3C are potent inhibitors of simian immunodeficiency virus replication. J Biol Chem **279:**53379-53386.
160. **Descours B, Cribier A, Chable-Bessia C, Ayinde D, Rice G, Crow Y, Yatim A, Schwartz O, Laguette N, Benkirane M.** 2012. SAMHD1 restricts HIV-1 reverse transcription in quiescent CD4(+) T-cells. Retrovirology **9:**87.
161. **Laguette N, Sobhian B, Casartelli N, Ringeard M, Chable-Bessia C, Segeral E, Yatim A, Emiliani S, Schwartz O, Benkirane M.** 2011. SAMHD1 is the dendritic- and myeloid-cell-specific HIV-1 restriction factor counteracted by Vpx. Nature **474:**654-657.
162. **White TE, Brandariz-Nunez A, Valle-Casuso JC, Amie S, Nguyen LA, Kim B, Tuzova M, Diaz-Griffero F.** 2013. The retroviral restriction ability of SAMHD1, but not its deoxynucleotide triphosphohydrolase activity, is regulated by phosphorylation. Cell Host Microbe **13:**441-451.
163. **Pauls E, Ruiz A, Badia R, Permanyer M, Gubern A, Riveira-Munoz E, Torres-Torronteras J, Alvarez M, Mothe B, Brander C, Crespo M, Menendez-Arias L, Clotet B, Keppler OT, Marti R, Posas F, Ballana E, Este JA.** 2014. Cell cycle control and HIV-1 susceptibility are linked by CDK6-dependent CDK2 phosphorylation of SAMHD1 in myeloid and lymphoid cells. J Immunol **193:**1988-1997.
164. **Cribier A, Descours B, Valadao AL, Laguette N, Benkirane M.** 2013. Phosphorylation of SAMHD1 by cyclin A2/CDK1 regulates its restriction activity toward HIV-1. Cell Rep **3:**1036-1043.

165. **St Gelais C, de Silva S, Hach JC, White TE, Diaz-Griffero F, Yount JS, Wu L.** 2014. Identification of cellular proteins interacting with the retroviral restriction factor SAMHD1. J Virol **88:**5834-5844.
166. **Doyle T, Goujon C, Malim MH.** 2015. HIV-1 and interferons: who's interfering with whom? Nat Rev Microbiol **13:**403-413.
167. **Colomer-Lluch M, Gollahon LS, Serra-Moreno R.** 2016. Anti-HIV Factors: Targeting Each Step of HIV's Replication Cycle. Curr HIV Res **14:**175-182.
168. **Garcia-Minambres A, Eid SG, Mangan NE, Pade C, Lim SS, Matthews AY, de Weerd NA, Hertzog PJ, Mak J.** 2017. Interferon epsilon promotes HIV restriction at multiple steps of viral replication. Immunol Cell Biol doi:10.1038/icb.2016.123.
169. **Li M.** 2015. Proteomics in the investigation of HIV-1 interactions with host proteins. Proteomics Clin Appl **9:**221-234.
170. **Park RJ, Wang T, Koundakjian D, Hultquist JF, Lamothe-Molina P, Monel B, Schumann K, Yu H, Krupzcak KM, Garcia-Beltran W, Piechocka-Trocha A, Krogan NJ, Marson A, Sabatini DM, Lander ES, Hacohen N, Walker BD.** 2016. A genome-wide CRISPR screen identifies a restricted set of HIV host dependency factors. Nat Genet doi:10.1038/ng.3741.
171. **Strack B, Calistri A, Craig S, Popova E, Göttlinger HG.** 2003. AIP1/ALIX is a binding partner for HIV-1 p6 and EIAV p9 functioning in virus budding. Cell **114:**689-699.
172. **Kudoh A, Takahama S, Sawasaki T, Ode H, Yokoyama M, Okayama A, Ishikawa A, Miyakawa K, Matsunaga S, Kimura H, Sugiura W, Sato H, Hirano H, Ohno S, Yamamoto N, Ryo A.** 2014. The phosphorylation of HIV-1 Gag by atypical protein kinase C facilitates viral infectivity by promoting Vpr incorporation into virions. Retrovirology **11:**9.
173. **Jager S, Kim DY, Hultquist JF, Shindo K, LaRue RS, Kwon E, Li M, Anderson BD, Yen L, Stanley D, Mahon C, Kane J, Franks-Skiba K, Cimermancic P, Burlingame A, Sali A, Craik CS, Harris RS, Gross JD, Krogan NJ.** 2011. Vif hijacks CBF-beta to degrade APOBEC3G and promote HIV-1 infection. Nature **481:**371-375.
174. **Rice AP.** 2016. Cyclin-dependent kinases as therapeutic targets for HIV-1 infection. Expert Opin Ther Targets **20:**1453-1461.
175. **Price AJ, Jacques DA, McEwan WA, Fletcher AJ, Essig S, Chin JW, Halambage UD, Aiken C, James LC.** 2014. Host cofactors and pharmacologic ligands share an essential interface in HIV-1 capsid that is lost upon disassembly. PLoS Pathog **10:**e1004459.
176. **Saito A, Henning MS, Serrao E, Dubose BN, Teng S, Huang J, Li X, Saito N, Roy SP, Siddiqui MA, Ahn J, Tsuji M, Hatziioannou T, Engelman AN, Yamashita M.** 2016. Capsid-CPSF6 Interaction Is Dispensable for HIV-1 Replication in Primary Cells but Is Selected during Virus Passage In Vivo. J Virol **90:**6918-6935.
177. **Sowd GA, Serrao E, Wang H, Wang W, Fadel HJ, Poeschla EM, Engelman AN.** 2016. A critical role for alternative polyadenylation factor CPSF6 in targeting HIV-1 integration to transcriptionally active chromatin. Proc Natl Acad Sci U S A **113:**E1054-1063.

178. **Yu X, Yu Y, Liu B, Luo K, Kong W, Mao P, Yu XF.** 2003. Induction of APOBEC3G ubiquitination and degradation by an HIV-1 Vif-Cul5-SCF complex. Science **302:**1056-1060.
179. **Brai A, Fazi R, Tintori C, Zamperini C, Bugli F, Sanguinetti M, Stigliano E, Este J, Badia R, Franco S, Martinez MA, Martinez JP, Meyerhans A, Saladini F, Zazzi M, Garbelli A, Maga G, Botta M.** 2016. Human DDX3 protein is a valuable target to develop broad spectrum antiviral agents. Proc Natl Acad Sci U S A **113:**5388-5393.
180. **Yedavalli VS, Neuveut C, Chi YH, Kleiman L, Jeang KT.** 2004. Requirement of DDX3 DEAD box RNA helicase for HIV-1 Rev-RRE export function. Cell **119:**381-392.
181. **Janardhan A, Swigut T, Hill B, Myers MP, Skowronski J.** 2004. HIV-1 Nef binds the DOCK2-ELMO1 complex to activate rac and inhibit lymphocyte chemotaxis. PLoS Biol **2:**E6.
182. **Cartier C, Deckert M, Grangeasse C, Trauger R, Jensen F, Bernard A, Cozzone A, Desgranges C, Boyer V.** 1997. Association of ERK2 mitogen-activated protein kinase with human immunodeficiency virus particles. J Virol **71:**4832-4837.
183. **Jacque JM, Mann A, Enslen H, Sharova N, Brichacek B, Davis RJ, Stevenson M.** 1998. Modulation of HIV-1 infectivity by MAPK, a virion-associated kinase. EMBO J **17:**2607-2618.
184. **Chen BJ, Lamb RA.** 2008. Mechanisms for enveloped virus budding: can some viruses do without an ESCRT? Virology **372:**221-232.
185. **Garrus JE, von Schwedler UK, Pornillos OW, Morham SG, Zavitz KH, Wang HE, Wettstein DA, Stray KM, Côté M, Rich RL, Myszka DG, Sundquist WI.** 2001. Tsg101 and the vacuolar protein sorting pathway are essential for HIV-1 budding. Cell **107:**55-65.
186. **Henne WM, Buchkovich NJ, Emr SD.** 2011. The ESCRT pathway. Dev Cell **21:**77-91.
187. **Votteler J, Sundquist WI.** 2013. Virus budding and the ESCRT pathway. Cell Host Microbe **14:**232-241.
188. **Bregnard C, Zamborlini A, Leduc M, Chafey P, Camoin L, Saib A, Benichou S, Danos O, Basmaciogullari S.** 2013. Comparative proteomic analysis of HIV-1 particles reveals a role for Ezrin and EHD4 in the Nef-dependent increase of virus infectivity. J Virol **87:**3729-3740.
189. **Vardabasso C, Manganaro L, Lusic M, Marcello A, Giacca M.** 2008. The histone chaperone protein Nucleosome Assembly Protein-1 (hNAP-1) binds HIV-1 Tat and promotes viral transcription. Retrovirology **5:**8.
190. **Woolaway K, Asai K, Emili A, Cochrane A.** 2007. hnRNP E1 and E2 have distinct roles in modulating HIV-1 gene expression. Retrovirology **4:**28.
191. **Marchand V, Santerre M, Aigueperse C, Fouillen L, Saliou JM, Van Dorsselaer A, Sanglier-Cianferani S, Branlant C, Motorin Y.** 2011. Identification of protein partners of the human immunodeficiency virus 1 tat/rev exon 3 leads to the discovery of a new HIV-1 splicing regulator, protein hnRNP K. RNA Biol **8:**325-342.
192. **Agostini I, Popov S, Li J, Dubrovsky L, Hao T, Bukrinsky M.** 2000. Heat-shock protein 70 can replace viral protein R of HIV-1 during

nuclear import of the viral preintegration complex. Exp Cell Res **259:**398-403.

193. **Manganaro L, Lusic M, Gutierrez MI, Cereseto A, Del Sal G, Giacca M.** 2010. Concerted action of cellular JNK and Pin1 restricts HIV-1 genome integration to activated CD4+ T lymphocytes. Nat Med **16:**329-333.
194. **Cherepanov P, Maertens G, Proost P, Devreese B, Van Beeumen J, Engelborghs Y, De Clercq E, Debyser Z.** 2003. HIV-1 integrase forms stable tetramers and associates with LEDGF/p75 protein in human cells. The Journal of Biological Chemistry **278:**372-381.
195. **Schweitzer CJ, Matthews JM, Madson CJ, Donnellan MR, Cerny RL, Belshan M.** 2012. Knockdown of the cellular protein LRPPRC attenuates HIV-1 infection. PLoS One **7:**e40537.
196. **Engeland CE, Oberwinkler H, Schumann M, Krause E, Muller GA, Krausslich HG.** 2011. The cellular protein lyric interacts with HIV-1 Gag. J Virol **85:**13322-13332.
197. **Kula A, Guerra J, Knezevich A, Kleva D, Myers MP, Marcello A.** 2011. Characterization of the HIV-1 RNA associated proteome identifies Matrin 3 as a nuclear cofactor of Rev function. Retrovirology **8:**60.
198. **Shelton MN, Huang MB, Ali SA, Powell MD, Bond VC.** 2012. Secretion modification region-derived peptide disrupts HIV-1 Nef's interaction with mortalin and blocks virus and Nef exosome release. J Virol **86:**406-419.
199. **Di Nunzio F, Fricke T, Miccio A, Valle-Casuso JC, Perez P, Souque P, Rizzi E, Severgnini M, Mavilio F, Charneau P, Diaz-Griffero F.** 2013. Nup153 and Nup98 bind the HIV-1 core and contribute to the early steps of HIV-1 replication. Virology **440:**8-18.
200. **Dharan A, Talley S, Tripathi A, Mamede JI, Majetschak M, Hope TJ, Campbell EM.** 2016. KIF5B and Nup358 Cooperatively Mediate the Nuclear Import of HIV-1 during Infection. PLoS Pathog **12:**e1005700.
201. **Di Nunzio F, Danckaert A, Fricke T, Perez P, Fernandez J, Perret E, Roux P, Shorte S, Charneau P, Diaz-Griffero F, Arhel NJ.** 2012. Human nucleoporins promote HIV-1 docking at the nuclear pore, nuclear import and integration. PLoS One **7:**e46037.
202. **Mancebo HS, Lee G, Flygare J, Tomassini J, Luu P, Zhu Y, Peng J, Blau C, Hazuda D, Price D, Flores O.** 1997. P-TEFb kinase is required for HIV Tat transcriptional activation in vivo and in vitro. Genes Dev **11:**2633-2644.
203. **Dos Santos Paparidis NF, Durvale MC, Canduri F.** 2016. The emerging picture of CDK9/P-TEFb: more than 20 years of advances since PITALRE. Mol Biosyst doi:10.1039/c6mb00387g.
204. **Roy BB, Hu J, Guo X, Russell RS, Guo F, Kleiman L, Liang C.** 2006. Association of RNA helicase a with human immunodeficiency virus type 1 particles. J Biol Chem **281:**12625-12635.
205. **Bolinger C, Yilmaz A, Hartman TR, Kovacic MB, Fernandez S, Ye J, Forget M, Green PL, Boris-Lawrie K.** 2007. RNA helicase A interacts with divergent lymphotropic retroviruses and promotes translation of human T-cell leukemia virus type 1. Nucleic Acids Res **35:**2629-2642.

206. **Berro R, Kehn K, de la Fuente C, Pumfery A, Adair R, Wade J, Colberg-Poley AM, Hiscott J, Kashanchi F.** 2006. Acetylated Tat regulates human immunodeficiency virus type 1 splicing through its interaction with the splicing regulator p32. J Virol **80:**3189-3204.
207. **Milev MP, Ravichandran M, Khan MF, Schriemer DC, Mouland AJ.** 2012. Characterization of staufen1 ribonucleoproteins by mass spectrometry and biochemical analyses reveal the presence of diverse host proteins associated with human immunodeficiency virus type 1. Front Microbiol **3:**367.
208. **Chatel-Chaix L, Abrahamyan L, Frechina C, Mouland AJ, DesGroseillers L.** 2007. The host protein Staufen1 participates in human immunodeficiency virus type 1 assembly in live cells by influencing pr55Gag multimerization. J Virol **81:**6216-6230.
209. **Valle-Casuso JC, Di Nunzio F, Yang Y, Reszka N, Lienlaf M, Arhel N, Perez P, Brass AL, Diaz-Griffero F.** 2012. TNPO3 is required for HIV-1 replication after nuclear import but prior to integration and binds the HIV-1 core. J Virol **86:**5931-5936.
210. **Larue R, Gupta K, Wuensch C, Shkriabai N, Kessl JJ, Danhart E, Feng L, Taltynov O, Christ F, Van Duyne GD, Debyser Z, Foster MP, Kvaratskhelia M.** 2012. Interaction of the HIV-1 intasome with transportin 3 protein (TNPO3 or TRN-SR2). J Biol Chem **287:**34044-34058.
211. **De Iaco A, Luban J.** 2011. Inhibition of HIV-1 infection by TNPO3 depletion is determined by capsid and detectable after viral cDNA enters the nucleus. Retrovirology **8:**98.
212. **Brass AL, Dykxhoorn DM, Benita Y, Yan N, Engelman A, Xavier RJ, Lieberman J, Elledge SJ.** 2008. Identification of host proteins required for HIV infection through a functional genomic screen. Science (New York, NY) **319:**921-926.
213. **Christ F, Thys W, De Rijck J, Gijsbers R, Albanese A, Arosio D, Emiliani S, Rain JC, Benarous R, Cereseto A, Debyser Z.** 2008. Transportin-SR2 imports HIV into the nucleus. Curr Biol **18:**1192-1202.
214. **Timani KA, Liu Y, He JJ.** 2013. Tip110 interacts with YB-1 and regulates each other's function. BMC Mol Biol **14:**14.
215. **Mu X, Li W, Wang X, Gao G.** 2013. YB-1 stabilizes HIV-1 genomic RNA and enhances viral production. Protein Cell **4:**591-597.
216. **Hatziioannou T, Perez-Caballero D, Cowan S, Bieniasz PD.** 2005. Cyclophilin interactions with incoming human immunodeficiency virus type 1 capsids with opposing effects on infectivity in human cells. J Virol **79:**176-183.
217. **Wiegers K, Rutter G, Schubert U, Grattinger M, Krausslich HG.** 1999. Cyclophilin A incorporation is not required for human immunodeficiency virus type 1 particle maturation and does not destabilize the mature capsid. Virology **257:**261-274.
218. **Llano M, Saenz DT, Meehan A, Wongthida P, Peretz M, Walker WH, Teo W, Poeschla EM.** 2006. An essential role for LEDGF/p75 in HIV integration. Science **314:**461-464.
219. **Ferris AL, Wu X, Hughes CM, Stewart C, Smith SJ, Milne TA, Wang GG, Shun MC, Allis CD, Engelman A, Hughes SH.** 2010. Lens epithelium-derived growth factor fusion proteins redirect HIV-1 DNA integration. Proc Natl Acad Sci U S A **107:**3135-3140.

220. **Hemonnot B, Cartier C, Gay B, Rebuffat S, Bardy M, Devaux C, Boyer V, Briant L.** 2004. The host cell MAP kinase ERK-2 regulates viral assembly and release by phosphorylating the p6gag protein of HIV-1. The Journal of biological chemistry **279:**32426-32434.
221. **Hurley JH, Emr SD.** 2006. The ESCRT complexes: structure and mechanism of a membrane-trafficking network. Annual Review of Biophysics and Biomolecular Structure **35:**277-298.
222. **Katzmann DJ, Babst M, Emr SD.** 2001. Ubiquitin-dependent sorting into the multivesicular body pathway requires the function of a conserved endosomal protein sorting complex, ESCRT-I. Cell **106:**145-155.
223. **Carlton JG, Martin-Serrano J.** 2007. Parallels between cytokinesis and retroviral budding: a role for the ESCRT machinery. Science (New York, NY) **316:**1908-1912.
224. **Raiborg C, Stenmark H.** 2009. The ESCRT machinery in endosomal sorting of ubiquitylated membrane proteins. Nature **458:**445-452.
225. **Raiborg C, Stenmark H.** 2009. The ESCRT machinery in endosomal sorting of ubiquitylated membrane proteins. Nature **458:**445-452.
226. **Sundquist WI, Krausslich HG.** 2012. HIV-1 assembly, budding, and maturation. Cold Spring Harb Perspect Med **2:**a006924.
227. **Weiss ER, Gottlinger H.** 2011. The role of cellular factors in promoting HIV budding. J Mol Biol **410:**525-533.
228. **Martin-Serrano J, Neil SJ.** 2011. Host factors involved in retroviral budding and release. Nat Rev Microbiol **9:**519-531.
229. **Bieniasz PD.** 2006. Late budding domains and host proteins in enveloped virus release. Virology **344:**55-63.
230. **Göttlinger HG, Dorfman T, Sodroski JG, Haseltine WA.** 1991. Effect of mutations affecting the p6 gag protein on human immunodeficiency virus particle release. Proceedings of the National Academy of Sciences of the United States of America **88:**3195-3199.
231. **Freed EO.** 2002. Viral late domains. J Virol **76:**4679-4687.
232. **Huang M, Orenstein JM, Martin MA, Freed EO.** 1995. p6Gag is required for particle production from full-length human immunodeficiency virus type 1 molecular clones expressing protease. Journal of Virology **69:**6810-6818.
233. **Martin-Serrano J, Zang T, Bieniasz PD.** 2001. HIV-1 and Ebola virus encode small peptide motifs that recruit Tsg101 to sites of particle assembly to facilitate egress. Nature Medicine **7:**1313-1319.
234. **VerPlank L, Bouamr F, LaGrassa TJ, Agresta B, Kikonyogo A, Leis J, Carter CA.** 2001. Tsg101, a homologue of ubiquitin-conjugating (E2) enzymes, binds the L domain in HIV type 1 Pr55(Gag). Proceedings of the National Academy of Sciences of the United States of America **98:**7724-7729.
235. **von Schwedler UK, Stuchell M, Müller B, Ward DM, Chung H-Y, Morita E, Wang HE, Davis T, He G-P, Cimbora DM, Scott A, Kräusslich H-G, Kaplan J, Morham SG, Sundquist WI.** 2003. The protein network of HIV budding. Cell **114:**701-713.
236. **Wollert T, Yang D, Ren X, Lee HH, Im YJ, Hurley JH.** 2009. The ESCRT machinery at a glance. Journal of Cell Science **122:**2163-2166.
237. **Parent LJ, Bennett RP, Craven RC, Nelle TD, Krishna NK, Bowzard JB, Wilson CB, Puffer BA, Montelaro RC, Wills JW.** 1995. Positionally independent and exchangeable late budding functions

of the Rous sarcoma virus and human immunodeficiency virus Gag proteins. Journal of Virology **69:**5455-5460.
238. **Hermle J, Anders M, Heuser A-M, Müller B.** 2010. A simple fluorescence based assay for quantification of human immunodeficiency virus particle release. BMC biotechnology **10**.
239. **Müller B, Patschinsky T, Kräusslich H-G.** 2002. The late-domain-containing protein p6 is the predominant phosphoprotein of human immunodeficiency virus type 1 particles. Journal of virology **76:**1015-1024.
240. **Da Q, Yang X, Xu Y, Gao G, Cheng G, Tang H.** 2011. TANK-binding kinase 1 attenuates PTAP-dependent retroviral budding through targeting endosomal sorting complex required for transport-I. J Immunol **186:**3023-3030.
241. **Radestock B, Morales I, Rahman SA, Radau S, Glass B, Zahedi RP, Muller B, Krausslich HG.** 2013. Comprehensive mutational analysis reveals p6Gag phosphorylation to be dispensable for HIV-1 morphogenesis and replication. J Virol **87:**724-734.
242. **Radestock B, Burk R, Muller B, Krausslich H.** 2014. Re-visiting the functional Relevance of the highly conserved Serine 40 Residue within HIV-1 p6 Gag. Retrovirology **11:**114.
243. **Bukrinskaya AG, Ghorpade A, Heinzinger NK, Smithgall TE, Lewis RE, Stevenson M.** 1996. Phosphorylation-dependent human immunodeficiency virus type 1 infection and nuclear targeting of viral DNA. Proc Natl Acad Sci U S A **93:**367-371.
244. **Burnette B, Yu G, Felsted RL.** 1993. Phosphorylation of HIV-1 gag proteins by protein kinase C. J Biol Chem **268:**8698-8703.
245. **Reil H, Bukovsky AA, Gelderblom HR, Gottlinger HG.** 1998. Efficient HIV-1 replication can occur in the absence of the viral matrix protein. EMBO J **17:**2699-2708.
246. **Freed EO, Englund G, Martin MA.** 1995. Role of the basic domain of human immunodeficiency virus type 1 matrix in macrophage infection. J Virol **69:**3949-3954.
247. **Gallay P, Swingler S, Aiken C, Trono D.** 1995. HIV-1 infection of nondividing cells: C-terminal tyrosine phosphorylation of the viral matrix protein is a key regulator. Cell **80:**379-388.
248. **Zhou Y, Ratner L.** 2000. Phosphorylation of human immunodeficiency virus type 1 Vpr regulates cell cycle arrest. J Virol **74:**6520-6527.
249. **Barnitz RA, Wan F, Tripuraneni V, Bolton DL, Lenardo MJ.** 2010. Protein kinase A phosphorylation activates Vpr-induced cell cycle arrest during human immunodeficiency virus type 1 infection. J Virol **84:**6410-6424.
250. **Agostini I, Popov S, Hao T, Li JH, Dubrovsky L, Chaika O, Chaika N, Lewis R, Bukrinsky M.** 2002. Phosphorylation of Vpr regulates HIV type 1 nuclear import and macrophage infection. AIDS Res Hum Retroviruses **18:**283-288.
251. **Liu RD, Wu J, Shao R, Xue YH.** 2014. Mechanism and factors that control HIV-1 transcription and latency activation. J Zhejiang Univ Sci B **15:**455-465.
252. **Simon V, Bloch N, Landau NR.** 2015. Intrinsic host restrictions to HIV-1 and mechanisms of viral escape. Nat Immunol **16:**546-553.

253. **Yan J, Hao C, DeLucia M, Swanson S, Florens L, Washburn MP, Ahn J, Skowronski J.** 2015. CyclinA2-Cyclin-dependent Kinase Regulates SAMHD1 Protein Phosphohydrolase Domain. J Biol Chem **290:**13279-13292.
254. **Francis AC, Di Primio C, Allouch A, Cereseto A.** 2011. Role of phosphorylation in the nuclear biology of HIV-1. Curr Med Chem **18:**2904-2912.
255. **Fire A, Xu S, Montgomery MK, Kostas SA, Driver SE, Mello CC.** 1998. Potent and specific genetic interference by double-stranded RNA in Caenorhabditis elegans. Nature **391:**806-811.
256. **Bartel DP.** 2004. MicroRNAs: genomics, biogenesis, mechanism, and function. Cell **116:**281-297.
257. **Cullen BR.** 2005. RNAi the natural way. Nature Genetics **37:**1163-1165.
258. **König R, Zhou Y, Elleder D, Diamond TL, Bonamy GMC, Irelan JT, Chiang C-Y, Tu BP, De Jesus PD, Lilley CE, Seidel S, Opaluch AM, Caldwell JS, Weitzman MD, Kuhen KL, Bandyopadhyay S, Ideker T, Orth AP, Miraglia LJ, Bushman FD, Young JA, Chanda SK.** 2008. Global analysis of host-pathogen interactions that regulate early-stage HIV-1 replication. Cell **135:**49-60.
259. **Zhou J, Yuan X, Dismuke D, Forshey BM, Lundquist C, Lee KH, Aiken C, Chen CH.** 2004. Small-molecule inhibition of human immunodeficiency virus type 1 replication by specific targeting of the final step of virion maturation. J Virol **78:**922-929.
260. **Prudencio M, Lehmann MJ.** 2009. Illuminating the host - how RNAi screens shed light on host-pathogen interactions. Biotechnol J **4:**826-837.
261. **Fennell M, Xiang Q, Hwang A, Chen C, Huang CH, Chen CC, Pelossof R, Garippa RJ.** 2014. Impact of RNA-guided technologies for target identification and deconvolution. J Biomol Screen **19:**1327-1337.
262. **Panda D, Cherry S.** 2012. Cell-based genomic screening: elucidating virus-host interactions. Curr Opin Virol **2:**784-792.
263. **Adachi A, Gendelman HE, Koenig S, Folks T, Willey R, Rabson A, Martin MA.** 1986. Production of acquired immunodeficiency syndrome-associated retrovirus in human and nonhuman cells transfected with an infectious molecular clone. Journal of Virology **59:**284-291.
264. **Lampe M, Briggs JAG, Endress T, Glass B, Riegelsberger S, Kräusslich H-G, Lamb DC, Bräuchle C, Müller B.** 2007. Double-labelled HIV-1 particles for study of virus-cell interaction. Virology **360:**92-104.
265. **Sena-Esteves M, Saeki Y, Camp SM, Chiocca EA, Breakefield XO.** 1999. Single-step conversion of cells to retrovirus vector producers with herpes simplex virus-Epstein-Barr virus hybrid amplicons. Journal of Virology **73:**10426-10439.
266. **Scherer WF, Syverton JT, Gey GO.** 1953. Studies on the propagation in vitro of poliomyelitis viruses. IV. Viral multiplication in a stable strain of human malignant epithelial cells (strain HeLa) derived from an epidermoid carcinoma of the cervix. The Journal of Experimental Medicine **97:**695-710.

267. **Charneau P, Alizon M, Clavel F.** 1992. A second origin of DNA plus-strand synthesis is required for optimal human immunodeficiency virus replication. Journal of Virology **66:**2814-2820.
268. **Miyoshi I, Taguchi H, Fujishita M, Niiya K, Kitagawa T, Ohtsuki Y, Akagi T.** 1982. Asymptomatic type C virus carriers in the family of an adult T-cell leukemia patient. Gann = Gan **73:**339-340.
269. **Erfle H, Neumann B, Liebel U, Rogers P, Held M, Walter T, Ellenberg J, Pepperkok R.** 2007. Reverse transfection on cell arrays for high content screening microscopy. Nature protocols **2:**392-399.
270. **Erfle H, Neumann B, Rogers P, Bulkescher J, Ellenberg J, Pepperkok R.** 2008. Work flow for multiplexing siRNA assays by solid-phase reverse transfection in multiwell plates. Journal of biomolecular screening **13:**575-580.
271. **Rieber N, Knapp B, Eils R, Kaderali L.** 2009. RNAither, an automated pipeline for the statistical analysis of high-throughput RNAi screens. Bioinformatics **25:**678-679.
272. **Boutros M, Bras LP, Huber W.** 2006. Analysis of cell-based RNAi screens. Genome Biol **7:**R66.
273. **Müller B, Daecke J, Fackler OT, Dittmar MT, Zentgraf H, Kräusslich H-G.** 2004. Construction and characterization of a fluorescently labeled infectious human immunodeficiency virus type 1 derivative. Journal of Virology **78:**10803-10813.
274. **Börner K, Hermle J, Sommer C, Brown NP, Knapp B, Glass B, Kunkel J, Torralba G, Reymann J, Beil N, Beneke J, Pepperkok R, Schneider R, Ludwig T, Hausmann M, Hamprecht F, Erfle H, Kaderali L, Kräusslich H-G, Lehmann MJ.** 2010. From experimental setup to bioinformatics: an RNAi screening platform to identify host factors involved in HIV-1 replication. Biotechnology journal **5:**39-49.
275. **Cleveland WS.** 1981. LOWESS: A Program for Smoothing Scatterplots by Robust Locally Weighted Regression. The American Statistician **35**.
276. **Huang da W, Sherman BT, Lempicki RA.** 2009. Systematic and integrative analysis of large gene lists using DAVID bioinformatics resources. Nat Protoc **4:**44-57.
277. **Huang da W, Sherman BT, Lempicki RA.** 2009. Bioinformatics enrichment tools: paths toward the comprehensive functional analysis of large gene lists. Nucleic Acids Res **37:**1-13.
278. **Huang DW, Sherman BT, Tan Q, Collins JR, Alvord WG, Roayaei J, Stephens R, Baseler MW, Lane HC, Lempicki RA.** 2007. The DAVID Gene Functional Classification Tool: a novel biological module-centric algorithm to functionally analyze large gene lists. Genome Biol **8:**R183.
279. **Huang DW, Sherman BT, Tan Q, Kir J, Liu D, Bryant D, Guo Y, Stephens R, Baseler MW, Lane HC, Lempicki RA.** 2007. DAVID Bioinformatics Resources: expanded annotation database and novel algorithms to better extract biology from large gene lists. Nucleic Acids Res **35:**W169-175.
280. **Kanehisa M, Sato Y, Kawashima M, Furumichi M, Tanabe M.** 2016. KEGG as a reference resource for gene and protein annotation. Nucleic Acids Res **44:**D457-462.

281. **Kanehisa M, Goto S.** 2000. KEGG: kyoto encyclopedia of genes and genomes. Nucleic Acids Res **28:**27-30.
282. **Kanehisa M, Furumichi M, Tanabe M, Sato Y, Morishima K.** 2017. KEGG: new perspectives on genomes, pathways, diseases and drugs. Nucleic Acids Res **45:**D353-D361.
283. **Zhou H, Xu M, Huang Q, Gates AT, Zhang XD, Castle JC, Stec E, Ferrer M, Strulovici B, Hazuda DJ, Espeseth AS.** 2008. Genome-scale RNAi screen for host factors required for HIV replication. Cell host & microbe **4:**495-504.
284. **Odqvist L, Sanchez-Beato M, Montes-Moreno S, Martin-Sanchez E, Pajares R, Sanchez-Verde L, Ortiz-Romero PL, Rodriguez J, Rodriguez-Pinilla SM, Iniesta-Martinez F, Solera-Arroyo JC, Ramos-Asensio R, Flores T, Palanca JM, Bragado FG, Franjo PD, Piris MA.** 2013. NIK controls classical and alternative NF-kappaB activation and is necessary for the survival of human T-cell lymphoma cells. Clin Cancer Res **19:**2319-2330.
285. **Li X, Josef J, Marasco WA.** 2001. Hiv-1 Tat can substantially enhance the capacity of NIK to induce IkappaB degradation. Biochem Biophys Res Commun **286:**587-594.
286. **Choudhary S, Boldogh S, Garofalo R, Jamaluddin M, Brasier AR.** 2005. Respiratory syncytial virus influences NF-kappaB-dependent gene expression through a novel pathway involving MAP3K14/NIK expression and nuclear complex formation with NF-kappaB2. J Virol **79:**8948-8959.
287. **Schoggins JW, Wilson SJ, Panis M, Murphy MY, Jones CT, Bieniasz P, Rice CM.** 2011. A diverse range of gene products are effectors of the type I interferon antiviral response. Nature **472:**481-485.
288. **Schoggins JW, Rice CM.** 2011. Interferon-stimulated genes and their antiviral effector functions. Curr Opin Virol **1:**519-525.
289. **Dinkel H, Van Roey K, Michael S, Kumar M, Uyar B, Altenberg B, Milchevskaya V, Schneider M, Kuhn H, Behrendt A, Dahl SL, Damerell V, Diebel S, Kalman S, Klein S, Knudsen AC, Mader C, Merrill S, Staudt A, Thiel V, Welti L, Davey NE, Diella F, Gibson TJ.** 2016. ELM 2016-data update and new functionality of the eukaryotic linear motif resource. Nucleic Acids Res **44:**D294-300.
290. **Dinkel H, Van Roey K, Michael S, Davey NE, Weatheritt RJ, Born D, Speck T, Kruger D, Grebnev G, Kuban M, Strumillo M, Uyar B, Budd A, Altenberg B, Seiler M, Chemes LB, Glavina J, Sanchez IE, Diella F, Gibson TJ.** 2014. The eukaryotic linear motif resource ELM: 10 years and counting. Nucleic Acids Res **42:**D259-266.
291. **Khan KA, Abbas W, Varin A, Kumar A, Di Martino V, Dichamp I, Herbein G.** 2013. HIV-1 Nef interacts with HCV Core, recruits TRAF2, TRAF5 and TRAF6, and stimulates HIV-1 replication in macrophages. J Innate Immun **5:**639-656.
292. **Borner K, Hermle J, Sommer C, Brown NP, Knapp B, Glass B, Kunkel J, Torralba G, Reymann J, Beil N, Beneke J, Pepperkok R, Schneider R, Ludwig T, Hausmann M, Hamprecht F, Erfle H, Kaderali L, Krausslich HG, Lehmann MJ.** 2010. From experimental setup to bioinformatics: an RNAi screening platform to identify host factors involved in HIV-1 replication. Biotechnol J **5:**39-49.

293. **Jiang WM, Zhang XY, Zhang YZ, Liu L, Lu HZ.** 2014. A high throughput RNAi screen reveals determinants of HIV-1 activity in host kinases. Int J Clin Exp Pathol **7:**2229-2237.
294. **Wen X, Ding L, Hunter E, Spearman P.** 2014. An siRNA screen of membrane trafficking genes highlights pathways common to HIV-1 and M-PMV virus assembly and release. PLoS One **9:**e106151.
295. **Hisano Y, Nishi T, Kawahara A.** 2012. The functional roles of S1P in immunity. J Biochem **152:**305-311.
296. **Spiegel S, Milstien S.** 2011. The outs and the ins of sphingosine-1-phosphate in immunity. Nat Rev Immunol **11:**403-415.
297. **Carr JM, Mahalingam S, Bonder CS, Pitson SM.** 2013. Sphingosine kinase 1 in viral infections. Rev Med Virol **23:**73-84.
298. **Jelicic K, Cimbro R, Nawaz F, Huang da W, Zheng X, Yang J, Lempicki RA, Pascuccio M, Van Ryk D, Schwing C, Hiatt J, Okwara N, Wei D, Roby G, David A, Hwang IY, Kehrl JH, Arthos J, Cicala C, Fauci AS.** 2013. The HIV-1 envelope protein gp120 impairs B cell proliferation by inducing TGF-beta1 production and FcRL4 expression. Nat Immunol **14:**1256-1265.
299. **Kersh EN, Luo W, Adams DR, Mitchell J, Garcia-Lerma JG, Butera S, Folks T, Otten R.** 2009. Evaluation of the lymphocyte trafficking drug FTY720 in SHIVSF162P3-infected rhesus macaques. J Antimicrob Chemother **63:**758-762.
300. **Morris M, Aubert RD, Butler K, Henning T, Mitchell J, Jenkins L, Garber D, McNicholl J, Kersh EN.** 2014. Preclinical evaluation of the immunomodulatory lymphocyte trafficking drug FTY720 for HIV prevention in the female genital mucosa of macaques. J Med Primatol **43:**370-373.
301. **Dai L, Plaisance-Bonstaff K, Voelkel-Johnson C, Smith CD, Ogretmen B, Qin Z, Parsons C.** 2014. Sphingosine kinase-2 maintains viral latency and survival for KSHV-infected endothelial cells. PLoS One **9:**e102314.
302. **Qin Z, Dai L, Trillo-Tinoco J, Senkal C, Wang W, Reske T, Bonstaff K, Del Valle L, Rodriguez P, Flemington E, Voelkel-Johnson C, Smith CD, Ogretmen B, Parsons C.** 2014. Targeting sphingosine kinase induces apoptosis and tumor regression for KSHV-associated primary effusion lymphoma. Mol Cancer Ther **13:**154-164.
303. **Diez-Guerra FJ.** 2010. Neurogranin, a link between calcium/calmodulin and protein kinase C signaling in synaptic plasticity. IUBMB Life **62:**597-606.
304. **Duskova K, Nagilla P, Le HS, Iyer P, Thalamuthu A, Martinson J, Bar-Joseph Z, Buchanan W, Rinaldo C, Ayyavoo V.** 2013. MicroRNA regulation and its effects on cellular transcriptome in human immunodeficiency virus-1 (HIV-1) infected individuals with distinct viral load and CD4 cell counts. BMC Infect Dis **13:**250.
305. **Bowden TA, Jones EY, Stuart DI.** 2011. Cells under siege: viral glycoprotein interactions at the cell surface. J Struct Biol **175:**120-126.
306. **Bruce JW, Ahlquist P, Young JA.** 2008. The host cell sulfonation pathway contributes to retroviral infection at a step coincident with provirus establishment. PLoS Pathog **4:**e1000207.
307. **Murry JP, Godoy J, Mukim A, Swann J, Bruce JW, Ahlquist P, Bosque A, Planelles V, Spina CA, Young JA.** 2014. Sulfonation

pathway inhibitors block reactivation of latent HIV-1. Virology **471-473:**1-12.

308. **Guo JH, Hexige S, Chen L, Zhou GJ, Wang X, Jiang JM, Kong YH, Ji GQ, Wu CQ, Zhao SY, Yu L.** 2006. Isolation and characterization of the human D-glyceric acidemia related glycerate kinase gene GLYCTK1 and its alternatively splicing variant GLYCTK2. DNA Seq **17:**1-7.
309. **Van Rompay AR, Johansson M, Karlsson A.** 2003. Substrate specificity and phosphorylation of antiviral and anticancer nucleoside analogues by human deoxyribonucleoside kinases and ribonucleoside kinases. Pharmacol Ther **100:**119-139.
310. **Suzuki NN, Koizumi K, Fukushima M, Matsuda A, Inagaki F.** 2004. Structural basis for the specificity, catalysis, and regulation of human uridine-cytidine kinase. Structure **12:**751-764.
311. **Dooley S, Seib T, Engel M, Theisinger B, Janz H, Piontek K, Zang KD, Welter C.** 1994. Isolation and characterization of the human genomic locus coding for the putative metastasis control gene nm23-H1. Hum Genet **93:**63-66.
312. **Laplante M, Sabatini DM.** 2009. mTOR signaling at a glance. J Cell Sci **122:**3589-3594.
313. **Lee C, Tomkowicz B, Freedman BD, Collman RG.** 2005. HIV-1 gp120-induced TNF-{alpha} production by primary human macrophages is mediated by phosphatidylinositol-3 (PI-3) kinase and mitogen-activated protein (MAP) kinase pathways. J Leukoc Biol **78:**1016-1023.
314. **Cheung R, Ravyn V, Wang L, Ptasznik A, Collman RG.** 2008. Signaling mechanism of HIV-1 gp120 and virion-induced IL-1beta release in primary human macrophages. J Immunol **180:**6675-6684.
315. **Nookala AR, Shah A, Noel RJ, Kumar A.** 2013. HIV-1 Tat-mediated induction of CCL5 in astrocytes involves NF-kappaB, AP-1, C/EBPalpha and C/EBPgamma transcription factors and JAK, PI3K/Akt and p38 MAPK signaling pathways. PLoS One **8:**e78855.
316. **Gangwani MR, Noel RJ, Jr., Shah A, Rivera-Amill V, Kumar A.** 2013. Human immunodeficiency virus type 1 viral protein R (Vpr) induces CCL5 expression in astrocytes via PI3K and MAPK signaling pathways. J Neuroinflammation **10:**136.
317. **Blagoveshchenskaya AD, Thomas L, Feliciangeli SF, Hung CH, Thomas G.** 2002. HIV-1 Nef downregulates MHC-I by a PACS-1- and PI3K-regulated ARF6 endocytic pathway. Cell **111:**853-866.
318. **Hung CH, Thomas L, Ruby CE, Atkins KM, Morris NP, Knight ZA, Scholz I, Barklis E, Weinberg AD, Shokat KM, Thomas G.** 2007. HIV-1 Nef assembles a Src family kinase-ZAP-70/Syk-PI3K cascade to downregulate cell-surface MHC-I. Cell Host Microbe **1:**121-133.
319. **Chugh P, Bradel-Tretheway B, Monteiro-Filho CM, Planelles V, Maggirwar SB, Dewhurst S, Kim B.** 2008. Akt inhibitors as an HIV-1 infected macrophage-specific anti-viral therapy. Retrovirology **5:**11.
320. **Francois F, Klotman ME.** 2003. Phosphatidylinositol 3-kinase regulates human immunodeficiency virus type 1 replication following viral entry in primary CD4+ T lymphocytes and macrophages. J Virol **77:**2539-2549.

321. **Chugh P, Fan S, Planelles V, Maggirwar SB, Dewhurst S, Kim B.** 2007. Infection of human immunodeficiency virus and intracellular viral Tat protein exert a pro-survival effect in a human microglial cell line. J Mol Biol **366:**67-81.
322. **Swann SA, Williams M, Story CM, Bobbitt KR, Fleis R, Collins KL.** 2001. HIV-1 Nef blocks transport of MHC class I molecules to the cell surface via a PI 3-kinase-dependent pathway. Virology **282:**267-277.
323. **Law ME, Corsino PE, Narayan S, Law BK.** 2015. Cyclin-Dependent Kinase Inhibitors as Anticancer Therapeutics. Mol Pharmacol **88:**846-852.
324. **Guen VJ, Gamble C, Flajolet M, Unger S, Thollet A, Ferandin Y, Superti-Furga A, Cohen PA, Meijer L, Colas P.** 2013. CDK10/cyclin M is a protein kinase that controls ETS2 degradation and is deficient in STAR syndrome. Proc Natl Acad Sci U S A **110:**19525-19530.
325. **Fraser ID, Tavalin SJ, Lester LB, Langeberg LK, Westphal AM, Dean RA, Marrion NV, Scott JD.** 1998. A novel lipid-anchored A-kinase Anchoring Protein facilitates cAMP-responsive membrane events. EMBO J **17:**2261-2272.
326. **Giroud C, Chazal N, Gay B, Eldin P, Brun S, Briant L.** 2013. HIV-1-associated PKA acts as a cofactor for genome reverse transcription. Retrovirology **10:**157.
327. **Takeuchi H, Takeuchi T, Gao J, Cantley LC, Hirata M.** 2010. Characterization of PXK as a protein involved in epidermal growth factor receptor trafficking. Mol Cell Biol **30:**1689-1702.
328. **Vaughn SE, Foley C, Lu X, Patel ZH, Zoller EE, Magnusen AF, Williams AH, Ziegler JT, Comeau ME, Marion MC, Glenn SB, Adler A, Shen N, Nath S, Stevens AM, Freedman BI, Tsao BP, Jacob CO, Kamen DL, Brown EE, Gilkeson GS, Alarcon GS, Reveille JD, Anaya JM, James JA, Moser KL, Criswell LA, Vila LM, Alarcon-Riquelme ME, Petri M, Scofield RH, Kimberly RP, Ramsey-Goldman R, Binjoo Y, Choi J, Bae SC, Boackle SA, Vyse TJ, Guthridge JM, Namjou B, Gaffney PM, Langefeld CD, Kaufman KM, Kelly JA, Harley IT, Harley JB, Kottyan LC.** 2014. Lupus risk variants in the PXK locus alter B-cell receptor internalization. Front Genet **5:**450.
329. **Takazawa K, Perret J, Dumont JE, Erneux C.** 1991. Molecular cloning and expression of a human brain inositol 1,4,5-trisphosphate 3-kinase. Biochem Biophys Res Commun **174:**529-535.
330. **Takazawa K, Perret J, Dumont JE, Erneux C.** 1990. Human brain inositol 1,4,5-trisphosphate 3-kinase cDNA sequence. Nucleic Acids Res **18:**7141.
331. **Erneux C, Roeckel N, Takazawa K, Mailleux P, Vassart G, Mattei MG.** 1992. Localization of the genes for human inositol 1,4,5-trisphosphate 3-kinase A (ITPKA) and B (ITPKB) to chromosome regions 15q14-q21 and 1q41-q43, respectively, by in situ hybridization. Genomics **14:**546-547.
332. **Maricato JT, Furtado MN, Takenaka MC, Nunes ER, Fincatti P, Meliso FM, da Silva ID, Jasiulionis MG, Cecilia de Araripe Sucupira M, Diaz RS, Janini LM.** 2015. Epigenetic modulations in

activated cells early after HIV-1 infection and their possible functional consequences. PLoS One **10:**e0119234.
333. **Hetzer C, Bisgrove D, Cohen MS, Pedal A, Kaehlcke K, Speyerer A, Bartscherer K, Taunton J, Ott M.** 2007. Recruitment and activation of RSK2 by HIV-1 Tat. PLoS One **2:**e151.
334. **Anneren C, Lindholm CK, Kriz V, Welsh M.** 2003. The FRK/RAK-SHB signaling cascade: a versatile signal-transduction pathway that regulates cell survival, differentiation and proliferation. Curr Mol Med **3:**313-324.
335. **Lolli G, Johnson LN.** 2005. CAK-Cyclin-dependent Activating Kinase: a key kinase in cell cycle control and a target for drugs? Cell Cycle **4:**572-577.
336. **Nekhai S, Zhou M, Fernandez A, Lane WS, Lamb NJ, Brady J, Kumar A.** 2002. HIV-1 Tat-associated RNA polymerase C-terminal domain kinase, CDK2, phosphorylates CDK7 and stimulates Tat-mediated transcription. Biochem J **364:**649-657.
337. **Cujec TP, Okamoto H, Fujinaga K, Meyer J, Chamberlin H, Morgan DO, Peterlin BM.** 1997. The HIV transactivator TAT binds to the CDK-activating kinase and activates the phosphorylation of the carboxy-terminal domain of RNA polymerase II. Genes Dev **11:**2645-2657.
338. **Jia M, Souchelnytskyi S.** 2010. Kinase suppressor of Ras 2 is involved in regulation of cell proliferation and is up-regulated in human invasive ductal carcinomas of breast. Exp Oncol **32:**209-212.
339. **Wang X, Wang TT, White JH, Studzinski GP.** 2007. Expression of human kinase suppressor of Ras 2 (hKSR-2) gene in HL60 leukemia cells is directly upregulated by 1,25-dihydroxyvitamin D(3) and is required for optimal cell differentiation. Exp Cell Res **313:**3034-3045.
340. **Zarubin T, Han J.** 2005. Activation and signaling of the p38 MAP kinase pathway. Cell Res **15:**11-18.
341. **Kim N, Kukkonen S, Martinez-Viedma Mdel P, Gupta S, Aldovini A.** 2013. Tat engagement of p38 MAP kinase and IRF7 pathways leads to activation of interferon-stimulated genes in antigen-presenting cells. Blood **121:**4090-4100.
342. **Hao HX, Cardon CM, Swiatek W, Cooksey RC, Smith TL, Wilde J, Boudina S, Abel ED, McClain DA, Rutter J.** 2007. PAS kinase is required for normal cellular energy balance. Proc Natl Acad Sci U S A **104:**15466-15471.
343. **Wilson WA, Skurat AV, Probst B, de Paoli-Roach A, Roach PJ, Rutter J.** 2005. Control of mammalian glycogen synthase by PAS kinase. Proc Natl Acad Sci U S A **102:**16596-16601.
344. **DeMille D, Grose JH.** 2013. PAS kinase: a nutrient sensing regulator of glucose homeostasis. IUBMB Life **65:**921-929.
345. **Cardon CM, Beck T, Hall MN, Rutter J.** 2012. PAS kinase promotes cell survival and growth through activation of Rho1. Sci Signal **5:**ra9.
346. **Sgadari C, Barillari G, Palladino C, Bellino S, Taddeo B, Toschi E, Ensoli B.** 2011. Fibroblast Growth Factor-2 and the HIV-1 Tat Protein Synergize in Promoting Bcl-2 Expression and Preventing Endothelial Cell Apoptosis: Implications for the Pathogenesis of AIDS-Associated Kaposi's Sarcoma. Int J Vasc Med **2011:**452729.

347. **Xie X, Colberg-Poley AM, Das JR, Li J, Zhang A, Tang P, Jerebtsova M, Gutkind JS, Ray PE.** 2014. The basic domain of HIV-tat transactivating protein is essential for its targeting to lipid rafts and regulating fibroblast growth factor-2 signaling in podocytes isolated from children with HIV-1-associated nephropathy. J Am Soc Nephrol **25:**1800-1813.
348. **Ray PE, Al-Attar A, Liu XH, Das JR, Tassi E, Wellstein A.** 2014. Expression of a Secreted Fibroblast Growth Factor Binding Protein-1 (FGFBP1) in Angioproliferative Kaposi Sarcoma. J AIDS Clin Res **5**.
349. **Langford D, Hurford R, Hashimoto M, Digicaylioglu M, Masliah E.** 2005. Signalling crosstalk in FGF2-mediated protection of endothelial cells from HIV-gp120. BMC Neurosci **6:**8.
350. **Chaudhary D, Robinson S, Romero DL.** 2015. Recent advances in the discovery of small molecule inhibitors of interleukin-1 receptor-associated kinase 4 (IRAK4) as a therapeutic target for inflammation and oncology disorders. J Med Chem **58:**96-110.
351. **Pathak S, De Souza GA, Salte T, Wiker HG, Asjo B.** 2009. HIV induces both a down-regulation of IRAK-4 that impairs TLR signalling and an up-regulation of the antibiotic peptide dermcidin in monocytic cells. Scand J Immunol **70:**264-276.
352. **Coulombe P, Meloche S.** 2007. Atypical mitogen-activated protein kinases: structure, regulation and functions. Biochim Biophys Acta **1773:**1376-1387.
353. **Ishitani T, Ishitani S.** 2013. Nemo-like kinase, a multifaceted cell signaling regulator. Cell Signal **25:**190-197.
354. **Flory E, Hoffmeyer A, Smola U, Rapp UR, Bruder JT.** 1996. Raf-1 kinase targets GA-binding protein in transcriptional regulation of the human immunodeficiency virus type 1 promoter. J Virol **70:**2260-2268.
355. **Folgueira L, Algeciras A, MacMorran WS, Bren GD, Paya CV.** 1996. The Ras-Raf pathway is activated in human immunodeficiency virus-infected monocytes and particpates in the activation of NF-kappa B. J Virol **70:**2332-2338.
356. **Popik W, Pitha PM.** 1996. Binding of human immunodeficiency virus type 1 to CD4 induces association of Lck and Raf-1 and activates Raf-1 by a Ras-independent pathway. Mol Cell Biol **16:**6532-6541.
357. **Flory E, Weber CK, Chen P, Hoffmeyer A, Jassoy C, Rapp UR.** 1998. Plasma membrane-targeted Raf kinase activates NF-kappaB and human immunodeficiency virus type 1 replication in T lymphocytes. J Virol **72:**2788-2794.
358. **Hodge DR, Dunn KJ, Pei GK, Chakrabarty MK, Heidecker G, Lautenberger JA, Samuel KP.** 1998. Binding of c-Raf1 kinase to a conserved acidic sequence within the carboxyl-terminal region of the HIV-1 Nef protein. J Biol Chem **273:**15727-15733.
359. **Hofmann F, Wegener JW.** 2013. cGMP-dependent protein kinases (cGK). Methods Mol Biol **1020:**17-50.
360. **Jain S, Desai N, Bhangoo A.** 2013. Pathophysiology of GHRH-growth hormone-IGF1 axis in HIV/AIDS. Rev Endocr Metab Disord **14:**113-118.
361. **Xu Y, Kulkosky J, Acheampong E, Nunnari G, Sullivan J, Pomerantz RJ.** 2004. HIV-1-mediated apoptosis of neuronal cells: Proximal molecular mechanisms of HIV-1-induced encephalopathy. Proc Natl Acad Sci U S A **101:**7070-7075.

362. **Wong S, Bhasin S, Serra C, Yu Y, Deng L, Guo W.** 2013. Lopinavir/Ritonavir Impairs Physical Strength in Association with Reduced Igf1 Expression in Skeletal Muscle of Older Mice. J AIDS Clin Res **4:**216.
363. **Suh HS, Lo Y, Choi N, Letendre S, Lee SC.** 2015. Insulin-like growth factors and related proteins in plasma and cerebrospinal fluids of HIV-positive individuals. J Neuroinflammation **12:**72.
364. **Bowden DW, Akots G, Rothschild CB.** 1991. An insertion deletion polymorphism associated with C-FES. Nucleic Acids Res **19:**4311.
365. **Craig AW.** 2012. FES/FER kinase signaling in hematopoietic cells and leukemias. Front Biosci (Landmark Ed) **17:**861-875.
366. **Shiramizu B, Herndier BG, McGrath MS.** 1994. Identification of a common clonal human immunodeficiency virus integration site in human immunodeficiency virus-associated lymphomas. Cancer Res **54:**2069-2072.
367. **Ivanov VN, Ronai Z.** 2000. p38 protects human melanoma cells from UV-induced apoptosis through down-regulation of NF-kappaB activity and Fas expression. Oncogene **19:**3003-3012.
368. **Li T, Wang W, Zhao JH, Zhou X, Li YM, Chen H.** 2015. Pseudolaric acid B inhibits T-cell mediated immune response in vivo via p38MAPK signal cascades and PPARgamma activation. Life Sci **121:**88-96.
369. **Grove JR, Banerjee P, Balasubramanyam A, Coffer PJ, Price DJ, Avruch J, Woodgett JR.** 1991. Cloning and expression of two human p70 S6 kinase polypeptides differing only at their amino termini. Mol Cell Biol **11:**5541-5550.
370. **Zhao XF, Zhao MY, Chai L, Kukuruga D, Tan M, Stass SA.** 2013. Amplified RPS6KB1 and CDC2 genes are potential biomarkers for aggressive HIV+/EBV+ diffuse large B-cell lymphomas. Int J Clin Exp Pathol **6:**148-154.
371. **Tang L, Gao Y, Yan F, Tang J.** 2012. Evaluation of cyclin-dependent kinase-like 1 expression in breast cancer tissues and its regulation in cancer cell growth. Cancer Biother Radiopharm **27:**392-398.
372. **Song Z, Lin J, Sun Z, Ni J, Sha Y.** 2015. RNAi-mediated downregulation of CDKL1 inhibits growth and colony-formation ability, promotes apoptosis of human melanoma cells. J Dermatol Sci **79:**57-63.
373. **Aguirre E, Renner O, Narlik-Grassow M, Blanco-Aparicio C.** 2014. Genetic Modeling of PIM Proteins in Cancer: Proviral Tagging and Cooperation with Oncogenes, Tumor Suppressor Genes, and Carcinogens. Front Oncol **4:**109.
374. **Duverger A, Wolschendorf F, Anderson JC, Wagner F, Bosque A, Shishido T, Jones J, Planelles V, Willey C, Cron RQ, Kutsch O.** 2014. Kinase control of latent HIV-1 infection: PIM-1 kinase as a major contributor to HIV-1 reactivation. J Virol **88:**364-376.
375. **Wells L, Vosseller K, Hart GW.** 2003. A role for N-acetylglucosamine as a nutrient sensor and mediator of insulin resistance. Cell Mol Life Sci **60:**222-228.
376. **Sharif SR, Lee H, Islam MA, Seog DH, Moon IS.** 2015. N-acetyl-D-glucosamine kinase is a component of nuclear speckles and paraspeckles. Mol Cells **38:**402-408.

377. **Jochmann R, Thurau M, Jung S, Hofmann C, Naschberger E, Kremmer E, Harrer T, Miller M, Schaft N, Sturzl M.** 2009. O-linked N-acetylglucosaminylation of Sp1 inhibits the human immunodeficiency virus type 1 promoter. J Virol **83:**3704-3718.
378. **Ryazanov AG, Pavur KS, Dorovkov MV.** 1999. Alpha-kinases: a new class of protein kinases with a novel catalytic domain. Curr Biol **9:**R43-45.
379. **Hosoda T, Monzen K, Hiroi Y, Oka T, Takimoto E, Yazaki Y, Nagai R, Komuro I.** 2001. A novel myocyte-specific gene Midori promotes the differentiation of P19CL6 cells into cardiomyocytes. J Biol Chem **276:**35978-35989.
380. **Van Sligtenhorst I, Ding ZM, Shi ZZ, Read RW, Hansen G, Vogel P.** 2012. Cardiomyopathy in alpha-kinase 3 (ALPK3)-deficient mice. Vet Pathol **49:**131-141.
381. **Guo C, Ludvik AE, Arlotto ME, Hayes MG, Armstrong LL, Scholtens DM, Brown CD, Newgard CB, Becker TC, Layden BT, Lowe WL, Reddy TE.** 2015. Coordinated regulatory variation associated with gestational hyperglycaemia regulates expression of the novel hexokinase HKDC1. Nat Commun **6:**6069.
382. **Lin CW, Kuo JH, Jan MS.** 2012. The global gene-expression profiles of U-937 human macrophages treated with Tat peptide and Tat-FITC conjugate. J Drug Target **20:**515-523.
383. **Sun L, Gu S, Li X, Sun Y, Zheng D, Yu K, Ji C, Tang R, Xie Y, Mao Y.** 2006. [Identification of a novel human MAST4 gene, a new member of the microtubule associated serine-threonine kinase family]. Mol Biol (Mosk) **40:**808-815.
384. **Garland P, Quraishe S, French P, O'Connor V.** 2008. Expression of the MAST family of serine/threonine kinases. Brain Res **1195:**12-19.
385. **Robinson DR, Kalyana-Sundaram S, Wu YM, Shankar S, Cao X, Ateeq B, Asangani IA, Iyer M, Maher CA, Grasso CS, Lonigro RJ, Quist M, Siddiqui J, Mehra R, Jing X, Giordano TJ, Sabel MS, Kleer CG, Palanisamy N, Natrajan R, Lambros MB, Reis-Filho JS, Kumar-Sinha C, Chinnaiyan AM.** 2011. Functionally recurrent rearrangements of the MAST kinase and Notch gene families in breast cancer. Nat Med **17:**1646-1651.
386. **Bristow JM, Reno TA, Jo M, Gonias SL, Klemke RL.** 2013. Dynamic phosphorylation of tyrosine 665 in pseudopodium-enriched atypical kinase 1 (PEAK1) is essential for the regulation of cell migration and focal adhesion turnover. J Biol Chem **288:**123-131.
387. **Wang Y, Kelber JA, Tran Cao HS, Cantin GT, Lin R, Wang W, Kaushal S, Bristow JM, Edgington TS, Hoffman RM, Bouvet M, Yates JR, 3rd, Klemke RL.** 2010. Pseudopodium-enriched atypical kinase 1 regulates the cytoskeleton and cancer progression [corrected]. Proc Natl Acad Sci U S A **107:**10920-10925.
388. **Nada S, Okada M, MacAuley A, Cooper JA, Nakagawa H.** 1991. Cloning of a complementary DNA for a protein-tyrosine kinase that specifically phosphorylates a negative regulatory site of p60c-src. Nature **351:**69-72.
389. **McCarthy SD, Jung D, Sakac D, Branch DR.** 2014. c-Src and Pyk2 protein tyrosine kinases play protective roles in early HIV-1 infection of CD4+ T-cell lines. J Acquir Immune Defic Syndr **66:**118-126.

390. **Wang PJ, Page DC.** 2002. Functional substitution for TAF(II)250 by a retroposed homolog that is expressed in human spermatogenesis. Hum Mol Genet **11:**2341-2346.
391. **Sakamaki J, Fu A, Reeks C, Baird S, Depatie C, Al Azzabi M, Bardeesy N, Gingras AC, Yee SP, Screaton RA.** 2014. Role of the SIK2-p35-PJA2 complex in pancreatic beta-cell functional compensation. Nat Cell Biol **16:**234-244.
392. **Shen A, Yang HC, Zhou Y, Chase AJ, Boyer JD, Zhang H, Margolick JB, Zink MC, Clements JE, Siliciano RF.** 2007. Novel pathway for induction of latent virus from resting CD4(+) T cells in the simian immunodeficiency virus/macaque model of human immunodeficiency virus type 1 latency. J Virol **81:**1660-1670.
393. **Bressler P, Pantaleo G, Demaria A, Fauci AS.** 1991. Anti-CD2 receptor antibodies activate the HIV long terminal repeat in T lymphocytes. J Immunol **147:**2290-2294.
394. **Iglesias-Ussel M, Vandergeeten C, Marchionni L, Chomont N, Romerio F.** 2013. High levels of CD2 expression identify HIV-1 latently infected resting memory CD4+ T cells in virally suppressed subjects. J Virol **87:**9148-9158.
395. **Wen X, Ding L, Wang JJ, Qi M, Hammonds J, Chu H, Chen X, Hunter E, Spearman P.** 2014. ROCK1 and LIM kinase modulate retrovirus particle release and cell-cell transmission events. J Virol **88:**6906-6921.
396. **Strasner AB, Natarajan M, Doman T, Key D, August A, Henderson AJ.** 2008. The Src kinase Lck facilitates assembly of HIV-1 at the plasma membrane. J Immunol **181:**3706-3713.
397. **Schiralli Lester GM, Akiyama H, Evans E, Singh J, Gummuluru S, Henderson AJ.** 2013. Interleukin 2-inducible T cell kinase (ITK) facilitates efficient egress of HIV-1 by coordinating Gag distribution and actin organization. Virology **436:**235-243.
398. **Yeung ML, Houzet L, Yedavalli VS, Jeang KT.** 2009. A genome-wide short hairpin RNA screening of jurkat T-cells for human proteins contributing to productive HIV-1 replication. J Biol Chem **284:**19463-19473.
399. **Rato S, Maia S, Brito PM, Resende L, Pereira CF, Moita C, Freitas RP, Moniz-Pereira J, Hacohen N, Moita LF, Goncalves J.** 2010. Novel HIV-1 knockdown targets identified by an enriched kinases/phosphatases shRNA library using a long-term iterative screen in Jurkat T-cells. PLoS One **5:**e9276.
400. **Hirsch AJ.** 2010. The use of RNAi-based screens to identify host proteins involved in viral replication. Future Microbiol **5:**303-311.
401. **Le Sage V, Cinti A, Amorim R, Mouland AJ.** 2016. Adapting the Stress Response: Viral Subversion of the mTOR Signaling Pathway. Viruses **8**.
402. **Manning BD, Toker A.** 2017. AKT/PKB Signaling: Navigating the Network. Cell **169:**381-405.
403. **Mori S, Nada S, Kimura H, Tajima S, Takahashi Y, Kitamura A, Oneyama C, Okada M.** 2014. The mTOR pathway controls cell proliferation by regulating the FoxO3a transcription factor via SGK1 kinase. PLoS One **9:**e88891.

404. **Hay N.** 2011. Interplay between FOXO, TOR, and Akt. Biochim Biophys Acta **1813:**1965-1970.
405. **Jacinto E, Loewith R, Schmidt A, Lin S, Ruegg MA, Hall A, Hall MN.** 2004. Mammalian TOR complex 2 controls the actin cytoskeleton and is rapamycin insensitive. Nat Cell Biol **6:**1122-1128.
406. **Devreotes P, Horwitz AR.** 2015. Signaling networks that regulate cell migration. Cold Spring Harb Perspect Biol **7:**a005959.
407. **Carlson LA, de Marco A, Oberwinkler H, Habermann A, Briggs JA, Krausslich HG, Grunewald K.** 2010. Cryo electron tomography of native HIV-1 budding sites. PLoS Pathog **6:**e1001173.
408. **Rahman SA, Koch P, Weichsel J, Godinez WJ, Schwarz U, Rohr K, Lamb DC, Krausslich HG, Muller B.** 2014. Investigating the role of F-actin in human immunodeficiency virus assembly by live-cell microscopy. J Virol **88:**7904-7914.
409. **Daussy CF, Beaumelle B, Espert L.** 2015. Autophagy restricts HIV-1 infection. Oncotarget **6:**20752-20753.
410. **Dinkins C, Pilli M, Kehrl JH.** 2015. Roles of autophagy in HIV infection. Immunol Cell Biol **93:**11-17.
411. **Heredia A, Le N, Gartenhaus RB, Sausville E, Medina-Moreno S, Zapata JC, Davis C, Gallo RC, Redfield RR.** 2015. Targeting of mTOR catalytic site inhibits multiple steps of the HIV-1 lifecycle and suppresses HIV-1 viremia in humanized mice. Proc Natl Acad Sci U S A **112:**9412-9417.
412. **Perkovic M, Schmidt S, Marino D, Russell RA, Stauch B, Hofmann H, Kopietz F, Kloke B-P, Zielonka J, Ströver H, Hermle J, Lindemann D, Pathak VK, Schneider G, Löchelt M, Cichutek K, Münk C.** 2009. Species-specific inhibition of APOBEC3C by the prototype foamy virus protein bet. The Journal of biological chemistry **284:**5819-5826.

12 Appendix

12.1 Appendix 1: Primary screen kinase library (Ambion)

Table 23 List of all genes targeted by the kinase library.

Gene Symbol	RefSeq ID	Gene Symbol	RefSeq ID	Gene Symbol	RefSeq ID
AAK1	NM_014911	GNE	NM_005476	PDGFRB	NM_002609
ABL1	NM_007313	GOSR1	NM_004871	PDGFRL	NM_006207
ABL2	NM_007314	GRIP2	XM_042936	PDK1	NM_002610
ACK1	NM_005781	GRK1	NM_002929	PDK2	NM_002611
ACVR1	NM_001105	GRK4	NM_001004056	PDK3	NM_005391
ACVR1B	NM_020328	GRK5	NM_005308	PDK4	NM_002612
ACVR1C	NM_145259	GRK6	NM_001004106	PDPK1	NM_002613
ACVR2	NM_001616	GRK7	NM_139209	PDXK	NM_003681
ACVR2B	NM_001106	GSG2	NM_031965	PFKL	NM_002626
ACVRL1	NM_000020	GSK3A	NM_019884	PFKM	NM_000289
ADCK2	NM_052853	GSK3B	NM_002093	PFKP	NM_002627
ADCK4	NM_024876	GUK1	NM_000858	PFTK1	NM_012395
ADCK5	NM_174922	HAK	NM_052947	PGK1	NM_000291
ADK	NM_001123	HCK	NM_002110	PGK2	NM_138733
ADRBK1	NM_001619	HCV_138	-	PHKG1	NM_006213
ADRBK2	NM_005160	HCV_321	-	PHKG2	NM_000294
AIP1	NM_012301	HGS	NM_004712	PI4K2B	NM_018323
AK1	NM_000476	HIPK1	NM_198269	PI4KII	NM_018425
AK2	NM_172199	HIPK2	NM_022740	PIK3AP1	NM_152309
AK3	NM_203464	HIPK3	NM_005734	PIK3C2A	NM_002645
AK3L1	NM_016282	HIPK4	NM_144685	PIK3C2B	NM_002646
AK5	NM_012093	HK1	NM_033497	PIK3C2G	NM_004570
AK7	NM_152327	HK2	NM_000189	PIK3C3	NM_002647
AKAP12	NM_144497	HK3	NM_002115	PIK3CA	NM_006218
AKAP2	NM_001004065	HRI	NM_014413	PIK3CB	NM_006219
AKAP28	NM_178813	HSMDPKIN	NM_017525	PIK3CD	NM_005026
AKAP7	NM_016377	HUNK	NM_014586	PIK3CG	NM_002649
AKAP8	NM_005858	ICK	NM_016513	PIK3R3	NM_003629
AKAP8L	NM_014371	IGF1R	NM_000875	PIK3R4	NM_014602
AKIP	NM_017900	IHPK1	NM_001006115	PIK4CA	NM_002650
AKT1	NM_005163	IHPK2	NM_001005909	PIK4CB	NM_002651
AKT2	NM_001626	IHPK3	NM_054111	PIM1	NM_002648
AKT3	NM_181690	IKBKB	NM_001556	PIM2	NM_006875
ALDH18A1	NM_002860	IKBKE	NM_014002	PIM3	NM_001001852
ALK	NM_004304	IKBKG	NM_003639	PINK1	NM_032409
ALS2CR2	NM_018571	ILK	NM_004517	PIP5K1A	NM_003557
ALS2CR7	NM_139158	INCENP	NM_020238	PIP5K1B	NM_001031687
AMHR2	NM_020547	INSR	NM_000208	PIP5K1C	NM_012398
ANKK1	NM_178510	INSRR	NM_014215	PIP5K2A	NM_005028
ARAF1	NM_001654	IPMK	NM_152230	PIP5K2B	NM_138687
ARK5	NM_014840	IRAK1	NM_001025242	PIP5K2C	NM_024779
ASB10	NM_080871	IRAK2	NM_001570	PIP5KL1	NM_173492
ATM	NM_000051	IRAK3	NM_007199	PKLR	NM_000298
ATR	NM_001184	IRAK4	NM_016123	PKM2	NM_182471
AURKB	NM_004217	ITGB1BP3	NM_014446	PKMYT1	NM_182687
AURKC	NM_001015878	ITK	NM_005546	PKN1	NM_002741
AXL	NM_001699	ITPK1	NM_014216	PKN2	NM_006256
BAIAP1	NM_001033057	ITPKA	NM_002220	PKN3	NM_013355
BCKDK	NM_005881	ITPKB	NM_002221	PLK1	NM_005030
BLK	NM_001715	ITPKC	NM_025194	PLK2	NM_006622
BMP2K	NM_198892	JAK1	NM_002227	PLK3	NM_004073
BMP2KL	XM_293293	JAK2	NM_004972	PLK4	NM_014264
BMPR1A	NM_004329	JAK3	NM_000215	PLXNA1	NM_032242
BMPR1B	NM_001203	JIK	NM_016281	PLXNA2	NM_025179
BMPR2	NM_033346	KDR	NM_002253	PLXNA3	NM_017514
BMX	NM_001721	KHK	NM_006488	PLXNA4A	XM_379927
BRAF	NM_004333	KIAA0431	NM_015251	PLXNB1	NM_002673
BTK	NM_000061	KIAA0551	NM_015028	PLXNB2	NM_012401
BUB1	NM_004336	KIAA0999	NM_025164	PLXNB3	NM_005393
BUB1B	NM_001211	KIAA1361	NM_020791	PLXNC1	NM_005761
C14orf20	NM_174944	KIAA1639	XM_290923	PLXND1	NM_015103
C19orf35	NM_198532	KIAA1765	XM_047355	PMVK	NM_006556
C21orf7	NM_020152	KIAA1804	NM_032435	PNCK	NM_198452
C9orf12	NM_022755	KIAA1811	NM_032430	PNKP	NM_007254
C9orf95	NM_017881	KIAA2002	XM_370878	PRKAA1	NM_006251
C9orf96	NM_153710	KIS	NM_144624	PRKAA2	NM_006252
C9orf98	NM_152572	KIT	NM_000222	PRKACA	NM_002730
CALM1	NM_006888	KSR2	NM_173598	PRKACB	NM_207578
CALM2	NM_001743	LAK	NM_025144	PRKACG	NM_002732
CALM3	NM_005184	LATS1	NM_004690	PRKCA	NM_002737
CAMK1	NM_003656	LATS2	NM_014572	PRKCABP	NM_012407
CAMK1D	NM_020397	LCK	NM_005356	PRKCB1	NM_212535
CAMK1G	NM_020439	LEDGF/p75	-	PRKCBP1	NM_183048
CAMK2A	NM_171825	LIMK1	NM_016735	PRKCD	NM_006254
CAMK2B	NM_172083	LIMK2	NM_005569	PRKCDBP	NM_145040
CAMK2D	NM_172128	LMTK2	NM_014916	PRKCE	NM_005400
CAMK2G	NM_172171	LMTK3	XM_055866	PRKCG	NM_002739
CAMK4	NM_001744	LOC149420	NM_152835	PRKCH	NM_006255

Gene Symbol	RefSeq ID	Gene Symbol	RefSeq ID	Gene Symbol	RefSeq ID
CaMKIINalpha	NM_018584	LOC283846	NM_199284	PRKCI	NM_002740
CAMKK1	NM_032294	LOC340156	NM_001012418	PRKCM	NM_002742
CAMKK2	NM_153499	LOC340371	NM_178564	PRKCN	NM_005813
CARKL	NM_013276	LOC375328	NM_199347	PRKCQ	NM_006257
CASK	NM_003688	LOC388221	XM_370939	PRKCSH	NM_001001329
CCRK	NM_178432	LOC389599	XM_372002	PRKCZ	NM_002744
CD2	NM_001767	LOC390777	XM_372663	PRKD2	NM_016457
CD4	-	LOC390877	XM_372705	PRKDC	NM_006904
CDC2	NM_001786	LOC390975	XM_372749	PRKG1	NM_006258
CDC2L2	NM_033534	LOC391295	XM_497791	PRKG2	NM_006259
CDC2L5	NM_003718	LOC391533	XM_497921	PRKR	NM_002759
CDC42BPA	NM_014826	LOC392226	XM_498286	PRKWNK1	NM_018979
CDC42BPB	NM_006035	LOC392265	XM_498294	PRKWNK2	NM_006648
CDC42SE2	NM_020240	LOC392347	XM_373298	PRKWNK3	NM_020922
CDC7	NM_003503	LOC400301	XM_375150	PRKWNK4	NM_032387
CDK10	NM_003674	LOC440332	XM_496112	PRKX	NM_005044
CDK11	NM_015076	LOC440345	XM_496125	PRKXP1	XM_497470
CDK2	NM_001798	LOC440451	XM_496234	PRKY	NM_002760
CDK3	NM_001258	LOC441047	XM_496720	PRPF4B	NM_003913
CDK4	NM_052984	LOC441708	XM_497433	PRPS1	NM_002764
CDK5	NM_004935	LOC441777	XM_497521	PRPS1L1	NM_175886
CDK6	NM_001259	LOC441787	XM_497532	PRPS2	NM_002765
CDK7	NM_001799	LOC442075	XM_496630	PRPSAP1	NM_002766
CDK8	NM_001260	LOC442141	XM_498022	PRPSAP2	NM_002767
CDK9	NM_001261	LOC91807	NM_182493	PSKH1	NM_006742
CDKL1	NM_004196	LRRK1	NM_024652	PSKH2	NM_033126
CDKL2	NM_003948	LRRK2	NM_198578	PTK2	NM_153831
CDKL3	NM_016508	LTK	NM_206961	PTK2B	NM_173176
CDKL4	NM_001009565	LY6G5B	NM_021221	PTK6	NM_005975
CDKL5	NM_003159	LYK5	NM_153335	PTK7	NM_152883
CERK	NM_182661	LYN	NM_002350	PTK9	NM_198974
CHEK1	NM_001274	MADD	NM_003682	PTK9L	NM_007284
CHEK2	NM_145862	MAGI1	NM_173515	PXK	NM_017771
CHKA	NM_001277	MAGI-3	NM_020965	RAB1A	NM_004161
CHKB	NM_152253	MAK	NM_005906	RAB6A	NM_002869
CHUK	NM_001278	MAP2K1	NM_002755	RAF1	NM_002880
CIB1	NM_006384	MAP2K1IP1	NM_021970	RAGE	NM_014226
CIB4	NM_001029881	MAP2K2	NM_030662	RBKS	NM_022128
CIT	NM_007174	MAP2K3	NM_002756	RET	NM_020630
CKB	NM_001823	MAP2K4	NM_003010	RFK	NM_018339
CKI-alpha	-	MAP2K5	NM_145162	RIOK1	NM_031480
CKI-delta	-	MAP2K6	NM_002758	RIOK2	NM_018343
CKM	NM_001824	MAP2K7	NM_145185	RIOK3	NM_145906
CKMT1	NM_020990	MAP3K1	XM_042066	RIPK1	NM_003804
CKMT2	NM_001825	MAP3K10	NM_002446	RIPK2	NM_003821
CLK1	NM_001024646	MAP3K11	NM_002419	RIPK3	NM_006871
CLK2	NM_001291	MAP3K12	NM_006301	RIPK4	NM_020639
CLK3	NM_001292	MAP3K13	NM_004721	RIPK5	NM_199462
CLK4	NM_020666	MAP3K14	NM_003954	RNASEL	NM_021133
CNKSR1	NM_006314	MAP3K2	NM_006609	ROCK1	NM_005406
COASY	NM_025233	MAP3K3	NM_203351	ROCK2	NM_004850
COL4A3BP	NM_031361	MAP3K4	NM_006724	ROR1	NM_005012
COPB	NM_016451	MAP3K5	NM_005923	ROR2	NM_004560
CRIM1	NM_016441	MAP3K6	NM_004672	ROS1	NM_002944
CRK7	NM_016507	MAP3K7	NM_145332	RP26	NM_001030312
CSF1R	NM_005211	MAP3K7IP2	NM_015093	RPS6KA1	NM_001006665
CSK	NM_004383	MAP3K8	NM_005204	RPS6KA2	NM_001006932
CSNK1A1	NM_001892	MAP3K9	NM_033141	RPS6KA3	NM_004586
CSNK1A1L	NM_145203	MAP4K1	NM_007181	RPS6KA4	NM_001006944
CSNK1D	NM_139062	MAP4K2	NM_004579	RPS6KA5	NM_004755
CSNK1E	NM_001894	MAP4K3	NM_003618	RPS6KA6	NM_014496
CSNK1G1	NM_022048	MAP4K4	NM_145686	RPS6KB1	NM_003161
CSNK1G2	NM_001319	MAP4K5	NM_006575	RPS6KB2	NM_001007071
CSNK1G3	NM_004384	MAPK1	NM_138957	RPS6KL1	NM_031464
CSNK2A1	NM_177560	MAPK10	NM_138981	RYK	NM_002958
CSNK2A2	NM_001896	MAPK11	NM_138993	SBK1	NM_001024401
CXCR4	-	MAPK12	NM_002969	SCAP1	NM_003726
DAPK1	NM_004938	MAPK13	NM_002754	SCGB2A1	NM_002407
DAPK2	NM_014326	MAPK14	NM_139013	Scrambled	-
DAPK3	NM_001348	MAPK3	NM_002746	SCYL1	NM_020680
DCAMKL1	NM_004734	MAPK4	NM_002747	SGK	NM_005627
DCK	NM_000788	MAPK6	NM_002748	SGK2	NM_016276
DDR1	NM_001954	MAPK7	NM_139032	SGKL	NM_013257
DDR2	NM_001014796	MAPK8	NM_139049	SH3BP4	NM_014521
DGKA	NM_201444	MAPK9	NM_139068	SIK2	NM_015191
DGKB	NM_145695	MAPKAPK2	NM_032960	SKP2	NM_032637
DGKD	NM_152879	MAPKAPK3	NM_004635	SLAMF6	NM_052931
DGKE	NM_003647	MAPKAPK5	NM_139078	SLK	NM_014720
DGKG	NM_001346	MARK1	NM_018650	SMG1	NM_014006
DGKH	NM_152910	MARK2	NM_017490	SNARK	NM_030952
DGKI	NM_004717	MARK3	NM_002376	SNF1LK	NM_173354
DGKK	NM_001013742	MARK4	NM_031417	SNRK	NM_017719
DGKQ	NM_001347	MAST1	NM_014975	SNX16	NM_152837
DGKZ	NM_003646	MAST2	NM_015112	SPHK1	NM_021972
DGUOK	NM_001929	MAST3	XM_038150	SPHK2	NM_020126
DKFZp434B1231	NM_178275	MAST4	XM_291141	SRC	NM_005417
DKFZP434C131	NM_015518	MASTL	NM_032844	SRMS	NM_080823
DKFZp434C1418	NM_173655	MATK	NM_139354	SRPK1	NM_003137
DKFZp434G0625	NM_181775	MELK	NM_014791	SRPK2	NM_182692
DKFZP586B1621	NM_015533	MERTK	NM_006343	SSTK	NM_032037
DKFZp761P0423	XM_291277	MET	NM_000245	STK10	NM_005990
DMPK	NM_004409	MFHAS1	NM_004225	STK11	NM_000455
DNAJC6	NM_014787	MGC40579	NM_152776	STK11IP	NM_052902

Gene Symbol	RefSeq ID		Gene Symbol	RefSeq ID		Gene Symbol	RefSeq ID
DOK1	NM_001381		MGC42105	NM_153361		STK16	NM_001008910
DTYMK	NM_012145		MGC45428	NM_152619		STK17A	NM_004760
DV-E	-		MGC4796	NM_032017		STK17B	NM_004226
DV-NS3	-		MGC8407	NM_024046		STK19	NM_004197
DV-NS5	-		MIDORI	NM_020778		STK22B	NM_053006
DYRK1A	NM_130438		MINK	NM_170663		STK22C	NM_052841
DYRK1B	NM_006484		MKNK1	NM_003684		STK22D	NM_032028
DYRK2	NM_003583		MKNK2	NM_017572		STK23	NM_014370
DYRK3	NM_003582		MOS	NM_005372		STK24	NM_001032296
DYRK4	NM_003845		MPP1	NM_002436		STK25	NM_006374
EEF2K	NM_013302		MPP2	NM_005374		STK29	NM_003957
EGFR	NM_201284		MPP3	NM_001932		STK3	NM_006281
EIF2AK3	NM_004836		MPP4	NM_033066		STK32A	NM_145001
EIF2AK4	NM_001013703		MPP5	NM_022474		STK32B	NM_018401
Emerin	-		MPP6	NM_016447		STK32C	NM_173575
EPHA1	NM_005232		MPP7	NM_173496		STK33	NM_030906
EPHA2	NM_004431		MRC2	NM_006039		STK35	NM_080836
EPHA3	NM_182644		MST1R	NM_002447		STK36	NM_015690
EPHA4	NM_004438		MST4	NM_016542		STK38	NM_007271
EPHA5	NM_004439		MUSK	NM_005592		STK38L	NM_015000
EPHA7	NM_004440		MVK	NM_000431		STK39	NM_013233
EPHA8	NM_020526		MYLK	NM_053031		STK4	NM_006282
EPHB1	NM_004441		MYLK2	NM_033118		STK6	NM_198433
EPHB2	NM_017449		NAGK	NM_017567		STYK1	NM_018423
EPHB3	NM_004443		NEK1	NM_012224		SYK	NM_003177
EPHB4	NM_004444		NEK11	NM_145910		T3JAM	NM_025228
EPHB6	NM_004445		NEK2	NM_002497		TAF1	NM_004606
ERBB2	NM_004448		NEK3	NM_002498		TAF1L	NM_153809
ERBB3	NM_001982		NEK4	NM_003157		TAO1	NM_016151
ERBB4	NM_005235		NEK5	NM_199289		TBK1	NM_013254
ERK8	NM_139021		NEK6	NM_014397		TEC	NM_003215
ERN1	NM_001433		NEK7	NM_133494		TEK	NM_000459
ERN2	NM_033266		NEK8	NM_178170		TESK1	NM_006285
ETNK1	NM_018638		NEK9	NM_033116		TESK2	NM_007170
ETNK2	NM_018208		NIPA	NM_016478		TEX14	NM_031272
FASTK	NM_025096		NLK	NM_016231		TGFBR1	NM_004612
FER	NM_005246		NME1	NM_000269		TGFBR2	NM_001024847
FES	NM_002005		NME2	NM_001018137		TIE	NM_005424
FGFR1	NM_023108		NME3	NM_002513		TK1	NM_003258
FGFR2	NM_023031		NME4	NM_005009		TK2	NM_004614
FGFR3	NM_000142		NME5	NM_003551		TLK1	NM_012290
FGFR4	NM_002011		NME6	NM_005793		TLK2	NM_006852
FGFRL1	NM_021923		NME7	NM_197972		TNK1	NM_003985
FGR	NM_005248		NRBP	NM_013392		TNNI3K	NM_015978
FLJ10074	NM_017988		NRGN	NM_006176		TOPK	NM_018492
FLJ10842	NM_018238		NRK	NM_198465		TPK1	NM_022445
FLJ10986	NM_018291		NTRK1	NM_001012331		TRIB1	NM_025195
FLJ12476	NM_001031715		NTRK2	NM_001018065		TRIB2	NM_021643
FLJ13052	NM_023018		NTRK3	NM_002530		TRIB3	NM_021158
FLJ16518	NM_001001671		NYD-SP25	NM_033516		Trim5alpha	-
FLJ20574	NM_017886		OSR1	NM_005109		TRRAP	NM_003496
FLJ22761	NM_025130		OSRF	NM_012382		TSKS	NM_021733
FLJ22955	NM_024819		p24	-		TTBK1	NM_032538
FLJ23074	NM_001018046		p53	-		TTK	NM_003318
FLJ25006	NM_144610		PACE-1	NM_181093		TXK	NM_003328
FLJ32685	NM_152534		PACSIN1	NM_020804		TXNDC3	NM_016616
FLJ33655	NM_173641		PACSIN2	NM_007229		TXNDC6	NM_178130
FLJ34389	NM_152649		PACSIN3	NM_016223		TYK2	NM_003331
FLJ37794	NM_173588		PAK1	NM_002576		TYRO3	NM_006293
FLT1	NM_002019		PAK2	NM_002577		UCK1	NM_031432
FLT3	NM_004119		PAK3	NM_002578		UCK2	NM_012474
FLT4	NM_002020		PAK4	NM_001014833		UCKL1	NM_017859
FN3K	NM_022158		PAK6	NM_020168		ULK1	NM_003565
FN3KRP	NM_024619		PAK7	NM_177990		ULK2	NM_014683
FRAP1	NM_004958		PANK1	NM_138316		UMP-CMPK	NM_016308
FRK	NM_002031		PANK2	NM_153638		VRK1	NM_003384
FUK	NM_145059		PANK3	NM_024594		VRK2	NM_006296
FYN	NM_153048		PANK4	NM_018216		VRK3	NM_016440
GAK	NM_005255		PAPSS1	NM_005443		WEE1	NM_003390
GALK1	NM_000154		PAPSS2	NM_004670		XM_290793	NM_014238
GALK2	NM_001001556		PASK	NM_015148		XYLB	NM_005108
GCK	NM_033507		PCM1	NM_006197		YES1	NM_005433
GCKR	NM_001486		PCTK1	NM_006201		ZAK	NM_133646
GK	NM_000167		PCTK2	NM_002595		ZAP70	NM_207519
GK2	NM_033214		PCTK3	NM_002596			
GLYCTK	NM_145262		PDGFRA	NM_006206			

12.2 Appendix 2: Reconfirmation screen library

Table 24 List of all genes targeted by the reconfirmation screen library.

Gene Symbol	RefSeq ID	Full Gene Name	Gene ID	Ambion siRNA ID	Sense siRNA Sequence	Antisense siRNA Sequence	Z-score
ACVR2A	NM_001616	activin A receptor, type IIA	92	s980	GCCCAGUUGCUUAACGAAUtt	AUUCGUUAAGCAACUGGGCtt	-2.73300511
ACVR2A	NM_001616	activin A receptor, type IIA	92	s981	GGAUGAUAUCAACUGCUAUtt	AUAGCAGUUGAUAUCAUCCag	-3.70856555
ACVR2A	NM_001616	activin A receptor, type IIA	92	s982	CAGACUUUCUUAAGGCUAAtt	UUAGCCUUAAGAAAGUCUGat	0.157403425
AKAP7	NM_004842	A kinase (PRKA) anchor protein 7	9465	s18135	AACUAGUAAGGCUCAGUAAtt	UUACUGAGCCUUACUAGUUca	0.418438436
AKAP7	NM_004842	A kinase (PRKA) anchor protein 7	9465	s225138	AGUGCUAAGUUUAAAAUAAtt	UUAUUUUAAACUUAGCACUtg	-3.81524755
AKAP7	NM_004842	A kinase (PRKA) anchor protein 7	9465	s225139	CCGAAGCAGCUGAUCAGAAtt	UUCUGAUCAGCUGCUUCGGtt	-0.31091666
AKAP8L	NM_014371	A kinase (PRKA) anchor protein 8-like	26993	s25667	GGAACACUUUAAGUACGUAtt	UACGUACUUAAAGUGUUCCtt	-1.39975422
AKAP8L	NM_014371	A kinase (PRKA) anchor protein 8-like	26993	s25668	CCAUGGAUCACAACCGGAAtt	UUCCGGUUGUGAUCCAUGGtc	-1.4377644
AKAP8L	NM_014371	A kinase (PRKA) anchor protein 8-like	26993	s25669	CAGUCGACAUACUCGGAUAtt	UAUCCGAGUAUGUCGACUGca	1.570650326
ALPK3	NM_020778	alpha-kinase 3	57538	s33259	GACUAGGCCUUUCAACAGAtt	UCUGUUGAAAGGCCUAGUCgg	-2.25198529
ALPK3	NM_020778	alpha-kinase 3	57538	s33260	GGUACAAGGAUGAUACGGAtt	UCCGUAUCAUCCUUGUACCag	-1.7383512
ALPK3	NM_020778	alpha-kinase 3	57538	s33261	CCAUGGAUAUGGAAACCCAtt	UGGGUUUCCAUAUCCAUGGgt	-1.77638445
AURKAIP1	NM_017900	aurora kinase A interacting protein 1	54998	s195269	AGAUCAAGUUCGAGAAAGAtt	UCUUUCUCGAACUUGAUCUgc	-1.95451317
AURKAIP1	NM_017900	aurora kinase A interacting protein 1	54998	s29953	GCAGAUCAAGUUCGAGAAAtt	UUUCUCGAACUUGAUCUGCtt	-0.43108357
AURKAIP1	NM_017900	aurora kinase A interacting protein 1	54998	s29954	CCACCGCAAUCCUACCAGUtt	ACUGGUAGGAUUGCGGUGGag	-2.10077712
BLK	NM_001715	B lymphoid tyrosine kinase	640	s1994	GCUCCUUUCUUAUCAGAGAtt	UCUCUGAUAAGAAAGGAGCcg	0.530277633
BLK	NM_001715	B lymphoid tyrosine kinase	640	s1995	UCUACGCAGUGGUCACCAAtt	UUGGUGACCACUGCGUAGAgt	-0.44898079
BLK	NM_001715	B lymphoid tyrosine kinase	640	s1996	UGAUGGAAGUUGUCACUUAtt	UAAGUGACAACUUCCAUCAgg	-0.9561952
BRAF	NM_004333	v-raf murine sarcoma viral oncogene homolog B1	673	s2080	CAGAGGAUUUUAGUCUAUAtt	UAUAGACUAAAAUCCUCUGtt	-1.39602365
BRAF	NM_004333	v-raf murine sarcoma viral oncogene homolog B1	673	s2081	GCAUAAUCCACCAUCAAUAtt	UAUUGAUGGUGGAUUAUGCtc	-0.57195702
BRAF	NM_004333	v-raf murine sarcoma viral oncogene homolog B1	673	s2082	CAGUUGUCUGGAUCCAUUUtt	AAAUGGAUCCAGACAACUGtt	-2.89227483
BRSK2	NM_003957	BR serine/threonine kinase 2	9024	s17197	CGGAAAGAAAGGUACCCGAtt	UCGGGUACCUUUCUUUCCGgt	-0.3725711
BRSK2	NM_003957	BR serine/threonine kinase 2	9024	s17198	GCACUUGUCAGACACCACUtt	AGUGGUGUCUGACAAGUGCtg	-0.20152294
BRSK2	NM_003957	BR serine/threonine kinase 2	9024	s17199	AGAAUGAGCCCGAACCAGAtt	UCUGGUUCGGGCUCAUUCUtg	-0.35589065
CD2	NM_001767	CD2 molecule	914	s225090	GAGAGGGUCUCAAAACCAAtt	UUGGUUUUGAGACCCUCUCtt	2.111036276

Gene Symbol	RefSeq ID	Full Gene Name	Gene ID	Ambion siRNA ID	Sense siRNA Sequence	Antisense siRNA Sequence	Z-score
CD2	NM_001767	CD2 molecule	914	s225091	GCACUGCUCGUUUUCUAUAtt	UAUAGAAAACGAGCAGUGCca	-0.54939342
CD2	NM_001767	CD2 molecule	914	s2565	GGACAUCUAUCUCAUCAUUtt	AAUGAUGAGAUAGAUGUCCag	-0.5586411
CDK10	NM_052987	cyclin-dependent kinase 10	8558	s262	GUUUCCAACUUGCUCAUGAtt	UCAUGAGCAAGUUGGAAACct	-2.19817594
CDK10	NM_052987	cyclin-dependent kinase 10	8558	s263	GGCCUAUGGUGUCCCAGUAtt	UACUGGGACACCAUAGGCCcg	-3.86335008
CDK10	NM_052987	cyclin-dependent kinase 10	8558	s264	AGAUCGACUUGAUCGUGCAtt	UGCACGAUCAAGUCGAUCUgg	0.935507477
CDK4	NM_000075	cyclin-dependent kinase 4	1019	s2822	UGCUGACUUUUAACCCACAtt	UGUGGGUUAAAAGUCAGCAtt	-1.65740479
CDK4	NM_000075	cyclin-dependent kinase 4	1019	s2823	GGCUUUUGAGCAUCCCAAUtt	AUUGGGAUGCUCAAAAGCCtc	-0.09868773
CDK4	NM_000075	cyclin-dependent kinase 4	1019	s2824	CACCCGUGGUUGUUACACUtt	AGUGUAACAACCACGGGUGta	1.916087317
CDK6	NM_001259	cyclin-dependent kinase 6	1021	s51	GUUUGUAACAGAUAUCGAUtt	AUCGAUAUCUGUUACAAACtt	1.093543646
CDK6	NM_001259	cyclin-dependent kinase 6	1021	s52	GGAUAUGAUGUUUCAGCUUtt	AAGCUGAAACAUCAUAUCCtt	-1.13512646
CDK6	NM_001259	cyclin-dependent kinase 6	1021	s53	GCAGAAAUGUUUCGUAGAAtt	UUCUACGAAACAUUUCUGCaa	-0.6869506
CDK7	NM_001799	cyclin-dependent kinase 7	1022	s2828	CAACAUUGGAUCCUACAUAtt	UAUGUAGGAUCCAAUGUUGat	-0.79226092
CDK7	NM_001799	cyclin-dependent kinase 7	1022	s2829	CCUUAAAGGAGCAAUCAAAtt	UUUGAUUGCUCCUUUAAGGtt	-0.164398
CDK7	NM_001799	cyclin-dependent kinase 7	1022	s2830	GGACAUAGAUCAGAAGCUAtt	UAGCUUCUGAUCUAUGUCCaa	-3.56290634
CDKL1	NM_004196	cyclin-dependent kinase-like 1 (CDC2-related kinase)	8814	s16804	GUACUUCAGUGGAGUGAAAtt	UUUCACUCCACUGAAGUACtg	-0.29432686
CDKL1	NM_004196	cyclin-dependent kinase-like 1 (CDC2-related kinase)	8814	s16805	GGACCGAGUGACUACUAUAtt	UAUAGUAGUCACUCGGUCCag	-2.40689095
CDKL1	NM_004196	cyclin-dependent kinase-like 1 (CDC2-related kinase)	8814	s16806	CGAAUGCUCAAGCAACUCAtt	UGAGUUGCUUGAGCAUUCGga	-2.10035665
CSK	NM_004383	c-src tyrosine kinase	1445	s223346	ACAAUUUCGUGCAUCGAGAtt	UCUCGAUGCACGAAAUUGUtg	0.281948305
CSK	NM_004383	c-src tyrosine kinase	1445	s3613	CGAUUACCGAGGGAACAAAtt	UUUGUUCCCUCGGUAAUCGcc	-1.84391909
CSK	NM_004383	c-src tyrosine kinase	1445	s3614	CGCGCCUCAUUAAACCAAAtt	UUUGGUUUAAUGAGGCGCGta	4.936097316
DCAKD	NM_024819	dephospho-CoA kinase domain containing	79877	s36551	AGCACACCGUGGUAGUAUAtt	UAUACUACCACGGUGUGCUtc	0.09974558
DCAKD	NM_024819	dephospho-CoA kinase domain containing	79877	s36552	GUACAGUAAUUAGCCGAAAtt	UUUCGGCUAAUUACUGUACtg	-0.38220487
DCAKD	NM_024819	dephospho-CoA kinase domain containing	79877	s36553	ACCGCUACGUGAUUCUGGAtt	UCCAGAAUCACGUAGCGGUat	-2.52388272
DGKH	NM_152910	diacylglycerol kinase, eta	160851	s46227	GGAGUAUAAUGACAUAUGAtt	UCAUAUGUCAUUAUACUCCac	-2.23512579
DGKH	NM_152910	diacylglycerol kinase, eta	160851	s46228	GGAUUGGAUUAGAUGCAAAtt	UUUGCAUCUAAUCCAAUCCca	-1.74788994
DGKH	NM_152910	diacylglycerol kinase, eta	160851	s46229	GGAGUUCGAUUAUCAACAAtt	UUGUUGAUAAUCGAACUCCca	-0.83951009
EPHA10	NM_001004338	EPH receptor A10	284656	s200587	GCAGGAUAAUAAAAACUUGtt	CAAGUUUUUAUUAUCCUGCac	-0.66307715

Gene Symbol	RefSeq ID	Full Gene Name	Gene ID	Ambion siRNA ID	Sense siRNA Sequence	Antisense siRNA Sequence	Z-score
EPHA10	NM_173641	EPH receptor A10	284656	s200588	GCAUCUUCGUGGAACUGCAtt	UGCAGUUCCACGAAGAUGCgc	-1.38698414
EPHA10	NM_001004338	EPH receptor A10	284656	s200589	CCAAGGAACUGGAUGCGAAtt	UUCGCAUCCAGUUCCUUGGcg	-0.47513084
EPHB4	NM_004444	EPH receptor B4	2050	s243	GGACAAACACGGACAGUAUtt	AUACUGUCCGUGUUUGUCCga	0.210799592
EPHB4	NM_004444	EPH receptor B4	2050	s244	GCAGAGCAAUGGGAGAGAAtt	UUCUCUCCCAUUGCUCUGCtt	-1.45727549
EPHB4	NM_004444	EPH receptor B4	2050	s245	GCUGCUGCCUUCAUAUUGAtt	UCAAUAUGAAGGCAGCAGCtg	-1.46266266
ERBB3	NM_001005915	v-erb-b2 erythroblastic leukemia viral oncogene homolog 3 (avian)	2065	s4778	CAGUGGAUUCGAGAAGUGAtt	UCACUUCUCGAAUCCACUGca	-1.64049237
ERBB3	NM_001005915	v-erb-b2 erythroblastic leukemia viral oncogene homolog 3 (avian)	2065	s4779	UCGUCAUGUUGAACUAUAAtt	UUAUAGUUCAACAUGACGAag	-4.35611139
ERBB3	NM_001005915	v-erb-b2 erythroblastic leukemia viral oncogene homolog 3 (avian)	2065	s4780	GAAUGAAUUCUCUACUCUAtt	UAGAGUAGAGAAUUCAUUCat	1.435105765
FES	NM_002005	feline sarcoma oncogene	2242	s5112	CCACGCUGGAGAUCCUUAAtt	UUAAGGAUCUCCAGCGUGGgt	-0.69818285
FES	NM_002005	feline sarcoma oncogene	2242	s5113	CCUCAGCAAUCAGCAGACAtt	UGUCUGCUGAUUGCUGAGGtt	-2.67613108
FES	NM_002005	feline sarcoma oncogene	2242	s5114	AGUGGGUGCUGAACCAUGAtt	UCAUGGUUCAGCACCCACUtg	-2.24959041
FGFR2	NM_000141	fibroblast growth factor receptor 2	2263	s5173	GGAGUACUCCUAUGACAUUtt	AAUGUCAUAGGAGUACUCCat	1.17449117
FGFR2	NM_000141	fibroblast growth factor receptor 2	2263	s5174	GUAGGACUGUAGACAGUGAtt	UCACUGUCUACAGUCCUACtg	-3.18462741
FGFR2	NM_000141	fibroblast growth factor receptor 2	2263	s5175	GAACAGUAUUCACCUAGUUtt	AACUAGGUGAAUACUGUUCga	-3.38086396
FGFR4	NM_002011	fibroblast growth factor receptor 4	2264	s223533	UCAAGAUGCUCAAAGACAAtt	UUGUCUUUGAGCAUCUUGAcg	-1.11417248
FGFR4	NM_002011	fibroblast growth factor receptor 4	2264	s5176	CAUUGACUACUAUAAGAAAtt	UUUCUUAUAGUAGUCAAUGtg	-2.25209678
FGFR4	NM_002011	fibroblast growth factor receptor 4	2264	s5178	ACACCUGCCUGGUAGAGAAtt	UUCUCUACCAGGCAGGUGUat	-0.21674311
FRK	NM_002031	fyn-related kinase	2444	s5363	GCAACUACAAGGCUAUAUUtt	AAUAUAGCCUUGUAGUUGCtg	-3.27402184
FRK	NM_002031	fyn-related kinase	2444	s5364	CCAUUUGAUUUGUCGUAUAtt	UAUACGACAAAUCAAAUGGag	-0.22508165
FRK	NM_002031	fyn-related kinase	2444	s5365	GCAGACAAGUCAACCGUGAtt	UCACGGUUGACUUGUCUGCct	-3.61201873
GAK	NM_005255	cyclin G associated kinase	2580	s5527	GUCCGUCGCUAAUUAUGCAtt	UGCAUAAUUAGCGACGGACtg	-2.69483594
GAK	NM_005255	cyclin G associated kinase	2580	s5528	CACCAGAAAUCAUAGACUUtt	AAGUCUAUGAUUUCUGGUGtt	-1.81880586
GAK	NM_005255	cyclin G associated kinase	2580	s5529	CGAGGAAUACAACACCAAUtt	AUUGGUGUUGUAUUCCUCGtg	-2.77921267
GLYCTK	NM_145262	glycerate kinase	132158	s43670	GGAUGACAGGUACCAAUGUtt	ACAUUGGUACCUGUCAUCCct	-4.61141529
GLYCTK	NM_145262	glycerate kinase	132158	s43671	GCCCACAAUGACUCACAUAtt	UAUGUGAGUCAUUGUGGGCta	-3.37966716
GLYCTK	NM_145262	glycerate kinase	132158	s43672	ACAUAGCCGUGUCCAGGUAtt	UACCUGGACACGGCUAUGUgg	-0.4452919

Gene Symbol	RefSeq ID	Full Gene Name	Gene ID	Ambion siRNA ID	Sense siRNA Sequence	Antisense siRNA Sequence	Z-score
GRK4	NM_001004056	G protein-coupled receptor kinase 4	2868	s6084	GGACUGUCAAUCUUAGAUAtt	UAUCUAAGAUUGACAGUCCac	-1.88692667
GRK4	NM_001004056	G protein-coupled receptor kinase 4	2868	s6085	GAGUUGGAACAGUCGGCUAtt	UAGCCGACUGUUCCAACUCtt	0.05572894
GRK4	NM_001004056	G protein-coupled receptor kinase 4	2868	s6086	GAAUCAAGAAUGAUACCGAtt	UCGGUAUCAUUCUUGAUUCtt	-0.26950322
GSK3B	NM_002093	glycogen synthase kinase 3 beta	2932	s6239	CUCAAGAACUGUCAAGUAAtt	UUACUUGACAGUUCUUGAGtg	-1.50710918
GSK3B	NM_002093	glycogen synthase kinase 3 beta	2932	s6240	CGAGAGCUCCAGAUCAUGAtt	UCAUGAUCUGGAGCUCUCGat	-3.81397019
GSK3B	NM_002093	glycogen synthase kinase 3 beta	2932	s6241	GCUAGAUCACUGUAACAUAtt	UAUGUUACAGUGAUCUAGCtt	-1.53526973
HKDC1	NM_025130	hexokinase domain containing 1	80201	s37044	GGAGCUCUUUGAUCACAUUtt	AAUGUGAUCAAAGAGCUCCtc	-2.05782072
HKDC1	NM_025130	hexokinase domain containing 1	80201	s37045	GUGCGAAUGUACAACAAGAtt	UCUUGUUGUACAUUCGCACtg	1.379561321
HKDC1	NM_025130	hexokinase domain containing 1	80201	s37046	CCCUCACUUUUCUAGAAUAtt	UAUUCUAGAAAAGUGAGGGtg	-2.13134621
IGF1R	NM_000875	insulin-like growth factor 1 receptor	3480	s223917	CGUCUUCCAUAGAAAGAGAtt	UCUCUUUCUAUGGAAGACGta	-2.79148155
IGF1R	NM_000875	insulin-like growth factor 1 receptor	3480	s223918	GAAGAAUCGCAUCAUCAUAtt	UAUGAUGAUGCGAUUCUUCga	-2.32157228
IGF1R	NM_000875	insulin-like growth factor 1 receptor	3480	s223919	GAAUCCCAAUGGAUUGAUUtt	AAUCAAUCCAUUGGGAUUCtc	-0.28334771
ILK	NM_001014794	integrin-linked kinase	3611	s7404	GCCGUAGUGUAAUGAUUGAtt	UCAAUCAUUACACUACGGCta	-2.75918875
ILK	NM_001014794	integrin-linked kinase	3611	s7405	CGACCCAAAUUUGACAUGAtt	UCAUGUCAAAUUUGGGUCGct	-2.06260796
ILK	NM_001014794	integrin-linked kinase	3611	s7406	GAAUCACUCUGGAGAGCUAtt	UAGCUCUCCAGAGUGAUUCtc	-1.70913408
IPMK	NM_152230	inositol polyphosphate multikinase	253430	s48411	CCAAACGAUUUAUACCUAAtt	UUAGGUAUAAAUCGUUUGGtg	-2.0982205
IPMK	NM_152230	inositol polyphosphate multikinase	253430	s48412	CAGCUUAAUUUUUACGCAAtt	UUGCGUAAAAAUUAAGCUGct	-2.55355925
IPMK	NM_152230	inositol polyphosphate multikinase	253430	s48413	GCAUUACGGAAGAAGCUUAtt	UAAGCUUCUUCCGUAAUGCtg	-1.84394487
IRAK4	NM_016123	interleukin-1 receptor-associated kinase 4	51135	s27527	GGUUGACAUUACUACUGAAtt	UUCAGUAGUAAUGUCAACCat	-2.24908088
IRAK4	NM_016123	interleukin-1 receptor-associated kinase 4	51135	s27528	GCCUAAUGGUUCAUUGCUAtt	UAGCAAUGAACCAUUAGGCat	0.012825897
IRAK4	NM_016123	interleukin-1 receptor-associated kinase 4	51135	s27529	GGUGUGGUUUUACUAGAAAtt	UUUCUAGUAAAACCACACCaa	-3.01037423
ITPKA	NM_002220	inositol 1,4,5-trisphosphate 3-kinase A	3706	s7625	GAAGGACAUGUACAAGAAAtt	UUUCUUGUACAUGUCCUUCcg	-3.76057724
ITPKA	NM_002220	inositol 1,4,5-trisphosphate 3-kinase A	3706	s7626	GGACUUACCUAGAGGAGGAtt	UCCUCCUCUAGGUAAGUCCtg	-0.38656832
ITPKA	NM_002220	inositol 1,4,5-trisphosphate 3-kinase A	3706	s7627	CGAGGACGUGGGUCAGAAAtt	UUUCUGACCCACGUCCUCGcc	-1.96698587
KSR2	NM_173598	kinase suppressor of ras 2	283455	s49244	CGAAAACUGAUACACUUGAtt	UCAAGUGUAUCAGUUUUCGgg	0.150613393
KSR2	NM_173598	kinase suppressor of ras 2	283455	s49245	GCAUCCCACUACUACAAAUtt	AUUUGUAGUAGUGGGAUGCtg	-3.55889714

Gene Symbol	RefSeq ID	Full Gene Name	Gene ID	Ambion siRNA ID	Sense siRNA Sequence	Antisense siRNA Sequence	Z-score
KSR2	NM_173598	kinase suppressor of ras 2	283455	s49246	CAGGCAGAUUGCUCAAGAAtt	UUCUUGAGCAAUCUGCCUGgt	1.188541147
LIMK1	NM_002314	LIM domain kinase 1	3984	s8188	GCAUGACCCUCACGAUACAtt	UGUAUCGUGAGGGUCAUGCtc	-3.6170902
LIMK1	NM_002314	LIM domain kinase 1	3984	s8189	CCUCACGUGUGGGACCUUUtt	AAAGGUCCCACACGUGAGGca	-2.74048765
LIMK1	NM_002314	LIM domain kinase 1	3984	s8190	GCAUGAGCCCAGAUGUGAAtt	UUCACAUCUGGGCUCAUGCag	-1.11277666
LOC731914	XM_001131241	hypothetical protein LOC731914	731914	s61460	GAAUAACCAAUGCAGAGAAtt	UUCUCUGCAUUGGUUAUUCta	-2.10839829
MAP2K3	NM_002756	mitogen-activated protein kinase kinase 3	5606	s11173	GGUCGACUGUUUCUACACUtt	AGUGUAGAAACAGUCGACCgt	-0.93270745
MAP2K3	NM_002756	mitogen-activated protein kinase kinase 3	5606	s11174	ACAGAAACUUUGAGGUGGAtt	UCCACCUCAAAGUUUCUGUct	-3.44139616
MAP2K3	NM_002756	mitogen-activated protein kinase kinase 3	5606	s11175	CCCGGACCUUCAUCACCAUtt	AUGGUGAUGAAGGUCCGGGag	-1.83271687
MAP3K14	NM_003954	mitogen-activated protein kinase kinase kinase 14	9020	s17186	GUCCAAAUACAGUCUCUUAtt	UAAGAGACUGUAUUUGGACtt	-2.87396925
MAP3K14	NM_003954	mitogen-activated protein kinase kinase kinase 14	9020	s17187	GGAUUGACCUCACCCAGAAtt	UUCUGGGUGAGGUCAAUCCtg	-6.53870706
MAP3K14	NM_003954	mitogen-activated protein kinase kinase kinase 14	9020	s17188	GGAUUAUGAGUACCGAGAAtt	UUCUCGGUACUCAUAAUCCac	-1.59496375
MAP4K1	NM_001042600	mitogen-activated protein kinase kinase kinase kinase 1	11184	s22080	GGGACAUCAAGGGAGCUAAtt	UUAGCUCCCUUGAUGUCCCtg	-4.83883586
MAP4K1	NM_001042600	mitogen-activated protein kinase kinase kinase kinase 1	11184	s22082	GCUCAGUCAUCAACUGGUAtt	UACCAGUUGAUGACUGAGCat	-8.65459049
MAP4K1	NM_001042600	mitogen-activated protein kinase kinase kinase kinase 1	11184	s223205	CAAGAUCCAGGACACCAAAtt	UUUGGUGUCCUGGAUCUUGgt	-1.05307597
MAP4K2	NM_004579	mitogen-activated protein kinase kinase kinase kinase 2	5871	s11687	CCAAGAUUCCUGACACCAAtt	UUGGUGUCAGGAAUCUUGGtg	2.210484059
MAP4K2	NM_004579	mitogen-activated protein kinase kinase kinase kinase 2	5871	s11688	CCUAUGACAUGUUUCCAGAtt	UCUGGAAACAUGUCAUAGGtc	-2.61744
MAP4K2	NM_004579	mitogen-activated protein kinase kinase kinase kinase 2	5871	s11689	GCAGCUACCUCAGGAAUGAtt	UCAUUCCUGAGGUAGCUGCca	-2.52282258
MAP4K4	NM_004834	mitogen-activated protein kinase kinase kinase kinase 4	9448	s18095	CCUAUGGACAAGUCUAUAAtt	UUAUAGACUUGUCCAUAGGtg	-0.40119442
MAP4K4	NM_004834	mitogen-activated protein kinase kinase kinase kinase 4	9448	s18096	CGGCUAGAAGAGCAACAAAtt	UUUGUUGCUCUUCUAGCCGtc	0.145233521
MAP4K4	NM_004834	mitogen-activated protein kinase kinase kinase kinase 4	9448	s18097	CGAAGACGAUUUCAACAAAtt	UUUGUUGAAAUCGUCUUCGgt	-0.33933447
MAPK3	NM_001040056	mitogen-activated protein kinase 3	5595	s11140	GGAUCAGCUCAACCACAUUtt	AAUGUGGUUGAGCUGAUCCag	-2.79715075

Gene Symbol	RefSeq ID	Full Gene Name	Gene ID	Ambion siRNA ID	Sense siRNA Sequence	Antisense siRNA Sequence	Z-score
MAPK3	NM_001040056	mitogen-activated protein kinase 3	5595	s11141	GGACCGGAUGUUAACCUUUtt	AAAGGUUAACAUCCGGUCCag	-5.05574453
MAPK3	NM_001040056	mitogen-activated protein kinase 3	5595	s11142	GACCUGAAUUGUAUCAUCAtt	UGAUGAUACAAUUCAGGUCct	-4.02594643
MAST4	NM_198828	microtubule associated serine/threonine kinase family member 4	375449	s51708	GAAGUUUGAUAGAUUCCCAtt	UGGGAAUCUAUCAAACUUCct	-1.72817562
MAST4	NM_198828	microtubule associated serine/threonine kinase family member 4	375449	s51709	CGAGGAGCUUGACCACAUAtt	UAUGUGGUCAAGCUCCUCGtc	-2.04915713
MAST4	NM_198828	microtubule associated serine/threonine kinase family member 4	375449	s51710	GGCCCUGGAAAAUCACUGAtt	UCAGUGAUUUUCCAGGGCCag	-0.49925156
NAGK	NM_017567	N-acetylglucosamine kinase	55577	s31007	GGCUAGGGAUACUCACUCAtt	UGAGUGAGUAUCCCUAGCCga	-2.27703979
NAGK	NM_017567	N-acetylglucosamine kinase	55577	s31008	GCUACUUAAUCACCACCGAtt	UCGGUGGUGAUUAAGUAGCtt	1.096946297
NAGK	NM_017567	N-acetylglucosamine kinase	55577	s31009	GAUCGGCUAGGGAUACUCAtt	UGAGUAUCCCUAGCCGAUCtg	-1.34768554
NLK	NM_016231	nemo-like kinase	51701	s28543	CCAGAAAUCCUGAUGGGCAtt	UGCCCAUCAGGAUUUCUGGag	-2.99836453
NLK	NM_016231	nemo-like kinase	51701	s28544	GGUGUUGUCUGGUCAGUAAtt	UUACUGACCAGACAACACCaa	-1.5718544
NLK	NM_016231	nemo-like kinase	51701	s28545	CCAAAAGAAUAUCCGCUAAtt	UUAGCGGAUAUUCUUUUGGat	0.174938031
NME1	NM_000269	non-metastatic cells 1, protein (NM23A) expressed in	4830	s224120	CCAGCAUAGGAUUCAUUGAtt	UCAAUGAAUCCUAUGCUGGga	-1.04313976
NME1	NM_000269	NME/NM23 nucleoside diphosphate kinase 1	4830	s224121	GGAAAUCUAGUUAUUUACAtt	UGUAAAUAACUAGAUUUCCta	-0.66070655
NME1	NM_000269	NME/NM23 nucleoside diphosphate kinase 1	4830	s9590	CUGAGGAACUGGUAGAUUAtt	UAAUCUACCAGUUCCUCAGgg	-3.98750233
NRGN	NM_006176	neurogranin (protein kinase C substrate, RC3)	4900	s224138	UGCUCUGACCGGAAGAGAAtt	UUCUCUUCCGGUCAGAGCAag	-7.90994574
NRGN	NM_006176	neurogranin (protein kinase C substrate, RC3)	4900	s9723	CACACUCACUUAAAGAAAAtt	UUUUCUUUAAGUGAGUGUGct	-0.41008579
NRGN	NM_006176	neurogranin (protein kinase C substrate, RC3)	4900	s9724	GCCGGACGACGACAUUCUAtt	UAGAAUGUCGUCGUCCGGCtt	-2.27692255
NRK	NM_198465	Nik related kinase	203447	s47517	CUUAUACGCUGGAUUCGUAtt	UACGAAUCCAGCGUAUAAGat	-0.07511407
NRK	NM_198465	Nik related kinase	203447	s47518	GGAGUUCGCAAAAUCGUCAtt	UGACGAUUUUGCGAACUCCtt	-1.14727431
NRK	NM_198465	Nik related kinase	203447	s47519	CUGUAUACUUGACAAACGAtt	UCGUUUGUCAAGUAUACAGgg	-3.06969038
PAPSS1	NM_005443	3'-phosphoadenosine 5'-phosphosulfate synthase 1	9061	s17282	GGAUCGAUUCUGAAUAUGAtt	UCAUAUUCAGAAUCGAUCCca	-5.49237051
PAPSS1	NM_005443	3'-phosphoadenosine 5'-phosphosulfate synthase 1	9061	s17283	GCAUCGCAGAAGUUGCUAAtt	UUAGCAACUUCUGCGAUGCgt	-3.61204507

Gene Symbol	RefSeq ID	Full Gene Name	Gene ID	Ambion siRNA ID	Sense siRNA Sequence	Antisense siRNA Sequence	Z-score
PAPSS1	NM_005443	3'-phosphoadenosine 5'-phosphosulfate synthase 1	9061	s17284	GGCUUAGUGUGCAUCACAAtt	UUGUGAUGCACACUAAGCCag	-3.8865677
PAPSS2	NM_001015880	3'-phosphoadenosine 5'-phosphosulfate synthase 2	9060	s17279	GGGUAGCUAUCUUACGAGAtt	UCUCGUAAGAUAGCUACCCtc	-1.67413236
PAPSS2	NM_001015880	3'-phosphoadenosine 5'-phosphosulfate synthase 2	9060	s17280	CAUUCGCAAAGGAUCGUGAtt	UCACGAUCCUUUGCGAAUGga	0.638272518
PAPSS2	NM_001015880	3'-phosphoadenosine 5'-phosphosulfate synthase 2	9060	s17281	CCACCAAUGUAGUCUAUCAtt	UGAUAGACUACAUUGGUGGat	-1.63067477
PASK	NM_015148	PAS domain containing serine/threonine kinase	23178	s23211	GAAUCUUGCUGACUAUACAtt	UGUAUAGUCAGCAAGAUUCac	-3.40515466
PASK	NM_015148	PAS domain containing serine/threonine kinase	23178	s23212	CCUGGUUGCUAACGACAAAtt	UUUGUCGUUAGCAACCAGGat	-0.74375964
PASK	NM_015148	PAS domain containing serine/threonine kinase	23178	s23213	GCCUAGACCUCUUCGCUUUtt	AAAGCGAAGAGGUCUAGGCcg	-0.53418841
PFTK2	NM_139158	PFTAIRE protein kinase 2	65061	s35180	GAGUCCCAUUUACAGCUAUtt	AUAGCUGUAAAUGGGACUCct	-3.37022586
PFTK2	NM_139158	PFTAIRE protein kinase 2	65061	s35181	GCUCUUAUGCGACAGUUUAtt	UAAACUGUCGCAUAAGAGCct	-2.70560461
PFTK2	NM_139158	PFTAIRE protein kinase 2	65061	s35182	CCUGAAACCUCAGAACUUAtt	UAAGUUCUGAGGUUUCAGGtc	-8.11626326
PIK3CG	NM_002649	phosphoinositide-3-kinase, catalytic, gamma polypeptide	5294	s10532	GCUUUAGAGUUCCAUAUGAtt	UCAUAUGGAACUCUAAAGCtt	0.04345312
PIK3CG	NM_002649	phosphoinositide-3-kinase, catalytic, gamma polypeptide	5294	s10533	GCUGCACGACUUUACCCAAtt	UUGGGUAAAGUCGUGCAGCat	-3.89243546
PIK3CG	NM_002649	phosphoinositide-3-kinase, catalytic, gamma polypeptide	5294	s10534	GUAAUCGAGAUGUUACAAAtt	UUUGUAACAUCUCGAUUACtt	-0.12603174
PIM1	NM_002648	pim-1 oncogene	5292	s10526	ACAUCCUUAUCGACCUCAAtt	UUGAGGUCGAUAAGGAUGUtt	-2.31710326
PIM1	NM_002648	pim-1 oncogene	5292	s10527	CCGUCUACACGGACUUCGAtt	UCGAAGUCCGUGUAGACGGtg	-0.47406254
PIM1	NM_002648	pim-1 oncogene	5292	s10528	CCUUCGAAGAAAUCCAGAAtt	UUCUGGAUUUCUUCGAAGGtt	0.159971941
PLK2	NM_006622	polo-like kinase 2 (Drosophila)	10769	s64	GCUAGUAUGUUGUCCAAAAtt	UUUUGGACAACAUACUAGCaa	-2.67846486
PLK2	NM_006622	polo-like kinase 2 (Drosophila)	10769	s65	GGUUGAUUACUCUAACAAAtt	UUUGUUAGAGUAAUCAACCca	-5.79636429
PLK2	NM_006622	polo-like kinase 2 (Drosophila)	10769	s66	CUACUUCGAGGACAAAGAAtt	UUCUUUGUCCUCGAAGUAGtg	-0.70834094
PLXNA2	NM_025179	plexin A2	5362	s10699	GGCACUAUGGUGACCAUUAtt	UAAUGGUCACCAUAGUGCCtc	-7.06665261
PLXNA2	NM_025179	plexin A2	5362	s10700	GGAUCGCCCAUCAUUCUGAtt	UCAGAAUGAUGGGCGAUCCtg	0.406796243
PLXNA2	NM_025179	plexin A2	5362	s10701	GGGAAGAUAUUUGUCAGCAtt	UGCUGACAAAUAUCUUCCCtg	2.683179691
PLXNA3	NM_017514	plexin A3	55558	s224372	GAGCUGUAUUUCUAUGUCAtt	UGACAUAGAAAUACAGCUCgt	-1.56357873
PLXNA3	NM_017514	plexin A3	55558	s30977	CAGUGAACCGAGUCUUUAAtt	UUAAAGACUCGGUUCACUGcg	-0.17803423

Gene Symbol	RefSeq ID	Full Gene Name	Gene ID	Ambion siRNA ID	Sense siRNA Sequence	Antisense siRNA Sequence	Z-score
PLXNA3	NM_017514	plexin A3	55558	s30979	CAUCAUCAAUGGAAGCACUtt	AGUGCUUCCAUUGAUGAUGct	0.058227048
PLXNC1	NM_005761	plexin C1	10154	s19775	CCACUAUAAAAGUCUUUAAtt	UUAAAGACUUUUAUAGUGGat	-1.94673018
PLXNC1	NM_005761	plexin C1	10154	s19776	GGGCAUCGAACAUCACAAUtt	AUUGUGAUGUUCGAUGCCCgg	0.073539825
PLXNC1	NM_005761	plexin C1	10154	s19777	GGAGAAUUCGUGUUGCAAAtt	UUUGCAACACGAAUUCUCCtc	-4.54430511
PRKG2	NM_006259	protein kinase, cGMP-dependent, type II	5593	s11134	GCUAUGAAGUGUAUAAGGAtt	UCCUUAUACACUUCAUAGCaa	-2.83705674
PRKG2	NM_006259	protein kinase, cGMP-dependent, type II	5593	s11135	GCCUGGUUAUAGAUCGAGAtt	UCUCGAUCUAUAACCAGGCat	0.664397714
PRKG2	NM_006259	protein kinase, cGMP-dependent, type II	5593	s11136	GAGAUUACAUCAUUAGAGAtt	UCUCUAAUGAUGUAAUCUCct	-2.71827223
PRPS1	NM_002764	phosphoribosyl pyrophosphate synthetase 1	5631	s11233	GCACUAUUGUCUCACCUGAtt	UCAGGUGAGACAAUAGUGCag	-1.49676735
PRPS1	NM_002764	phosphoribosyl pyrophosphate synthetase 1	5631	s11235	GACUUUGCCUUGAUUCACAtt	UGUGAAUCAAGGCAAAGUCca	1.735552175
PRPS1	NM_002764	phosphoribosyl pyrophosphate synthetase 1	5631	s224421	AGGCAGUAGUAGUCACCAAtt	UUGGUGACUACUACUGCCUca	0.326178948
PSKH1	NM_006742	protein serine kinase H1	5681	s11324	ACCGAGACCUCAAACCUGAtt	UCAGGUUUGAGGUCUCGGUgt	-0.26944883
PSKH1	NM_006742	protein serine kinase H1	5681	s11325	GCACUAAGAGUGACGUGUAtt	UACACGUCACUCUUAGUGCca	0.83238745
PSKH1	NM_006742	protein serine kinase H1	5681	s11326	GGUGAUGACUGCUUGAUGAtt	UCAUCAAGCAGUCAUCACCct	-3.72342369
PTK6	NM_005975	PTK6 protein tyrosine kinase 6	5753	s11487	CAUCCAUGGUUAAGUCAUAtt	UAUGACUUAACCAUGGAUGaa	1.80420224
PTK6	NM_005975	PTK6 protein tyrosine kinase 6	5753	s11488	GGUUUUGACUCACCUGAAAtt	UUUCAGGUGAGUCAAAACCaa	-0.76476776
PTK6	NM_005975	PTK6 protein tyrosine kinase 6	5753	s11489	CCGCGACUCUGAUGAGAAAtt	UUUCUCAUCAGAGUCGCGGag	-0.90175548
PXK	NM_017771	PX domain containing serine/threonine kinase	54899	s29710	CGGAAUAUAUUAUUCGAGUtt	ACUCGAAUAAUAUAUUCCGtg	-1.5744343
PXK	NM_017771	PX domain containing serine/threonine kinase	54899	s29711	GGAUCUGAUCUACAAGGCAtt	UGCCUUGUAGAUCAGAUCCtt	1.163692223
PXK	NM_017771	PX domain containing serine/threonine kinase	54899	s29712	GACAUAGGUUGGAGAAUAAtt	UUAUUCUCCAACCUAUGUCtt	-3.80122921
RBKS	NM_022128	ribokinase	64080	s34394	GAAUUUACAUAUCAGACUAtt	UAGUCUGAUAUGUAAAUUCtg	-4.5071576
RBKS	NM_022128	ribokinase	64080	s34395	GGUGGUAAUCAUUACCUUAtt	UAAGGUAAUGAUUACCACCtg	0.482226343
RBKS	NM_022128	ribokinase	64080	s34396	GAUUGCUAUUAGUCCCAAAtt	UUUGGGACUAAUAGCAAUCaa	-1.17818663
RIPK3	NM_006871	receptor-interacting serine-threonine kinase 3	11035	s21740	GGCAAGUCUGGAUAACGAAtt	UUCGUUAUCCAGACUUGCCat	-0.96548289
RIPK3	NM_006871	receptor-interacting serine-threonine kinase 3	11035	s21741	GAACUGUUUGUUAACGUAAtt	UUACGUUAACAAACAGUUCtg	0.538533505
RIPK3	NM_006871	receptor-interacting serine-threonine kinase 3	11035	s21742	GGAGAACCAUAGAAAACCAtt	UGGUUUUCUAUGGUUCUCCta	-1.01402074

Gene Symbol	RefSeq ID	Full Gene Name	Gene ID	Ambion siRNA ID	Sense siRNA Sequence	Antisense siRNA Sequence	Z-score
ROR1	NM_001083592	receptor tyrosine kinase-like orphan receptor 1	4919	s9755	GUACUGCGAUGAAACUUCAtt	UGAAGUUUCAUCGCAGUACgg	0.197976281
ROR1	NM_001083592	receptor tyrosine kinase-like orphan receptor 1	4919	s9756	GGAUGAAAACUUUAAGUCUtt	AGACUUAAAGUUUUCAUCCaa	1.550257095
ROR1	NM_001083592	receptor tyrosine kinase-like orphan receptor 1	4919	s9757	CCGUCUAUAUGGAGUCUUUtt	AAAGACUCCAUAUAGACGGtg	2.391194414
RPS6KA2	NM_001006932	ribosomal protein S6 kinase, 90kDa, polypeptide 2	6196	s12276	CGAUAUCUGACGCAGCUAAtt	UUAGCUGCGUCAGAUAUCGag	2.259012425
RPS6KA2	NM_001006932	ribosomal protein S6 kinase, 90kDa, polypeptide 2	6196	s12277	CGAGCUCUCUUCAAACGGAtt	UCCGUUUGAAGAGAGCUCGca	-1.89003944
RPS6KA2	NM_001006932	ribosomal protein S6 kinase, 90kDa, polypeptide 2	6196	s12278	GAGUAUGCCGUGAAGAUCAtt	UGAUCUUCACGGCAUACUCgg	-3.67254772
RPS6KA4	NM_001006944	ribosomal protein S6 kinase, 90kDa, polypeptide 4	8986	s17138	CCUCCAUUCUCUUUGACCAtt	UGGUCAAAGAGAAUGGAGGgt	1.988825974
RPS6KA4	NM_001006944	ribosomal protein S6 kinase, 90kDa, polypeptide 4	8986	s17139	GCACUUCAGCGAGUCGGAAtt	UUCCGACUCGCUGAAGUGCcg	-3.14152089
RPS6KA4	NM_001006944	ribosomal protein S6 kinase, 90kDa, polypeptide 4	8986	s17140	UCAUUUACCGAGACCUGAAtt	UUCAGGUCUCGGUAAAUGAtg	1.190876116
RPS6KB1	NM_003161	ribosomal protein S6 kinase, 70kDa, polypeptide 1	6198	s12282	CAUGGAACAUUGUGAGAAAtt	UUUCUCACAAUGUUCCAUGcc	-1.64403391
RPS6KB1	NM_003161	ribosomal protein S6 kinase, 70kDa, polypeptide 1	6198	s12283	GGUUUUUCAAGUACGAAAAtt	UUUUCGUACUUGAAAAACCtt	-2.13559989
RPS6KB1	NM_003161	ribosomal protein S6 kinase, 70kDa, polypeptide 1	6198	s12284	GGACUAUGCAAAGAAUCUAtt	UAGAUUCUUUGCAUAGUCCaa	-2.60647388
SGK269	XM_370878	NKF3 kinase family member	79834	s36441	CAUUGUCUCCUGUUCGAUUtt	AAUCGAACAGGAGACAAUGtg	0.924951648
SGK269	XM_370878	NKF3 kinase family member	79834	s36443	GCAUGAUAGGUGGGAUAAAtt	UUUAUCCCACCUAUCAUGCaa	-2.01471094
SLK	NM_014720	STE20-like kinase (yeast)	9748	s18812	GGAAAUUGAGAAUCUAGAAtt	UUCUAGAUUCUCAAUUUCCtg	-2.25386571
SLK	NM_014720	STE20-like kinase (yeast)	9748	s18813	GAUCGAUAUCUUUACAAGAtt	UCUUGUAAAGAUAUCGAUCca	0.560007632
SLK	NM_014720	STE20-like kinase (yeast)	9748	s18814	GCAGAAACAGACUAUCGAAtt	UUCGAUAGUCUGUUUCUGCtg	-0.15897564
SNF1LK2	NM_015191	SNF1-like kinase 2	23235	s23355	CCAUAGCCCAAAUCAAGGAtt	UCCUUGAUUUGGGCUAUGGtt	2.361630407
SNF1LK2	NM_015191	SNF1-like kinase 2	23235	s23356	GGAAGAUUGUGCACCGUGAtt	UCACGGUGCACAAUCUUCCga	-1.97456601
SNF1LK2	NM_015191	SNF1-like kinase 2	23235	s23357	GAAGGAUGUUGGUCCUAGAtt	UCUAGGACCAACAUCCUUCgg	0.116645576
SPHK1	NM_021972	sphingosine kinase 1	8877	s16957	AACUACUUCUGGAUGGUCAtt	UGACCAUCCAGAAGUAGUUtg	-8.0236657
SPHK1	NM_021972	sphingosine kinase 1	8877	s16958	GGAAGAGUGGGUUCCAAGAtt	UCUUGGAACCCACUCUUCCta	2.343972585
SPHK1	NM_021972	sphingosine kinase 1	8877	s16959	UCACGCUGAUGCUCACUGAtt	UCAGUGAGCAUCAGCGUGAag	-1.81824975
SPHK2	NM_020126	sphingosine kinase 2	56848	s32283	CCCUCACCCUUACAUCGCAtt	UGCGAUGUAAGGGUGAGGGca	-0.44826073
SPHK2	NM_020126	sphingosine kinase 2	56848	s32284	CGGCCUACUUCUGCAUCUAtt	UAGAUGCAGAAGUAGGCCGct	-2.55359907
SPHK2	NM_020126	sphingosine kinase 2	56848	s32285	CAAGGCAGCUCUACACUCAtt	UGAGUGUAGAGCUGCCUUGgg	1.828391289
STK16	NM_001008910	serine/threonine kinase 16	8576	s16337	AUAUAUUGCUUGGAGAUGAtt	UCAUCUCCAAGCAAUAUAUtg	-5.8898735

Gene Symbol	RefSeq ID	Full Gene Name	Gene ID	Ambion siRNA ID	Sense siRNA Sequence	Antisense siRNA Sequence	Z-score
STK16	NM_001008910	serine/threonine kinase 16	8576	s16338	CCAACUCAGCAUCCCACAAtt	UUGUGGGAUGCUGAGUUGGtt	-0.01183599
STK16	NM_001008910	serine/threonine kinase 16	8576	s16339	GGUACGCUGUGGAAUGAGAtt	UCUCAUUCCACAGCGUACCtc	-3.04285898
STK32B	NM_018401	serine/threonine kinase 32B	55351	s30804	AGAUGAUUCUAGAAUCCAAtt	UUGGAUUCUAGAAUCAUCUct	-3.39114677
STK32B	NM_018401	serine/threonine kinase 32B	55351	s30805	ACAUAGCGACGGUAGUGAAtt	UUCACUACCGUCGCUAUGUtg	-0.79711601
STK32B	NM_018401	serine/threonine kinase 32B	55351	s30806	CAUUACAGACUUCAACAUAtt	UAUGUUGAAGUCUGUAAUGtg	-2.06882053
SYK	NM_003177	spleen tyrosine kinase	6850	s13679	GGAUAAGAACAUCAUAGAAtt	UUCUAUGAUGUUCUUAUCCtt	-3.44984136
SYK	NM_003177	spleen tyrosine kinase	6850	s13680	CGCUCUUAAAGAUGAGUUAtt	UAACUCAUCUUUAAGAGCGgg	-1.23978621
SYK	NM_003177	spleen tyrosine kinase	6850	s13681	GCACUAUCGCAUCGACAAAtt	UUUGUCGAUGCGAUAGUGCag	0.029946936
TAF1L	NM_153809	TAF1 RNA polymerase II, TATA box binding protein (TBP)-associated factor, 210kDa-like	138474	s44115	CACUGUUCAUUGUGACUAUtt	AUAGUCACAAUGAACAGUGgt	3.184645079
TAF1L	NM_153809	TAF1 RNA polymerase II, TATA box binding protein (TBP)-associated factor, 210kDa-like	138474	s44116	CCGUGAAAAUGUGCGUAAAtt	UUUACGCACAUUUUCACGGag	0.951053759
TAF1L	NM_153809	TAF1 RNA polymerase II, TATA box binding protein (TBP)-associated factor, 210kDa-like	138474	s44117	CAGUGUAUCUUCAUAAGAUtt	AUCUUAUGAAGAUACACUGga	-3.86782375
UCK2	NM_012474	uridine-cytidine kinase 2	7371	s14669	AGCUUCUACCGUGUCCUUAtt	UAAGGACACGGUAGAAGCUat	-3.92192338
UCK2	NM_012474	uridine-cytidine kinase 2	7371	s14670	GAUUUUAUCUCAGUACAUUtt	AAUGUACUGAGAUAAAAUCtg	-4.14093842
UCK2	NM_012474	uridine-cytidine kinase 2	7371	s14671	GUACGAGACCUGUUCCAGAtt	UCUGGAACAGGUCUCGUACct	1.593472577

12.3 Appendix 3: KEGG protein pathway maps

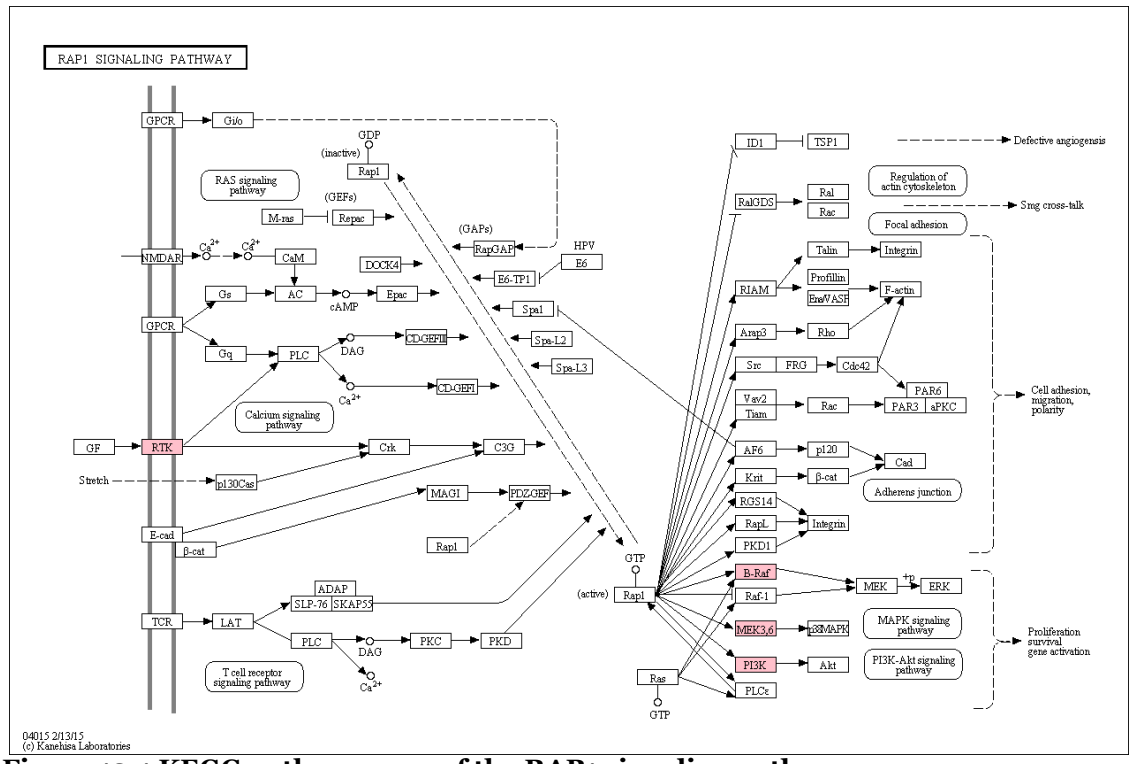

Figure 12-1 KEGG pathway map of the RAP1 signaling pathway.
The map shows the RAP1 signaling pathway based on the KEGG database. The four hits, falling into this network, are indicated in pink. Figure created using KEGG Mapper v2.5.

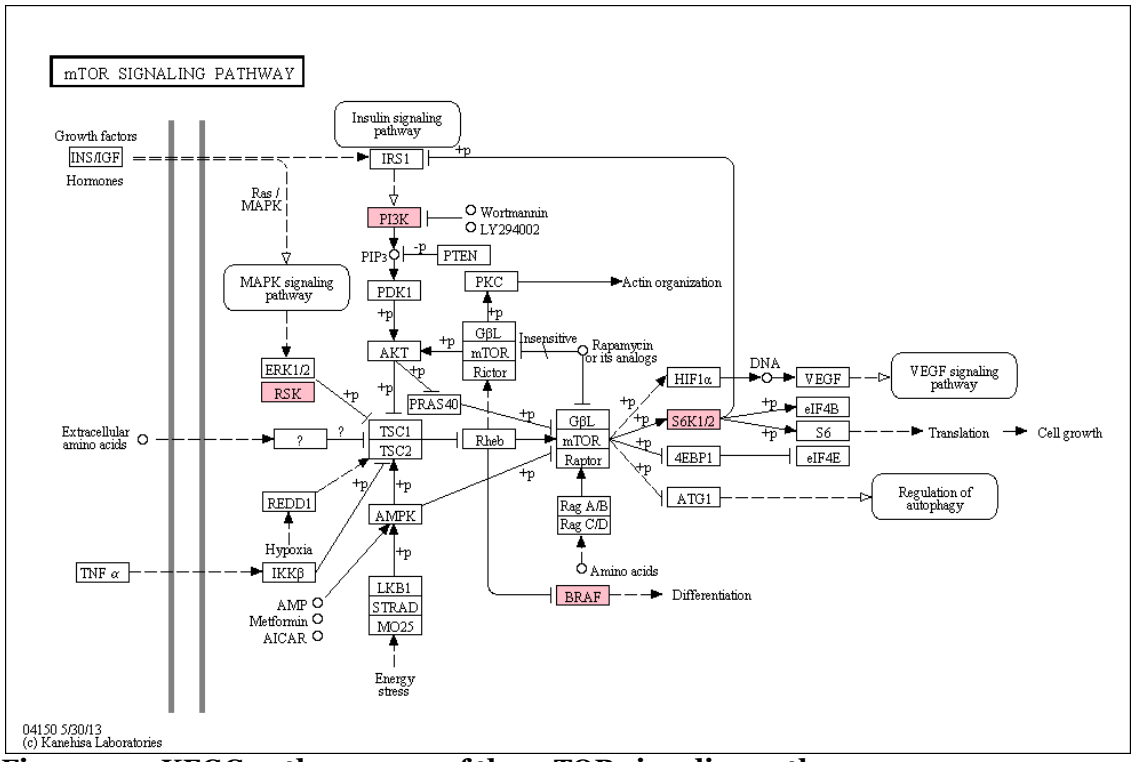

Figure 12-2 KEGG pathway map of the mTOR signaling pathway.
The map shows the mTOR signaling pathway based on the KEGG database. The four hits, falling into this network, are indicated in pink. Figure created using KEGG Mapper v2.5.

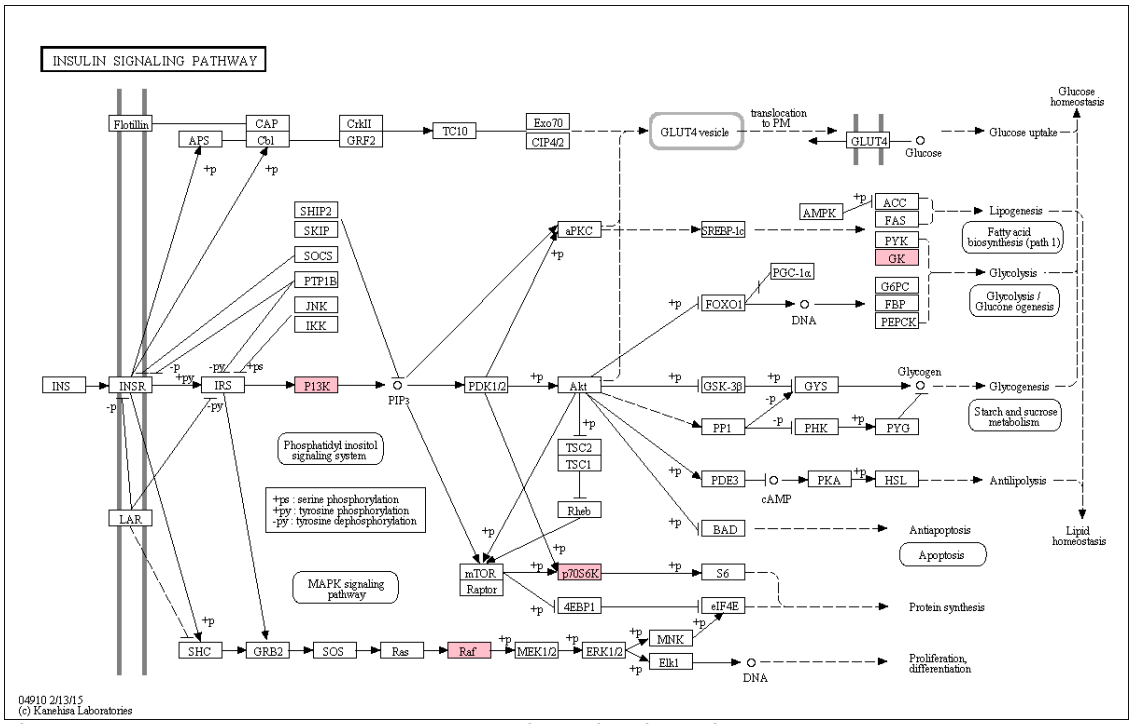

Figure 12-3 KEGG pathway map of the insulin signaling pathway.
The map shows the insulin signaling pathway based on the KEGG database. The four hits, falling into this network, are indicated in pink. Figure created using KEGG Mapper v2.5.

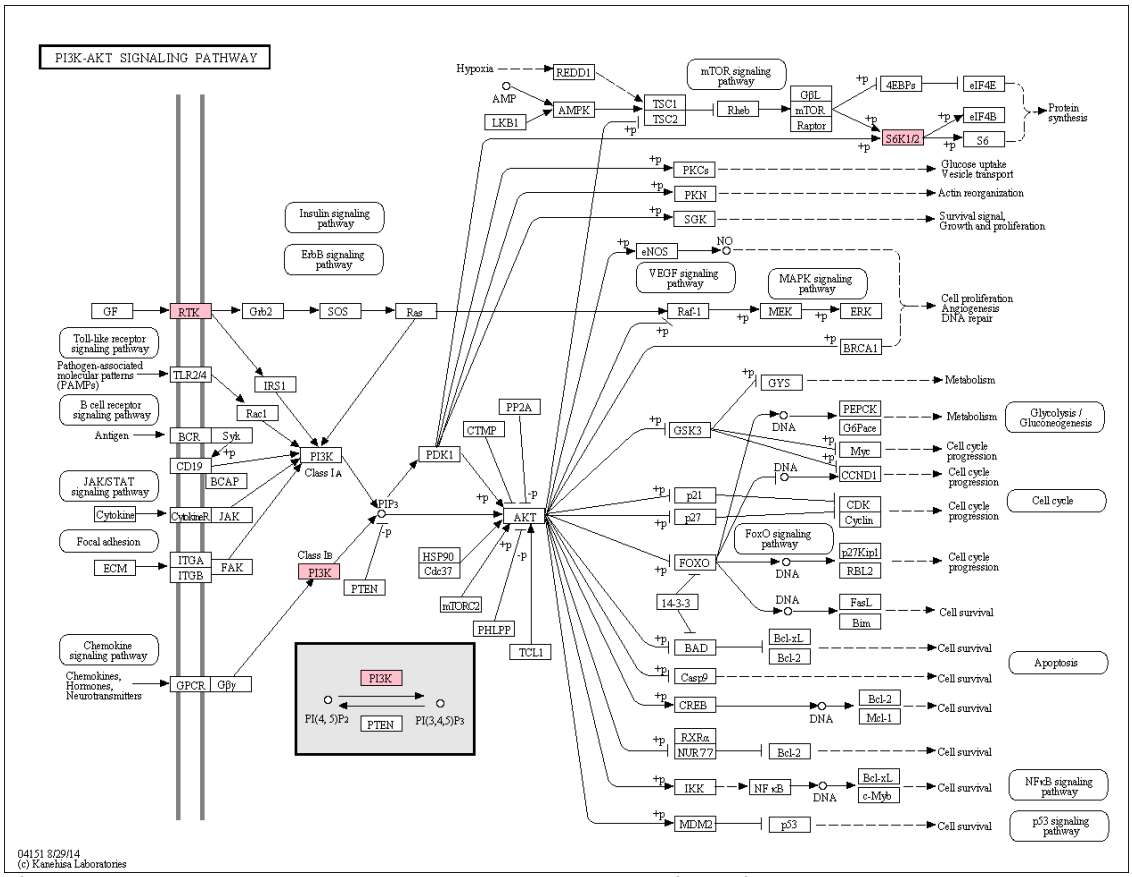

Figure 12-4 KEGG pathway map of the PI3K-Akt signaling pathway.
The map shows the PI3K-Akt signaling pathway based on the KEGG database. The four hits, falling into this network, are indicated in pink. Figure created using KEGG Mapper v2.5.

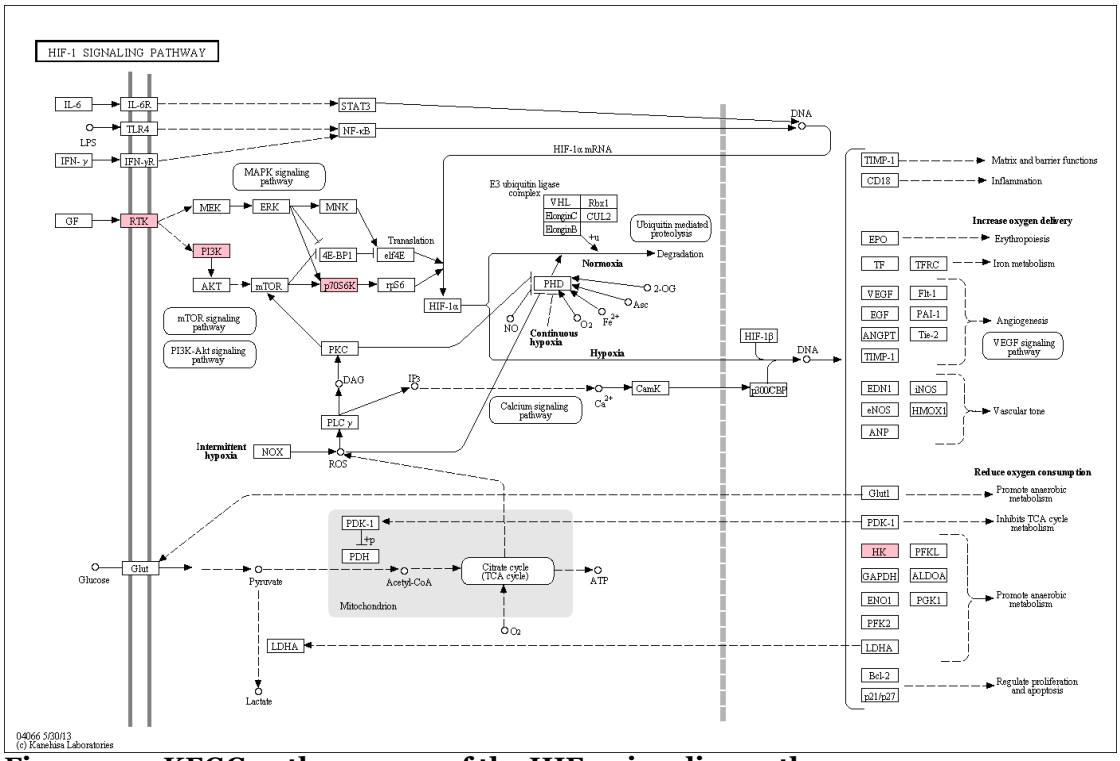

Figure 12-5 KEGG pathway map of the HIF-1 signaling pathway.
The map shows the HIF-1 signaling pathway based on the KEGG database. The four hits, falling into this network, are indicated in pink. Figure created using KEGG Mapper v2.5.

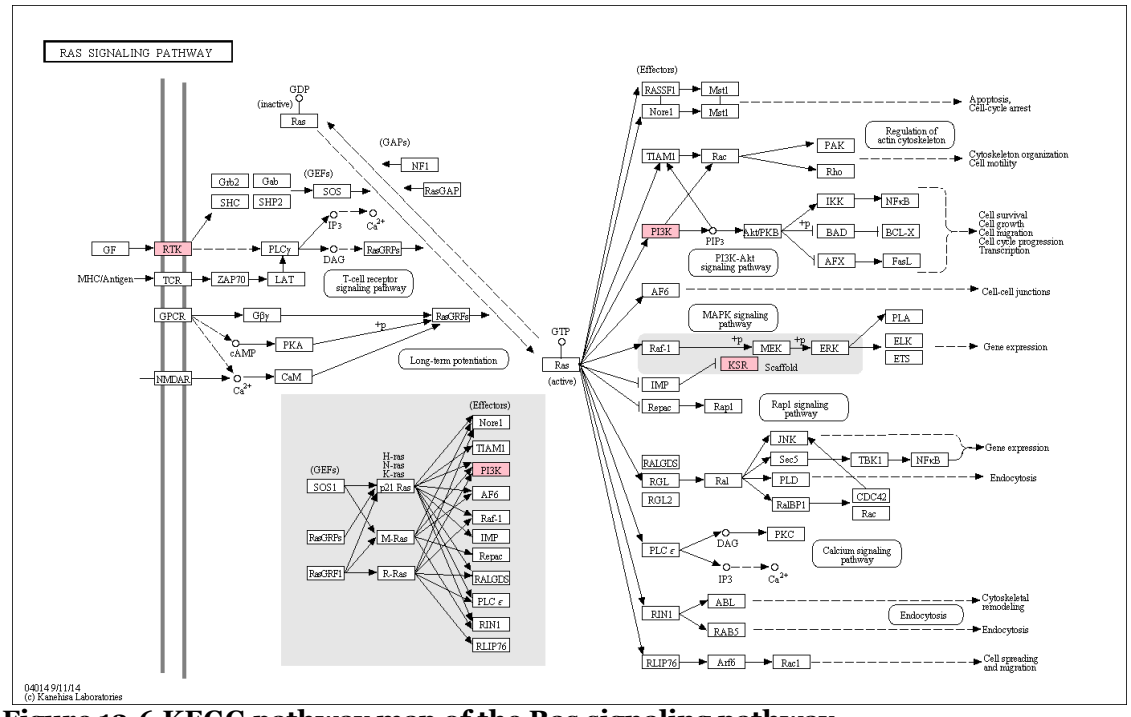

Figure 12-6 KEGG pathway map of the Ras signaling pathway.
The map shows the Ras signaling pathway based on the KEGG database. The four hits, falling into this network, are indicated in pink. Figure created using KEGG Mapper v2.5.

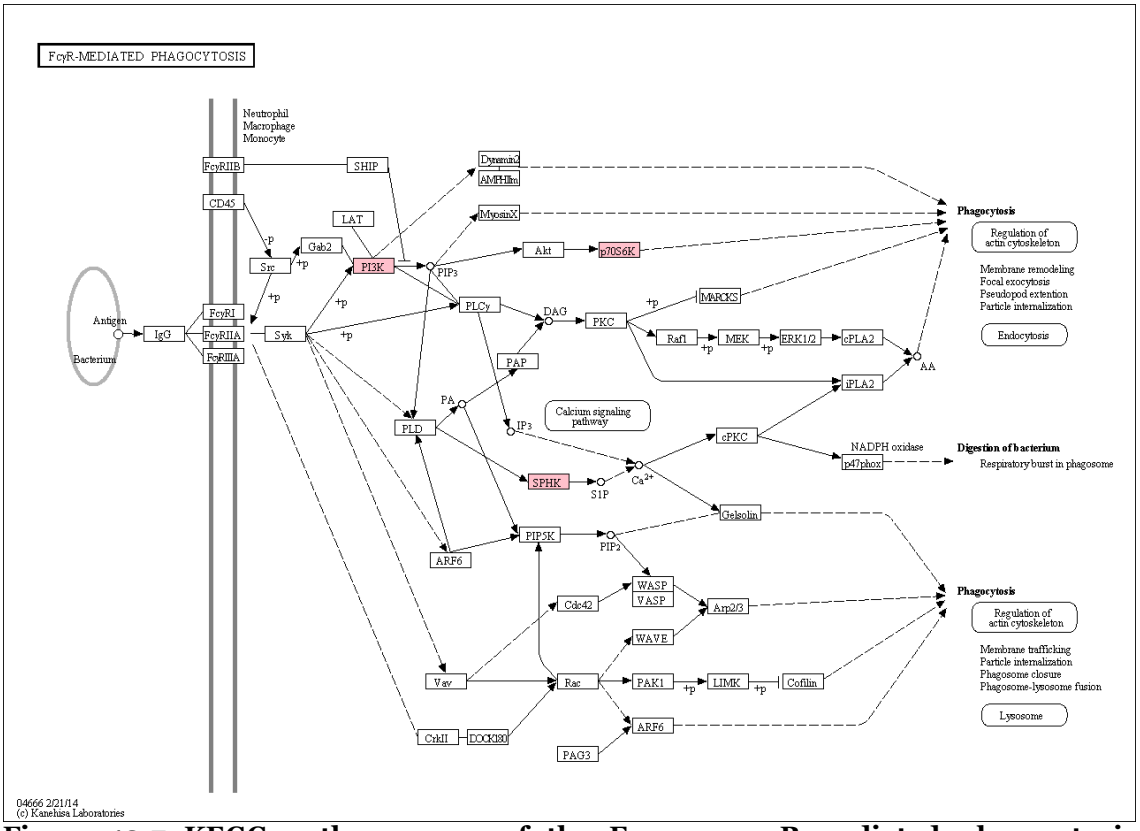

Figure 12-7 KEGG pathway map of the Fc gamma R-mediated phagocytosis pathway.
The map shows the Fc gamma R-mediated phagocytosis pathway based on the KEGG database. The four hits, falling into this network, are indicated in pink. Figure created using KEGG Mapper v2.5.

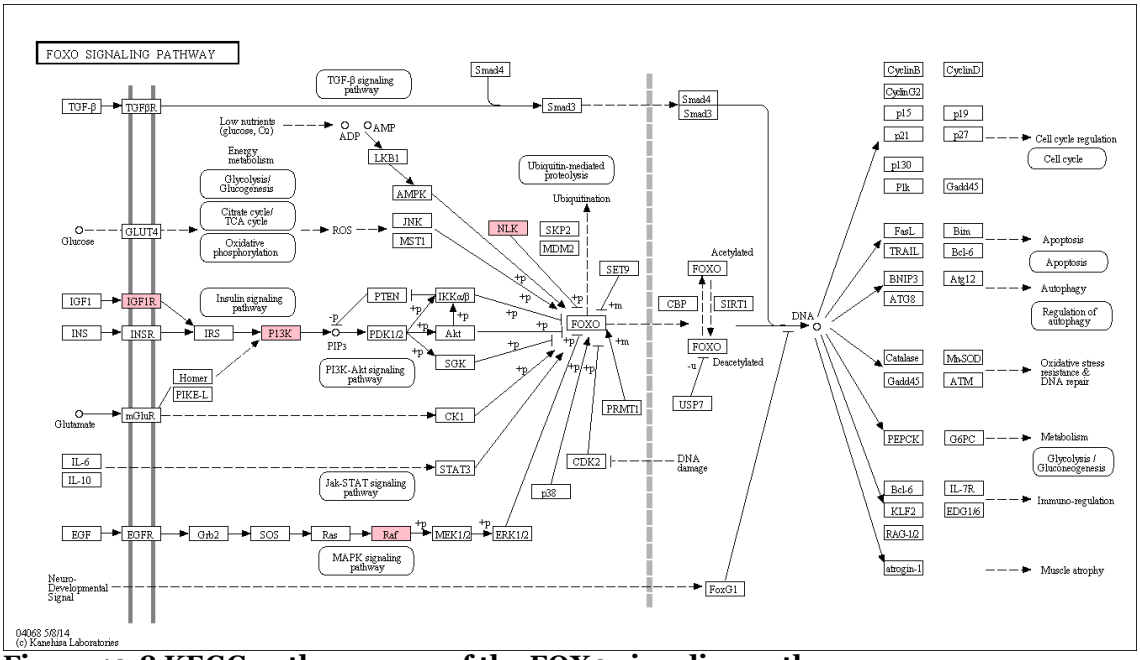

Figure 12-8 KEGG pathway map of the FOX0 signaling pathway.
The map shows the FOX0 signaling pathway based on the KEGG database. The four hits, falling into this network, are indicated in pink. Figure created using KEGG Mapper v2.5.

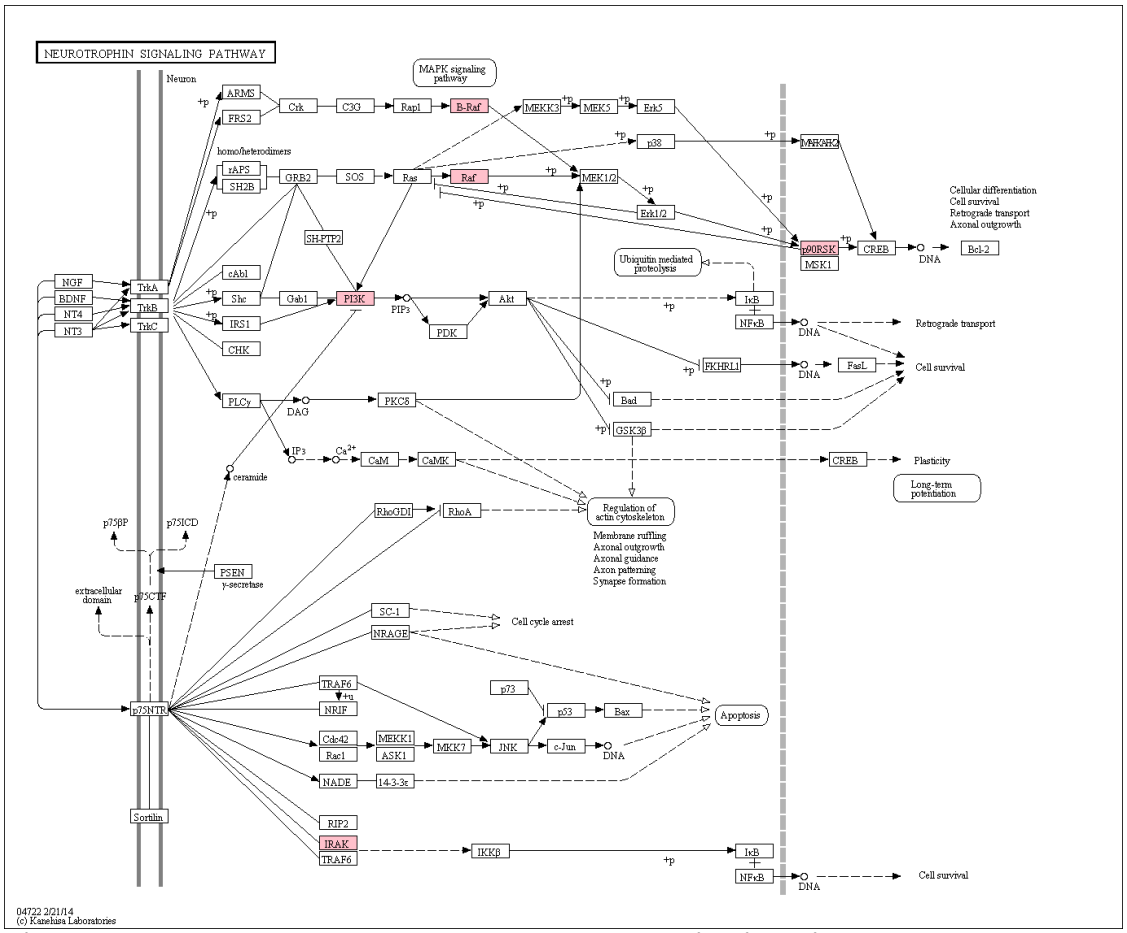

Figure 12-9 KEGG pathway map of the Neurotrophin signaling pathway.
The map shows the Neurotrophin signaling pathway based on the KEGG database. The four hits, falling into this network, are indicated in pink. Figure created using KEGG Mapper v2.5.

12.4 Appendix 4: NCBI HIV-1 interaction database

Table 25 Overlap between the results of this work and the NCBI HIV-1 interaction database.

HIV-1 protein	Interaction	Screen Hit	Pubmed ID
Envelope surface glycoprotein gp120	inhibited by	CD2	7589092
Envelope surface glycoprotein gp120	interacts with	CD2	9475352
Envelope transmembrane glycoprotein gp41	inhibits	CD2	1832084
capsid	interacts with	CD2	1385321, 2111780, 7517794, 8809126, 9743208, 10722370
capsid	interacts with	CD2	7517794
capsid	interacts with	CD2	8809126, 9743208
nucleocapsid	downregulates	CD2	18051367

HIV-1 protein	Interaction	Screen Hit	Pubmed ID
Tat	binds	CDK7	8628270, 8934526, 9184228, 9334327, 9765201
Tat	binds	CDK7	9311822, 10639311, 12049628, 19732026
Tat	interacts with	CDK7	12049628, 19732026
Tat	interacts with	CDK7	8849451, 8934526, 9054383, 9121429, 19732026, 23827503, 24565118
Tat	interacts with	CDK7	9651670, 10066804, 10082552, 10866664, 14569024
Tat	requires	CDK7	8934526, 9184228, 9334327
Tat	stimulates	CDK7	8934526, 9184228, 9311822, 9334327, 9570510, 9651670, 10438593, 10866664, 14569024, 19732026
Tat	synergizes with	CDK7	8934526, 19732026
Vpr	enhanced by	CDK7	12379213
Vpr	inhibited by	CDK7	12379213
Envelope surface glycoprotein gp120	activates	CSK	21562048
Tat	activates	CSK	9621077
Envelope surface glycoprotein gp120	upregulates	IGF1R	15103018
HIV-1 virus replication	enhanced by expression of human gene	ITPKA	18187620
HIV-1 virus replication	enhanced by expression of human gene	NME1	19266025
Tat	upregulates	PIM1	23898208
Envelope surface glycoprotein gp120	activates	PIK3CG	12551992, 12960231, 20041213
Envelope surface glycoprotein gp120	activates	PIK3CG	18453587
Envelope surface glycoprotein gp120	activates	PIK3CG	23251686
Envelope surface glycoprotein gp120	inhibited by	PIK3CG	20818790
Envelope surface glycoprotein gp120	mediated by	PIK3CG	16081599
Envelope surface glycoprotein gp120	modulated by	PIK3CG	16524887
Envelope surface glycoprotein gp120	regulated by	PIK3CG	15689238
Envelope surface glycoprotein gp120	relocalizes	PIK3CG	18453587

HIV-1 protein	Interaction	Screen Hit	Pubmed ID
Envelope surface glycoprotein gp160, precursor	activates	PIK3CG	9341793
Envelope surface glycoprotein gp160, precursor	inhibits	PIK3CG	9808187
Nef	activates	PIK3CG	25104021
Nef	complexes with	PIK3CG	18854243
Nef	downregulates	PIK3CG	8636073, 9247029, 10208934
Nef	interacts with	PIK3CG	11289809, 12526811, 12584329, 17632570, 20702582, 23215766
Nef	upregulates	PIK3CG	10985305
Tat	activates	PIK3CG	17157319
Tat	activates	PIK3CG	20019835
Tat	activates	PIK3CG	21029719
Tat	activates	PIK3CG	21765914
Tat	activates	PIK3CG	8798481, 9394803, 9708406, 11156964, 11994280, 17157319
Tat	induces phosphorylation of	PIK3CG	23301033
Tat	inhibited by	PIK3CG	12077252
Tat	interacts with	PIK3CG	11154208
Tat	interacts with	PIK3CG	14602571
Tat	interacts with	PIK3CG	23077641
Tat	interacts with	PIK3CG	9446795
Tat	regulated by	PIK3CG	24073214
HIV-1 virus replication	enhanced by expression of human gene	PIK3CG	19460752
Tat	activates	MAP2K3	24742347
Tat	interacts with	MAP2K3	23535064
Envelope transmembrane glycoprotein gp41	activates	RPS6KB1	10089566, 10807185
Tat	inhibits	RPS6KB1	20433920
nucleocapsid	upregulates	UCK2	18051367
Tat	downregulates	CDK10	22632162
Envelope surface glycoprotein gp120	upregulates	SPHK1	24162774
Tat	enhances	MAP3K14	11511100

HIV-1 protein	Interaction	Screen Hit	Pubmed ID
HIV-1 virus replication	enhanced by expression of human gene	MAP3K14	18976975
Vpu	binds	NLK	23047923
Tat	Downregulates	HKDC1	22632162